Attachment 7

CRITICALITY SAFETY EVALUATION REPORT - (NON-PROPRIETARY)

VIRGINIA ELECTRIC AND POWER COMPANY
NORTH ANNA POWER STATION UNITS 1 AND 2

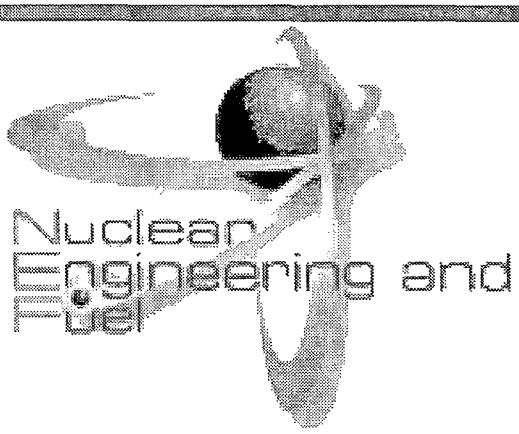

Criticality Safety Evaluation of the North Anna New Fuel Storage Area and Spent Fuel Pool Allowing 5 wt% U-235 Enriched Fuel

Nuclear Engineering and Fuel

Dominion Resources Services, Inc.

November 2016

Table of Contents

Note: Page numbers in the Appendix start with "A-" which is not shown in the Table of Contents, List of Figures, or List of Tables.

List of Tables

List of Figures

Annotation of proprietary information herein corresponds as follows to the specific reasons delineated in the respective affidavits executed by the owners of the information:

1) **AREVA information: denoted with "A" superscript**
2) **Westinghouse information: denoted with "a,c" superscripts**
3) **AREVA/EPRI jointly-owned information: denoted with "A,E" superscripts.**

LIST OF ACRONYMS AND ABBREVIATIONS

BPRA	Burnable Poison Rod Assembly which is a group of boron containing rodlets for the guide tubes held together by a plate that rests on the assembly top nozzle. The number of rodlets and boron content can vary. The BPRA is typically removed after the first cycle of burnup. An AREVA product.
BARAP	Burnup Averaged Relative Assembly Power
CAL	Confirmatory Action Letter
DOE	Department of Energy (USA)
EALF	Energy of the Average Lethargy of a neutron causing Fission
EOL	End of Life
FA	Fuel Assembly
FBMPC	Fuel Building Movable Platform Crane
FFSC	Failed Fuel Storage Cans
FP	Fission Product
FRSR	Fuel Rod Storage Rack is a container for 52 fuel rods that fits in a rack cell position.
GWd/MTU	Gigawatt*day per Metric Ton (Tonne) of Uranium. A unit of burnup.
HTC	Haut Taux de Combustion. This is a set of critical experiments done in France that uses fuel that represents the uranium and plutonium content of 4.5 wt% fuel burned to 37.5 GWd/MTU
ID	Inner Diameter
IFBA	Integral Fuel Burnable Absorber which is a ZrB_2 coating placed on the outside of the fuel pellet. A Westinghouse product.
ISG	Interim Staff Guidance from the NRC
LOCA	Loss of Coolant Accident
MOX	Mixed Oxide fuel. Contains both UO_2 and PuO_2.
MPS	Millstone Power Station
MW/MTU	Megawatt per Metric Ton (Tonne) of Uranium. A unit of specific power.
MWd/MTU	Megawatt*day per Metric Ton (Tonne) of Uranium. A unit of burnup.
NAIF	North Anna Improved Fuel is a fuel design manufactured by Westinghouse with zirconium based grids, Reconstitutable Top Nozzle, and a Debris Filter Bottom Nozzle. Variations are NAIF/P+, NAIF/P+Z and NAIF/P+Z2 which account for an additional protective grid and a change to Zirlo.
NAPS	North Anna Power Station
NCS	Nuclear Criticality Safety
NFSA	New Fuel Storage Area also known as the new fuel storage racks
OD	Outer Diameter

pcm	**0.00001 in k (acronym from percent milli)**
ppm	**Parts per million by weight**
PS	**Poison Stop which is a piece of steel used in the racks to position the Boraflex panels**
PWR	**Pressurized Water Reactor**
RCCA	**Rod Cluster Control Assembly (control rod)**
RCS	**Reactor Cooling System**
RFA	**Robust Fuel Assembly is fuel design manufactured by Westinghouse. This is short for RFA-2.**
RSS	**square Root of the Sum of the Squares**
RTP	**Rated Total Power**
SER	**Safety Evaluation Report**
SFP	**Spent Fuel Pool.**
SNF	**Spent Nuclear Fuel**
SS	**Stainless Steel**
VF	**Volume Fraction**
VSDA	**Vibration Suppression Damping Assemblies. These are an array of solid Zircaloy rods that inserted into the guide tubes which suspended from a plate that rests on the assembly top nozzle.**
WABA	**Wet Annular Burnable Absorbers. This is a Westinghouse removable burnable absorber product.**

1 Introduction

This criticality analysis of the North Anna Power Station new fuel storage area and spent fuel pool has been performed to allow an increase in the maximum allowable fuel enrichment to 5 wt% U-235, simplify spent fuel storage configurations, and increase identified margin to k-effective limits. The current enrichment limit for the North Anna new fuel storage area and spent fuel pool is 4.6 wt% U-235.

The North Anna spent fuel pool has 1737 storage cell locations in 16 rack modules. The cell design for all the rack modules is the same. The rack modules were designed to have flux traps with Boraflex panels. Boraflex credit was removed prior to this criticality analysis and no credit for the Boraflex is included in this analysis. For the previous criticality analysis, fuel assemblies could be loaded in matrix and non-matrix locations. Matrix locations are 5x5 groups of cells with a cell blocker in the center. The burnup restrictions for matrix and non-matrix locations differed.

For this criticality analysis, the matrix terminology has been dropped and replaced by two configurations, Region 1 and Region 2. Region 1 checkerboards fuel assemblies and empty cells and has no burnup requirements. Cell blockers are no longer needed due to analysis of the multiple misload accident provided in Section 13.2. Region 2 has two sets of minimum burnup requirements; one for fuel assemblies with no cooling to 3 years cooling and another for fuel assemblies that have been cooled more than 3 years. Region 1 can be anywhere in the pool (except 6 cells near the new fuel elevator) as long as the following four requirements are met:

1) Region 1 blocks must have empty cells at the outer corners.

2) At least two Region 2 rows must exist between Region 1 blocks.

3) Each Region 1 block shall be fully contained in a single rack module where a rack module is adjacent to another rack module.

4) Spent fuel cells AA21, AA22, BB21, BB22, CC21, and CC22 may not be part of a Region 1 block due to the proximity of the new fuel elevator. (See Figure 9.7 for location of these cells.)

No absorber panels are credited in this criticality analysis, however, credit is taken for control rods (fresh or used). If a fuel assembly has a control rod in it, then it can be loaded in Region 2 with no burnup credit (valid for all enrichments up to the 5 wt% U-235).

The following terms used in this report need to be clearly defined. **Burnup** when used to compare to loading criteria is the volume averaged burnup of the assembly as determined using the measured reaction rates.
Enrichment when used to compare to loading criteria is the maximum planar volume averaged enrichment in the fuel assembly. If the fuel assembly has axial blankets the lower enriched fuel is not credited in determining the enrichment. This enrichment uses the as built data not the nominal ordered enrichment.

2 Acceptance Criteria and Regulatory Guidance

The Code of Federal Regulations Title 10 Part 50 Section 68 (b)(4) states:

> *"If credit is taken for soluble boron, the k-effective of the spent fuel storage racks loaded with fuel of the maximum fuel assembly reactivity must not exceed 0.95, at a 95 percent probability, 95 percent confidence level, if flooded with borated water, and the k-effective must remain below 1.0 (subcritical), at a 95 percent probability, 95 percent confidence level, if flooded with unborated water. "*

This analysis shows at a 95 percent probability and 95 percent confidence level that if the fuel loaded in the spent fuel pool meets the Technical Specification for enrichment and burnup, the k-effective will be less than 0.95 crediting soluble boron and less than 1.0 with unborated water as specified in 10CFR50.68(b)(4). [1]

Further, Title 10 Part 50 Section 68 (b) paragraphs (2) and (3) specify:

> *"(2) The estimated ratio of neutron production to neutron absorption and leakage (k-effective) of the fresh fuel in the fresh fuel storage racks shall be calculated assuming the racks are loaded with fuel of the maximum fuel assembly reactivity and flooded with unborated water and must not exceed 0.95, at a 95 percent probability, 95 percent confidence level. This evaluation need not be performed if administrative controls and/or design features prevent such flooding or if fresh fuel storage racks are not used.*

(3) If optimum moderation of fresh fuel in the fresh fuel storage racks occurs when the racks are assumed to be loaded with fuel of the maximum fuel assembly reactivity and filled with low-density hydrogenous fluid, the k-effective corresponding to this optimum moderation must not exceed 0.98, at a 95 percent probability, 95 percent confidence level. This evaluation need not be performed if administrative controls and/or design features prevent such moderation or if fresh fuel storage racks are not used"

This analysis of the fresh fuel storage racks shows that 5 wt% U-235 fuel loaded into the new fuel storage area meets the requirements of paragraphs (2) and (3).

Meeting the requirements of 10 CFR 50.68 will also satisfy 10 CFR 50, Appendix A, General Design Criterion 62, [2] which specify:

"Criticality in the fuel storage and handling system shall be prevented by physical systems or processes, preferably by use of geometrically safe configurations."

Standard Review Plan, NUREG-0800, Section 9.1.1, "Criticality Safety of Fresh and Spent Fuel Storage and Handling." [3] provides the regulatory review criteria used by the NRC in evaluating whether a licensee meets the NRC's regulations

Provided below are the thirteen review criteria from NUREG-0800, Section 9.1.1 and a cross reference to where the information is provided in this report, if applicable.

1. *Fuel assembly design to verify that appropriate fuel assembly data were used.*

   Fuel assembly design data is provided in Section 4.

2. *Fuel storage rack design to verify that appropriate fuel storage rack data were used.*

   Storage rack design data is provided in Section 3.

3. *Evaluation of performance effectiveness of the neutron absorbing materials in the fresh and spent fuel racks.*

   No absorbers are credited except for control rods in the fuel assembly.

4. *Computational methods and related data to verify that acceptable computational methods and data were used.*

   Computational methods are described in Sections 5 and 6.

5. *Computational method validation to verify that the validation study is thorough and uses benchmark critical experiments that are similar to the normal-conditions and abnormal conditions models and to verify that the neutron distribution coefficient (K(eff)) bias and bias uncertainty values are conservatively determined.*

Validation is summarized in Section 6 and the details are provided in Appendix A.

6. *Identification of normal conditions to verify that the scope of specified normal conditions is comprehensive.*

Range of normal conditions is identified in Section 12

7. *Normal-conditions models to verify that normal conditions are modeled conservatively and that all modeling approximations and assumptions are appropriate.*

Normal conditions models and the tolerances and uncertainties in these models are described in Sections 7, 9, 10, 11 and 12.

8. *Identification of abnormal conditions to verify that the scope of considered abnormal conditions is comprehensive.*

Abnormal conditions are described in Section 13.

9. *Abnormal-conditions models to verify that abnormal conditions are modeled conservatively and that all modeling approximations and assumptions are appropriate.*

Abnormal condition models are described in Section 13.

10. *Analysis of normal and credible abnormal conditions to verify that the analysis is complete and logically sound and that assumptions, limits, and controls are clearly stated.*

The analysis is contained in Sections 7, through 13. The limitations of the analysis are listed in Section 14.

11. *Analysis conclusions to verify the applicant's conclusions regarding maintaining subcriticality for all normal and credible abnormal conditions.*

The final conclusion of the analysis is provided in Section 14.

12. *Inspections, Tests, Analyses, and Acceptance Criteria (ITAAC). For design certification (DC) and combined license (COL) reviews, the staff reviews the applicant's proposed ITAAC associated with the structures, systems, and components (SSCs) related to this SRP section in accordance with SRP Section 14.3, "Inspections, Tests, Analyses, and Acceptance Criteria." The staff recognizes that the review of ITAAC cannot be completed until after the rest of this portion of the application has been reviewed against acceptance criteria contained in this SRP section. Furthermore, the*

staff reviews the ITAAC to ensure that all SSCs in this area of review are identified and addressed as appropriate in accordance with SRP Section 14.3.

Not applicable to License Amendment Requests.

13. COL Action Items and Certification Requirements and Restrictions. For a DC application, the review will also address COL action items and requirements and restrictions (e.g., interface requirements and site parameters). For a COL application referencing a DC, a COL applicant must address COL action items (referred to as COL license information in certain DCs) included in the referenced DC. Additionally, a COL applicant must address requirements and restrictions (e.g., interface requirements and site parameters) included in the referenced DC.

Not applicable to License Amendment Requests.

Guidance for spent fuel pool criticality analysis is given in DSS-ISG-2010-01. [4]

Table 2.1: Use of DSS-ISG-2010-01

Guidance from DSS-ISG-2010-01	Implementation	Section(s) in this Report
1. Fuel Assembly Selection The NCS analysis must adequately bound all designs and variations within a design.	All the fuel designs and variations in the designs in the pool are described. The design features are bounded by the analysis for both depletions and criticality calculations. A single limiting fuel design was used but augmented by a grid bias to cover all designs. The new fuel storage rack used hybrid guide tube dimensions to conservatively cover the design variations.	Sections 4, 7.12, 7.13, 8.8, 9.2.1 and, 10.4.1
2. Depletion Analysis a.i. Depletion uncertainty (5%) covers only isotopic concentration uncertainty.	Critical experiments cover the major actinide cross section uncertainty. A bias of 1.5% of the fission production and minor actinides worth covers their bias and uncertainty in reactivity worth. Used fuel assembly burnup uncertainty is covered by a separate term (4%).	Sections 6.2, 6.3, 10.4.6
2. Depletion Analysis a.ii. Reactivity decrement should not include the worth of the burnable absorbers.	Followed.	Section 10.4.5
2. Depletion Analysis b.i. Bounding values should be used.	Bounding values are identified and used.	Sections 8.2 through 8.9
2. Depletion Analysis b.ii. Use the more limiting bounding parameter when a conflict occurs.	Fuel and moderator temperatures are maximized based on high specific power. A bias is added for low power at end of life.	Sections 8.4, 8.6, 8.7 and 10.4.7

Guidance from DSS-ISG-2010-01	Implementation	Section(s) in this Report
2. Depletion Analysis b.iii. Non-bounding values are outside scope of ISG.	Bounding values were used for all parameters.	Section 8.10
2. Depletion Analysis c.i. All removable burnable absorbers must be considered.	All removable burnable absorbers are identified and the most limiting burnable absorbers are used.	Section 8.9
2. Depletion Analysis c.ii. Limiting integral burnable absorbers should be used.	The reference depletions use BPRA which bounds the maximum worth IFBA. If IFBA is used, BPRAs used in the same assembly in addition to IFBA are limited to 8 fingers or less.	Section 8.9.1
2. Depletion Analysis c.iii. Model the burnable absorbers appropriately.	Burnable absorbers are modeled appropriately. The BPRA are conservatively modeled as full length and contain the maximum design B-10 loading in the depletion analysis.	Section 8.9.1
2. Depletion Analysis c.iv. Consider competing effects	The depletion model correctly accounts for competing effects.	Section 8.9
2. Depletion Analysis d.i. Spectrum hardening from rodded operation should be considered.	The rodded operation was reviewed and it was determined that the modeling conservatively covered the rodded operation.	Section 8.9.2
2. Depletion Analysis d.ii. Effect of control rods on the axial burnup profile should be considered	The NUREG/CR-6801 axial burnup profiles were used which included rodded operation. Therefore, the axial burnup profiles used covered rodded operation.	Section 8.5
3. Criticality Analysis a. Axial Burnup Profile	The NUREG/CR-6801 axial burnup profiles were used. Also, analysis was done with uniform burnup. The most limiting of the two was used.	Section 8.5
3. Criticality Analysis b. Rack Model i. Model inputs should be traceable.	The rack dimensions and materials are taken from the manufacturer's drawings.	Section 3
3. Criticality Analysis b. Rack Model ii. Efficiency of the neutron absorber should be established.	Absorber panels are not credited in this analysis. Ag/In/Cd control rods do not introduce efficiency concerns. The control rod absorption was reduced by conservative depletion analysis.	Section 10.7
3. Criticality Analysis b. Rack Model iii. Conservative degradation should be used.	Conservative degradation of the control rods is assumed via a conservative depletion analysis.	Section 10.7
3. Criticality Analysis c. Interfaces - Use the maximum uncertainties from either side.	The maximum uncertainty from either side is used.	Section 11
3. Criticality Analysis d. Normal Conditions - All normal conditions such as movement of fuel and inspections should be considered.	All normal conditions are considered.	Section 12

Guidance from DSS-ISG-2010-01	Implementation	Section(s) in this Report
3. Criticality Analysis e. Accident Conditions	All normal initial conditions are considered as base conditions for the accident analysis.	Section 13
4. Criticality Code Validation NUREG/CR-6698 endorsed	NUREG/CR-6698 was followed for the validation.	Appendix A
4. Criticality Code Validation a. Area of Applicability i. Include the HTC criticals	The HTC critical experiments are included in the analysis.	Appendix A
4. Criticality Code Validation a. Area of Applicability ii. Use appropriate criticals	Appropriate critical experiments are used.	Appendix A
4. Criticality Code Validation a. Area of Applicability iii. Sufficient criticals for analysis and appropriate grouping.	A large sample of critical experiments is used, providing adequate statistics for all the conclusions made.	Appendix A
4. Criticality Code Validation a. Area of Applicability iv. Be sure the set is not highly correlated.	Due to the large number of experiments from multiple critical facilities, the critical experiments are not highly correlated.	Appendix A
4. Criticality Code Validation b. Trend Analysis Adequate, appropriate, not rejected.	The trend analysis is performed on the major parameters. The trend analysis finds the best linear fit. No trends are rejected to be conservative. The most limiting bias and uncertainty for the area of applicability is applied assuming both that all trends are real and there are no trends.	Appendix A
4. Criticality Code Validation c. Statistical Treatment i. Use the variance of the population about the mean	The statistical approach recommended in NUREG/CR-6698 is used. Thus, the variance of the population about the mean rather than the variance of the mean is used.	Appendix A
4. Criticality Code Validation c. Statistical Treatment ii. Use correct confidence factors.	The statistical approach recommended in NUREG/CR-6698 is used. The correct confidence factors were used.	Appendix A
4. Criticality Code Validation c. Statistical Treatment iii. Consider Normality	Normality testing was performed and the appropriate statistical treatment was applied.	Appendix A
4. Criticality Code Validation d. Lumped Fission Products	Lumped Fission Products are not used.	Section 6
4. Criticality Code Validation e. Code-to-Code Comparisons	5% of the Delta k of depletion as recommended in this ISG is used but to confirm this is appropriate for SCALE TRITON comparisons to CASMO 4 and 5 were performed.	Section 6.2.1
5. Miscellaneous a. Precedence b. References c. Assumptions	Precedence is not quoted as a licensing basis. References used were carefully chosen to be applicable to the point being made. Assumptions are identified and justified.	

3 Storage Rack Description

3.1 New Fuel Storage Area

The layout of the New Fuel Storage Area (NFSA) is displayed below in Figure 3.1. There is air behind the south and east wall and underneath the concrete floor. Figure 3.2 shows two pictures of the NFSA.The dimensions applicable to the NFSA rack are provided in Table 3.1.

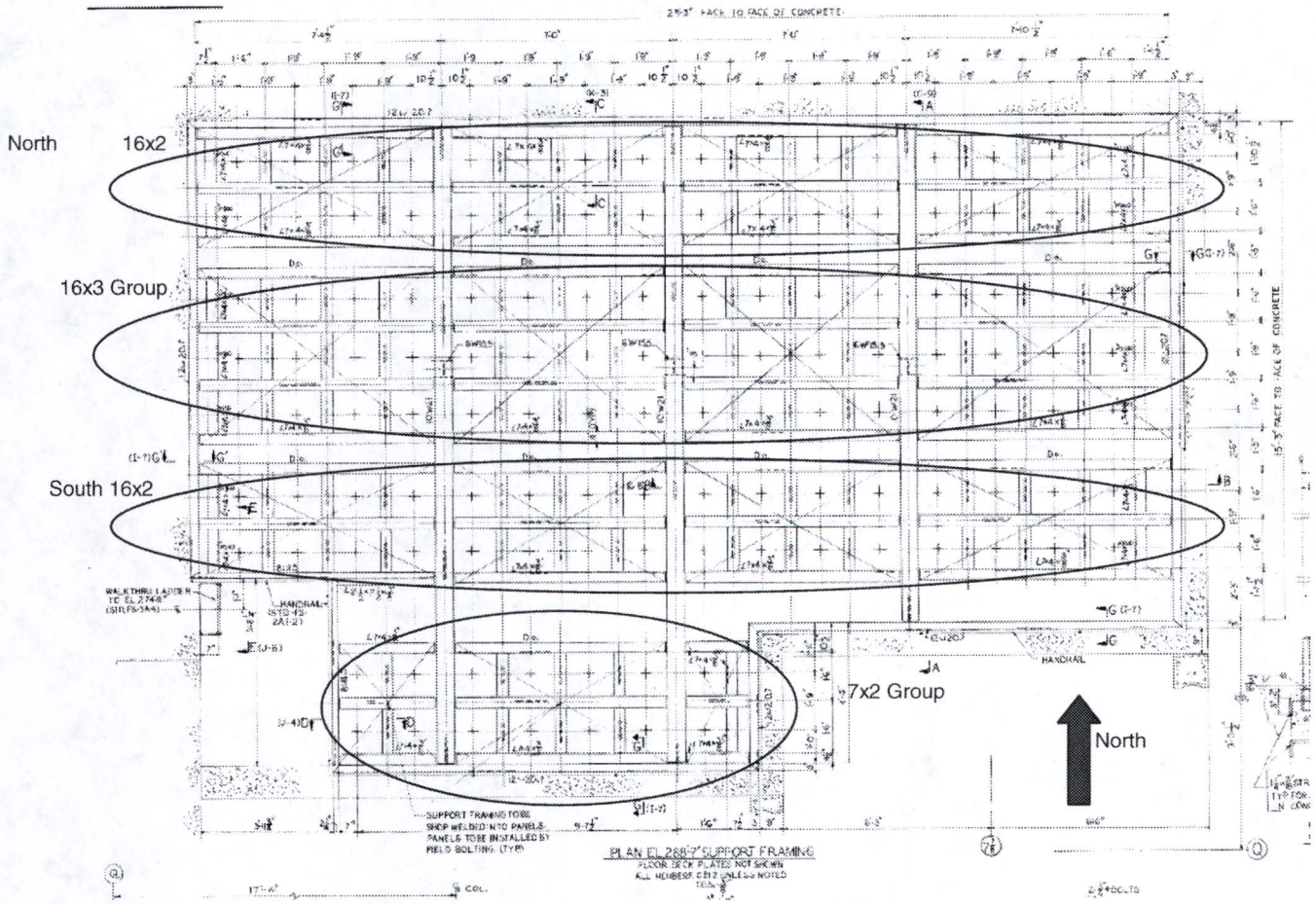

Figure 3.1: North Anna New Fuel Storage Area [5]

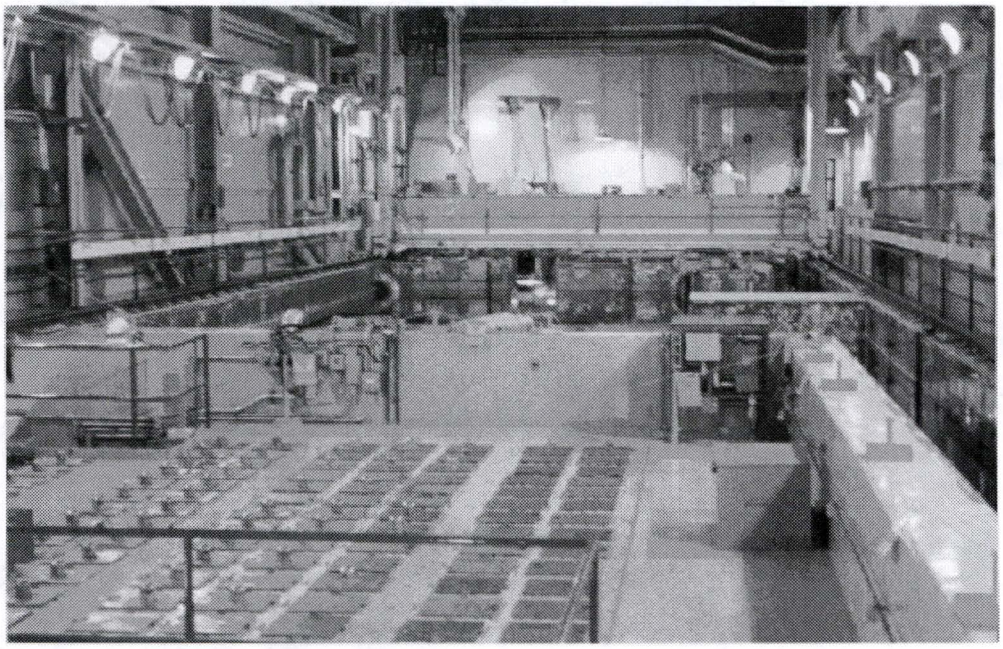

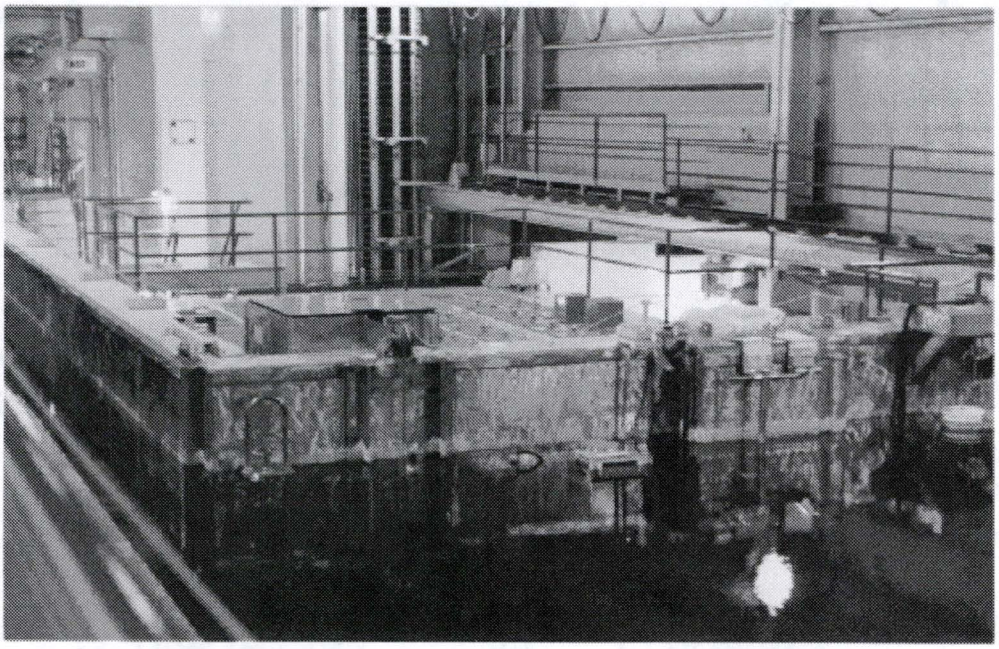

Figure 3.2: Pictures of the New Fuel Storage Area

Table 3.1: New Fuel Storage Area Rack Dimensions

Measurement Description	Dimension in cm
Stainless Steel Tube Pitch	53.340 ± 0.635
Stainless Steel Tube Inner Diameter	22.86
Stainless Steel Tube Thickness	0.3175 ± 0.0250
Stainless Steel Tube Length	420
Lower Structural L-Beams	See Figure 3.3
Distance from NFSA floor to bottom of active fuel	9.030 ± 0.085
South and East Concrete wall and Concrete floor Thickness	30.48 ± 15.24

The new fuel storage area rack tubes are attached at the bottom to 7x4x3/8 inch L beams bolted to the concrete floor. These L beams are 4 feet 8.25 inches long for the rows that contain 3 tubes and 2 feet 11.25 inches for the rows that contain 2 tubes. The distance between the left and right L beam is approximately the outside diameter of a tube. These beams set the east west location of the rack tubes. The 4 inch legs of the two L beams place about 8 inches wide (slightly less accounting for the thickness of the L beam) of steel at the bottom of the tube over the concrete floor. The fuel assembly bottom nozzle sits on the 4 inch sides of the L beam. There is a gap between the L beams that allows for water drainage (along with holes at the bottom of the SS tube). Some of the fuel is over the L beams and some is directly over the concrete.

In order to position the tubes in the north/south direction 1x1x1/8 inch L beams are welded to the larger L beams. These small L beams create a box that corresponds to the tube outer diameter thus positioning the bottom of the tube. The tubes flare out at the top to help in loading the assemblies. At the top the tubes are held in position between I beams. Since the

upper structure is considerably above the active fuel and above the upper structure is air the details of the upper structure are not important. Figure 3.3 shows an axial representation of the new fuel storage area racks.

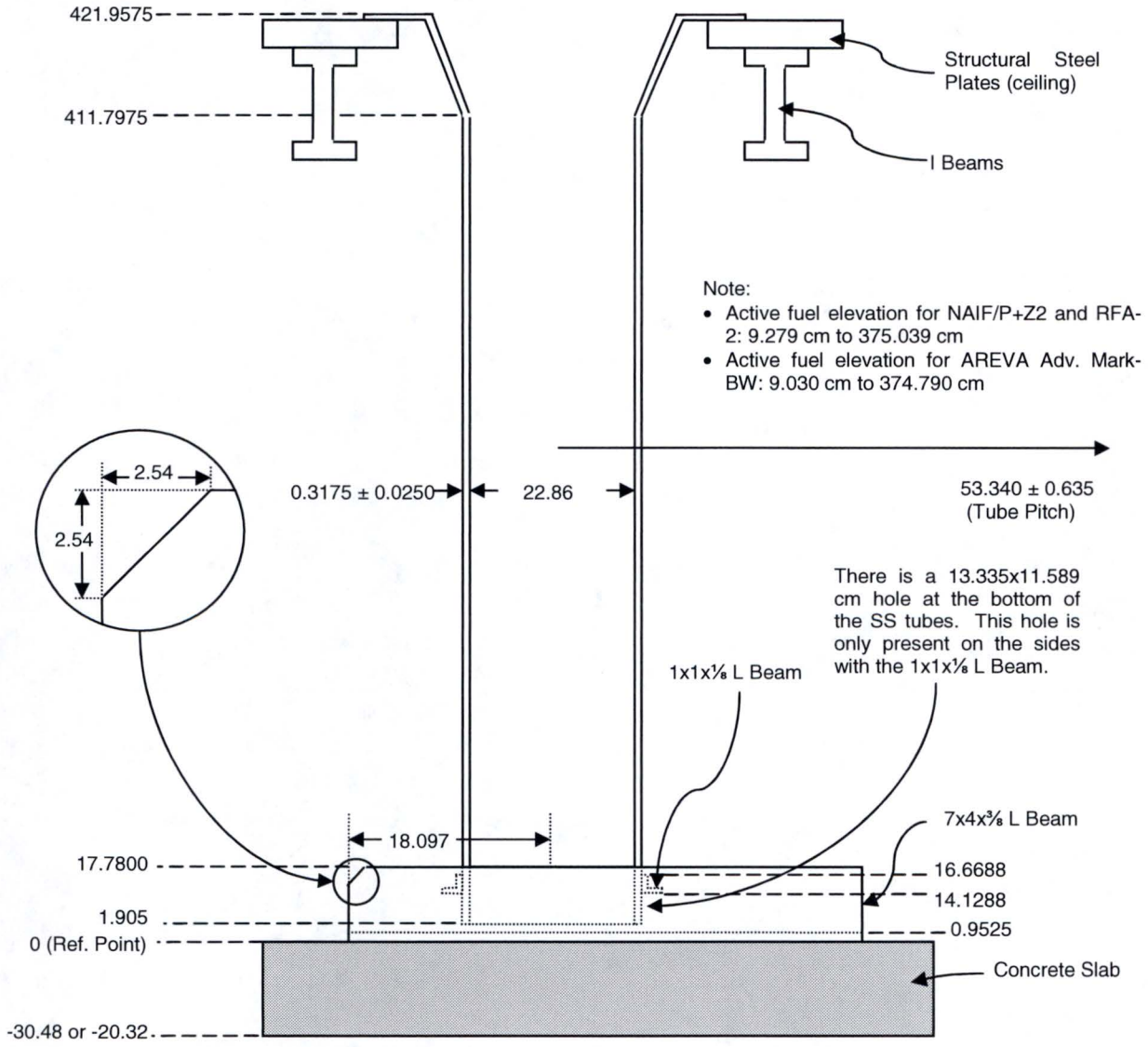

Not to scale. Dimensions in cm (except the L Beams are described by their nominal inches).

Figure 3.3: Axial Representation of the New Fuel Storage Area Racks

3.2 Spent Fuel Pool

There is only one rack module design (of 6 different sizes) located in the North Anna Spent Fuel Pool. The criticality analysis presented herein describes a Region 1 and a Region 2. These specific expressions refer to different arrangements of fuel rather than physically different rack modules. Figure 3.4 shows the layout of the spent fuel pool with the rack modules. The cask loading pit is through a gate on the west side of the spent fuel pool.

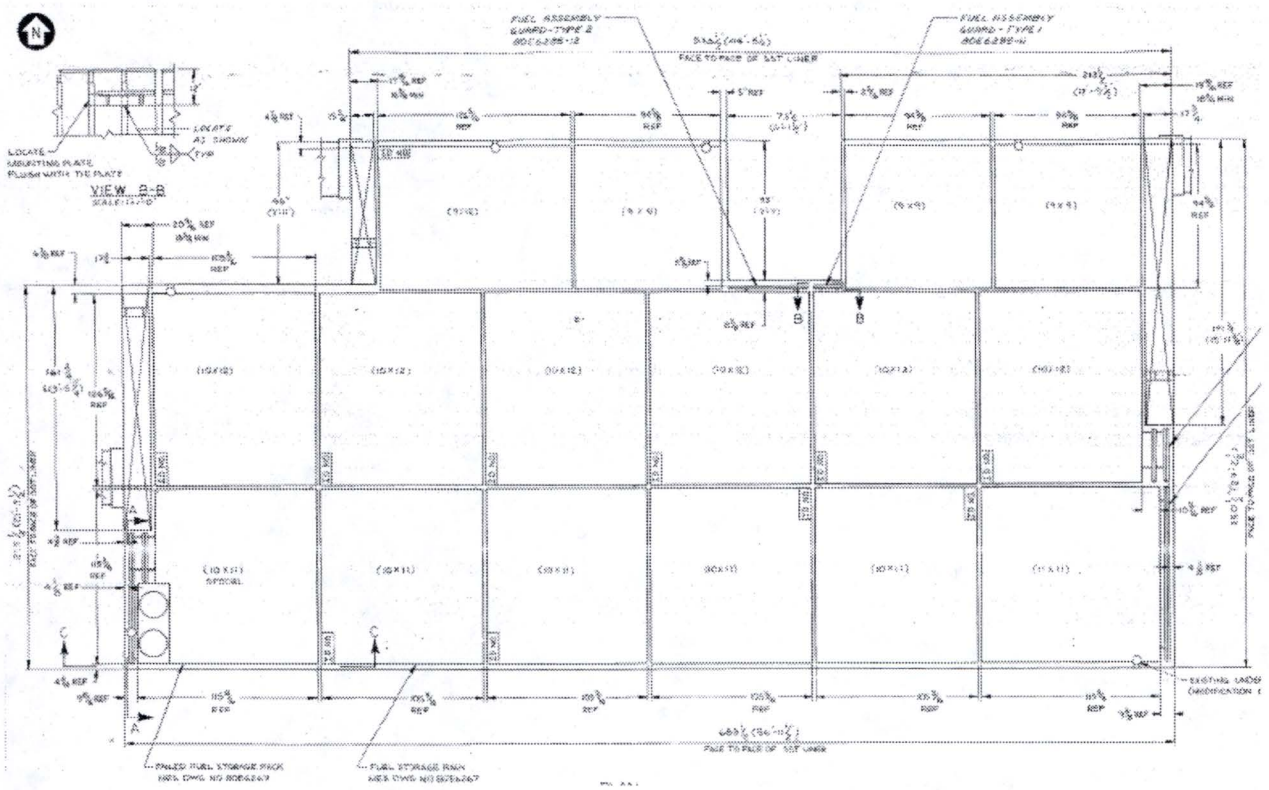

Figure 3.4: North Anna Spent Fuel Pool

The rack modules consist of rectangular tubes of stainless steel with Boraflex panels on all four sides. Over the Boraflex panels is placed a thin cover of stainless steel which will be called the "wrapper." The bottom of about a quarter of the wrappers is thickened and lengthened. The bottom 30 inches of those wrappers is called a "stiffener." The Boraflex panels do not extend the full length of the tube so there are stainless steel "stops" above and below the Boraflex panels. The tubes are held in place by tie plates. The tie plates are roughly the length of the tube. Figure 3.5 shows how the tie plates connect multiple tubes. The circles highlight the tie

plates around one tube. Figure 3.6 is a picture looking down at the rack showing the cells and tie plates.

At the top of the cell the cell walls are flared out to make a chute for the fuel assemblies to enter the cells. This flare out prevents the wrappers from being visible. Under the cell boxes is a half inch steel baseplate with holes for water flow. Beneath that is a support structure with a high water fraction. Figure 3.7 provides an axial description of the modules. (Figure 3.7 shows a support leg under the cell, but the actual structure has about one leg per every nine cells.) Table 3.2 provides the dimensions for the spent fuel pool and rack modules.

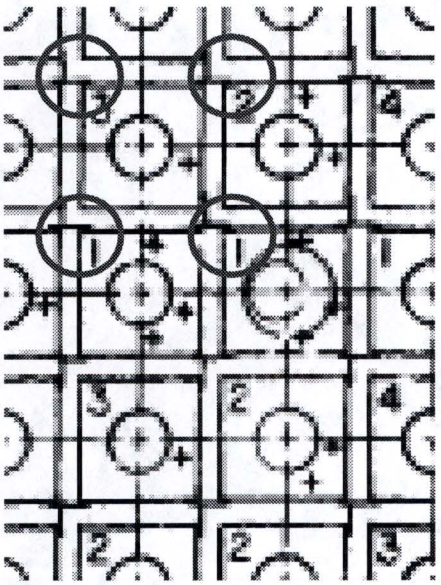

Figure 3.5: Tie Plates in the North Anna Spent Fuel Pool Rack Modules

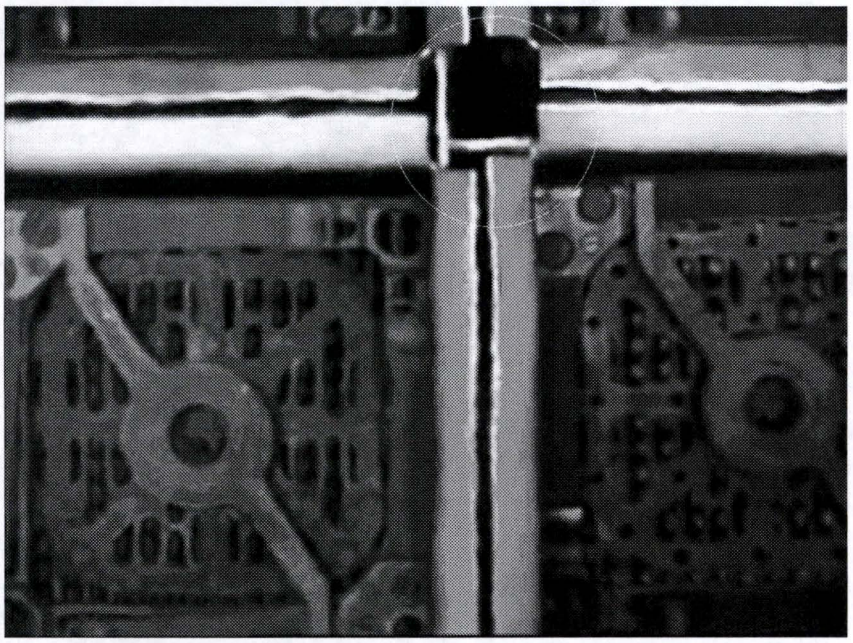

Figure 3.6: Photo From Above the Racks Showing Tie Plates

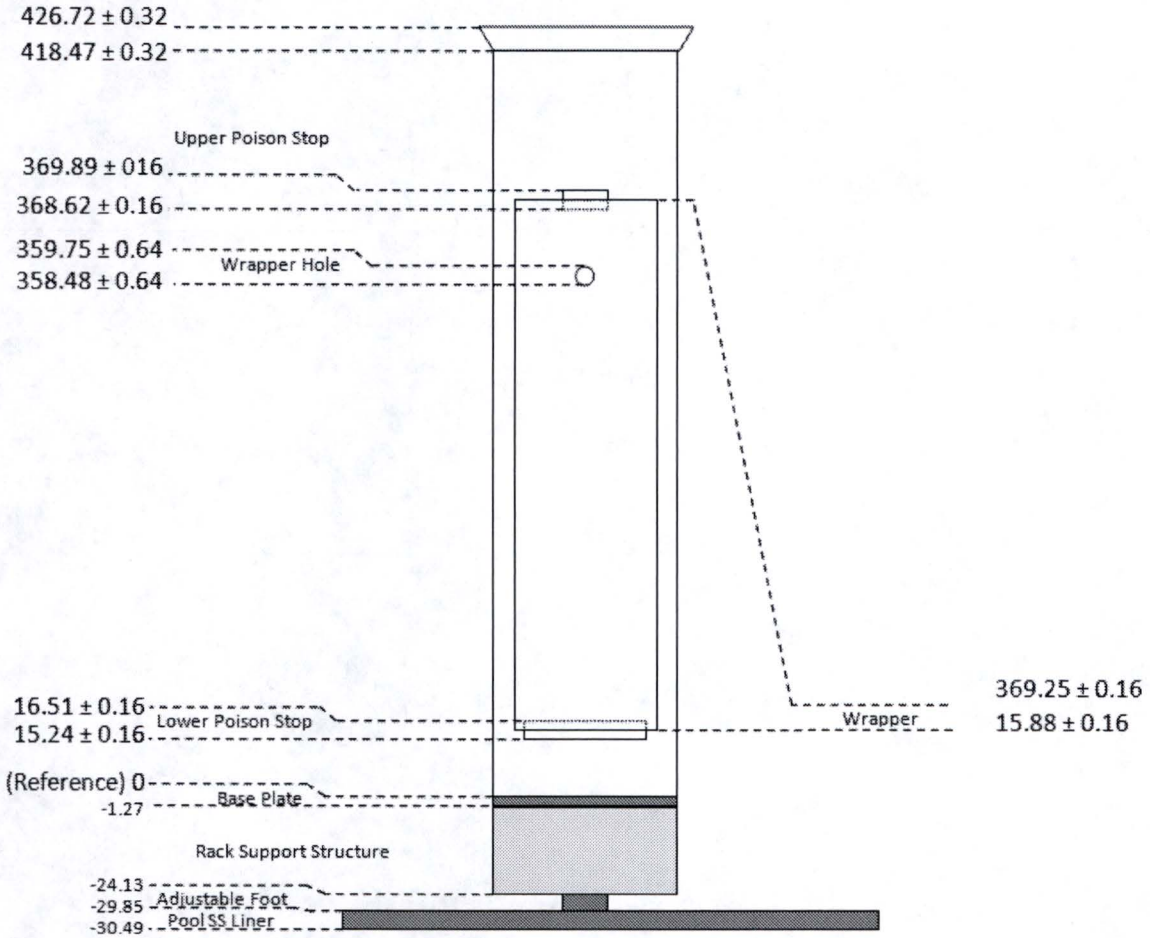

Dimensions are in cm. Bounding design active fuel position is between 8.15 to 373.91 cm

Figure 3.7: Axial Description of a Cell in the Rack Modules

Table 3.2: Spent Fuel Pool Dimensions

Component	Dimension(cm)
Cell Pitch	26.83 ± 0.32*
Cell Inside Dimension	22.5425 ± 0.12
Cell Wall Thickness	0.2286 ± 0.013
Absorber Gap	0.254 ± 0.025
Wrapper Thickness	0.0744 ± 0.013
Wrapper Width	19.37 ± 0.16
Wrapper Vent Hole	1.27
Stiffener Thickness	0.2286 ± 0.013
Tie Plate-1 Width	5.08 ± 0.08
Tie Plate-1 Thickness	0.305 ± 0.013
Tie Plate-2 Width	4.13 ± 0.08
Tie Plate-2 Thickness	0.305 ± 0.013
Lower Poison Stop Width	17.939 ± 0.159
Upper Poison Stop Width	7.78 ± 0.16
Lower and Upper Poison Stop Thickness	0.2286 ± 0.013
Lower and Upper Poison Stop Height	1.27 ± 0.16
Pool Liner	0.635 ± 0.159
Baseplate Thickness	1.270 ± 0.318
Rack Support Structure Thickness	22.86
Adjustable Foot Height	5.72
Cell Height	426.7 ± 0.32
Wrapper Height	353.4 ± 0.16
Wrapper Hole to Top of Wrapper	10.16 ± 0.64
Stiffener Height	76.20 ± 0.16
Bottom of Cell to Top of Lower Poison Stop	16.51 ± 0.16
Top of Lower Poison Stop to Bottom of Wrapper	0.64 ± 0.16
Top of Lower PS to Bottom of Upper PS	352.11 ± 0.16
Top Flair Out Height	8.26 ± 0.32
Tie Plate-1 and 2 Height	416.56 ± 0.32

*The rack drawing gives the cell pitch uncertainty of 1/8 of an inch. The same rack drawing gives the dimension of 5 cells with the same uncertainty (1/8 of an inch). A note on the rack drawing states that the uncertainty is not to accumulate. Since moving a single cell by a small uncertainty has little reactivity worth, it is assumed that the pitch will uniformly increase or decrease by +/- 0.3175 cm divided by 5 or 0.0635 cm per cell.

4 Fuel Design Description

4.1 Fuel Description

North Anna uses a 17x17 lattice fuel with a center instrument tube and 24 guide tubes. Four fuel designs (Standard, NAIF, AREVA, and RFA) have been used, all with very similar designs. The initial fuel design, designated "Standard," used all Inconel grids. The current fuel design is the Westinghouse RFA design. This design includes annular pellets at the ends of the IFBA rods. Table 4.1 provides the dimensions of the four fuel designs.

Table 4.1: Fuel Design Dimensions
(Dimensions in inches)

	Standard	NAIF	AREVA	RFA
Pellet Diameter	0.3225	0.3225	0.3225	0.3225
Clad Inner Diameter	0.329	0.329	0.329	0.329
Clad Outer Diameter	0.374	0.374	0.374	0.374
Clad Material	Zirc4	ZIRLO	M5	Opt. ZIRLO
Rod Pitch	0.496	0.496	0.496	0.496
Guide Tube and Instrument Tube				
Inner Diameter	0.450	0.442	0.450	0.442
Outer Diameter	0.482	0.474	0.482	0.482
Grid Volume (cubic inches)[1]	[ ]^{a,c}	[ ]^{a,c}	[ ]^{A}	[ ]^{a,c}

[1]The grid volume is the volume of the grids plus sleeves in the active fuel ignoring the bottom grid. The grids are a zirconium alloy except for the Standard fuel which used all Inconel grids.

The fuel pellet is dished and chamfered. The fuel batch stack density (density of the pellet reduced by the dishing and chamfering) has ranged from [ ]^{a,c}. The manufacturing tolerances for the fuel are found on Table 4.2. The RFA fuel has annular pellets for the IFBA rods in the top and bottom 6 inches. The annular pellets have the same outer diameter but have a void center with a diameter of 0.155 inches

The active length of the fuel is 144 inches plus or minus [ ]^{a,c}. The distance from the bottom of the fuel assembly to the bottom of the active fuel has varied by design but the smallest distance (AREVA fuel) is [ ]^{A}. Axial blankets have not been used at North Anna. All fuel pins in an assembly are the same enrichment.

The assembly pitch in the core is 8.466 inches. The location of the guide tubes in the assembly is given on Figure 4.1. Table 4.3 lists the fuel design and enrichment history for North Anna.

Table 4.2: Fuel Design Tolerances

Pellet Diameter	[ ]^{a,c}
Clad Inner Diameter	[ ]^{a,c}
Clad Outer Diameter*	[ ]^{a,c}
Rod Pitch	[ ]^{A}
Guide Tube and Instrument Tube Inner Diameter	[ ]^{a,c}
Guide Tube and Instrument Tube Outer Diameter	[ ]^{a,c}
Stack Density	[ ]^{a,c}

*Some older fuel had a [ ]^{A} tolerance so [ ]^{a,c} is used for the new fuel racks and [ ]^{A} is used for the spent fuel racks.

**Determined by the distribution of assembly uranium dioxide weights in assemblies in a batch. This is the highest deviation of all batches analyzed. Average batch uncertainty (2 sigma) is less than 0.3%.

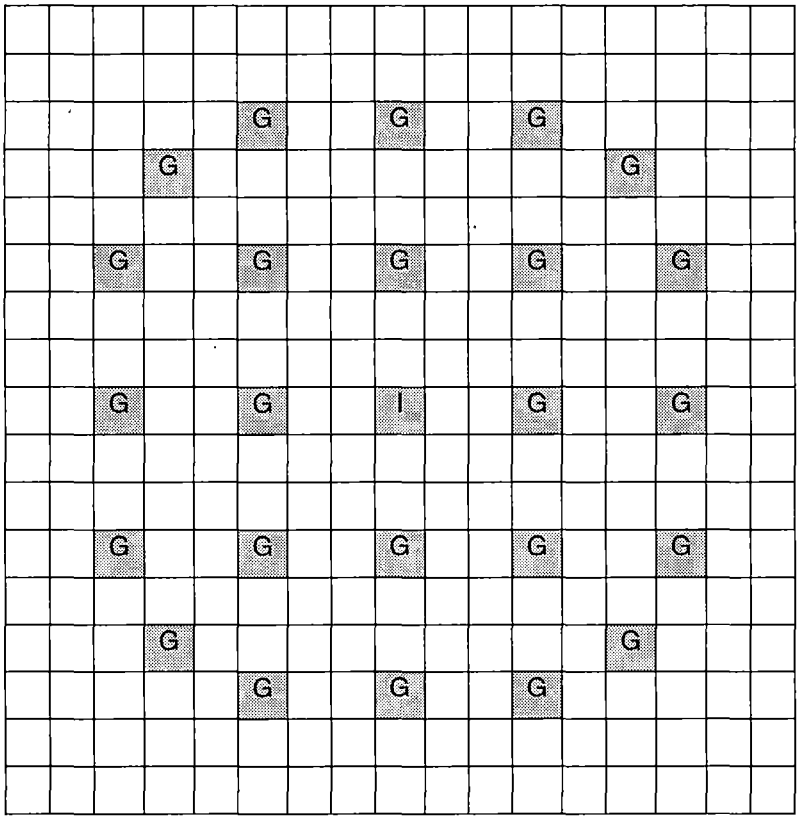

Figure 4.1: Westinghouse 17x17 Fuel Design

Table 4.3: Fuel Design and Enrichment History for North Anna

(Difference in NAIF designs do not impact criticality)

Unit 1			Unit 2		
Cycle	**Assembly Type**	**Enrichment**	**Cycle**	**Assembly Type**	**Enrichment**
1	Standard	2.11, 2.60, 3.10	1	Standard	2.11, 2.60, 3.10
2	Standard	3.21	2	Standard	3.41
3	Standard	3.41	3	Standard	3.59
4	Standard	3.59	4	Standard	3.60
5	Standard	3.60	5	Standard	3.60, 3.79
6	Standard	3.60, 3.80	6	Standard	3.79, 4.00
7	Standard	3.79, 3.99	7	Standard	3.80, 4.00
8	Standard	3.80, 4.00, 3.82	8	NAIF	3.99, 4.21
9	NAIF	4.01, 4.19	9	NAIF	4.02, 4.21
10	NAIF	4.00, 4.21	10	NAIF/P+	4.01, 4.20
11	NAIF/P+Z	4.01, 4.21	11	NAIF/P+Z	4.01, 4.21
12	NAIF/P+Z	4.00, 4.20	12	NAIF/P+Z	4.01, 4.21
13	NAIF/P+Z	4.00, 4.21	13	NAIF/P+Z	4.10, 4.25
13*	AREVA Adv Mark-BW	4.20			
14	NAIF/P+Z	4.15, 4.25	14	NAIF/P+Z	4.16, 4.24
15	NAIF/P+Z	4.15, 4.25	15	NAIF/P+Z	4.15, 4.25
16	NAIF/P+Z	4.25, 4.40	16	NAIF/P+Z	4.30,4.45
17	NAIF/P+Z2	4.45, 4.55	17	AREVA Adv Mark-BW	4.25, 4.40
18	AREVA Adv Mark-BW	4.25, 4.55	18	AREVA Adv Mark-BW	4.20, 4.40
19	AREVA Adv Mark-BW	4.50, 4.55	19	AREVA Adv Mark-BW	4.50, 4.55
20	AREVA Adv Mark-BW	4.45, 4.55	20	AREVA Adv Mark-BW	4.25, 4.50
21	AREVA Adv Mark-BW	4.39, 4.55	21	AREVA Adv Mark-BW	4.25, 4.45
22	AREVA Adv Mark-BW	4.55	22	AREVA Adv Mark-BW	4.25, 4.49
23	RFA-2	4.40, 3.66	23	RFA-2	3.81, 4.01, 4.45
24	RFA-2	4.55	24**	RFA-2	1.50, 4.30, 4.40
25	RFA-2	4.40, 4.55			

*Two fuel designs were loaded in Cycle 13 of Unit 1, NAIF/P+Z and an AREVA Adv Mark-BW lead test assembly.

**In the most recent completed cycle of Unit 2 (cycle 24) a fresh fuel assembly with 1.5 wt% U-235 and 7 stainless steel pins was used to help reduce the effect of baffle jetting.

4.2 Fuel Inserts Description

4.2.1 Burnable Absorbers

Four types of burnable absorbers have been used at North Anna: Pyrex, BPRA (Burnable Poison Rod Assembly), WABA (Wet Annular Burnable Absorber), and IFBA (Integral Fuel Burnable Absorber). The Pyrex burnable absorbers were used with the Standard fuel in the early cycles. The Pyrex burnable absorbers consist of an annulus of borosilicate glass with an inner and outer clad. When the fuel was changed to NAIF the burnable absorber was changed to BPRA which uses solid $Al_2O_3 - B_4C$ pellets. WABAs were introduced with the RFA fuel as part of a transition to IFBA. Table 4.4 provides the information needed to model the Pyrex, BPRA, and WABA burnable absorbers. Pyrex, BPRA, and WABA are composed of rods suspended from a baseplate that rests on the fuel assembly top nozzle. The rods are often referred to as "fingers." There are 24 locations (Guide Tubes) for the fingers. The number of fingers are part of the core design. The maximum number of Pyrex fingers was 20. The maximum number of BPRA and WABA fingers used is 24.

An IFBA rod is a fuel rod with a thin ZrB_2 coating on the surface of the fuel pellets. The pellets at the top and bottom 6 inches of an IFBA rod are annular to allow for more volume for the Helium created by the n,α reaction with the Boron. Table 4.5 provides IFBA data. Figure 4.2 provides the locations of the IFBA rods in the assembly. .

Table 4.4: Description of Fuel Inserts

Component	Design Characteristics
Pyrex Burnable absorber rods	
Inner Cladding	
Inner Diameter	0.1685 in (0.428 cm)
Outer Diameter	0.1815 in (0.4610 cm)
Inner Clad Material	SS-304
Tubing Glass	
Inner Diameter	0.1900 in (0.4826 cm)
Outer Diameter	0.3360 in (0.8534 cm)
Tubing Glass Material	Borosilicate glass
BP content, B_2O_3	12.5 w/o
B^{10} Linear Loading	6.25 mg/cm

Component	Design Characteristics
Outer Cladding	
Inner Diameter	0.3440 in (0.8738 cm)
Outer Diameter	0.3810 in (0.9677 cm)
Outer Clad Material	SS-304
BPRA (Al_2O_3-B_4C Pellets)	
Burnable Absorber Pellets	
Diameter	[ ]A
Pellet Material	Al_2O_3-B_4C
Maximum B^{10} Linear Loading	[ ]A
Cladding	
Inner Diameter	[ ]A
Outer Diameter	[ ]A
Outer Clad Material	[ ]A
WABA	
Inner Cladding	
Inner Diameter	0.2250 in (0.572 cm)
Outer Diameter	0.2670 in (0.6782 cm)
Inner Clad Material	Zircaloy-4
Absorber Pellet	
Inner Diameter	0.278 in (0.706 cm)
Outer Diameter	0.318 in (0.808 cm)
Absorber Material	Al_2O_3-B_4C
B^{10} Linear Loading	6.03 mg/cm
Outer Cladding	
Inner Diameter	0.3290 in (0.8357 cm)
Outer Diameter	0.3810 in (0.968 cm)
Outer Clad Material	Zircaloy-4
Control Rods	
Absorber Diameter top 130 inches	[ ]a,c
Absorber Diameter bottom 12 inches	[ ]a,c
Clad Inner Diameter (full length)	0.344 [ ]a,c (0.874 cm)
Clad Outer Diameter (full length)	0.381 [ ]a,c (0.968 cm)
Absorber Material	Ag(80 w/o)- In(15 w/o)- Cd(5 w/o)
Maximum Distance Between the End of the Absorber Material and the End of the Active Fuel	[ ]a,c
Vibration suppression damping assemblies (VSDA)	
Material	[ ]a,c
Outer Diameter	[ ]a,c

In-Core Instrument Thimble	
Thimble Inner Diameter	[ ]^{a,c}
Thimble Outer Diameter	[ ]^{a,c}
Thimble Material	Stainless Steel 316
Material inside Thimble	Helium

Table 4.5: Integral Fuel Burnable Absorber Data

Component	**Design Characteristics**
IFBA Loading 1.0x	0.00157 g/in (0.6181 mg/cm)
IFBA Loading 1.5x	0.00235 g/in (0.9252 mg/cm)
Thickness (1.5x)	0.0003125 in (0.0007938 cm)
IFBA Coating Length (centered in active fuel)	[ ]^{a,c}

[a,c]

4.2.2 Control Rods

Control rods are generally withdrawn during full power operation. The amount of control rod insertion is discussed in Section 8.9.2. Full length control rods can be used in a fuel assembly in order to place the fuel assembly in Region 2 when the fuel assembly does not meet the burnup requirements. A control rod has 24 fingers. When fully inserted, the control rod neutron absorber extends above the top of the active fuel, but can leave a maximum of [ ]^{a,c} of the bottom of the active fuel unpoisoned. At the bottom of the control rod is a [ ]^{a,c} end plug of stainless steel. Some of the historical control rods did not have the smaller diameter absorber at the end that was added to account for swelling; however, to be conservative it was assumed that all the control rods have the reduced diameter of absorber at the bottom [ ]^{a,c}.

Five part length control rods were part of the initial design for North Anna. There are 6 part length control rods in the North Anna spent fuel pool (from Unit 1 and a spare). Although part length control rods were installed in Unit 1 in the first cycle, based on core follow records, they were never used. No credit for the part length control rods is allowed in the criticality analysis.

4.2.3 Sources and Other Inserts

Primary and secondary neutron sources have been used at North Anna. These sources are contained in fingers attached to a baseplate similar to the burnable absorber rods, and sometimes in combination with burnable absorber rods. These source fingers displace water and affect the depletion. The outer diameter of the source rods is the same as the burnable absorbers and control rods, 0.381 inches. Since the source rods do not contain a strong absorber material, the impact of a source rod is less than a BPRA rod. Since this criticality analysis will not take credit for removing BPRAs, the source rods are conservatively covered by the BPRAs and no further information on the source rods is needed.

North Anna has employed Vibration Suppression Damping Assemblies (VSDA). These are solid Zircaloy 4 rods attached to a baseplate similar to burnable absorbers. These displace water and affect the depletion. However, these rods are also [ ]^{a,c} in diameter and are conservatively covered by the BPRA's used in the analysis.

Thimble plugs to reduce the bypass flow have been used at North Anna, but these do not hang down into the active fuel region and have no effect on criticality.

Prior to operation, thimbles for the incore flux monitoring are inserted into the instrument tubes of about one third of the fuel assemblies. Since these thimbles displace water they have a small effect on the depletion. Table 4.4 provides the dimensions of the thimbles.

4.3 Non-Standard Items in the Pool

There are a number of items in the spent fuel pool that are not fuel assemblies. If the item does not have fuel in it, it can be placed in any cell that is allowed to have fuel in it. The following is a current list of non-fuel items in the spent fuel pool (with the short designator):

- A Basket which stores debris from B&W equipment/products (B&WDBPAN)
- A Basket which stores ANF rod clips (CLB)
- A dummy assembly (DUM) which does not have any fuel.
- A Core sample can (SC1). Has not been used or moved in 16 years.
- A dummy assembly from Surry (SDM)
- A skeleton of the old AM2 fuel assembly (SKL)
- A basket for Tri-Nuc filters (TFB1)
- U1PINCAN and U2PINCAN: Baskets for the debris from the split pin replacement work. Note that "Split Pins" are Reactor Upper Internal Guide Tube Support Pins not fuel.
- Three upflow mod canisters (UFMCANA, UFMCANB, and UFMCANC)

There are also control rods that are suspended using cell blockers. These are allowed to be in the empty credited cells in Region 1.

There are two "Fuel Rod Storage Racks" that can contain fuel pins. Figure 4.3 is a picture of one of these baskets. These two Fuel Rod Storage Racks have [ ]^{a,c} stainless steel tubes that have a pitch of [ ]^{a,c}.

Over the years there have been fuel assemblies that have been damaged or reconstituted. The list of these fuel assemblies and where they can be placed in the spent fuel pool is found in Section 12.5.

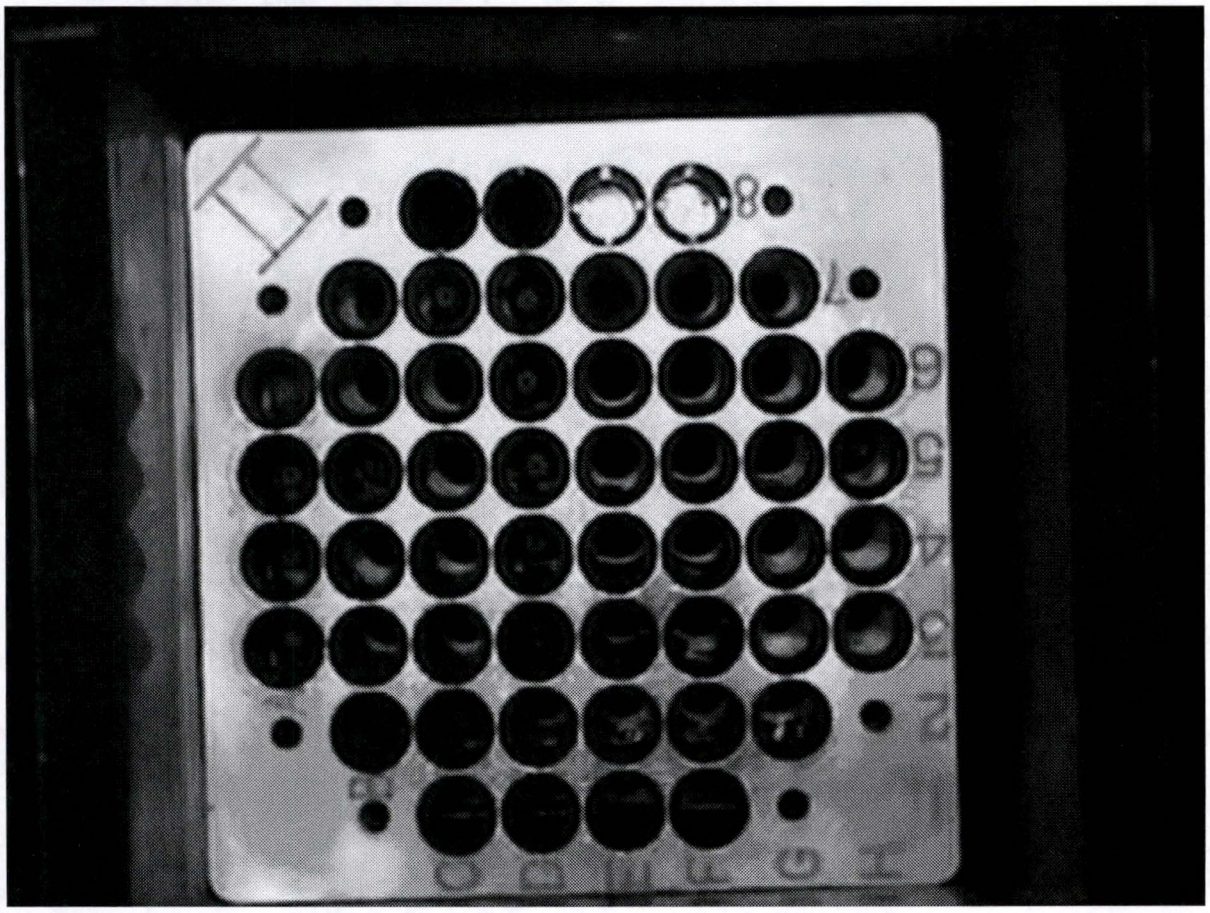

Figure 4.3: Fuel Rod Storage Rack

5 Overview of the Method of Analysis

The criticality analysis of the New Fuel Storage Area (NFSA) is performed assuming two accident conditions, fully flooded with water and optimum moderation. The analysis of the NFSA assumes the most reactive fuel at the highest enrichment (5 wt% U-235) and does not use any geometric restriction or credit for burnable absorbers. The analysis assumes each fuel assembly is located in the cell at its most reactive location (eccentricity built into the base case). All the analyses are for a full NFSA and the boundaries are extended to where zero flux boundary conditions are appropriate. The temperature of the water in the fully flooded cases is the most reactive, which was shown to be when water is most dense (277 K).

For the optimum moderation analysis a water temperature range of 273 K to 311 K (100 F) is used to cover the expected range of temperatures. (The density of the water and temperatures are not linked for this case since the water represents a foam.) The concrete composition, which is important to the optimum moderation cases, is conservatively determined. The validation of the criticality calculations for low moderator density is done by increasing the bias and uncertainty using a reasonable extrapolation needed for the harder neutron spectrum. The final determination of the 95/95 k includes uncertainties for manufacturing tolerances of both the fuel and rack calculated at both the full and optimum moderation. In order to cover the variation in zirconium alloys, pure zirconium is used in the analysis since it was determined that the alloying elements reduce reactivity.

The spent fuel storage rack analysis credits soluble boron, thus the criticality analysis shows k is less than 1.0 rather than 0.95 when the spent fuel pool has no soluble boron. Two configurations are analyzed:1) a checkerboard with empty cells, and 2) a fully loaded condition. A single limiting bounding fuel is used, but a bias is added for the variation in grid volume. For the checkerboard arrangement (labeled Region 1) no credit for burnup is required for even the maximum allowed enrichment (5 wt% U-235).

For the arrangement with all cells loaded (labeled Region 2), burnup credit is taken. A single loading curve (minimum burnup as a function of enrichment) is developed that covers the most reactive cooling condition. A second loading curve is developed for fuel cooled more than 3 years. No interpolation between the two curves is allowed. If an assembly does not meet the burnup requirements for Region 2, it is shown that it is acceptable to load in Region 2 if it

contains a control rod (even including unburned 5 wt% U-235 fuel). Although the racks have Boraflex absorber panels, no credit is taken for the Boraflex and no other fixed neutron absorbers are credited. No credit is taken for either the original or final content of any integral burnable absorbers except as part of a justification argument in Section 8.9.1.

The analysis is done using SCALE 6.0 and the ENDF/B-VII cross section library. [6] The criticality calculations are done with the CSAS5 module [7] and the depletion analysis is done with the t5-depl option of TRITON [8] which uses KENO-V.a for the flux calculations needed to collapse the cross sections spatially and in energy for the depletion. The TRITON depletion analysis is confirmed by comparison to CASMO (as well as the EPRI depletion benchmarks but no credit for the agreement is taken). [21, 22] The uncertainty in the depletion is covered by the 5% of delta k depletion allowed by DSS-ISG-2010 [4]. The rest of the validation is done consistent with the DSS-ISG-2010 and NUREG/CRs 6698 and 7109. [25, 28]

The limiting depletion conditions are determined by first selecting a fuel assembly average power that is bounding compared to the power an actual assembly could sustain from initial use through the fuel burnup being analyzed. The axial burnup profiles generated by the Department of Energy (DOE) database and reviewed in NUREG/CR-6801 [40] are used within their respective burnup ranges. With the fuel assembly power and the axial burnup profile known, the nodal moderator temperature is determined for each of the 18 axial nodes starting from the core inlet and integrating the enthalpy added in each successive node. The enthalpy calculation uses a bounding low moderator flow rate and an axial relative power shape that is the same as the axial relative burnup profile. Fuel temperatures likewise are determined by node using the nodal moderator temperature and fuel temperature difference from the moderator temperature which is dependent on the nodal fuel power. The fuel temperature data was taken from the SIMULATE data used by Dominion for its licensed fuel management analysis. [22] Fuel temperatures are pellet average, which bound the resonance effective fuel temperatures.

All isotopes produced during depletion are used in the analysis but there is a correction for fission gases and volatile elements.

Maximum grid volume is used in the depletion analysis and a bias is used for the minimum grid volume in the criticality calculations.

The depletion analysis assumes the burnable absorber that maximizes depleted fuel reactivity (24 finger BPRA) is in each assembly and is not withdrawn throughout the burnup. The analysis further determines the number of BPRA fingers that can be used with the maximum IFBA loading ([ ]^{a,c} with 1.5X loading) to match the reactivity effect of depleting with the 24 finger BPRAs.

North Anna normally operates with the control rods out at full power. The control rod history was reviewed to confirm the maximum historical average control rod insertion during at-power operation. Since the BPRA and control rods cannot both be in the guide tubes, the BPRA assumption covers the minimal control rod insertion history that exists (only 5% of the assemblies are under the control bank).

A bias to cover the maximum horizontal burnup distribution is calculated and used. Changes in the fuel geometry with depletion are included in the analysis. Specifically, grid growth as well as clad creep is included in the analysis.

Eccentric loading in the cells is done by determining the maximum number of co-located eccentric assemblies and then the analysis is performed with the co-located eccentric assemblies. Thus, this effect is handled as a bias rather than an uncertainty.

Since there is only one rack module design at North Anna, the interface analysis is simple. Further, since the region with the higher uncertainties is also the region with the highest calculated k, the uncertainty is at the interface, and therefore is determined using the largest uncertainty of either region.

The accident analysis is dominated by the multiple misload. In this analysis it is assumed that all assemblies in the pool are unburned 5 wt% U-235 and they are loaded in every cell. With credit for the technical specification minimum soluble boron, the 95/95 k is well below 0.95. An assembly misplacement and drop are analyzed and are considerably less limiting than the multiple misload. For a postulated boron dilution event, it is shown that the 95/95 k is much less than 0.95. Analysis for moderator temperatures up to and including boiling shows that in an over temperature accident the 95/95 k is much less than 0.95.

Analysis is performed for all normal operating conditions including movement, inspection, and reconstitution. All fuel-bearing containers in the North Anna spent fuel pool are identified and analyzed to determine the limitations on location in the pool.

6 Cross Sections, Computer Codes, and Validation

6.1 Cross Sections and Computer Codes

This analysis uses the CSAS5 [7] module of SCALE 6.0 [6] for the rack k analysis and the t5-depl TRITON [8] module for the depletion analysis. These analyses are performed using the 238 group ENDF/B-VII cross section library (v7-238).

6.1.1 CSAS5

The CSAS5 module uses the BONAMI code to provide resonance corrected cross sections in the unresolved resonance range and computer codes WORKER, CENTRM, and PMC to provide resonance-corrected cross sections in the resolved resonance range. This is followed by KENO V.a, which uses the processed cross sections to calculate the k* of three dimensional system models. Most of the CSAS5 computer runs use a Monte Carlo sampling of at least 3000 generations and 12000 neutrons per generation to achieve a statistical uncertainty in k of less than 0.00016.

Unless otherwise specified, all of the k values reported in this document are raw calculated k values with no adjustment for bias and uncertainty. The final values to be compared to the criticality criteria are the calculated values plus the total bias and uncertainty (notated as "$k_{95/95}$").

It was assumed that the initial source distribution was uniform in fissile material for the k calculations (the default option in CSAS5).

Due to the large number of generations, neutrons per generation, and generation skipped, convergence is not a major concern. k convergence of KENO cases was verified by checking for satisfaction of the chi-squared test for normality at the 95% level in the log file and by looking for excessive variation or trend in the k versus generation plot from the KENO output file edit. Cases which failed the screening were either rerun with additional generations and generations skipped, or were shown to be non-limiting or otherwise non applicable cases.

* Throughout this document, k is used as a short hand notation for k-effective or k_{eff}

Table 6.1 shows the 251 isotopes used for the fuel in the criticality analysis. Depending on the burnup, some of these isotopes had insignificant atom densities and were not placed in the output file by SCALE. For some analyses, where less precision is needed, the isotope set was reduced to the 28 isotopes plus oxygen specified in Table 3.1 of NUREG/CR-7108. [20]

Table 6.1: Isotopes Used in the Criticality Analysis

^{16}O	^{69}Ga	^{71}Ga	^{70}Ge	^{72}Ge	^{73}Ge	^{74}Ge	^{76}Ge	^{74}As	^{75}As
^{74}Se	^{76}Se	^{77}Se	^{78}Se	^{79}Se	^{80}Se	^{82}Se	^{79}Br	^{81}Br	^{80}Kr
^{82}Kr	^{83}Kr	^{84}Kr	^{85}Kr	^{86}Kr	^{85}Rb	^{86}Rb	^{87}Rb	^{84}Sr	^{86}Sr
^{87}Sr	^{88}Sr	^{89}Sr	^{90}Sr	^{89}Y	^{90}Y	^{91}Y	^{90}Zr	^{91}Zr	^{92}Zr
^{93}Zr	^{94}Zr	^{95}Zr	^{96}Zr	^{93}Nb	^{94}Nb	^{95}Nb	^{94}Mo	^{95}Mo	^{96}Mo
^{97}Mo	^{98}Mo	^{99}Mo	^{100}Mo	^{99}Tc	^{98}Ru	^{99}Ru	^{100}Ru	^{101}Ru	^{102}Ru
^{103}Ru	^{104}Ru	^{106}Ru	^{103}Rh	^{105}Rh	^{102}Pd	^{104}Pd	^{105}Pd	^{106}Pd	^{107}Pd
^{108}Pd	^{110}Pd	^{107}Ag	^{109}Ag	^{110m}Ag	^{111}Ag	^{108}Cd	^{110}Cd	^{111}Cd	^{112}Cd
^{113}Cd	^{114}Cd	^{115m}Cd	^{116}Cd	^{113}In	^{115}In	^{114}Sn	^{115}Sn	^{116}Sn	^{117}Sn
^{118}Sn	^{119}Sn	^{120}Sn	^{122}Sn	^{123}Sn	^{124}Sn	^{125}Sn	^{126}Sn	^{121}Sb	^{123}Sb
^{124}Sb	^{125}Sb	^{126}Sb	^{122}Te	^{123}Te	^{124}Te	^{125}Te	^{126}Te	^{127m}Te	^{128}Te
^{129m}Te	^{130}Te	^{132}Te	^{127}I	^{129}I	^{130}I	^{131}I	^{135}I	^{126}Xe	^{128}Xe
^{129}Xe	^{130}Xe	^{131}Xe	^{132}Xe	^{133}Xe	^{134}Xe	^{135}Xe	^{136}Xe	^{133}Cs	^{134}Cs
^{135}Cs	^{136}Cs	^{137}Cs	^{132}Ba	^{133}Ba	^{134}Ba	^{135}Ba	^{136}Ba	^{137}Ba	^{138}Ba
^{140}Ba	^{138}La	^{139}La	^{140}La	^{138}Ce	^{139}Ce	^{140}Ce	^{141}Ce	^{142}Ce	^{143}Ce
^{144}Ce	^{141}Pr	^{142}Pr	^{143}Pr	^{142}Nd	^{143}Nd	^{144}Nd	^{145}Nd	^{146}Nd	^{147}Nd
^{148}Nd	^{150}Nd	^{147}Pm	^{148}Pm	^{148m}Pm	^{149}Pm	^{151}Pm	^{147}Sm	^{148}Sm	^{149}Sm
^{150}Sm	^{151}Sm	^{152}Sm	^{153}Sm	^{154}Sm	^{151}Eu	^{152}Eu	^{153}Eu	^{154}Eu	^{155}Eu
^{156}Eu	^{157}Eu	^{152}Gd	^{153}Gd	^{154}Gd	^{155}Gd	^{156}Gd	^{157}Gd	^{158}Gd	^{160}Gd
^{159}Tb	^{160}Tb	^{158}Dy	^{160}Dy	^{161}Dy	^{162}Dy	^{163}Dy	^{164}Dy	^{165}Ho	^{166m}Ho
^{164}Er	^{166}Er	^{167}Er	^{168}Er	^{170}Er	^{208}Pb	^{228}Th	^{229}Th	^{230}Th	^{232}Th
^{234}Th	^{231}Pa	^{233}Pa	^{232}U	^{233}U	^{234}U	^{235}U	^{236}U	^{237}U	^{238}U
^{235}Np	^{236}Np	^{237}Np	^{238}Np	^{239}Np	^{236}Pu	^{237}Pu	^{238}Pu	^{239}Pu	^{240}Pu
^{241}Pu	^{242}Pu	^{244}Pu	^{241}Am	^{242}Am	^{242m}Am	^{243}Am	^{244}Am	^{241}Cm	^{242}Cm
^{243}Cm	^{244}Cm	^{245}Cm	^{246}Cm	^{247}Cm	^{248}Cm	^{249}Bk	^{249}Cf	^{250}Cf	^{251}Cf
^{252}Cf									

The densities for the isotopic atoms listed above are directly from the initial fuel content or the depletion analysis except for an adjustment for gaseous or volatile fission products (hereafter called fission gases). Table 6.2 lists the fission gases used in the criticality analysis. Two of the isotopes, Cs-133 and Xe-131, are about 80% of the reactivity worth of the fission gases. The treatment of the fission gases for this criticality analysis is the same as was done for the recently

approved Millstone 2 criticality analysis [9] and the key elements of the position are repeated here.

Table 6.2: Fission Product Gases and Volatiles

Noble Gases	^{80}Kr, ^{82}Kr, ^{83}Kr, ^{84}Kr, ^{85}Kr, ^{86}Kr ^{126}Xe, ^{128}Xe, ^{129}Xe, ^{130}Xe, **^{131}Xe**, ^{132}Xe, ^{133}Xe, ^{134}Xe, ^{135}Xe, ^{136}Xe
Alkali Metals	^{85}Rb, ^{86}Rb, ^{87}Rb **^{133}Cs**, ^{134}Cs, ^{135}Cs, ^{136}Cs, ^{137}Cs
Halogens	^{79}Br, ^{81}Br ^{127}I, ^{129}I, ^{130}I, ^{131}I, ^{135}I

Most of the fission gases remain in the active fuel near where they were created. The mobility of fission gases is important in assessing the consequences of reactor accidents. There is data on fission gas release that has been reviewed and approved by the NRC. Regulatory Guide (RG) 1.183 provides conservative release fractions for fission gases. [10]

It is expected that RG 1.183 will be updated to reflect higher linear powers than were used in developing the current limits. PNNL-18212 Rev. 1, "Update of Gap Release Fractions for Non-LOCA Events Utilizing the Revised ANS 5.4 Standard," which was completed in June 2011, provides a new analysis. [11] Table 2.9 of PNNL-18212 provides new limiting release rates. PNNL-18212, Appendix C also provides an example of calculated release rates when the linear power is known. Using the North Anna assembly average peaking factors (see Section 8.2) and the average linear heat rate of 5.9 kw/ft (See Section 8.4 for operating power), it is clear that the Appendix C example release rates are representative for North Anna.

Table 6.3 shows the fission gas release fractions from the current revision of RG 1.183, the PNNL-18212 recommended change to RG 1.183, the PNNL-18212 plant dependent release rate from Appendix C, and the release rate assumed for the North Anna criticality analysis (the same as was used for Millstone Unit 2 [9]). As shown in Table 6.3, the fission gas release fraction selected is generous compared to Appendix C of PNNL-18212 and is more bounding than the current revision of RG 1.183 (note that I-131 is low worth).

Table 6.3: Fission Gas Release Fractions

Isotopes	Current RG 1.183	Bounding Proposed in PNNL-18212	Appendix C of PNNL-18212	Implemented in North Anna Criticality Analysis
Kr-85	0.10	0.38	0.13	0.20
I-131	0.08	0.08	0.02	0.05
Other Nobles Gases	0.05	0.08	0.02	0.05
Other Halogens	0.05	0.05	0.01	0.05
Alkali Metals	0.12	0.50	0.16	0.20

The release rates for PNNL-18212 assume cladding breach. For the criticality analysis the concern is for the fission products moving into the plenum and therefore no longer acting as effective absorbers. The boiling point of Cesium (951 K) is much higher than the clad temperature during normal fuel use (boiling point of water at 2250 psia is 618 K). It is unlikely that a significant amount of Cesium can migrate away from the fuel due to the clad acting as a condensing surface. This contention is supported by a couple of observations. It is common to use Cs-137 as a measure of burnup. The agreement between Cs-137 and Nd-148 as a burnup measurement for chemical assays has been generally good [13-17] Also, the BNFL burnup measurement device which is based on Cs-137 has agreed well with the reactor record burnup. [18] For this analysis it is assumed that 20% of the Cs-133 is lost, and Cs-133 is about a third of the worth of the fission gases. Therefore, the fission gas loss assumptions are conservative.

6.1.2 TRITON

The t5-depl sequence of SCALE's TRITON [8] enables depletion calculations to be performed by coordinating iterative calls between cross-section processing codes (CENTRM and BONAMI), KENO-V.a, and the ORIGEN-S point-depletion code. A 2D KENO model of the fuel assembly in the core provides the flux distribution needed to collapse the cross sections spatially and in energy for the ORIGEN-S depletion calculations. All the fuel pins are treated as a single depletion material. For this analysis each KENO calculation uses 3000 generations and 3000 neutrons per generation. Past analysis have shown that fewer neutron histories than this provide adequate convergence, [9, 19] however; to confirm this a depletion was run with 6000 neutrons per generation (same number of generations) showing agreement on the assembly k for each depletion step to within the Monte Carlo uncertainty.

The analysis employed the TRITON parameter addnux=3 to maximize the number of isotopes included in the analysis. The spent fuel reactivity was maximized by using the isotopic content after five days of decay. Other than removing light elements (less than oxygen) the set of isotopes (shown on Table 6.1) is taken directly from the TRITON output.

It is important that the depletion time steps are short enough to assure convergence. For this analysis time steps of 10, 40, 50, 50, and 50 days are used for the low burnups. The time steps for the rest of the calculations are uniform to meet the desired burnup. The "nlib" is set so that all the remaining time steps are less than 70 days. These time step sizes were used previously for Millstone 2 and were shown by analysis of various time steps to be converged, [9] however; to confirm that the time steps were sufficiently small for North Anna, a case (2.5 wt% U-235 at 10 GWd/MTU) was run with time steps half the normal size and the agreement on k in the rack was within the Monte Carlo uncertainty.

The reactivity after discharge changes fairly rapidly in the first few days due to the decay of short half life isotopes such as Xe-135. For Millstone 2 [9] an analysis was performed that showed the peak reactivity occurs at 5 days (100 hour results were statistically the same as 5 days). A 5 day cooling is selected for the peak reactivity for the North Anna analysis. This was confirmed with the analysis provided in Table 6.4.

Table 6.4: Confirming Peak Reactivity at 5 Days Cooling

Enrichment (wt% U-235)	Boron (ppm)	Burnup (GWd/MTU)	Decay Days	Calculated k	Uncertainty
3.0	0	20	4	0.9409	0.00008
3.0	0	20	5	0.9411	0.00008
3.0	0	20	6	0.9410	0.00008
3.0	0	20	7	0.9410	0.00008
3.0	0	20	10	0.9407	0.00008
3.0	0	20	20	0.9407	0.00008
3.0	0	20	50	0.9406	0.00008

6.2 Validation of Isotopic Content (Depletion Analysis)

The validation of isotopic content (depletion analysis) is difficult due to a limited amount of measured data. The NRC has sponsored research at Oak Ridge National Laboratory (ORNL) to determine a bias and uncertainty using chemical assay data. [20] EPRI uses power distribution data to infer a bias and uncertainty as a function of burnup. [19, 21] At the time of this submittal the NRC's interim staff guidance, DSS-ISG-2010-01 [4], allows using the historical estimate of 5% of the depletion reactivity for the uncertainty and a zero bias. The zero bias is supported by the ORNL chemical assay work [20] and most of the cases in the EPRI analysis [19] when using SCALE and the 238 group ENDF/B-VII cross sections as is done for this analysis.

A depletion reactivity uncertainty of 5% has been supported based on a conservative estimate of the state of the art of fuel management analysis computer codes. Since SCALE has not been used for fuel management, a study has been performed to compare the delta k depletion predicted using the TRITON t5-depl sequence of SCALE to North Anna's licensed fuel management code, CASMO-4, as well as CASMO-5. [22] The study shows that using TRITON atom densities is more conservative than using CASMO atom densities. Similar results were found when CASMO was compared to TRITON for Millstone 2. [9] Section 6.2.1 describes the analysis.

6.2.1 Comparison of CASMO and TRITON Depletion Reactivity

To confirm that TRITON is acceptable for depletion analysis for North Anna, representative comparisons are provided for North Anna (17x17 fuel assembly) Region 2 (all cells loaded) fuel rack k using TRITON, CASMO-4 and CASMO-5 to generate depleted fuel isotopic content. The same conservative depletion conditions were used in all 3 codes, including 24 BPRA, 1100 ppm soluble boron, and high moderator and fuel temperature. A single node (Node 15; nodes run from 1 at the bottom of fuel to 18 at the top) was used as a reasonable representation of the fuel for this comparison. No grids were used in the depletion models for simplicity. Two enrichment and burnup combinations representing the lowest and highest burnup credit requirement for Region 2 are modeled. Conservative depletion conditions consistent with this critical analysis were used (ie: 1100 ppm, 24 BPRA, bounding high moderator and fuel temperatures).

For CASMO-4, isotopes common to both CASMO-4 and TRITON (49 nuclides) were used in the KENO rack models. CASMO-5 [60] has no lumped fission products, so all nuclides available in the SCALE standard composition library were retained. All depletions end with 5 days decay after shutdown. CASMO-4 has been reviewed and approved by the NRC for use in North Anna core design calculations, calculation of key core parameters, and core follow [22]. CASMO-5 has previously been used as part of the Millstone Unit 2 spent fuel pool criticality License Amendment Request. [9]

Results of the KENO Region 2 fuel rack k cases are provided in Table 6.5. For 2.45 w/o fuel depleted to 10 GWd/MTU and 49 nuclides (all CASMO-4 nuclides available in both CASMO and SCALE), the TRITON depletion produces a fuel rack k approximately 0.008 Δk higher than CASMO-4, and 0.0018 higher than the CASMO-5 depletion. With all available nuclides included, the TRITON case fuel rack k is higher than the CASMO-5 case by 0.00035 Δk.

For 5.0 w/o fuel depleted to 44 GWd/MTU and 49 nuclides, the TRITON depletion produces a fuel rack k approximately 0.015 Δk higher than the equivalent CASMO-4 depletion. With all available nuclides included, the TRITON case fuel rack k is higher than the CASMO-5 case by 0.0014 Δk.

Table 6.5 results show that depletion with TRITON produces the highest rack k as compared to depletion with CASMO-4 and CASMO-5. TRITON results are much closer to CASMO-5 results, probably because CASMO-5 and TRITON use ENDF/B-VII cross sections and CASMO-4 uses an earlier cross section set. Use of the older CASMO-4 cross section data to produce isotopic content that is then used in a KENO rack model with newer (ENDF/B-VII) cross section data creates a potential mismatch that may explain some of the large difference in fuel rack k results between TRITON and CASMO-4.

Table 6.5: Comparison of CASMO and TRITON Depletion Worth

Enrich. (U235 w/o)	Number of Nuclides	Burnup (GWd/MTU)	Depletion Code	Calculated Rack k	Monte Carlo Sigma	Burnup Worth (Δk)
2.45	N/A	0	N/A	1.025768	0.000059	N/A
2.45	49	10	TRITON	0.957684	0.000056	0.0681
2.45	49	10	CASMO4	0.949563	0.000053	0.0762
2.45	49	10	CASMO5	0.955930	0.000054	0.0698
2.45	ALL	10	TRITON	0.951871	0.000053	0.0739
2.45	ALL*	10	CASMO5	0.951523	0.000056	0.0742
5.0	N/A	0	N/A	1.190491	0.000064	N/A
5.0	49	44	TRITON	0.930972	0.000055	0.2595
5.0	49	44	CASMO4	0.916284	0.000053	0.2742
5.0	ALL	44	TRITON	0.914146	0.000052	0.2763
5.0	ALL*	44	CASMO5	0.912796	0.000054	0.2777

*Some minor nuclides not in SCALE 6.0 library

6.3 Validation of Criticality Analysis

Criticality computer codes and cross sections must be validated for their ability to predict k. The criticality validation must attempt to best match the North Anna racks for isotopic content, spectrum and geometry. A perfect match however is never possible with a large but limited set of critical experiments.

Due to isotopic limitations in the critical experiments the validation is done in two steps. The first step is to use laboratory critical experiments to validate the structural materials and major actinides in a variety of geometries which produce a range of neutron spectra. The second step is to validate the minor actinides and fission products. Since there is little to no use of these isotopes in critical experiments, this validation is based on the uncertainty in the cross section measurement.

6.3.1 Major Actinides and Structural Materials

The validation for the major actinides and structural materials follows NUREG/CR-6698 [25]. Three hundred twenty one (321) critical experiments were selected from the OECD/NEA handbook [26] and the HTC critical experiments [27] that match the conditions of the North Anna new fuel storage area and spent fuel pool. These experiments were analyzed with SCALE 6.0 using the 238-group ENDF/B-VII cross-section library. The resulting predicted k's

were then fit for trends on the key parameters influencing k. Using these trends, the most limiting bias and uncertainty in the area of applicability was determined. Although some of the trends may not be statistically significant, it is conservative to use all of the trends in determining the limiting bias and uncertainty. Table A.6.1 is the area of applicability for the validation. The North Anna spent fuel pool is covered by the area of applicability of the validation. Specifically,

1. Enrichment: The benchmarks selected range from 2.35 to 4.74 wt% U-235. The fuel in the spent fuel pool ranges from 1.5 to 5 wt% U-235. The bias decreases with enrichment and the slope is small allowing for a small extrapolation for higher enrichments. For the low enrichments the extrapolated bias and uncertainty is acceptable since the single 1.5 wt% assembly and the 2.1 wt% assemblies from the first core all have burnups well in excess of the burnup requirements.

2. Spectrum: The benchmarks cover a wide range of spectrum by varying the pin pitch. The Energy of the Average Lethargy causing Fission (EALF) of the benchmarks ranges from 0.0605 to 0.8432 eV. This covers the range of spectrum in borated and non-borated conditions in the spent fuel pool and the full moderated condition in the new fuel storage area. Some extrapolation is required for the optimum moderator condition in the new fuel storage area.

3. Fuel Pin Pitch: The fuel pin pitch of the benchmarks ranges from 1.075 to 2.54 cm. The North Anna fuel pin pitch is 1.26 cm.

4. Assembly Spacing: The benchmarks include spacing between assemblies of 0 to 15.4 cm of water. The spent fuel pool average spacing between the outside of the assemblies is 5.4 cm. The NFSA has a separation 31.9 cm but neutron transport through >15.4 cm of water has small affect on k. If the water has decreased density, then the separation effectively decreases. Therefore, the NFSA optimum moderation cases are covered.

5. Boron Areal Density: North Anna does not use absorber panels so no critical experiments which used boron absorber panels were selected. Cd containing experiments were included to cover credited control rods.

6. Soluble Boron: The benchmarks have soluble boron concentrations up to 5030 ppm. The soluble boron credited to meet k less than 0.95 and credited for the accident analysis is well within the range of experiments.

Details on the area of applicability can be found in Appendix A.

For the spent fuel pool, the bias and uncertainty depends on the burnup since at low burnup the dominant fissile material is U-235 and at high burnup the dominant fissile material is Pu-239. In order to avoid trying to properly weight the critical experiments for the amount of U-235 and Pu-239, two sets of bias and uncertainty are employed; one from the fresh UO_2 critical experiments and one from the MOX critical experiments. The final bias and uncertainty employed is that which produces the highest 95/95 k.

The UO_2 critical experiments have a higher bias but lower uncertainty than the MOX experiments. Since the uncertainty is statistically combined with other uncertainties it is not possible to determine which set is more limiting until the other uncertainties due to factors such as manufacturing tolerances are determined. The UO_2 based bias and uncertainty for most cases is 0.0035 and 0.0050 respectively. This set of UO_2 based bias and uncertainty is limited to a maximum EALF of 0.4 eV which covers all but the borated cases. For cases with an EALF greater than 0.4 but less than 0.8, the UO_2 bias is 0.0060 and uncertainty 0.0060. Simultaneously, the analysis must be performed using the MOX bias and uncertainty. For EALF up to 0.4 eV the MOX bias and uncertainty is 0.0020 and 0.0089 respectively. For the harder spectra, 0.4 to 0.8 eV, the MOX based bias and uncertainty is 0.0034 and 0.0135 respectively. Table 6.6 summaries this paragraph.

Table 6.6: Summary of Validation Bias and Uncertainty from Major Actinides and Structural Materials

	EALF Range (eV)	UO_2	MOX
Bias			
	< 0.4	0.0035	0.0020
	0.4 – 0.8	0.0060	0.0034
	0.8 – 1.1	0.0070	
Uncertainty			
	< 0.4	0.0050	0.0089
	0.4 – 0.8	0.0060	0.0135
	0.8 – 1.1	0.0063	

For unburned fuel in the spent fuel pool the UO_2 set from Table 6.6 is used. For depleted fuel calculations, both bias and uncertainty sets (UO_2 and MOX) are considered, The set used is the one that provides the highest 95/95 k.

For the new fuel storage area in the fully flooded condition, the UO_2 set from Table 6.6 is used. For the optimum moderation case, the EALF can be higher. Extrapolation of the measured critical experiments is required. The range of the EALF in the criticality data is 0.06 to 0.84 eV. The optimum moderation case requires a bias and uncertainty for 1.1 eV. The extrapolation needed is only a third of the range. The bias and uncertainty from extrapolation to 1.1 eV are 0.0070 and 0.0063, respectively.

6.3.2 Minor Actinides and Fission Products

Since there are few to no critical experiments that contain some of the isotopes used in this criticality evaluation, validation is done by estimating the maximum error in k due to cross section measurement uncertainty. NUREG-7109 has shown that applying a bias of 1.5% of the worth of the minor actinides and fission products conservatively accounts for both the bias and uncertainty due to the minor actinides and fission products. [28] NUREG-7109 mainly addresses the 28 highest worth isotopes, but on the last sentence of page 106 indicates, "An upper value of 1.5% of the worth is also applicable for SNF isotopic compositions consisting of all nuclides in the SFP configuration." NUREG-7109 limits the applicability to certain cross section sets, but ENDF/B-VII used here is one of those sets. The use of the 1.5% is part of the NRC's transport division in ISG-8 Rev.3. [29]

The minor actinides are defined as actinides not contained in the criticality validation benchmarks. Table 6.1 lists all the isotopes used in the analysis. The major actinides are U-234, U-235, U-238, Pu-238, Pu-239, Pu-240, Pu-241, Pu-242, and Am-241. U-236 is not a major actinide although it has a significant worth in spent fuel. Am-241 is a major actinide since it decays from Pu-241 after the MOX pins were made for MOX critical experiments.

The fission products used are listed on Table 6.1. Pb-208 is neither a fission product nor an actinide, but is included in the analysis of burned fuel. Its atom density is extremely small with no real impact on the criticality analysis. It is treated as a fission product.

6.3.3 Temperature Dependence

All of the critical experiments utilized in Section 6.3.1 were done at room temperature. There is one set of critical experiments which were run as a function of temperature in the range of interest for spent fuel pools. There are a couple of sets of experiments with temperatures greater than 200 C [37, 38], but LEU-COMP-THERM-046 [39] is ideal for determining a bias as a function of temperature in the range of interest. LEU-COMP-THERM-046 is not used in the set of experiments from Section 6.3.1 since in general they are at elevated temperatures and as such represent a unique set. The analysis of this temperature dependent set is detailed in Appendix A, Section 8.

The analysis of the only set of thermal critical experiments in the International Handbook that uses elevated temperatures has shown a small increase in the bias with temperature. This increase can be conservatively handled by a bias from room temperature (293K) of 1.7E-05 $\Delta k/\Delta^{\circ}C$.

7 Criticality Safety Analysis of the New Fuel Storage Area

7.1 New Fuel Storage Area KENO Model

The description of the New Fuel Storage Area (NFSA) is given in Section 3.1. The SCALE CSAS5 (KENO) model for the NFSA is a three dimensional model of the entire rack including the concrete walls and floor. Table 3.1 provides the dimensions and tolerances. The fuel that can be placed in the NFSA is given on Table 4.1. The clad is modeled as pure zirconium. The maximum inner diameter and the minimum outer diameter of the design is used to model the guide tubes. The grids are conservatively ignored. The fuel tolerances are given on Table 4.2. The fuel is assumed to have the maximum enrichment of 5 wt% U-235 and a stack density (density after homogenizing the dishing and chamfering) of 95.5% of the UO2 theoretical density. The fuel assemblies are positioned asymmetrically in the cells to maximize the reactivity.

Figure 7.1 shows the axial representation of the NFSA model. This should be compared to the actual rack shown on Figure 3.3. The key simplification is the area above the active fuel. The cell walls are assumed to be straight rather than flare out at the top. The steel I beams, steel plates at the top of the rack, and the cell lids are conservatively ignored. Except for the cell wall, the area above the active fuel is assumed to be water at the same density, as throughout the rack. The top and bottom nozzles are also modeled as water.

Figure 7.2 shows a view of the NFSA KENO model from the top. The concrete walls have been cut back in this figure to allow more rack features to be seen. (In a following section on concrete the extent of the concrete walls are presented.)

Unless otherwise noted, each of the KENO cases run use 3000 generations, 12000 neutrons per generation, and skips at least 100 generations. The initial source distribution of neutrons was uniform in the fuel. Void boundary conditions are used on the six sides of the model.

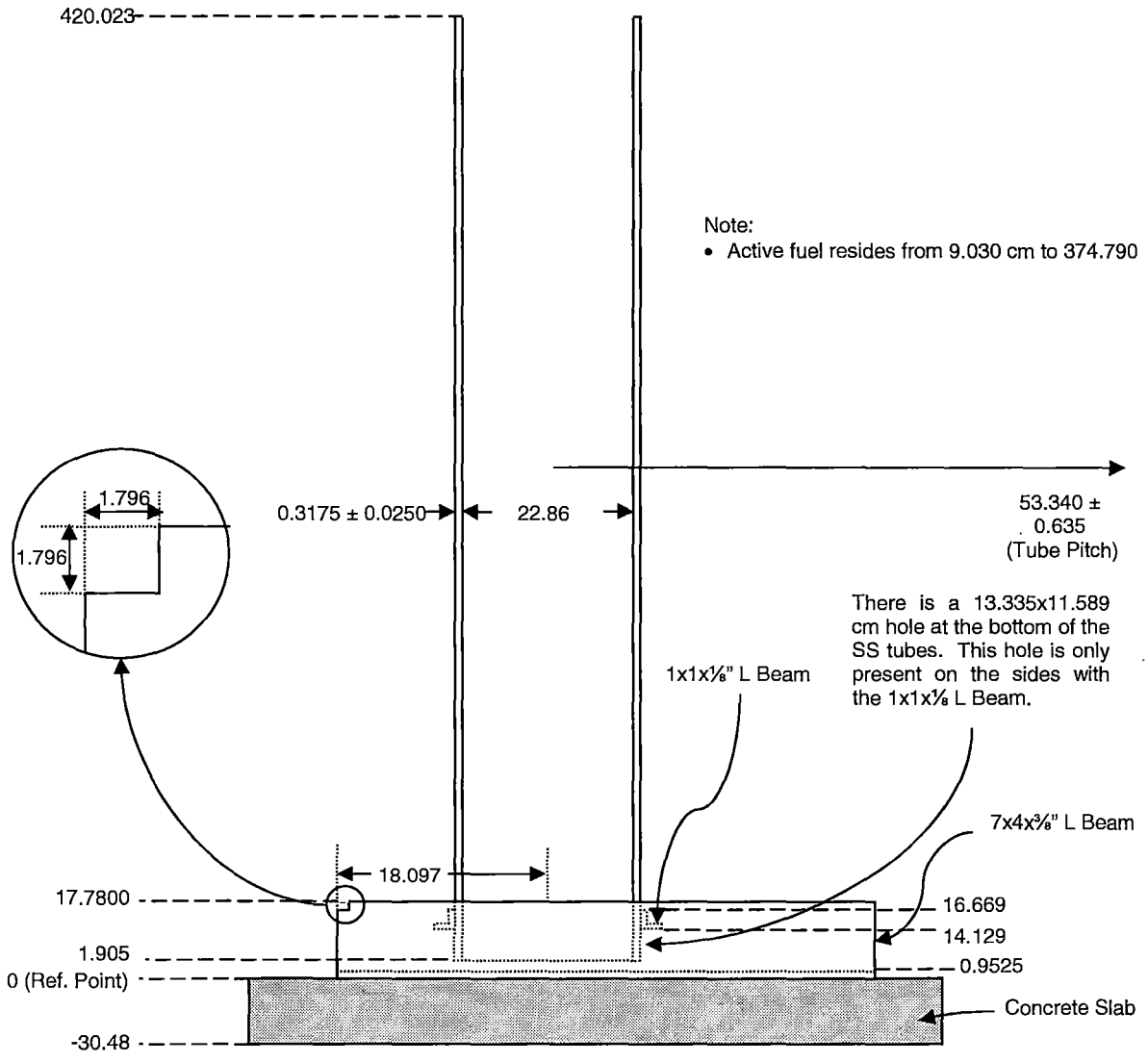

Figure 7.1: Axial representation of the New Fuel Storage Area Model

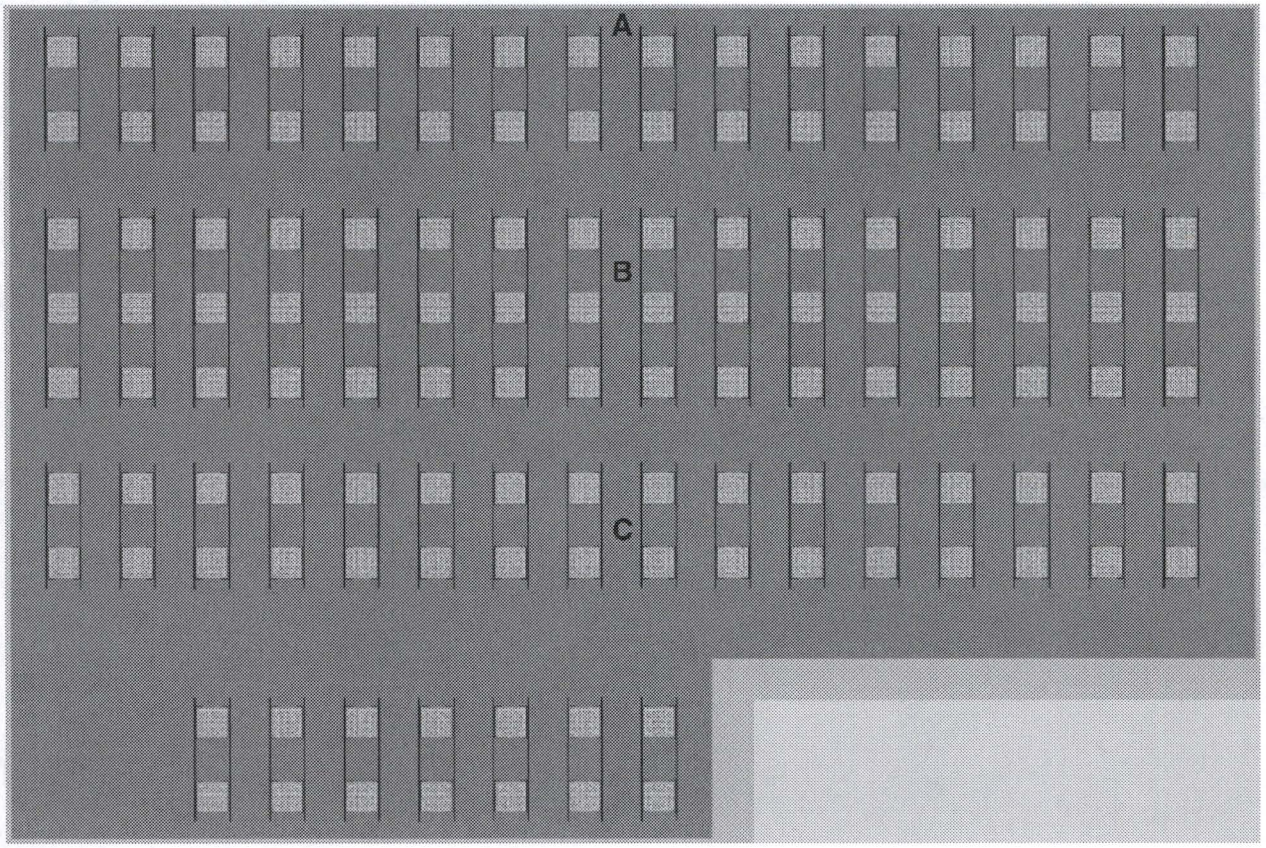

Figure 7.2: Top View of the New Fuel Storage Area Model

The following subsections describe model confirmation calculations.

7.1.1 Zirconium Alloys

Throughout the history of North Anna, the following four zirconium alloys have been used in the cladding and grids: Zircaloy-4, ZIRLO, Optimized ZIRLO, and M5. Sensitivity cases have been performed to discover if there is a significant difference between the zirconium alloys with respect to the k of the NFSA.

Table 7.1 shows that the alloying elements decrease k. To allow for future cladding changes, pure zirconium is used for the clad.

Table 7.1: Sensitivity of k to Various Zirconium Alloys

Case Description	k-eff	σ	Δk	Δk/rss(σ)	k-eff	σ	Δk	Δk/rss(σ)
	Water Density 1 gm/cc				Water Density 0.0625 gm/cc			
Zirconium	0.9034	0.00005	N/A	N/A	0.9440	0.00004	N/A	N/A
Zircaloy-4	0.9032	0.00014	-0.0002	-114%	0.9435	0.00013	-0.0005	-376%
ZIRLO	0.9027	0.00015	-0.0006	-405%	0.9431	0.00013	-0.0009	-663%
Optimized ZIRLO	0.9029	0.00014	-0.0005	-323%	0.9431	0.00012	-0.0009	-713%
M5 Alloy	0.9028	0.00015	-0.0006	-380%	0.9433	0.00013	-0.0007	-546%

7.1.2 Conservative Guide and Instrument Tubes

The instrument and guide tube design varies with different fuel types. To quantify the effect that this design input has on the k of the NFSA, sensitivity cases were run. The dimensions of the guide and instrumentation tubes are given in Table 4.1. Adding more zirconium in the active fuel region generally decreases k-eff. Therefore, to bound potential future fuel types, a hypothetical thin tube design was tested (labeled "Hypothetical Thin Walled Tube" in Table 7.2). This hypothetical design took the largest inner diameter (1.143 cm) and smallest outer diameter (1.204 cm) of the fuel designs to obtain a bounding tube wall.

Table 7.2: Sensitivity of k to Various Guide Tube Designs

Fuel Type	k-eff	σ	Δk	Δk/rss(σ)	k-eff	σ	Δk	Δk/rss(σ)
	Water Density 1 gm/cc				Water Density 0.0625 gm/cc			
Hypothetical Thin Walled Tube	0.9034	0.00005	N/A	N/A	0.9440	0.00004	N/A	N/A
Standard and AREVA	0.9022	0.00015	-0.0012	-729%	0.9437	0.00012	-0.0004	-294%
NAIF	0.9021	0.00014	-0.0012	-836%	0.9438	0.00013	-0.0002	-171%
RFA	0.9005	0.00015	-0.0029	-1834%	0.9436	0.00013	-0.0004	-281%

Table 7.2 shows that the Hypothetical Thin Walled Tube results in the largest k for both the optimum moderation and full density water scenarios. Therefore, this analysis uses the hypothetical instrument and guide tube design to calculate the maximum k of the NFSA.

7.1.3 Grids

To simplify the model of the fuel assembly, the grids will be ignored. Section 7.1.2 (Instrument and Guide Tubes) varies the thickness of the instrument and guide tubes to measure the reactivity affect. It was determined that the thinnest instrument and guide tube walls resulted in the largest k. In other words, the least amount of cladding within the fuel lattice yielded the most conservative case. Therefore, modeling no grids in the North Anna NFSA is conservative.

7.1.4 Fuel Hardware Above and Below the Active Fuel

The top assembly reflector is defined here as the material within the assembly radial profile that is between the active fuel and the top of the assembly. The bottom assembly reflector is defined as the material within the assembly radial profile that is between the bottom of the active fuel and the bottom of the assembly. The top and bottom reflector designs have changed more frequently than the active fuel region, but generally have no affect on the criticality analysis. To confirm this several of the top and bottom designs are tested. Tables 7.3a and 7.3b provide the volume fractions of the top and bottom hardware, respectively.

Table 7.3a: Top Assembly Reflector Volume Fractions

Parameter	Design 1	Design 2	Design 3
Stainless Steel	6%	10%	7%
Cladding	7%	7%	7%
Helium	18%	14%	17%
Water	68%	68%	68%
Inconel	1%	1%	1%

Table 7.3b: Bottom Assembly Reflector Volume Fractions

Parameter	Design 1	Design 2	Design 3
Stainless Steel	17%	13%	18%
Cladding	10%	7%	10%
Water	71%	80%	71%
Inconel	1%	0%	1%

Table 7.4 shows that replacing the bottom nozzle with water at the optimum moderation is conservative. Since the flux is bottom peaked due to the concrete, the top nozzle assumptions do not have a significant effect on k. For the fully flooded analysis, replacing the top and bottom nozzle with water does not have a significant effect on k. The variations seen are consistent with the Monte Carlo uncertainty.

Table 7.4: Sensitivity of k to Top and Bottom Nozzle Modeling

Reflector	k-eff	σ	Δk	Δk/rss(σ)	k-eff	σ	Δk	Δk/rss(σ)
	Water Density 1 gm/cc				Water Density 0.0625 gm/cc			
Pure Water Reflector	0.9034	0.00005	N/A	N/A	0.9440	0.00004	N/A	N/A
Design 2 Bottom Nozzle	0.9035	0.00013	0.0002	124%	0.9430	0.00013	-0.0010	-766%
Design 3 Bottom Nozzle	0.9031	0.00013	-0.0002	-150%	0.9425	0.00012	-0.0015	-1180%
Design 2 Top Nozzle	0.9035	0.00014	0.0002	103%	0.9442	0.00013	0.0002	131%
Design 1 Top Nozzle	0.9033	0.00014	-0.0001	-39%	0.9441	0.00012	0.0001	93%
Design 3 Top Nozzle	0.9032	0.00014	-0.0001	-93%	0.9440	0.00014	0.0000	0%

7.1.5 Cutout in Rack Bottom Angle Beams

There is a small cutout in the top corner of the 7"x4"x3/8" angle beams. This cutout is circled in Figure 3.3. The volume of the cutout is 3/16 in^3 or 3.072 cm^3 (right triangle with leg lengths of 1 inch each and the beam has a thickness of 3/8 inch). Due to the difficulties of modeling a triangular prism in Scale 6.0, this cutout was modeled as a cuboid of equal volume to the cutout (3.072 cm^3). To make sure that the shape difference is insignificant, a test case was run with a double sized cutout (1"x1"x3/8^{th}" cuboid cutout). The shape difference will not make a significant difference because Table 7.5 shows that the test case k, with twice the cutout volume, was approximately the same.

Table 7.5: Reactivity Impact of the Angle Beam Cutout

Case	k-eff	σ	Δk	Δk/rss(σ)	k-eff	σ	Δk	Δk/rss(σ)
	Water Density 1 gm/cc				Water Density 0.0625 gm/cc			
Equivalent Volume Cutout	0.9034	0.00005	N/A	N/A	0.9440	0.00004	N/A	N/A
Large Cutout	0.9030	0.00014	-0.0004	-235%	0.9440	0.00014	-0.0001	-49%

7.1.6 U-234 and U-236 Content

Figure 7.3 shows the fresh fuel as-built U-234 and U-236 data for the last 6 fuel batches that North Anna has received. Uranium 234 accounts for 0.0054 ± 0.0005% of natural uranium. This isotope is enriched during the enrichment process because it is lighter than U-235 and U-238. Uranium-236 is also present in fresh fuel, but the content of U-236 is not stable so it will be conservatively ignored.

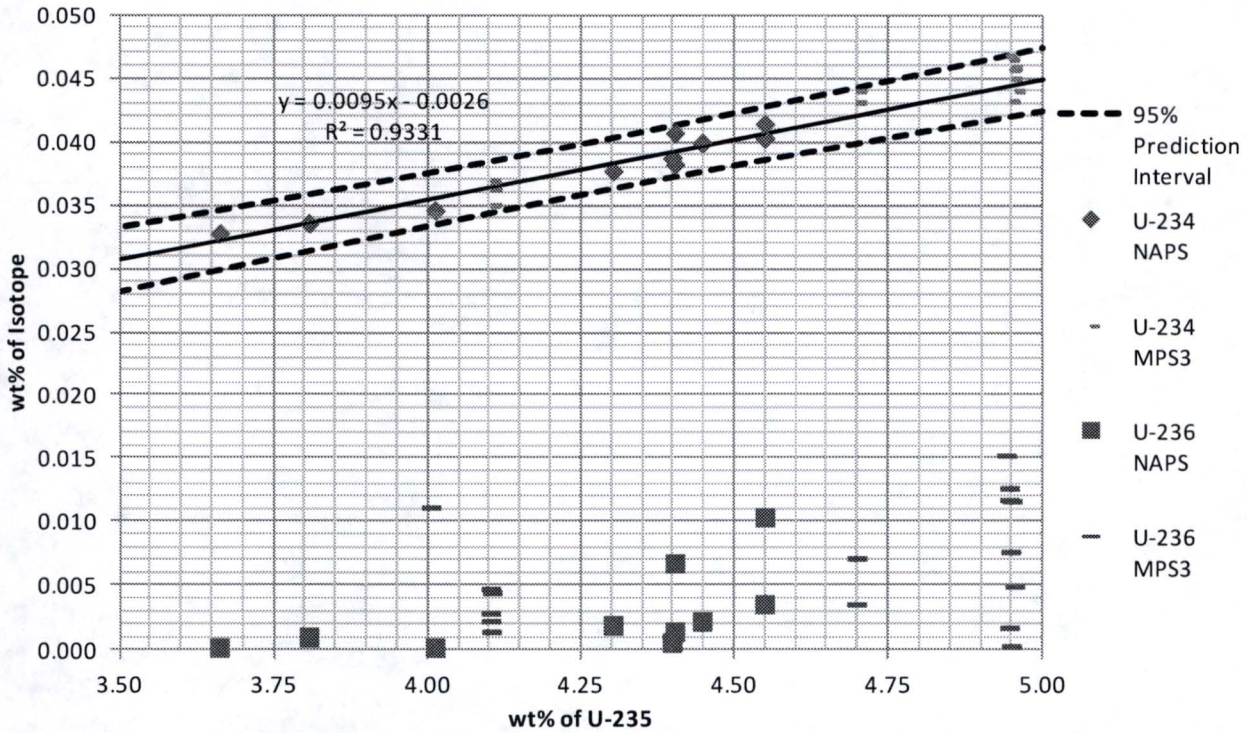

Figure 7.3: As-Built Enrichment of U-234 and U-236 versus Enrichment of U-235

Since North Anna has never received fuel with over 4.55 U-235 wt%, extrapolations must be made to estimate how much U-234 and U-236 would be present in fuel that is enriched to 5.0 U-235 wt%.

The relationship between U-234 and U-235 will be assumed to be linear. The as-built data supports this assumption with a calculated R^2 value of 0.9331. Figure 7.3 also shows the 95% prediction interval. This interval was calculated using:

$$95\%\text{PI(x)} = \hat{y} \pm t^{\star} s_y \sqrt{1 + \frac{1}{n} + \frac{(\hat{x}-\bar{x})^2}{(n-1)s_x^2}}$$

Where:

$\hat{y}$ is the regression line y value

$t^{\star}$ is the t value for a two tailed cumulative probability of 95% and n-2 degrees of freedom ($t^{\star}$=2.306)

s_y is $\sqrt{\frac{\sum(y_i-\hat{y}_i)^2}{n-2}}$ (s_y=8.477E-4)

n is the number of measured data points (n=10)

$\hat{x}$ is the regression line x value

$\bar{x}$ is the mean x value of the measured data points ($\bar{x}$=4.254)

s_x is the standard deviation of the measured x values (s_x=0.3142)

To ensure that the extrapolation and prediction intervals are reasonable, 4.95 U-235 wt% as-built data was compiled from Millstone Unit 3. Figure 7.3 shows that the Prediction Interval bounds the Millstone Unit 3 as-built data. In addition, AREVA as-built data for Millstone Unit 2 was surveyed and all the higher enriched fuel (>3.0 wt%) had a U-234 enrichment of 9 mg U234/g U235 (if this ratio were to be plotted on Figure 7.3, it would land almost on top of the regression line). The Millstone Unit 3 as-built data showed that the lowest U-234 enrichment was 0.0432 wt% for a 4.95 wt% U-235 assembly. Since the Millstone Unit 3 data correlated well with the North Anna prediction intervals, rather than use the North Anna prediction interval which would involve extrapolation to 5 wt%, the lowest Millstone 3 U-234 enrichment of 0.0432 wt% is used for the NAPS NFSA analysis.

To be conservative, no credit will be taken for U-236 in the fuel. No credit is taken because of the unexplained source of U-236, and because Figure 7.3 shows that it is possible for U-236 to vary between 0 wt% to ~0.015 wt% at 5.00 U-235 wt%.

To determine the affect U-234 and U-236 content has on k, a couple of runs were made. Table 7.6 shows that including U-234 is worth a couple of tenths of a percent and that U-236 at the high end of the content is negligible. Therefore, for NFSA analysis 0.0432 wt% of U-234 and zero U-236 is used.

Table 7.6: Reactivity Impact U-234 and U-236

Case	k-eff	σ	Δk	k-eff	σ	Δk
	Water Density 1 gm/cc			Water Density 0.0625 gm/cc		
0.0432 wt% U-234 no U-236	0.9034	0.00005	N/A	0.9440	0.00004	N/A
No U-234, no U-236	0.9054	0.00014	0.0021	0.9455	0.00012	0.0015
0.0432 wt% U-234, 0.0154 wt% U-236	0.9034	0.00014	0.0001	0.9439	0.00012	-0.0001

7.1.7 Concrete Composition

Concrete has the capability to reflect leakage neutrons back towards the fuel, which increases the k of the NFSA.

The floor and two walls of the NFSA are 12" thick. The remaining walls are conservatively modeled to be 300 cm thick.

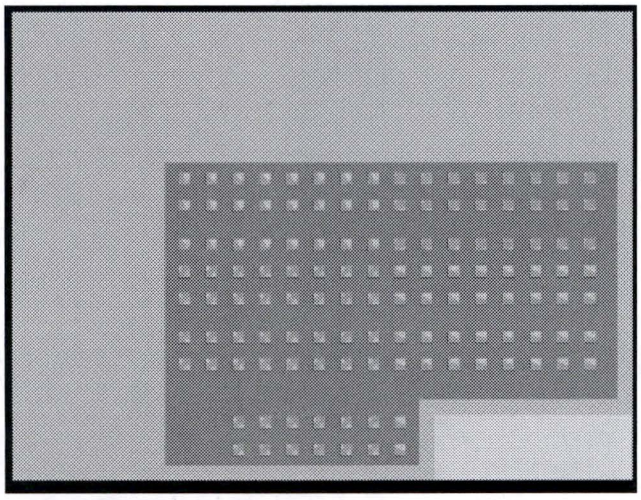

Figure 7.4: North Anna New Fuel Storage Area Walls (Yellow)

The exact composition of the concrete surrounding the North Anna NFSA is unknown. For this scenario, EPRI recommended two conservative concretes, dry and wet, that were determined by maximizing the isotopic content of the positive worth isotopes and minimizing the isotopic content of negative worth isotopes. [30] EPRI used the four concretes in the SCALE Standard Composition Library as a starting point. Nitrogen, Sulfur, Chlorine, Potassium, Titanium, and Manganese all had negative worths and at least one of the four concretes had zero weight percent of each of these elements. This resulted in elimination of these trace negative worth elements. The only remaining elements with negative worth were Hydrogen, Iron, and Calcium. All three of these elements are part of Portland cement.

The NRC review of the EPRI approach questioned whether the SCALE concrete compositions could be applied as a bounding concrete [31]:

The studies performed are mainly based on the four concrete compositions included in the SCALE libraries. There does not appear to be any effort to determine if the final "conservative" concrete composition is, in fact, conservative relative to a variety of real-world concrete compositions. Include some discussion of applicability to concrete from different geographic regions of the country, given their varying aggregates.

To address the NRC's concern, the following sections justify the use of the Hydrogen, Calcium, Iron, Carbon, and Oxygen weight percents.

Hydrogen in the Concrete

Hydrogen is a negative worth element in concrete. This means that minimizing the amount of hydrogen would produce a more conservative concrete.

Hydrogen exists in concrete in two principle forms. The first form is as H_2O located in the interstitial locations of the cement atomic lattice or in the air voids of the concrete. The second form is as OH^- chemically bounded to cations. As documented in the proceedings of ICAPP 2011, "Irradiation effects on concrete durability of nuclear power plants," Kontani [32] establishes that concrete can release hydrogen by gamma heating evaporating interstitial water or by radiation decomposing molecules to form hydrogen and oxygen gas. However, Kontani [32] also found that while, "hydrogen gas continued to be released after water release by

gamma heating came to the end, the amount of water released subsequently by radiolysis is very small." In addition, NUREG/CR-7171 [33, Section 6.3 and Section 3.5] shows that there is a non-releasable portion of water in concrete. Therefore, References 32 and 33 show that assuming all hydrogen can leave the concrete is unrealistically conservative.

Section 3.5 of NUREG/CR-7171 states that the amount of bound, non-releasable water in concrete is determined by:

$$W_b = 0.24\, m\, C \qquad \text{(Eq. 7.1)}$$

Where W_b is the weight of bound, non-releasable water, m is the maturity factor, and C is the total cement content of concrete.

The maturity factor comes from an article by H. K. Hilsdorf. [34] Figures 5a and 5b of Hilsdorf's article provide m. Using m=0.6 bounds both curves for all ages of concrete. The weight percentage of cement in the North Anna concrete is 15.4% wt%. [35, Design Mix 3NR, Structural Concrete, 3000 psi] Plugging 15.4 wt% into Equation 7.1 yields a bound water in cement weight percentage of 2.22%. Finally, multiplying 2.22% by the wt% of hydrogen in water will result in the weight percent of bound hydrogen of 0.249%. Therefore, the concrete used in this calculation will use a hydrogen weight percent of 0.25%. Note that this method takes no credit for hydrogen in the aggregate.

It is assumed that there is no water loss due to gamma heating since the NFSA walls receive very little gamma heating because fresh fuel is not radioactively hot and because the NFSA is empty the majority of the time.

Confirming Calcium and Iron in the Concrete

Calcium is a negative worth element in concrete. This means that minimizing the amount of calcium would produce a more conservative concrete.

North Anna used ASTM C150, Type II Portland Cement. [35, Section 2.1.1] ASTM C150 has requirements about the composition of Type II Portland Cement and although there is a range of calcium content, the minimum calcium is 24 wt%. Again, using the 15.4 wt% cement in the concrete, the calcium content in the concrete due only to the cement is greater than the 3.51

wt% in the EPRI wet concrete. [30] Therefore, it is conservative to use the EPRI calcium concentration.

Iron is a negative worth element in concrete. This means that minimizing the amount of iron would produce a more conservative concrete. There is significant rebar in the concrete that is not separately modeled. This rebar assures the iron content in the North Anna concrete exceeds that assumed in the EPRI wet concrete. [30] Calculations from station drawings have been used to confirm this.

Addition of Carbon and Oxygen

Carbon and oxygen are relatively large positive worth elements in concrete [30]. In order to maximize the carbon and oxygen it is assumed that all the CaO in the cement was oxidized to $CaCO_3$. To add additional conservatism it was assumed that the cement was 100% of the compound that has the highest CaO content (Tricalcium Silicate). This CO_2 was assumed to be added to the concrete in addition to the carbon and oxygen already in the EPRI wet concrete.

Final Concrete Composition

The EPRI wet concrete is adequately conservative for calcium and iron (negative worth elements) and close for hydrogen (a small 0.01% correction is done for this project). The highest worth positive elements, carbon and oxygen, are augmented. Table 7.7 shows the adjustments to the EPRI wet concrete and the final normalized wt%. Notice that the additional carbon and oxygen increases the density of the concrete to higher than common concretes, which is about 2.3 g/cc [6], so this composition and density is conservative.

Table 7.7: Concrete Composition

Element	EPRI Wet Concrete (wt%) [30]	Adjustment(wt%)	Adjusted Wet Concrete(wt%)	Renormalized, Adjusted Concrete (wt%)
Fe	0.45	+0	0.45	0.41
H	0.26	-0.01	0.25	0.23
C	13.97	+2.43	16.40	15.06
O	42.41	+6.49	48.90	44.90
Na	2.31	+0	2.31	2.12
Mg	7.51	+0	7.51	6.90
Al	2.71	+0	2.71	2.49
Si	26.87	+0	26.87	24.67
Ca	3.51	+0	3.51	3.22
Density (g/cm^3)	2.91	N/A	N/A	3.17

Table 7.8 shows that this concrete is more conservative than the EPRI Wet Concrete.

Table 7.8: Comparison of the EPRI Wet Concrete to the Adjusted Concrete

Case	k-eff	σ	Δk	Δk/rss(σ)	k-eff	σ	Δk	Δk/rss(σ)
	Water Density 1 gm/cc				Water Density 0.0625 gm/cc			
Adjusted, Bound Water Concrete	0.9034	0.00005	N/A	N/A	0.9440	0.00004	N/A	N/A
EPRI's Wet Concrete	0.9033	0.00014	-0.0000	-19%	0.9419	0.00012	-0.0021	-1662%

7.1.8 Asymmetric Positioning of Fuel Assemblies in the Rack Cells

To ensure that there will be no limitations on where the assemblies are placed within the stainless steel tubes, four cases were run to determine the assembly placement that achieves the highest possible k. The cases are:

1. All assemblies centered in their cells
2. All assemblies placed in their cells closest to Point A in Figure 7.2. This case would capture the highest k if the side concrete wall drove k.
3. All assemblies placed in their cells closest to Point B in Figure 7.2. This case is the center of the 8 rows of cells.

4. All assemblies placed in their cells closest to Point C in Figure 7.2. This case tests if the bottom short row and wall produces an increase in k.

Table 7.9 shows that the highest k is achieved when the assemblies are shifted towards the center of the NFSA (Location B). Placing the assemblies in the center of the cells is less reactive than asymmetric loading by about 0.002. The fully flooded k is less dependent on where the asymmetry is since the higher water density isolates the cells more than the optimum moderation water.

Table 7.9: Sensitivity of k to Asymmetric Placement in the Cell

Fuel Location	k-eff	σ	Δk	Δk/rss(σ)	k-eff	σ	Δk	Δk/rss(σ)
	Water Density 1 gm/cc				Water Density 0.0625 gm/cc			
All Fuel Toward the Center of Rack (point B)	0.9034	0.00005	N/A	N/A	0.9440	0.00004	N/A	N/A
Centered in Cells	0.9008	0.00014	-0.0026	-1735%	0.9418	0.00013	-0.0022	-1619%
Placed Toward North Wall (point A)	0.9031	0.00011	-0.0002	-199%	0.9432	0.00012	-0.0008	-634%
Placed Toward Center of Rows 6 and 7 (point C)	0.9031	0.00014	-0.0002	-155%	0.9432	0.00012	-0.0008	-634%

7.1.9 Temperature

For the fully flooded cases, the temperature sets the density of the water. However, for the optimum moderation condition, it is assumed that the water is foam, which could be at any temperature. Temperatures of 273K, 277K and 311K were used to calculate the maximum k of the NFSA. The rationale for each of these temperatures is detailed below:

- 273K is the coldest possible temperature for liquid water. The coolest temperature will minimize the Doppler Effect of the fuel.

- 277K is the temperature at which water has the highest density.

- 311K is 100°F. This temperature represents the hottest reasonable temperature that the water or foam in the NFSA could reasonably get. The basis for 100°F is that the temperature in Richmond only reached 100°F during one day of 2015. Further expansion of the fluid to make foam would normally cool the fluid. There is no heat source in the NFSA.

Table 7.10 shows that the maximum k occurs at 311K when the NFSA is flooded with an optimum moderator and that the maximum k occurs at 277K when flooded with water. Therefore, the maximum k-eff calculation will use a temperature of 311K when using low density water and 277K when using full density water.

Table 7.10: Sensitivity of k to Temperature

Temperature	k-eff	σ	Δk	Δk/rss(σ)	k-eff	σ	Δk	Δk/rss(σ)
	Water Density 0.9998, 1, or 0.9930 gm/cc				Water Density 0.0625 gm/cc			
273 K	0.9030	0.00014	-0.0003	-215%	0.9387	0.00012	-0.0053	-4215%
277 K	0.9034	0.00005	N/A	N/A	0.9386	0.00012	-0.0054	-4279%
311 K	0.9025	0.00014	-0.0008	-553%	0.9440	0.00004	N/A	N/A

7.1.10 Optimum Moderation

It is possible that the most reactive condition of the NFSA is with low density water caused by foam. Figure 7.5 shows the k of the NFSA over a range of moderator densities. Figure 7.6 expands Figure 7.5 near the reactivity peak. The k is maximized with a moderator density approximately 0.0625 gm/cc, which was used for all the optimum moderation analysis.

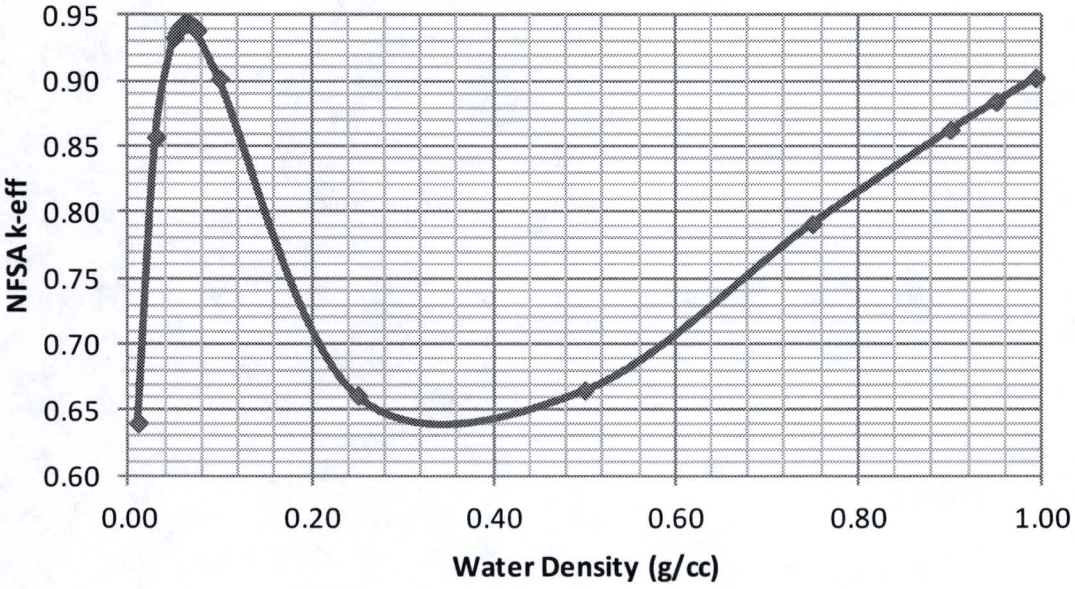

Figure 7.5: New Fuel Storage Area k as a Function of Water Density

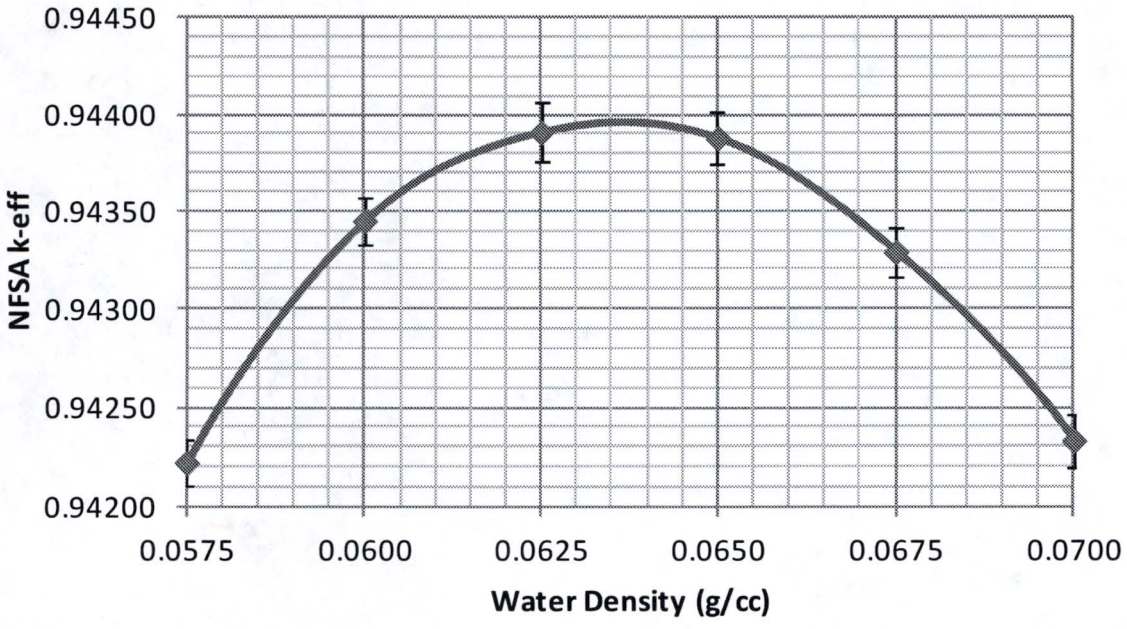

Figure 7.6: NFSA k as a Function of Water Density Near the Peak Reactivity

7.1.11 Summary of the Base Cases for the NFSA Analysis

Section 7.1 has determined the conditions for a conservative model of the NFSA k. The following describes the base cases that are used for the rest of the analysis:

1. Fuel is 5 wt% U-235 with no burnable absorbers.
2. The fuel contains 0.0432 wt% U-234 and no U-236.
3. The fuel stack density is 95.5% of the UO2 theoretical density.
4. The fuel pellet diameter is 0.3225 inches (0.81915 cm).
5. The fuel active length is 144 inches.
6. The fuel clad inner diameter is 0.329 inches (0.8357 cm).
7. The fuel clad outer diameter is 0.374 inches (0.9500 cm).
8. The fuel clad is pure zirconium.
9. The fuel rod pitch is 0.496 inches (1.260 cm).
10. The guide and instrument tubes have an ID of 0.450 inches (1.143 cm) and an OD of 0.47 inches (1.204 cm) which is the minimum cross sectional area.
11. The grids are conservatively ignored.
12. Above and below the active fuel is water plus rack structure and concrete.
13. The rack dimensions are shown on Figure 7.1.
14. The concrete composition is conservatively modeled assuming that hydrogen is only in the bound water in the cement.
15. The entire new fuel storage area is modeled and it is assumed that all the assemblies are placed in the cells so they are closest to the center of the model.
16. The fuel and moderator temperature for the fully moderated condition is 277 K (the temperature where the moderator density is the highest (1.0 gm/cc)).
17. The fuel and moderator temperature for the optimum moderated condition is 311 K (100 F) which is higher than normal temperatures and high for any expanding foam.
18. The water density for the fully flooded case is 1.0 gm/cc.
19. The water density for the optimum moderation condition is 0.0625 gm/cc.

The base cases were run with 9000 generations, 36000 neutrons/generation, and 300 generations skipped so the Monte Carlo uncertainty would be small for better final results and determination of tolerance reactivities. The k's of the base cases are shown on Table 7.11.

Table 7.11: Base Case k's for the North Anna NFSA

Case Description	k	σ
Optimum Moderation	0.94402	0.00004
Full Density Water	0.90335	0.00005
Air Moderated	0.46899	0.00008

7.2 Biases and Uncertainties for the New Fuel Storage Area Analysis

Tables 7.12 and 7.13 display the results of the tolerance sensitivity calculations for the optimum moderation and full density water condition, respectively. The "Total Manufacturing Uncertainty" is calculated using:

$$Total\ Manufacturing\ Unc. = \left[\sum \left(k_{\pm Unc.} - k_{Base} + 2 * \sqrt{\sigma^2_{\pm Unc.} + \sigma^2_{Base}}\right)^2\right]^{1/2}$$

The fuel manufacturing tolerances are given in Section 4.1. The rack tolerances are given in Section 3.1. Note that the fuel stack density is a bounding value but a typical batch averaged uncertainty is included in the analysis. No tolerances were available for the structural L-Beams at the bottom of the NFSA. Using ASTM 480/480M [36] the uncertainty in the thickness or the L beam would be equivalent to about 3% of the mass of the beam. For this analysis it will be assumed that the L beams have a 10% density uncertainty. The uncertainty for the distance between the bottom of the active fuel and the concrete is a combination of fuel assembly and L-Beam uncertainty and 0.085 cm was used. The uncertainty of the rack cell tube thickness is from ASTM A480/A480M [36]. The tolerance used is for cold-rolled stainless steel plates with a width of 12"-24" and a thickness of 0.100" to 0.125" (inclusive).

For the optimum moderation condition the total manufacturing uncertainty is dominated by the rack cell tube thickness uncertainty. For the fully flooded condition the tube thickness uncertainty is about half of the total uncertainty. Tolerances for rack distance from the storage area walls and rack storage cell inner dimension were not initially calculated. Review calculations were run to verify that these tolerances would not significantly change the total uncertainty. Including these two tolerances would not change the total uncertainty reported in Table 7.14. For optimum moderation (Table 7.12), the reactivity of the storage cell inner

dimension tolerance is 0.00025 Δk and the wall proximity tolerance is 0.00067 Δk. For flooded conditions (Table 7.13), the reactivity of the storage cell inner dimension tolerance is 0.00001 Δk and the wall proximity tolerance is 0.00004 Δk.

Table 7.12: Sensitivity Calculation for Manufacturing Tolerance in Optimum Moderation

Case Description	k-eff	σ	Δk
Base Model	**0.9440**	**0.00004**	**N/A**
Active Fuel Length - Increase	0.9441	0.00013	0.0000
Distance from Floor to Active Fuel - Decrease	0.9441	0.00012	0.0001
Cladding ID-Increase	0.9443	0.00013	0.0003
Cladding OD-Decrease	0.9443	0.00012	0.0002
Concrete Wall Thickness - Increase	0.9448	0.00013	0.0007
Fuel %TD - Increase	0.9445	0.00012	0.0005
Fuel Pellet OD-Increase	0.9444	0.00013	0.0004
Guide Tube ID-Increase	0.9441	0.00012	0.0001
Guide Tube OD-Decrease	0.9441	0.00008	0.0001
L-Beams Density - Decrease	0.9444	0.00012	0.0004
Pin Pitch – Increase*	0.9446	0.00013	0.0006
Rack Cell Tube Pitch - Decrease	0.9447	0.00012	0.0007
Rack Cell Tube Thickness - Decrease	0.9556	0.00013	0.0116
Total Manufacturing Uncertainty (Δk)			**0.0121**

*Pin pitch tolerance used was conservatively 0.0025 cm rather than [ ]^{a,c}.

Table 7.13: Sensitivity Calculation for Manufacturing Tolerance in Full Density Water

Case Description	k-eff	σ	Δk
Base Model	**0.9034**	**0.00005**	**N/A**
Active Fuel Length - Increase	0.9035	0.00009	0.0001
Distance from Floor to Active Fuel - Increase	0.9036	0.00014	0.0002
Cladding ID-Decrease	0.9038	0.00013	0.0005
Cladding OD-Decrease	0.9049	0.00014	0.0016
Concrete Wall Thickness - Increase	0.9037	0.00015	0.0003
Fuel %TD - Increase	0.9039	0.00015	0.0005
Fuel Pellet OD-Increase	0.9035	0.00014	0.0002
Guide Tube ID-Increase	0.9036	0.00015	0.0002
Guide Tube OD-Decrease	0.9036	0.00013	0.0002
L-Beams Density - Decrease	0.9035	0.00009	0.0001
Pin Pitch – Increase*	0.9044	0.00013	0.0011
Rack Cell Tube Pitch - Decrease	0.9034	0.00010	0.0000
Rack Cell Tube Thickness - Decrease	0.9052	0.00014	0.0018
Total Manufacturing Uncertainty (Δk)			**0.0036**

*Pin pitch tolerance used was conservatively 0.0025 cm rather than [ ]^{a,c}

Combination of Uncertainties

The base models have a Monte Carlo sigma of 0.00004 and 0.00005 for the optimum moderation and full density water condition, respectively. The sigma's will be doubled to achieve a 95%/95% probability and confidence level. Therefore, the base model Monte Carlo uncertainty is **0.0001** Δk for the optimum moderation (rounded up to 4 digits) and full density water conditions.

Section 6.3.1 produced a validation uncertainty of 0.0050 when the EALF is under 0.4 eV and 0.0063 for EALF between 0.8 and 1.1 eV. The EALF of the optimum moderation nominal case is 1.07 eV. The EALF of the full density water nominal case is 0.24 eV. Therefore, the validation uncertainty is **0.0063** and **0.0050** Δk for the optimum moderation and full density water condition, respectively.

The total manufacturing uncertainty, base model Monte Carlo uncertainty, and validation uncertainty are root sum squared to calculate a total uncertainty. The results are displayed in Table 7.14.

Table 7.14: Combining the NFSA's Uncertainties (Δk)

Parameter	Optimum Moderation	Full Density Water
Manufacturing Tolerance Uncertainty	0.0121	0.0036
Base Model Monte Carlo Uncertainty	0.0001	0.0001
Validation Uncertainty	0.0063	0.0050
Total Uncertainty	***0.0136***	***0.0061***

Biases

Since the critical experiments were done at room temperature except one, there is a temperature bias for temperatures above room temperature (See Section 6.3.3). The temperature bias is 1.7E-05 $\Delta k/\Delta\,^{\circ}C$ and needs to be applied for cases above room temperature. The optimum moderation case has a temperature of 311K and therefore needs to take a **0.0002** Δk bias [(311K-297K)* 1.7E-05 $\Delta k/\Delta\,^{\circ}C$=0.0002].

Section 6.3.1 determined a bias of 0.0035 when the EALF is under 0.4 eV and 0.0070 when the EALF is between 0.8 and 1.1 eV. The EALF of the optimum moderation base case is 1.07 eV. The EALF of the full density water base case is 0.24 eV. Therefore, the Code Uncertainty is **0.0070** and **0.0035** Δk for the optimum moderation and full density water conditions, respectively.

The total bias is 0.0072 and 0.0035 for the optimum moderation and full density water conditions, respectively.

7.3 Accident Conditions

It should be noted that it is almost impossible for the North Anna NFSA to be flooded with foam. This is because most of the NFSA is covered as can be seen in Figure 3.2. The only part that is not covered is a small opening in the Southwest corner to allow personnel to climb into the vault. Regardless, both the accident scenarios of flooding the NFSA with water and optimum moderator were analyzed throughout this calculation.

As can be seen on Figure 3.2 the New Fuel Storage Area has a cover that would prevent a misplaced assembly between cells. A dropped assembly as well as flooding would require two unlikely independent events and therefore, analysis is not required.

During a seismic event, free standing equipment shifts around which can move fuel closer or farther apart. However, the North Anna NFSA has no free standing equipment except for the assemblies inside the stainless steel tubes. Therefore, the fuel assemblies will shift inside the stainless steel tubes, but that scenario is covered by Section 7.1.8 (Asymmetric Positioning of Fuel Assemblies in the Rack Cells). No other components will shift around so no additional cases need to be run.

7.4 Comparison Between the New Fuel Storage Area k95/95 to the Acceptance Criteria

10CFR50.68 requires that the $k_{95/95}$ of the NFSA must not exceed 0.98 when flooded with low-density hydrogenous fluid and must not exceed 0.95 when flooded with unborated water. Table 7.15 displays the maximum k-eff of the NFSA and the margins to the limits.

To allow for any NRC review issues, a **0.0100** Δ k margin is included for both optimum moderation and full density water conditions.

This analysis demonstrates that the acceptance criteria are met for the North Anna NFSA for the storage of 126 fuel assemblies with a maximum enrichment up to 5.00wt% of U-235. The limiting condition by far is the optimum moderation condition. Generous margin exists to the fully flooded criteria.

Table 7.15: Comparison Between the New Fuel Storage Area $k_{95/95}$ to the Acceptance Criteria

	Optimum Moderation	Full Density Water
Base Model	0.9440	0.9034
Total Uncertainties	0.0136	0.0061
Total Biases	0.0072	0.0035
Margin for NRC Review	0.0100	0.0100
Maximum k-eff	**0.9748**	**0.9230**
10CFR50.68 Limit	**0.9800**	**0.9500**
Dominion Margin to the Limit	***0.0052***	***0.0270***

This analysis uses a combination of fuel assembly designs which bounds the historical fuel designs. New fuel designs will need to be compared to the model to see if they are bounded. The manufacturing tolerances on the fuel assembly dimensions do not need reviewed since the uncertainty is dominated by the uncertainty in the rack tube thickness (The optimum moderation case dominates so small impacts on the fully flooded analysis are also not important.). The following list summarizes the bounding assumptions for the fuel:

1. The design bottom of the active fuel is 8.078 cm or greater above the bottom of the fuel assembly.
2. The design stack density of the fuel is less than or equal to 95.5% of UO2 theoretical density.
3. The design fuel pellet diameter is less than or equal to 0.8192 cm.
4. The design clad OD is 0.95 cm or greater.
5. The design guide and instrument tube thickness is 0.061 cm or greater.

The effect of these parameters, in general, is small. However, fuel designs to be stored in the NFSA that are not bounded by these assumptions require additional analysis to ensure that criticality limits will be met.

8 Depletion Modeling

This section describes the North Anna SCALE 6.0 (TRITON) depletion models and conservative depletion conditions suitable for use in the North Anna spent fuel pool criticality calculations.

8.1 Depletion Method Overview

TRITON depletions are used to determine the isotopic content of depleted fuel for Spent Fuel Pool criticality analysis, specifically to develop burnup curves (required minimum fuel burnup as a function of initial enrichment). Performing TRITON depletions requires a SCALE model of a fuel assembly (or more specifically an axial segment of a fuel assembly) that includes geometry, material content, and depletion conditions (fuel temperature, moderator temperature and density, soluble boron, presence of burnable absorbers and or control rods, and depletion power).

Conservatism (maximizing spent fuel pool fuel reactivity) is incorporated via use of a bounding fuel assembly design and by choice of input depletion conditions that bound anticipated actual fuel depletion conditions. The methodology associated with determination of conservative models and conditions is consistent with that used for the recently accepted License Amendment Request for Millstone Unit 2. [9]

Section 6 provides the details on the computer code used (t5-depl sequence of SCALE 6.0 TRITON), the cross section library (238 group ENDF/B-VII), how it was run (number of neutrons followed, time step size, isotopes followed, and cooling time), and the validation.

The assembly is modeled as 18 equal size axial nodes. For each node the burnup is determined by the assembly burnup and the axial burnup distribution (See Section 8.5). The axial burnup distribution also provides the relative burnup averaged axial power distribution, which is used to determine depletion conditions for each node.

Each depletion node will consider the following parameters:

1. Assembly specific power (MW/MTU)
2. Soluble boron
3. Fuel design (pellet stack density, rod dimensions, and grids)

4. Burnable absorbers
5. Moderator temperature and density
6. Fuel temperature
7. Control rod insertion history

TRITON models will be conservative in the sense that fuel features and depletion conditions will be selected to accommodate past, present, and expected future fuel designs and depletion history in a way that maximizes spent fuel pool k. TRITON models are best estimate in the sense that uncertainties in fuel features (such as clad OD design tolerance) are not considered.

Each of these features or conditions will be evaluated using fuel design information, core design history, and operating history. Justification for the conservatism of each feature or condition will be provided using first principles, prior evaluations, or TRITON depletion sensitivity cases.

8.2 Burnup Averaged Relative Assembly Power

The fuel and moderator temperature depend in part on the fuel assembly power. For criticality, the assembly average power, not pin power, is important, since criticality requires assembly size masses not fuel pins. (Horizontal burnup gradients are addressed in Section 10.1.1) Further, the assembly average power for depletion to a particular fuel burnup is chosen to bound the average power an actual assembly could sustain from initial use through the fuel burnup being analyzed (the burnup averaged assembly power). Burnup averaged nodal fuel and moderator temperatures are calculated for the depletion analysis using the highest **b**urnup **a**veraged **r**elative **a**ssembly **p**ower (BARAP).

The BARAP at the end of each cycle is the accumulated assembly burnup divided by the sum of the cycle burnups for all cycles the assembly has resided in the core. For each assembly burned in the North Anna units, the burnup at the end of each cycle divided by the accumulated cycle burnup was calculated and plotted in Figure 8.1 against the assembly burnup. Figure 8.1 also shows a bounding a line for the BARAP as a function of burnup. Table 8.1 shows the breakpoints and values for the bounding (high) BARAP function. This BARAP function will be used as input to calculate depletion fuel and moderator temperature.

Table 8.1: Bounding Burnup Averaged Relative Assembly Power versus Burnup

(Interpolate for points between burnups on table)

Assembly Average Burnup (GWd/MTU)	Burnup Averaged Relative Assembly Power (BARAP)
0	1.44
30	1.44
53	1.30
60	1.00

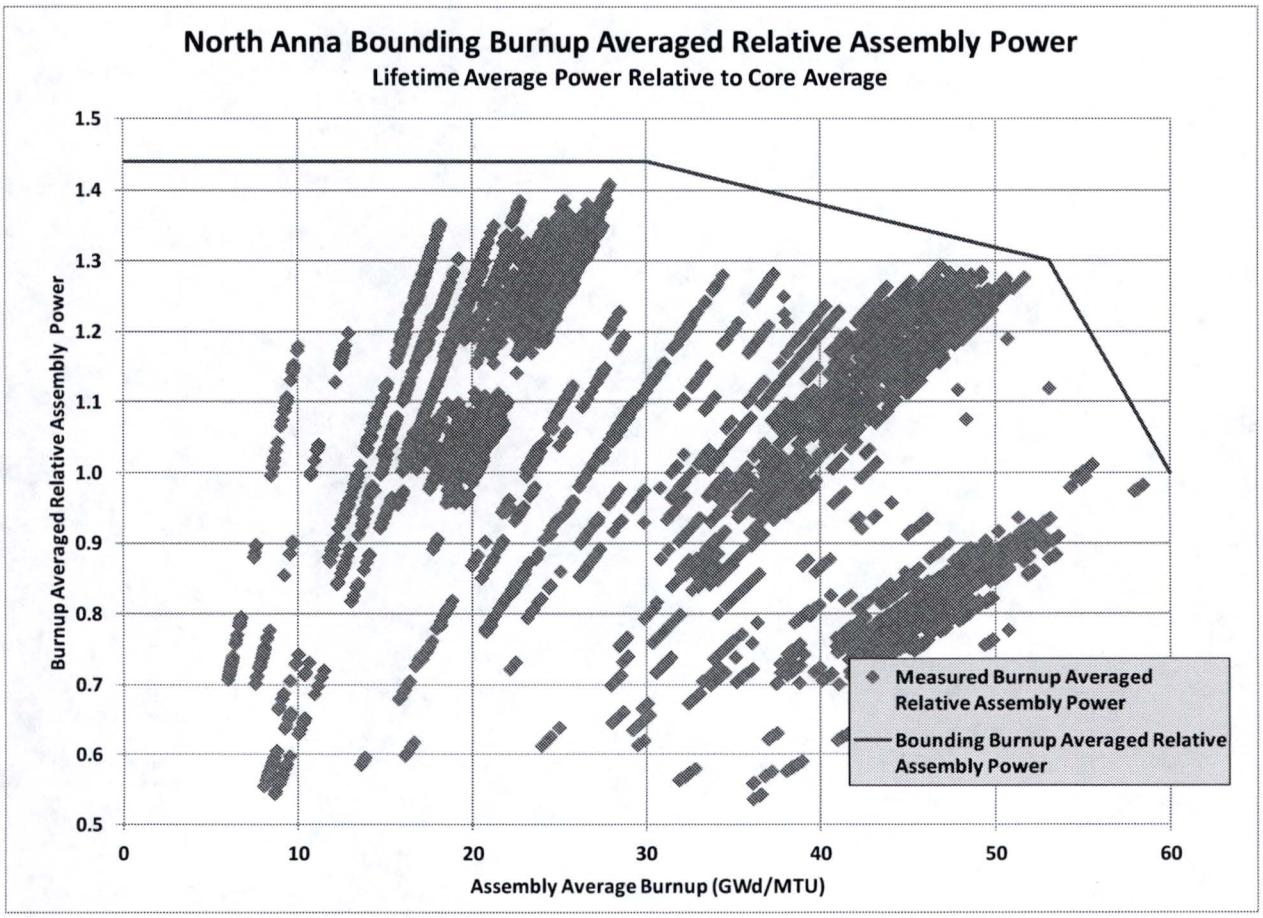

Figure 8.1: Bounding Burnup Averaged Relative Assembly Power

8.3 Depletion Boron for North Anna Cycles

Spent fuel reactivity is increased by depletion at higher soluble boron. Cycle average boron concentration is determined from measured data taken from Cycle 19 to the current cycle for both units. Average cycle boron is calculated by trapezoidal integrations of the boron versus burnup data from data taken about every shift. Results for the 11 most recent cycles (Table 8.2) are bounded by 1100 ppm soluble boron. The highest average boron occurs in the earthquake shortened cycle, which is North Anna Unit 1 Cycle 22. Fuel depletion soluble boron of 1100 ppm conservatively bounds all historical North Anna cycles.

Table 8.2: Cycle Average Soluble Boron

North Anna Unit	Cycle	Average boron (ppm)
1	24	840
2	23	815
1	23	919
2	22	996*
1	22	1051*
2	21	996*
1	21	899
2	20	958
1	20	865
2	19	905
1	19	858

*Cycle shortened due to earthquake. Earthquake occurred 8/23/2011 during N1C22 and N2C21. N1C22 resumed operation after approximately three months. N2C21 did not resume operation but entered a refueling outage early, shortening N2C21. The N2C21 refueling outage was longer than normal, shortening N2C22.

8.4 Bounding Average RCS Temperatures for North Anna Cycles

Higher depletion moderator temperature produces more plutonium and increases burned fuel k in the spent fuel pool. Calculation of the bounding high Reactor Cooling System (RCS) temperature is performed using a simple heat balance with the input variables: 1) minimum RCS flow (Section 3.4.1.3 of the Technical Specifications (TS)), 2) burnup averaged relative assembly power (maximum from Figure 8.1), 3) core power (maximum nominal power from TS), and 4) a high inlet temperature. The RCS flow is further reduced by a high bypass flow.

Rated core power, inlet temperature, RCS flow, and bypass flow data is given on Table 8.3. Average fuel assembly moderator exit temperature is calculated via simple heat balance to determine most limiting historical T/H conditions. Table 8.3 shows the results of the exit temperature calculation. The most limiting cycle is North Anna Unit 2 Cycle 7. Exit temperature is taken as the key metric for bounding RCS temperature because the reactivity of depleted PWR fuel is dominated by the top region of the fuel. The following conditions bound the exit temperature for all cycles:

- Power: 2940 MWth (highest of all cycles)
- RCS flow: 295000 gpm (TS minimum)
- Bypass flow: 5.1% (second highest of all cycles)
- Inlet Temperature: 551.1 F (2.2 F higher than current cycle value, set to bound exit temperature of all cycles)

Table 8.3: North Anna RCS Thermal/Hydraulic History

Unit and Cycle	Highest Rated Power (MWth)	Inlet Temp. (F)	RCS Flow (gpm)	RCS Flow (lbm/hr)	Bypass Flow (%)	Inlet Enthalpy (BTU/lbm)	Exit Enthalpy (BTU/lbm)	Average Moderator Exit Temp. (F)
N1C1	2775	549.5	304000	1.143E+08	3.00	546.5	631.9	612.9
N1C2	2775	549.5	304000	1.143E+08	3.00	546.5	631.9	612.9
N1C3	2775	549.5	304000	1.143E+08	3.00	546.5	631.9	612.9
N1C4	2775	552.1	304000	1.139E+08	3.00	549.7	635.5	615.3
N1C5	2775	557.4	304000	1.130E+08	3.00	556.4	642.8	620.0
N1C6	2893	555.1	304000	1.134E+08	3.00	553.5	643.3	620.3
N1C7	2893	554.9	301200	1.124E+08	3.00	553.2	643.8	620.7
N1C8	2893	554.9	301200	1.124E+08	3.00	553.2	643.8	620.7
N1C9	2893	550.1	293600	1.103E+08	4.50	547.2	641.0	618.9
N1C10	2893	549.2	308000	1.159E+08	4.50	546.1	635.4	615.2
N1C11	2893	549.2	308000	1.159E+08	4.50	546.1	635.4	615.2
N1C12	2893	549.2	308000	1.159E+08	4.50	546.1	635.4	615.2
N1C13	2893	549.4	308000	1.158E+08	4.50	546.4	635.7	615.4
N1C14	2893	549.4	315300	1.186E+08	4.50	546.4	633.6	614.0
N1C15	2893	549.4	315300	1.186E+08	4.50	546.4	633.6	614.0
N1C16	2893	549.4	315300	1.186E+08	4.50	546.4	633.6	614.0
N1C17	2893	549.4	315300	1.186E+08	4.50	546.4	633.6	614.0
N1C18	2893	549.4	315300	1.186E+08	4.50	546.4	633.6	614.0
N1C19	2893	549.4	315300	1.186E+08	4.50	546.4	633.6	614.0
N1C20	2893	549.4	314400	1.182E+08	4.50	546.4	633.8	614.2
N1C21	2940	548.9	317800	1.196E+08	4.50	545.7	633.6	614.1
N1C22	2940	548.9	311000	1.170E+08	4.50	545.7	635.6	615.3
N1C23	2940	548.9	311200	1.171E+08	4.75	545.7	635.7	615.4
N1C24	2940	548.9	311400	1.172E+08	5.10	545.7	636.0	615.6
N1C25	2940	548.9	311000	1.170E+08	5.50	545.7	636.5	616.0
N2C1	2775	549.5	304000	1.143E+08	3.00	546.5	631.9	612.9
N2C2	2775	549.5	304000	1.143E+08	3.00	546.5	631.9	612.9
N2C3	2775	552.1	304000	1.139E+08	3.00	549.7	635.5	615.3
N2C4	2775	557.4	304000	1.130E+08	3.00	556.4	642.8	620.0
N2C5	2893	555.1	304000	1.134E+08	3.00	553.5	643.3	620.3
N2C6	2893	555.1	304000	1.134E+08	3.00	553.5	643.3	620.3
N2C7	**2893**	**554.8**	**300100**	**1.120E+08**	**3.00**	**553.1**	**644.0**	**620.82**
N2C8	2893	548.4	299700	1.129E+08	4.50	545.1	636.8	616.1
N2C9	2893	547.7	293300	1.105E+08	4.50	544.2	637.8	616.8
N2C10	2893	547.6	292700	1.103E+08	4.50	544.1	637.9	616.9

Unit and Cycle	Highest Rated Power (MWth)	Inlet Temp. (F)	RCS Flow (gpm)	RCS Flow (lbm/hr)	Bypass Flow (%)	Inlet Enthalpy (BTU/lbm)	Exit Enthalpy (BTU/lbm)	Average Moderator Exit Temp. (F)
N2C11	2893	549.2	308000	1.159E+08	4.50	546.1	635.4	615.2
N2C12	2893	549.2	308000	1.159E+08	4.50	546.1	635.4	615.2
N2C13	2893	549.3	308000	1.158E+08	4.50	546.2	635.5	615.3
N2C14	2893	549.3	308000	1.158E+08	3.70	546.2	634.8	614.8
N2C15	2893	549.3	308000	1.158E+08	3.70	546.2	634.8	614.8
N2C16	2893	549.3	313300	1.178E+08	3.70	546.2	633.3	613.8
N2C17	2893	549.3	313300	1.178E+08	3.70	546.2	633.3	613.8
N2C18	2893	549.3	313300	1.178E+08	3.70	546.2	633.3	613.8
N2C19	2893	549.3	310000	1.166E+08	3.70	546.2	634.2	614.4
N2C20	2893	549.3	310000	1.166E+08	3.70	546.2	634.2	614.4
N2C21	2940	548.8	308000	1.159E+08	3.70	545.6	635.5	615.3
N2C22	2940	548.8	310000	1.167E+08	4.05	545.6	635.3	615.2
N2C23	2940	548.8	310000	1.167E+08	4.42	545.6	635.6	615.4
N2C24	2940	548.8	310400	1.168E+08	4.78	545.6	635.9	615.5
BOUND	**2940**	**551.1**	**295000**	**1.107E+08**	**5.10**	**548.5**	**644.0**	**620.84**

8.5 Bounding Axial Burnup Shapes

NRC Interim Staff Guidance *DSS-ISG-2010-01* [4] provides the following guidance on the use of axial burnup profiles:

> *"Axial Burnup Profile: One of the most important aspects of fuel characterization is the selection of the axial burnup profile. NUREG/CR-6801, "Recommendations for Addressing Axial Burnup in PWR Burnup Credit Analyses," issued March 2003 (Reference 12), provides an insightful discussion of the "end effect" and recommendations for selecting an appropriate axial burnup profile. Although NUREG/CR-6801 is a useful reference on axial burnup profiles, it is not an exhaustive study of all of the fuel designs, core operating parameters, storage conditions, and possible synergistic effects. Therefore, the staff should verify that each application includes a portion of the analysis that demonstrates its treatment of axial burnup profile is appropriate for its specific conditions. For example, the reviewer should consider the following:*
>
> *i. Use of the limiting axial burnup distributions from NUREG/CR-6801 are acceptable for existing PWRs, provided they are used in a manner consistent with NUREG/CR-6801, e.g. the profiles are used within the burnup ranges specified. The NRC staff reviewer should verify the applications for plant designs that set the limiting profiles in NUREG/CR-6801 provide a site specific justification for the axial burnup distributions.*

ii. Applications using site-specific profiles should consider all past and present profiles, and include licensee controls to ensure that future profiles are not more reactive. An appropriate control for the axial profiles would be a licensee procedure that would evaluate the profile of an assembly before it is placed in the SFP storage racks and treat those with more reactive profiles than those used in the SFP NCS analysis as fresh fuel.

iii. Use of uniform profiles is conservative at low burnup levels. At some amount of burnup, the use of a uniform profile will become non-conservative. The burnup point where that occurs is dependent on the specifics of the situation. Applications that use uniform axial burnup profiles should only use them when appropriate and provide appropriate justification."

Consistent with this guidance, the North Anna spent fuel pool burnup credit analysis will use the NUREG/CR-6801 [40] profiles and uniform profiles. Table 8.4 is the relative axial burnup distributions from NUREG/CR-6801.

Table 8.4: Bounding Axial Burnup Profiles by Burnup Group [40]

Burnup group	1	2	3	4	5	6	7	8	9	10	11	12
Axial height (%)	Burnup ranges (GWd/MTU)											
	>46	42-46	38-42	34-38	30-34	26–30	22–26	18–22	14–18	10–14	6–10	<6
2.8%	0.582	0.666	0.660	0.648	0.652	0.619	0.630	0.668	0.649	0.633	0.658	0.631
8.3%	0.920	0.944	0.936	0.955	0.967	0.924	0.936	1.034	1.044	0.989	1.007	1.007
13.9%	1.065	1.048	1.045	1.070	1.074	1.056	1.066	1.150	1.208	1.019	1.091	1.135
19.4%	1.105	1.081	1.080	1.104	1.103	1.097	1.103	1.094	1.215	0.857	1.070	1.133
25.0%	1.113	1.089	1.091	1.112	1.108	1.103	1.108	1.053	1.214	0.776	1.022	1.098
30.6%	1.110	1.090	1.093	1.112	1.106	1.101	1.109	1.048	1.208	0.754	0.989	1.069
36.1%	1.105	1.086	1.092	1.108	1.102	1.103	1.112	1.064	1.197	0.785	0.978	1.053
41.7%	1.100	1.085	1.090	1.105	1.097	1.112	1.119	1.095	1.189	1.013	0.989	1.047
47.2%	1.095	1.084	1.089	1.102	1.094	1.125	1.126	1.121	1.188	1.185	1.031	1.050
52.8%	1.091	1.084	1.088	1.099	1.094	1.136	1.132	1.135	1.192	1.253	1.082	1.060
58.3%	1.088	1.085	1.088	1.097	1.095	1.143	1.135	1.140	1.195	1.278	1.110	1.070
63.9%	1.084	1.086	1.086	1.095	1.096	1.143	1.135	1.138	1.190	1.283	1.121	1.077
69.4%	1.080	1.086	1.084	1.091	1.095	1.136	1.129	1.130	1.156	1.276	1.124	1.079
75.0%	1.072	1.083	1.077	1.081	1.086	1.115	1.109	1.106	1.022	1.251	1.120	1.073
80.6%	1.050	1.069	1.057	1.056	1.059	1.047	1.041	1.049	0.756	1.193	1.101	1.052
86.1%	0.992	1.010	0.996	0.974	0.971	0.882	0.871	0.933	0.614	1.075	1.045	0.996
91.7%	0.833	0.811	0.823	0.743	0.738	0.701	0.689	0.669	0.481	0.863	0.894	0.845
97.2%	0.515	0.512	0.525	0.447	0.462	0.456	0.448	0.373	0.284	0.515	0.569	0.525

Confirmation that these shapes are appropriate for the North Anna spent fuel pool criticality analysis will be performed using guidance from NUREG/CR-6801:

> *Although the end effect is dependent upon many factors, it is primarily dependent on the slope of the burnup profile near the ends of the fuel, which is influenced by the fuel burnup, assembly design, and reactor operating environment.*

For PWR fuel, depletion conditions (moderator temperature) at the top of the fuel cause the top of the fuel to be more reactive, so the portion of the burnup profile of interest for North Anna is the burnup profile at the top of the fuel. End of cycle axial burnup shapes from the fuel management analysis for North Anna Unit 1 cycles 20 through 24 and North Anna Unit 2 cycles 20 through 23 used to determine the fraction of the burnup at the top of the core. Figure 8.2 compares the relative burnup in the top 1/6 of the fuel to the analogous value for the NUREG/CR-6801 shapes. Figure 8.3 has the same comparison for the top 1/4 of the fuel. In all cases, the top of fuel relative burnup in the NUREG/CR-6801 shapes conservatively bounds the North Anna shapes.

Axial blankets (reduced enrichment near the top and bottom ends of the fuel rods) have not been used. Relative to an un-blanketed fuel assembly, axial blankets reduce the reactivity of the fuel assembly in the axial region where they are present. If axial blankets are used in the future, ignoring them in the blanketed fuel assemblies is conservative, provided that the fuel enrichment used for comparison to the loading curve is the highest enrichment of any axial zone in the fuel assembly.

North Anna units have never had significant burnup with control rods inserted a significant depth. This will be explored in more detail in Section 8.9.2. The NUREG/CR-6801 axial burnup shape for the range of 14 to 18 GWd/T comes from an assembly burned with significant control rod insertion. The depletion analysis of the pool is performed at 10, 20, 30, 38, and 44 GWd/T which implicitly assumes that the burnup requirements at the burnup in between can be interpolated. This would not be correct if the analysis required use of the 14 to 18 GWd/T shape. If in the future analysis is needed with burnup between 10 and 20 GWd/T then the NUREG 18 to 22 GWd/T shape can be used since it is more appropriate for North Anna.

Uniform burnup shapes are required to be considered as well. Uniform burnup shapes are often limiting at burnups less than 20 GWd/MTU, which makes the low burnup NUREG shapes of little importance.

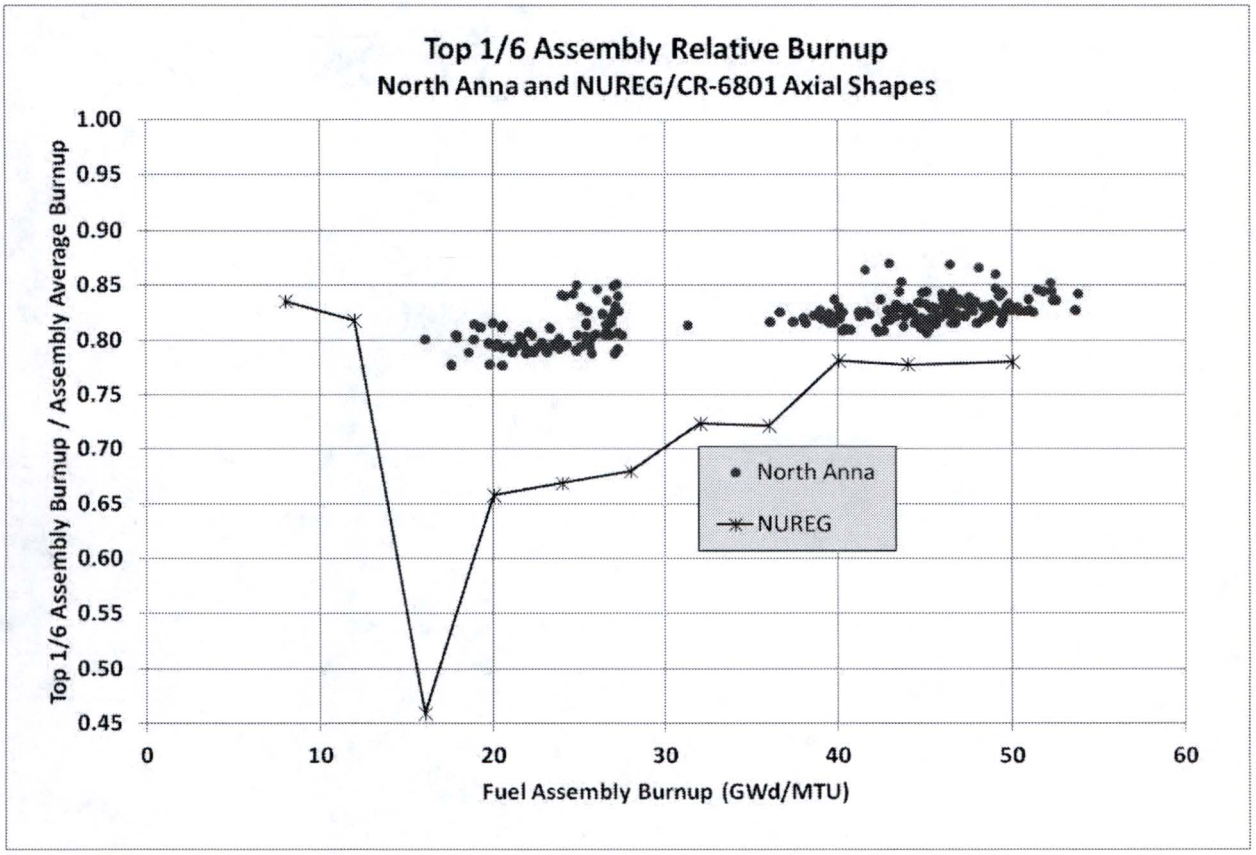

Figure 8.2: Comparison of the Average Burnup in the Top Sixth of the Fuel to Burnup Shapes

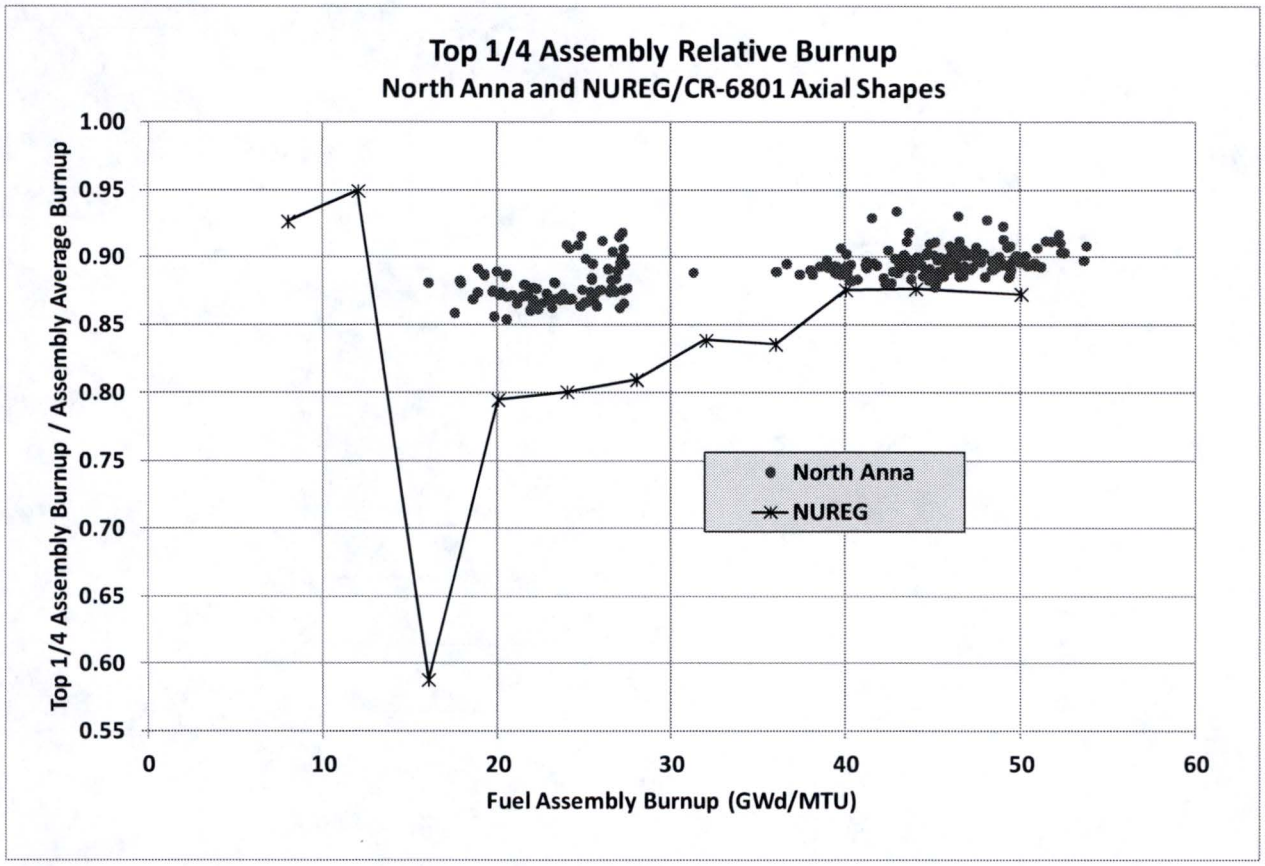

Figure 8.3: Comparison of the Average Burnup in the Top Quarter of the Fuel to Burnup Shapes

8.6 Bounding Moderator and Fuel Temperature

The moderator temperature of each of the 18 nodes is calculated. The fuel assembly average power for this calculation is BARAP times the core average assembly power. The axial power profile is the appropriate NUREG normalized burnup profile (Table 8.4). With the fuel assembly power and the axial power profile known, the nodal average moderator enthalpy (average of the enthalpy at the upper and lower boundaries of the node) is determined for each of the 18 axial nodes starting from the core inlet and integrating the enthalpy added in each successive node. The enthalpy calculation uses a bounding low moderator flow rate and a conservative inlet temperature (Table 8.3). Moderator temperature is determined from moderator enthalpy using a pressure of 2250 psia.

Fuel temperatures likewise are determined by node using the nodal moderator temperature and fuel temperature difference from the moderator temperature which is dependent on the nodal fuel power. The fuel temperature data was taken from the SIMULATE data used by Dominion for its licensed fuel management analysis. [22] Fuel temperatures are pellet average, which bound the resonance effective fuel temperatures. Fuel temperature data (a function of power and burnup) used for this calculation is also integrated to the burnup of interest to obtain an appropriate depletion average temperature rather than a point value at a particular burnup.

Table 8.5 and 8.6 provide the limiting moderator temperature and density as well as limiting fuel temperature for 10, 20, 30, 38, and 44 GWd/MTU. Note that for the 10 GWd/MTU case the uniform shape is assumed. For uniform shapes the same process is used, but the burnup profile is 1.0 for all 18 nodes.

Table 8.5: Limiting Depletion Parameters by Node for 10, 20, and 30 GWd/MTU

Burnup	10 GWd/MTU (Uniform)				20 GWd/MTU				30 GWd/MTU			
Depletion Days	172				343				515			
BARAP	1.440				1.440				1.440			
Axial Node	Mod. Temp. (K)	Mod. Den. (g/cc)	Fuel Temp. (k)	Power (MW/T)	Mod. Temp. (K)	Mod. Den. (g/cc)	Fuel Temp. (k)	Power (MW/T)	Mod. Temp. (K)	Mod. Den. (g/cc)	Fuel Temp. (k)	Power (MW/T)
1 Bottom	563	0.746	987	58.2	563	0.747	872	38.9	562	0.747	854	38.0
2	566	0.740	990	58.2	565	0.742	988	60.2	565	0.742	959	56.3
3	570	0.733	993	58.2	569	0.735	1036	67.0	569	0.735	1006	62.6
4	573	0.726	997	58.2	573	0.727	1018	63.7	572	0.728	1022	64.2
5	576	0.720	1000	58.2	576	0.720	1006	61.3	576	0.721	1028	64.5
6	579	0.713	1003	58.2	580	0.713	1007	61.0	579	0.713	1031	64.4
7	583	0.706	1006	58.2	583	0.705	1016	62.0	583	0.705	1032	64.2
8	586	0.698	1009	58.2	586	0.697	1031	63.8	586	0.697	1033	63.9
9	589	0.691	1012	58.2	590	0.689	1045	65.3	589	0.689	1035	63.7
10	592	0.684	1015	58.2	593	0.681	1054	66.1	593	0.681	1038	63.7
11	595	0.676	1018	58.2	596	0.672	1059	66.4	596	0.673	1042	63.8
12	597	0.668	1021	58.2	599	0.663	1062	66.3	599	0.664	1046	63.8
13	600	0.660	1024	58.2	602	0.654	1062	65.8	602	0.655	1048	63.8
14	603	0.652	1026	58.2	605	0.644	1055	64.4	605	0.646	1047	63.3
15	605	0.644	1029	58.2	608	0.635	1036	61.1	607	0.637	1038	61.7
16	608	0.635	1032	58.2	610	0.627	999	54.3	610	0.628	1005	56.6

Burnup	10 GWd/MTU (Uniform)				20 GWd/MTU				30 GWd/MTU			
Depletion Days	172				343				515			
BARAP	1.440				1.440				1.440			
17	610	0.626	1034	58.2	612	0.619	922	39.0	612	0.620	931	43.0
18 Top	613	0.617	1036	58.2	613	0.615	799	21.7	613	0.615	832	26.9

Table 8.6: Limiting Depletion Parameters by Node for 38 and 44 GWd/MTU

Burnup	38 GWd/MTU				44 GWd/MTU			
Depletion Days	675				803			
BARAP	1.391				1.355			
Axial Node	Mod. Temp. (K)	Mod. Den. (g/cc)	Fuel Temp. (k)	Power (MW/T)	Mod. Temp. (K)	Mod. Den. (g/cc)	Fuel Temp. (k)	Power (MW/T)
1 Bottom	562	0.747	840	37.1	562	0.747	831	36.5
2	565	0.742	933	52.7	565	0.742	925	51.7
3	568	0.736	978	58.8	568	0.736	968	57.4
4	572	0.729	997	60.8	571	0.730	986	59.2
5	575	0.722	1005	61.4	575	0.723	993	59.7
6	579	0.714	1010	61.5	578	0.716	996	59.7
7	582	0.707	1013	61.5	581	0.709	998	59.5
8	585	0.699	1015	61.3	584	0.701	1001	59.5
9	589	0.691	1018	61.3	588	0.694	1003	59.4
10	592	0.683	1021	61.2	591	0.686	1006	59.4
11	595	0.675	1024	61.2	594	0.679	1010	59.5
12	598	0.667	1026	61.1	596	0.671	1013	59.5
13	601	0.659	1028	61.0	599	0.663	1016	59.5
14	603	0.650	1027	60.6	602	0.654	1017	59.3
15	606	0.641	1021	59.5	605	0.646	1014	58.6
16	609	0.633	999	56.1	607	0.638	992	55.3
17	611	0.626	941	46.3	609	0.630	925	44.4
18 Top	612	0.620	841	29.5	611	0.625	825	28.1

8.7 Specific Power and Operating History

When parameters are in conflict, DSS-ISG-01-2010 [4] states:

> *"It may be physically impossible for the fuel assembly to simultaneously experience two bounding values (i.e., the moderator temperature associated with the "hot channel" fuel assembly and the minimum specific power). In those cases, the application should maximize the dominant parameter and use the nominal value for the subordinate parameter. Where this is done, the application should describe and justify the parameters used."*

The reactivity sensitivity to the moderator temperature/density and fuel temperature is much larger than the sensitivity to the specific power. Therefore, highest specific power matching that used to generate the temperatures is used. The depletion is done as a continuous full power burn. A continuous burn is the recommendation of NUREG/CR-6665. [41] NUREG/CR-6665 also recommended additional margin to cover additional reactivity due to low power at end of life. Rather than to add margin, low power at end of life was specifically analyzed. The atom densities used in most of the analysis did not include this low power operation, rather the low power at end of life was done in combination with grid growth, and clad creep and a net effect was included as a bias in the analysis. The results of this analysis are provided in Section 10.4.7.

The specific power used was calculated using the bounding power (2940 MWth) established in Section 8.4, the Burnup Averaged Relative Assembly Power (BARAP) established in Section 8.2, the axial burnup profile for the given node, and the MTU in the core. Isotopic content is a weak function of specific depletion power given the same fuel and moderator temperature, so a typical value of core MTU (0.463 MTU/assembly*157 assemblies) is used. Although the specific powers used are by node and with power peaking, for perspective the core average specific power is 40.45 MW/MTU.

Table 8.5 and 8.6 gives the specific power per node.

8.8 Bounding Assembly Design for Depletion and Rack Criticality

Fuel assembly design information is given in Section 4. North Anna fuel (historical and current) has these same nominal (cold) features:

- Array (17x17)
- Assembly pitch (21.50 cm)
- Rod pitch (1.26 cm)
- Active fuel length (365.76 cm)
- Fuel rods/assembly (264)
- Guide tubes (24)
- Instrument tubes (1)
- Fuel pellet diameter (0.8192 cm)
- Fuel clad OD (0.95 cm)
- Fuel clad ID (0.836 cm)

A few of features vary among the assembly designs:

- Stack Density (combination of density, dish, and chamfer)
- Grids (Use of intermediate flow mixers, grid material, and grid volume)
- Guide tube / instrument tube diameter (all similar)
- Clad alloy (all are Zr based)
- IFBA rods

The clad alloy has a very small effect on the spectrum and therefore very little importance to the depletion analysis. All the depletion analysis uses the SCALE Zircaloy-4 elemental mix. The reactivity effect of clad alloy variations was calculated for the new fuel storage area in Table 7.1. Modeling clad as Zircaloy-4 results in in-rack k 0.0003 or more higher than newer clad materials with full density water. Zircaloy-4 was replaced by newer clad materials in North Anna fuel designs over 20 years ago (Section 4.1). SFP rack calculations for Region 1 and 2 used Zircaloy-2 to represent the clad material. A sensitivity case for Region 1 indicated very little reactivity difference between the two materials (0.00008 dk lower using Zircaoly-2).

The combination of clad material results shows that modeling fuel clad as Zircaloy-2 is conservative for fuel designs used over the last 20 years. For older fuel designs, the slight non-conservatism of the clad modeling is insignificant when compared to other modeling conservatism. In particular, the fuel density of the older designs is more than 1% lower than the fuel density used in the analysis. The density effect on k is more than an order of magnitude larger than the clad effect (fuel density tolerance results are in Sections 9 and 10).

The following subsections cover the selection of the conservative stack density, grids, and guide tubes and IFBA. IFBA rods will be discussed with the burnable absorbers in Section 8.9. Tolerance cases in Sections 9 and 10 show that increased fuel density increases fuel reactivity in the SFP. A bounding high fuel density will be used. The maximum and minimum grid volume will be considered both for depletion effects and for SFP reactivity at unborated and borated conditions. Although the guide tube assessment is not performed at all storage configurations and conditions, guide tube design differences are small and the calculated effect on rack k is small. The depletion effect of IFBA rods will be discussed with the burnable absorbers in Section 8.9. No credit for IFBA is taken in the SFP rack k calculations..

8.8.1 Stack Density

Table 8.7 contains batch average fuel density data for fuel batches 1-27 (Unit 1) and 1-26 (Unit 2). Table 8.7 shows the net density (As-built density x (1-effective dish fraction)) which is also known as the stack density. A stack density of 95.5% of theoretical density of UO_2 is used since it is sufficient to bound all historical data and allow for slightly denser fuel in the future.

8.8.2 Grids

Grids displace water and harden the neutron spectrum during depletion, increasing Pu production (and k in the spent fuel pool). In the spent fuel pool, grids displace water and generally decrease k, except in highly borated conditions. In order to capture the effect of grids on both parts of the analysis, the depletion will be done with maximum grid volume. The final k analysis also uses the maximum grid volume but adds a bias to correct to the minimum grid volume for cases in which minimum grid volume increases k.

Table 4.1 contains grid data for the historical fuel designs at North Anna. The bottom Inconel grid may be ignored because it is a strong neutron absorber and it is in an unimportant neutronic region for depleted fuel. Depleted PWR fuel is more reactive in the top of the fuel because there is lower burnup in the top of the fuel and it depletes in a harder neutron spectrum (hotter moderator temperature).

With maximum grid volume, Zircaloy grids displace the equivalent of [ ]^{A} of the water surrounding the fuel rods if the grids are assumed to displace only water around fuel rods. Similarly, with minimum grid volume the displacement is equivalent to [ ]^{a,c}. A fraction of the

grid water displacement occurs around guide thimbles (25 of 289 lattice locations); however, for simplicity all grid water displacement will be associated with fuel rod lattice locations.

To verify that depletion with the maximum grid volume is conservative several cases were analyzed. The analysis was performed using one axial region in the spent fuel pool model. The depletion analysis was done for node 17 with the limiting depletion parameters. In order to save run time only 28 key isotopes were used in this analysis. All the spent fuel pool cases use a 4-out-of-4 loading of the pool at zero ppm soluble boron. The TRITON depletions were run with 0% and [ ]^{A} VF Zr grids (VF of water around fuel rods)

The results of the analysis are shown on Table 8.8 for Region 2 storage. Depletion with maximum Zr grids increases k by about 70 pcm at 10 GWd/MTU and by about 200 pcm at 40 GWd/MTU. It is conservative to deplete with maximum Zr grids. Table 8.8 also shows that at zero soluble boron and 10 GWd/MTU it is conservative to ignore the grids in both the depletion and spent fuel pool calculation. However, it is unrealistic to have no grids, and modeling maximum grid volume during the depletion increased k. **Therefore, for the North Anna criticality analysis the depletions are done with the maximum grid volume.**

Table 8.7: North Anna Pellet Density

Batch	Fuel Density (% Theoretical)	Dish and Chamfer (Volume %)	Stack Density (% Theoretical)	Fuel Density (% Theoretical)	Dish and Chamfer (Volume %)	Stack Density (% Theoretical)
	North Anna Unit 1			North Anna Unit 2		
1	94.96	1.207	93.81	94.565	1.207	93.42
2	95.06	1.207	93.91	94.72	1.207	93.58
3	95.06	1.207	93.91	94.619	1.207	93.48
4	94.55	1.207	93.41	94.914	1.207	93.77
5	94.579	1.207	93.44	94.879	1.207	93.73
6	94.58	1.207	93.44	95.145	1.207	94.00
7 (7A)	94.89	1.207	93.74	95.176	1.207	94.03
7B				95.062	1.207	93.91
8A	95.022	1.207	93.88	95.263	0.978	94.33
8B	94.847	1.207	93.70	95.14	0.978	94.21
9A	95.151	0.978	94.22	95.123	1.208	93.97
9B	95.011	0.978	94.08	95.341	1.208	94.19
10A	95.196	1.208	94.05	95.361	1.208	94.21
10B	95.358	1.208	94.21	95.39	1.208	94.24
10C	95.194	1.208	94.04			
11A	95.543	1.208	94.39	95.419	1.208	94.27
11B	95.514	1.208	94.36	95.365	1.208	94.21
12A	95.476	1.208	94.32	95.331	1.208	94.18
12B	95.402	1.208	94.25	95.389	1.208	94.24
13A	95.474	1.208	94.32	95.604	1.208	94.45
13B	95.656	1.208	94.50	95.384	1.208	94.23
14A	95.353	1.208	94.20	95.267	1.208	94.12
14B	95.513	1.208	94.36	95.446	1.208	94.29
15A	95.67	1.208	94.51	95.731	1.208	94.57
15B	95.717	1.208	94.56	95.571	1.208	94.42
15C	96.41	1.24	95.21			
16A	95.767	1.208	94.61	95.573	1.208	94.42
16B	95.679	1.208	94.52	95.554	1.208	94.40
17A	95.441	1.208	94.29	95.61	1.208	94.46
17B	95.761	1.208	94.60	95.667	1.208	94.51
18A	95.619	1.208	94.46	95.785	1.208	94.63
18B	95.601	1.208	94.45	95.864	1.208	94.71
19A	95.761	1.208	94.60	96.278	1.24	95.08
19B	95.626	1.208	94.47	96.434	1.24	95.24
20A	95.87	1.24	94.68	95.16	1.24	93.98
20B	95.76	1.24	94.57	96.12	1.24	94.93
21A	96.24	1.24	95.05	96.21	1.24	95.02

Batch	Fuel Density (% Theoretical)	Dish and Chamfer (Volume %)	Stack Density (% Theoretical)	Fuel Density (% Theoretical)	Dish and Chamfer (Volume %)	Stack Density (% Theoretical)
21B	96.09	1.24	94.90	96.24	1.24	95.05
22A	95.93	1.24	94.74	95.98	1.24	94.79
22B	95.93	1.24	94.74	96.27	1.24	95.08
23A	96.44	1.24	**95.24**	96.35	1.24	95.16
23B	96.4	1.24	95.20	96.31	1.24	95.12
24 (24A)	96	1.24	94.81	96.03	1.24	94.84
24B				96.07	1.24	94.88
25A	95.619	1.2074	94.46	95.51	1.2074	94.36
25B	95.561	1.2074	94.41	95.964	1.2074	94.81
25C				95.449	1.2074	94.30
26A	95.796	1.2074	94.64	95.857	1.2074	94.70
26B				95.901	1.2074	94.74
26C				95.647	1.2074	94.49
27A	95.672	1.2074	94.52			
27B	95.644	1.2074	94.49			

Table 8.8: Effect of Depleting with Maximum Volume Zirconium-based Grids

Enrichment (wt% U-235)	Burnup (GWd/MTU)	Depletion Grid Volume Fraction	Spent Fuel Pool Grid Volume Fraction	k	sigma
2.5	10	0	0	0.9714	0.00008
2.5	10	0	[ ]^{a,c}	0.9701	0.00008
2.5	10	[ ]^{A}	[ ]^{a,c}	0.9708	0.00008
4.5	40	0	[ ]^{a,c}	0.9531	0.00008
4.5	40	[ ]^{A}	[ ]^{a,c}	0.9551	0.00008

8.8.3 Guide Tube Dimensions

The difference in guide tube and instrument tube dimensions between the recent fuel designs (AREVA and RFA) is small. However, the RFA guide thimble displaces more water and will tend to increase spent fuel reactivity due to spectrum hardening (similar to the grid effect).

Table 8.9 shows the effect of depletion using the guide tube dimensions from the AREVA design versus the RFA design.

The RFA test cases show that the guide tube dimension change has a small effect such that a slightly more reactive fuel isotopic content is more than offset by water displacement in the spent fuel pool rack model. Therefore, **the AREVA design guide tubes are used in both the depletion and spent fuel pool analysis.**

Table 8.9: Effect of Depleting with Different Guide Tube Dimensions

Enrichment (wt% U-235)	Burnup (GWd/MTU)	Depletion Guide Tube	Spent Fuel Pool Guide Tube	k	sigma
3.0	20	AREVA	AREVA	0.9411	0.00008
3.0	20	RFA	RFA	0.9407	0.00008
3.0	20	RFA	AREVA	0.9415	0.00008

8.9 Bounding Fuel Assembly Inserts for Depletion Analysis

This section covers the various fuel inserts used at North Anna. These inserts include burnable absorbers, sources, control rods, vibration suppression damping assemblies, and in-core measurement thimbles. Although not an insert, this section also addresses IFBA. North Anna has also used "thimble plugs" to reduce the bypass flow, but since these are short and do not reach the active fuel they have no impact on the depletion analysis.

8.9.1 Burnable Absorbers and Sources

Burnable absorbers (BPRA, IFBA, WABA, Pyrex BP, gadolinium) harden the neutron spectrum during depletion by neutron absorption and in some cases water displacement, increasing Pu production and k in the spent fuel pool. In the spent fuel pool, residual poison from integral absorbers is not credited and removable absorber assemblies (WABA, BPRA, Pyrex BP) are not included in the spent fuel pool model. (Tables 9.1, 10.4, and 10.14 all show a negative reactivity for displacing water at the guide tubes so modeling the burnable absorbers as removed is conservative even if all the boron were depleted.)

The burnable absorbers used at North Anna are described in Section 4.2. BPRA history effects are bounded by leaving the maximum BPRA (24 rods with 3.0 w/o B_4C) inserted for the entire fuel assembly depletion. The BPRA are modeled as full length (every node). BPRA absorber length has been less than full length (a cutback region) since North Anna Unit 1 Cycle 13.

However, reducing BPRA neutron absorption softens the neutron spectrum, so modeling the BPRA as full length is conservative.

The Pyrex burnable absorber is similar to the BPRA burnable absorber. They both have the same outer clad diameter so they displace the same amount of water. The BPRA B^{10} linear loading per rodlet is slightly higher ([ ]^{A} versus 6.2 mg/cm Pyrex). The cladding on the Pyrex is stainless steel and is Zircaloy for the BPRAs. Due to having the same water displacement, the effect on the depletion would be similar. However, Pyrex burnable absorbers will not be used in the future so the depletion history of the old Pyrex bearing fuel assemblies is known. The maximum number of Pyrex rodlets used in North Anna fuel is 20 as compared to the 24 rodlet BPRA assumed in the depletion analysis. For these reasons, depleting with 24 fingered BPRA's bounds depletion with Pyrex.

Depletion with WABA is also bounded by depletion with BPRA. The maximum B^{10} loading is 6.0 and [ ]^{A} mgB^{10}/cm for WABA and BPRA, respectively. Both have the same clad outer diameter and use Zircaloy clad. The key difference is WABA is annular, open to the primary coolant and therefore displaces less water. NUREG/CR-6761 evaluations confirm that the displacement of water is significant to the delta k of depletion associated with burnable absorbers. [42]

Integral Fuel Burnable Absorber (IFBA) also hardens the neutron spectrum but less than 24 BPRA because it does not displace water. IFBA is the current burnable absorber used at North Anna and is described in Section 4.2.1 with the dimensions given on Table 4.5. It is possible that an assembly has a source rod inserts as well as IFBA. The maximum number of source rod fingers is 6. To confirm that the maximum loading of IFBA rods ([ ]^{a,c} at 1.5x) plus 6 source fingers is bounded by the 24 BPRA, depletion analysis and calculation of the spent fuel pool k were performed for a range of burnups. Each depletion was performed using the node 17 depletion parameters. Node 17 is typical of a node in the upper 1/4 of a fuel assembly, which is the most important region for PWR spent fuel pool criticality with burnup credit. IFBA is modeled as a thin layer of ZrB_2 with the volume fraction of B-10 set to obtain the correct loading. Secondary source rods are modeled as solid stainless steel rods with a 0.484 cm radius.

Table 8.10 shows the results of the burnable absorber depletions for fuel stored in the NAPS 4-out-of-4 spent fuel pool rack model at nominal conditions (fuel centered in the storage cell, 68 F

water temperature, 0 ppm soluble boron). In order to save run time only the 28 key burnup credit nuclides are used for this sensitivity study. The results show that the BPRA depletion produces the highest spent fuel pool k.

Table 8.10: Verification of Limiting Burnable Absorber Type for Burnup Credit

Enrichment (wt% U-235)	Burnup (GWd/MTU)	Burnable Absorber and Inserts	k	sigma
2.5	10	24 BPRA	0.9708	0.00008
2.5	10	[ ]^{a,c} IFBA plus 6 source rodlets	0.9699	0.00008
3.0	20	24 BPRA	0.9581	0.00008
3.0	20	[ ]^{a,c} IFBA plus 6 source rodlets	0.9542	0.00008
3.0	20	None	0.9418	0.00008
3.7	30	24 BPRA	0.9562	0.00008
3.7	30	[ ]^{a,c} IFBA plus 6 source rodlets	0.9504	0.00008
4.5	40	24 BPRA	0.9551	0.00008
4.5	40	[ ]^{a,c} IFBA plus 6 source rodlets	0.9479	0.00008
4.5	40	None	0.9389	0.00008

It is possible to use both WABA and IFBA in the same fuel assembly. The cases in Table 8.11 confirm that depletion with maximum IFBA ([ ]^{a,c} rods) plus 8 BPRA or less is bounded by the 24 BPRA @ 3 w/o B_4C depletion. BPRA was used instead of WABA for convenience, however, BPRA are conservative for WABA so this study also shows that [ ]^{a,c} IFBA plus 8 WABA is covered. The analysis for Table 8.11 was done differently than Table 8.10 so the k values should not be compared. Single node (Node 15) representative isotopic content was used in the full rack model with all TRITON isotopes retained for the analysis in Table 8.11. The low burnup (10 GWd/MTU) cases with no credit for residual IFBA show that the 24 BPRA depletion is not bounding. However, there are several mitigating reasons to accept this modest (0.0015 Δk) non conservatism for the purpose of determining the bounding IFBA/BPRA combination.

1) Although IFBA is not directly credited in this analysis, the worth of residual IFBA is large at low burnup, At 10 GWd/MTU residual IFBA worth (negative reactivity) is over 20 times the increase in k due to the effect of combined BP ([ ]^{a,c} IFBA and 8 BPRA).
2) IFBA cycles have substantially less soluble boron than the 1100 ppm bounding soluble boron. In Table 8.2, Cycles 23 and 24 are IFBA transition cycles.

3) In practice, a fuel assembly requiring maximum BPRA loading for cycle design would not be of low enough enrichment to store in Region 2 with only 10 GWd/MTU burnup (≤ 2.4 w/o U-235; see Figure 10.9). Fuel management would require any fuel assembly of high enough enrichment to require maximum burnable absorber to be depleted for more than one cycle before being stored in Region 2.

The 44 GWd/MTU [ ]^{a,c} IFBA plus 12 BPRA cases also show that the 24 BPRA depletion is bounding. Depleting with 12 instead of 8 BPRA is conservative for the purpose of this [ ]^{a,c} IFBA plus 8 BPRA confirmation. All cases (10, 20, and 44 GWd/MTU), with partial credit for residual IFBA (50% or less) show the spent fuel pool rack k is higher for depletion with 24 BPRA than with [ ]^{a,c} IFBA and 8 BPRA. Therefore, fuel depleted with up to [ ]^{a,c} IFBA in combination with up to 8 BPRA (or WABA) is bounded by the limiting fuel depletion using 24 BPRA.

Table 8.11: Effect of Depletion with Combined IFBA and BP

Enrichment (wt% U-235)	Burnup (GWd/MTU)	Burnable Absorber and Inserts	k	sigma	Delta k
2.45	10	24 BPRA	0.9519	.00005	N/A
2.45	10	[ ]^{a,c} IFBA plus 4 BPRA	0.9512	.00006	0.0007
2.45	10	[ ]^{a,c} IFBA plus 8 BPRA	0.9534	.00005	-0.0015
2.45	10	[ ]^{a,c} IFBA plus 8 BPRA	0.9113*	.00006	0.0406
3.075	20	24 BPRA	0.9384	.00006	N/A
3.075	20	[ ]^{a,c} IFBA plus 8 BPRA	0.9364	.00006	0.0020
5.0	44	24 BPRA	0.9141	.00005	N/A
5.0	44	[ ]^{a,c} IFBA plus 12 BPRA	0.9110	.00005	0.0031

* The SFP model includes the residual B10 in the IFBA from the Triton depletion.

Although Gadolinium has not been used at North Anna it may be used in the future. Studies have shown that Gadolinium burnable absorbers can be conservatively neglected [44, 30, 9]. The residual content of Gadolinium and the displacement of fissile material (UO_2) has more negative reactivity worth than the positive worth due to harder spectrum depletion, regardless of the burnup of the fuel assembly. The loading curves based on 24 BPRA depletion does not credit any reduction in fissile material due to Gadolinium and includes the greater spectrum hardening effect of the BPRA water displacement. If Gadolinium fuel is used, the planar averaged enrichment will be used for determination of the loading curve burnup requirement.

8.9.2 Control Rod Insertion History

Control rod position is logged daily for use in core follow calculations. Representative cycle average control rod insertion has been determined using control rod position and daily burnup data from North Anna cycles 19 to 24. Control rod insertion is integrated over burnup to calculate the average steps of insertion. A bank position of 225 steps or greater is fully withdrawn. Control rod insertion cannot occur with BPRA present.

Cycle average D-bank insertion (steps) is listed in Table 8.12. A step is 5/8 of an inch. Each node in the axial model is 8 inches. Maximum average insertion is less than 2 steps, which is approximately 16% of the top node height (less than 1% of the fuel stack length). D-bank insertion involves only 2% of fuel assemblies in the core (8 of 157 fuel assemblies residing in D-bank locations). Further, the limiting fuel assembly depletion condition includes the use of 24 BPRA. BPRA and control rod insertion is mutually exclusive. Water displacement by BPRA is roughly 6 times the water displacement of an RCCA inserted 2 steps because the BPRA occupies 100% of the top node height. For these reasons, control rod insertion will be ignored.

Table 8.12: North Anna Control Rod Insertion History

Cycle	Unit 1 Average D-bank insertion (steps)	Unit 2 Average D-bank insertion (steps)
19	0.4	0.9
20	0.4	0.8
21	0.8	1.6
22	1.2	0.7
23	**1.7**	0.7
24	0.7	-

8.9.3 Vibration Suppression Damping Assemblies

Vibration suppression damping assemblies (VSDA) are solid zircaloy rods inserted into the guide tubes. The outer diameter of the VSDA rods is the same as the BPRA so it displaces the same amount of water. Due to the displacement of water the VSDA do harden the neutron spectrum and increase spent fuel pool k. But, since the VSDA do not have any absorbing material they do not harden the spectrum as much as the BPRA so they are bounded by the depletion analysis that assumes 24 BPRA.

8.9.4 In-core Measurement Thimble in the Instrument Tube

In the North Anna core, 50 of 157 assembly locations contain an in-core measurement thimble in the center instrument tube. The in-core measurement thimble is a thin wall tube that displaces water and thereby hardens the neutron spectrum during depletion and increases k in the spent fuel pool. The in-core measurement thimble displaces roughly half of the water in the instrumentation tube. The in-core measurement thimble material (ASTM A213 Type 316 stainless steel) occupies about [ ]^{a,c} of the instrument tube inner volume and the [ ]^{a,c} is void space inside the in-core measurement thimble. To investigate the effect of a partially voided instrument tube, two of the Table 8.10 cases are re-depleted with the new homogenized material (water, void, and stainless steel) inside the instrument tube.

Table 8.13 shows the effect of depletion with an in-core measurement thimble in the instrument tube on the spent fuel pool k using Node 17 depleted fuel isotopic data. The results show that depletion with an in-core measurement thimble slightly increases spent fuel pool k. Both sensitivity cases produce a best estimate increase of about 0.0003 Δk. A bias of 0.00055 (includes 2 RSS uncertainty) applied to all depleted fuel will conservatively bound the in-core measurement thimble effect.

Table 8.13: Effect of Depletion with the Instrument Thimble in the Instrument Tube

Enrichment (wt% U-235)	Burnup (GWd/MTU)	Inside Instrument Tube	k	sigma	Delta k
3.0	20	Water	0.9581	.00008	N/A
3.0	20	Water plus Instrument Thimble	0.9584	.00008	0.0003
4.5	40	Water	0.9551	.00008	N/A
4.5	40	Water plus Instrument Thimble	0.9554	.00008	0.0003

8.10 Summary of Depletion Analysis Model

For burned fuel, the isotopic content comes from executing the t5-depl module of TRITON, which is a sequence of SCALE 6.0. The cross section library used is the 238 group ENDF/B-VII library. The model consists of an assembly in the core geometry where all the fuel pins are

depleted as a single fuel mixture. The guide tubes contain BPRAs with the maximum boron loading, which is 6.8 mg B^{10}/cm. It has been shown that this BPRA modeling covers WABAs, IFBAs, Pyrex, and gadolinia. Further, it has been shown that the 24 finger BPRA model covers IFBA plus secondary sources and vibration suppression damping assemblies (VSDA). Finally, it also covers IFBA with a reduced number of BPRA or WABA fingers. At this time, only credit for 8 finger BPRA or WABAs have been analyzed to be acceptable with any IFBA loading.

The TRITON depletions are run with 3000 generations and 3000 neutrons per generation and time steps of 10, 40, 50, 50, and 50 days are used for the low burnups followed by time steps less than 70 days. The burnable absorbers are depleted with the constant flux option. The depletion analysis follows the maximum number of isotopes permitted by SCALE (addnux=3). The TRITON module is used to decay the isotopes for 5 days for the peak reactivity and 3 years for cooling time credit.

The fission gases are reduced consistent with Table 6.3, but otherwise all isotopes in the fuel generated by TRITON are used in the pool model. The TRITON assembly model includes the maximum grid volume homogenized with the water around the fuel pins. The in-core measurement thimbles are not modeled in the instrument tube, but a reactivity bias of 0.00055 is used to cover this condition. The limiting fuel design has been shown to be the AREVA fuel design with a stack density of 95.5% of the theoretical density of UO_2. Other limiting conditions for the model are:

- Burnup Averaged Relative Assembly Power (bounding high, Table 8.1 and Figure 8.1)
- Burnup averaged soluble boron (1100 ppm)
- Bounding moderator temperature based on conditions shown at the bottom of Table 8.3. The temperatures are burnup and node dependent. Examples of the values for particular burnups are found on Tables 8.5 and 8.6.
- Bounding axial burnup shapes from NUREG/CR-6801 are used to determine the bounding fuel and moderator temperatures. At low burnups analysis with a uniform axial burnup is also performed.

- Bounding fuel temperature based on conditions shown at the bottom of Table 8.3. The temperatures are burnup and node dependent. Examples of the values for particular burnups are found on Tables 8.5 and 8.6.

- Control rod insertion history was reviewed and it was shown that the mutually exclusive BPRA depletion is conservative.

9 Region 1 Analysis

Region 1 allows fuel up to 5 %wt U-235 to be stored. No credit for burnup or absorbers is taken.

All of the rack modules in the North Anna spent fuel pool are identical. In order to allow for fresh fuel and once burned fuel, a portion of the racks are checker boarded with empty cells. These checker boarded areas are called Region 1. The Region 1 blocks can be anywhere in the pool as long as they meet the following four requirements:

1) Region 1 blocks must have empty cells at the outer corners.

2) At least two Region 2 rows must exist between Region 1 blocks.

3) Each Region 1 block shall be fully contained in a single rack module where a rack module is adjacent to another rack module. This requirement eliminates the need to perform an analysis postulating rack-to-rack misalignment (seismic event or installation) such that part of the checkerboard would not be properly aligned.

4) The spent fuel cells AA21, AA22, BB21, BB22, CC21, and CC22 may not be part of a Region 1 block due to the new fuel elevator. (See Figure 9.7 for location of these cells.)

Note that the outside row of a Region 1 block does not have an empty cell on all sides of the Region 1 assembly. For the outside row only three of the sides of the Region 1 cell are empty. Region 1 is sufficiently subcritical such that the increased reactivity for the edge assemblies is acceptable. This is demonstrated in the interface analysis found in Section 11. This is also the reason for the first requirement in the above list (empty cells at the outer corners). If the corner of a Region 1 block were a Region 1 assembly, it would have empty cells on only two of its faces and then the interface analysis would not be acceptable.

This section covers the analysis of an infinite area of Region 1. Section 11 covers the interface with Region 2.

9.1 Rack Model

Region 1 is a checkerboard arrangement with every other cell maintained empty of fuel and non-fuel items with the exception of a control rod. Analysis of Region 1 assumes fresh 17x17 fuel with maximum U-235 enrichment (5.0 w/o, all fuel pins, all axial regions of the fuel stack), no burnable absorbers, and no Boraflex credit.

Figure 9.1 shows the planar view with dimensions as modeled for the North Anna spent fuel pool.

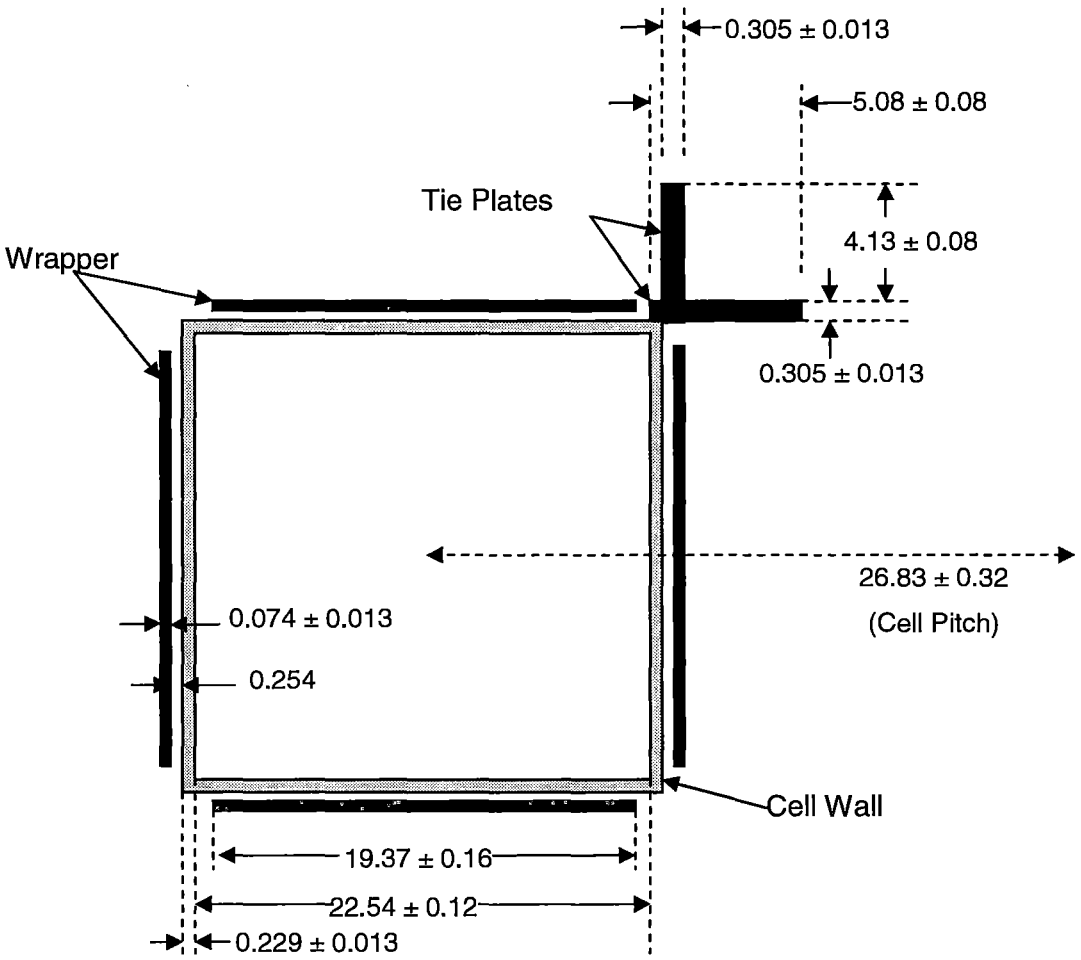

Figure 9.1: SFP Rack Model Planar Dimensions (All dimensions in cm and not to scale)

The following modeling simplifications are made:

- Water axial reflectors are used above and below the active fuel. This was confirmed for the new fuel storage area (See Section 7.1.4) and has been shown to be conservative in past analyzes. [9, 45]
- The ½ inch diameter vent hole, which is present near the top of each wrapper, is ignored. These holes are small and represent far less material than the upper and lower poison stops, which are also omitted. This simplification is verified to be acceptable later in this section.
- The wrapper width modeled does not include the curved edges, which are more than 0.1 inches on each side. Therefore, if it is conservative to omit some stainless steel, no wrapper width tolerance is needed. This simplification is verified via a wrapper thickness tolerance case.
- Tie plate length uncertainty is not modeled because the tie plates extend well below and above the active fuel region. The tie plates are modeled starting at the bottom of the fuel assembly (approximately 8 cm below the active fuel) and stop at the top of the active fuel.
- A component, called a "stiffener," was excluded from the model because it is not present on every cell. It is a thicker piece of stainless steel at the bottom of the cell extending up 30 inches. This exclusion is expected to have a small, conservative impact. This assumption is verified via the wrapper thickness tolerance cases.
- Boraflex is assumed to be completely degraded and is modeled as water. Boraflex binder material remaining in place inside the wrapper will contain some boron carbide. To assume none remains reduces neutron absorption in the Boraflex region (conservative).
- U-234 and U-236 in the fresh fuel is ignored. These are absorbers so ignoring them is conservative as shown in Section 7.1.6.

The storage cell walls are modeled nominal length and extend above and below the axial fuel region. The reflector region above the fuel (76 cm) and below the fuel (58 cm) is large enough to be considered neutronically infinite. Axial boundary conditions are reflective. Radial boundary conditions are periodic.

Figure 9.2 represents the X-Y plane of the 6x6 cell Region 1 KENO spent fuel pool rack model. Figure 9.3 is the same model showing the axial representation. A 6x6 model is used so that a 4x4 region of asymmetrically placed fuel may be modeled (see Section 9.2.3). Figure 9.4 is a

2x2 expanded view showing the tie plates. Figure 9.5 is the axial model with the cell walls removed so the other features of the axial model can be seen.

The SCALE 6.0 CSAS5 sequence is used for the calculation of spent fuel pool rack k. Consistent with the code benchmarking (Section 6 and Appendix A), the ENDF/B-VII 238 group cross sections are used. The number of neutron histories may vary, but 5000 generations, 16000 neutrons per generation and 1000 generations skipped are generally used and this provides a converged flux distribution with one sigma k uncertainty of about 0.00008. . Convergence is verified by inspecting the k versus generation trend for significant drift in key cases. One questionable case was rerun with a slight change to the number of neutrons pre generation. The difference in the final k was about 3 pcm (insignificant). No evidence of non-convergence was found.

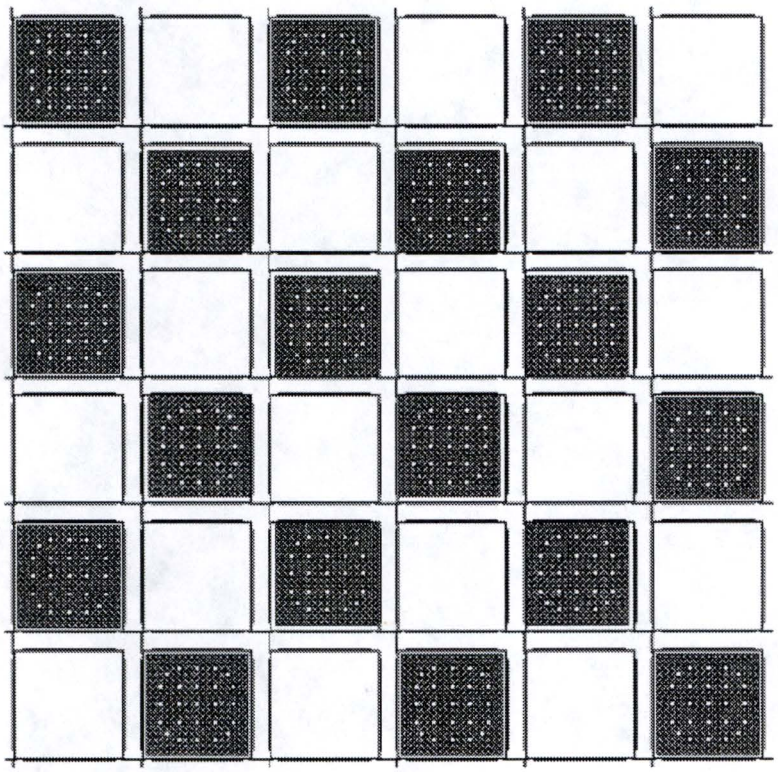

Figure 9.2: Region 1 Model X-Y View

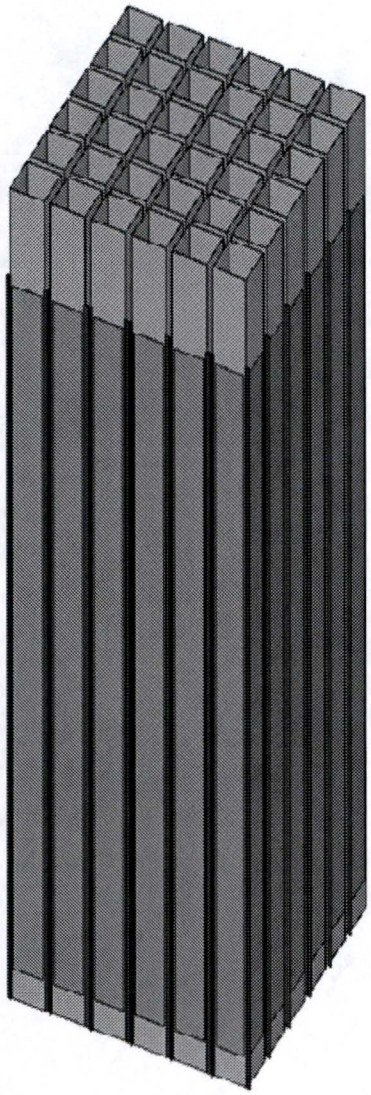

Figure 9.3: Axial View of the Region 1 Model

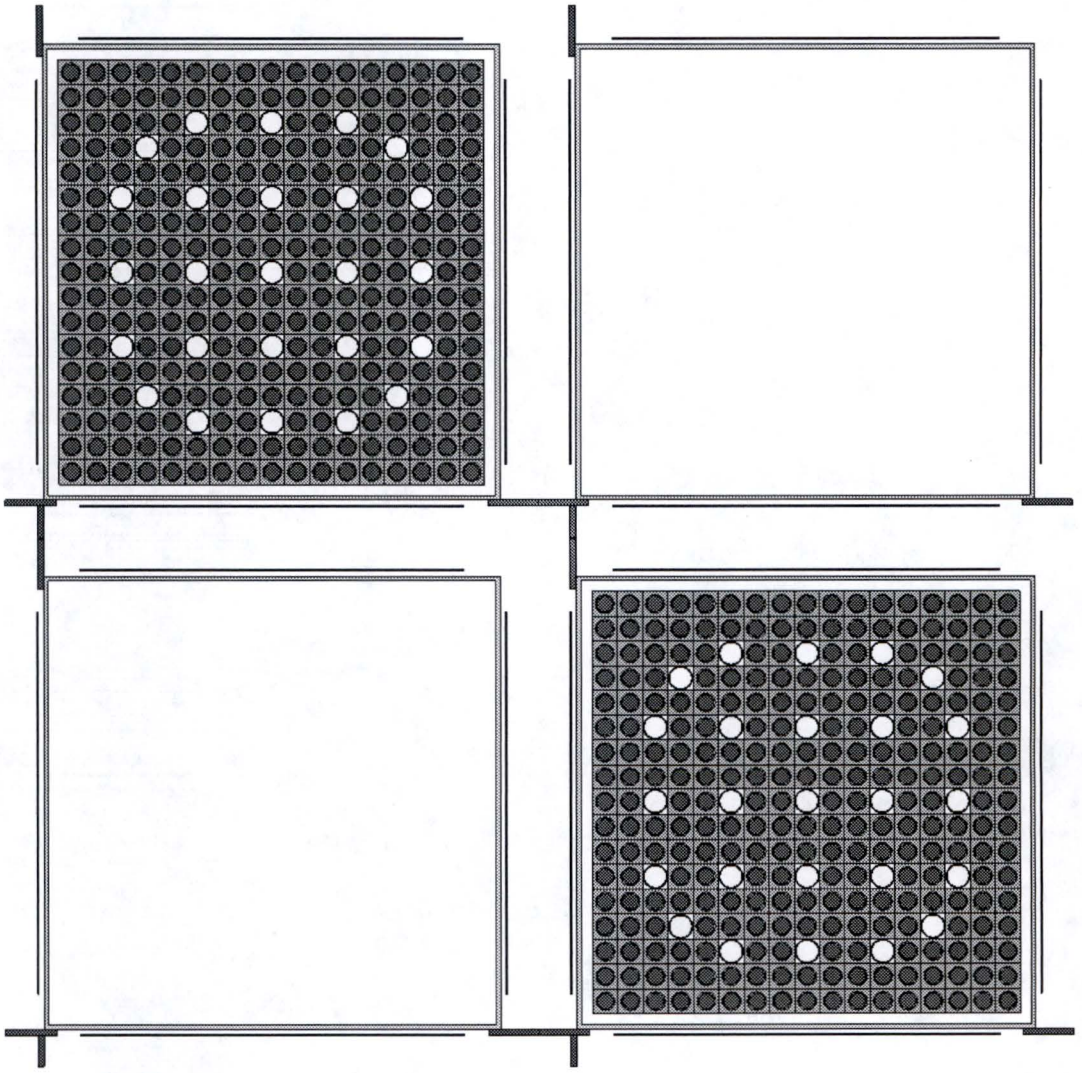

Figure 9.4: Region 1 Model X-Y View – 2x2 Blow-up

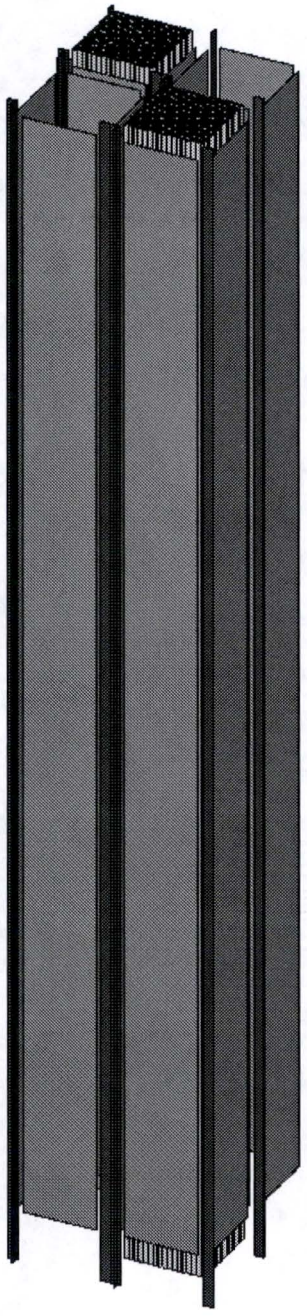

Figure 9.5: Region 1 Axial Model with the Cell Walls Removed

The tie plate configuration changes due to the finite size of a module. Generally three corners of each cell are connected to other cells via welded vertical "T" shaped tie plates. There is symmetry in the rack design such that a central row and column of cells is attached on all four corners. On the outer edges of the rack, cells are connected together by a flat tie plate. Figure 9.6 shows the arrangement of tie rods in a 10 by 10 rack module. Rather than model each module with its actual tie plate arrangement the uniform arrangement shown on Figure 9.4 is used. The reactivity effect of the detailed tie plate symmetry is small enough to ignore. This expectation is confirmed by direct KENO modeling. A 10x10 model including the details of the of tie plate arrangement was run and compared to a 2x2 model with the regular tie arrangement. Cases were run with 1.85 wt% U-235 (Region 2) and 5.0 wt% U-235 (Region 1) fuel at zero and 2000 ppm. In all cases the differences between the detailed tie plate and simplified tie plate models were within two times the Monte Carlo uncertainty.

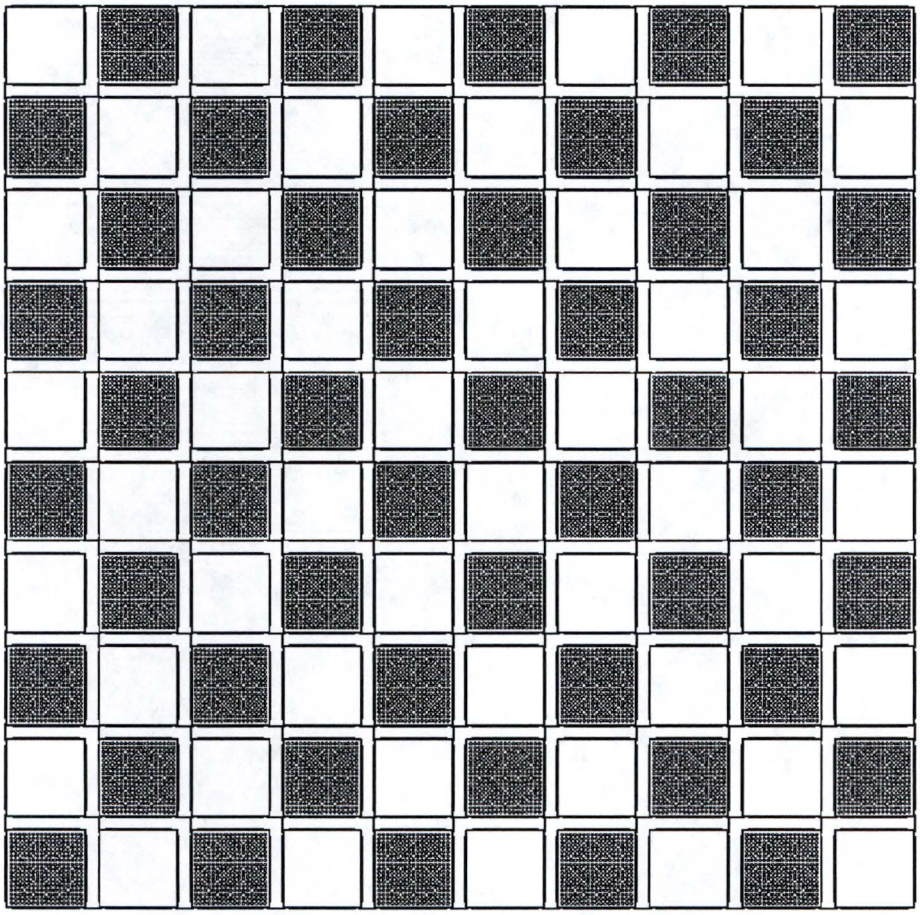

Figure 9.6: Tie Rod Arrangement in a 10x10 Module

In addition, cases are included to verify that wrapper holes, wrapper size variation, and poison stops need not be modeled. The more accurate modeling which increased the wrapper width (not thickness), added the hole in the wrapper, and added the poison stops showed there was not a statistically significant change in reactivity. (There was a slight indication that for the unborated analyses ignoring the stops and curved extra width of the wrapper is conservative but the maximum conservatism seen was only 2.3 times the Monte Carlo uncertainty.)

The AREVA fuel design is used for the analysis. The fuel pin dimensions are the same for all the fuel types used at North Anna. A smaller guide tube volume is more limiting since displacing water in the fuel is a negative reactivity (see tolerance calculations in the next section). The guide tubes are very similar for all designs. An earlier vintage fuel design has 1.45 cubic inches less guide tube volume in the assembly than the analysis design. However, a grid volume bias will be applied to the AREVA fuel to account for both the smaller grid and smaller guide tube volume in earlier design fuel.

9.2 Uncertainties and Biases

This section calculates the uncertainties associated with the fuel and rack manufacturing tolerances. This is followed by uncertainty and biases due to the modeling and validation.

9.2.1 Fuel Assembly Tolerances

The fuel assembly tolerances were previously given on Table 4.2. Table 9.1 provides the results of the analysis of the reactivity of the fuel tolerances. The reactivity due to fuel tolerances is small. Of the 10 tolerance reactivities on Table 9.1, Six are within two times the combined Monte Carlo uncertainty. The maximum delta k given on the table is the delta k from the base case plus two times the square root of the sum of the squares (RSS) of the Monte Carlo uncertainty. The grid reactivity on Table 9.1 is considered a bias rather than an uncertainty since it represents the low grid (and guide tube) volume fuel in the pool.

Table 9.1: Reactivity Associated with Fuel Tolerances for Region

Item	Change*	k	Sigma	Max Delta k
Base	N/A	0.9198	0.0001	N/A
Fuel Stack Density	95.5% increased by the theoretical density tolerance	0.9204	0.0001	0.0009
Pellet OD	0.8192 cm increased by the tolerance	0.9202	0.0001	0.0007
Fuel active length	Increase 1 cm	0.9197	0.0001	0.0003
Fuel Stack position	Lower fuel 1 cm	0.9198	0.0001	0.0003
Clad ID	0.836 cm decreased by the tolerance	0.9199	0.0001	0.0004
Clad OD	0.95 cm decreased by the tolerance	0.9221	0.0001	0.0026
Guide Tube ID	1.143 cm increased by the tolerance	0.9199	0.0001	0.0005
Guide Tube OD	1.224 cm decreased by the tolerance	0.9201	0.0001	0.0006
Pin Pitch	1.26 cm increased by the tolerance	0.9197	0.0001	0.0003
Grid	1/3 less grid volume	0.9210	0.0001	0.0016

*Only results from the limiting direction of the tolerance change are shown. The tolerances are given on Table 4.2.

9.2.2 Rack Manufacturing Tolerances

The spent fuel pool rack tolerances were previously given on Table 3.2. Table 9.2 provides the results of the analysis of the reactivity of the spent fuel pool rack tolerances. The cell wall and wrapper thickness tolerance produce the largest uncertainty in reactivity. There are a few tolerances on Table 3.2 that were not explicitly analyzed. The absorber gap thickness uncertainty only makes a slight change to the position of the wrapper, potentially making a small change to a flux trap effect. However, the cell inside dimension case suggests that this flux trap effect is small, likely because of the lack of a strong neutron absorber (no credit for Boraflex). The wrapper width is conservatively modeled as stated in Section 9.1. Also analysis mentioned in section 9.1 showed that the effect of the wrapper vent hole and poison stops was insignificant. Since the model is infinite with water reflectors, the tolerances on the pool liner, and rack base and foot are not important.

Table 9.2: Reactivity Associated with the Spent Fuel Pool Rack Tolerances for Region 1

Item	Change	k	Sigma	Max Delta k
Base	N/A	0.9198	0.0001	N/A
Cell wall thickness	From 0.229 cm to 0.2163 cm	0.9211	0.0001	0.0016
Cell pitch	From 26.83 cm to 26.7665 cm	0.9202	0.0001	0.0007
Cell inside dimension	From 22.54 to 22.66 cm	0.9201	0.0001	0.0005
Wrapper thickness	From 0.074 to 0.0617 cm	0.9209	0.0001	0.0014
Tie plates thickness*	From 0.305 to 0.287 cm	0.9198	0.0001	0.0004

*Tie plate width and thickness tolerance has been conservatively combined and modeled by reducing the thickness 6%. The thickness tolerance is 4.26%. The width tolerance is 1.57% (tie plate 1) or 1.94% (tie plate 2). The sum of width and thickness tolerances is 6.2% (tie plate 2) or 5.84% (tie plate 1). If width and thickness tolerances are combined by root sum square, the total tolerance is less than 4.7%. A conservative combined tie plate thickness tolerance of 6% will be used.

9.2.3 Eccentric Positioning

The reactivity effect of fuel placed asymmetrically in rack cells is included in the analysis base cases. Table 9.3 confirms that centered or uni-directional placement is less reactive than eccentric position in Region 1 and Region 2. The Region 2 analysis was done with 1.9 wt% U-235 with no burnup.

For this analysis it is assumed that there are a limited number of assemblies that are placed in their cells closest to a central point. The size of the block assemblies that are co-located about the central point is a 4x4 block of assemblies. This 4x4 block is in a 6x6 model where the box of assemblies outside the 4x4 co-located asymmetric loading are assemblies centered in the cells. This exceeds the maximum number of simultaneous and co-located asymmetric assembly placements expected. To determine the maximum number of assemblies expected to be simultaneously co-located, the method from Millstone Unit 2 spent fuel pool criticality analysis [9] is used. The method is summarized in these steps:

1) Asymmetry is considered a bias due to the size of the spent fuel pool and the number of fuel shuffles over the life of the pool. It is plausible that at some time and in some limited region of cells, an improbable asymmetric placement of fuel may occur.
2) The plausible number of co-located asymmetric assemblies in a region is based on a conservative probability estimate

a. There are 1737 locations in the spent fuel pool

b. In each cell there is a ¼ chance of placement in a cell corner that increases reactivity (conservatively assumes only four possible placement locations within the cell, each maximally shifted into a corner)

c. Assume 100 year spent fuel pool remaining life

d. Assume 1 complete spent fuel pool reshuffling per year

e. For Region 2, there are approximately 1400 storage locations (the balance are Region 1).

f. Assume that each cell in the region could be the center point for a 4x4 asymmetric set (not physically possible, but conservative).

g. For Region 2 it is expected that co-location of 16 symmetric fuel assemblies will occur 100 years*1400 positions* 0.25^{16} or 3.3×10^{-5} times over the life of the plant. Using this number we state that there is a greater than 95% probability that an asymmetric co-location of more than 16 assemblies is never expected to occur over the life of the spent fuel pool.

h. As with Region 2, for Region 1 the maximum asymmetry model will be a 4x4 region containing 8 maximally asymmetric fuel assemblies in the most reactive configuration within a centrally loaded 6x6.

i. For Region 1 (2-out-of-4 storage) the expected number of fuel storage locations is 178.

j. Rounding up 178 to 200 storage locations, it is expected that asymmetric co-location of 8 assemblies will occur 100*200* 0.25^{8} or 0.31 times over the life of the plant.

Since the expected outcome for a Region 1 asymmetric arrangement is greater than 0.05 occurrences during the lifetime of the plant, two additional cases were run (Table 9.3). The first case has a 4x6 asymmetric center in a 6x10 model. The second case is a 5x5 in 6x6 (center cell of 5x5 is empty).The k difference resulting from the larger asymmetric region is well within Monte Carlo uncertainty. For these cases, it is expected that an asymmetric loading of this size will occur 100*200* 0.25^{12} or 0.001 times during the life of the plant. This is interpreted as there is a greater than a 95% probability that a larger grouping of asymmetric placing of assemblies will never occur. Since there is no significant increase in k with these larger asymmetric models no additional bias will be applied.

Table 9.3: Reactivity Associated Eccentric Positioning of Assemblies in Region 1 and Region 2

Region	Enrichment	Case	k	sigma	Delta k
1	5 wt% U^{235}	4x4 eccentric array (8 assemblies) in the center of a 6x6 array (Outer row assemblies are centered in cell)	0.9198	0.0001	
1	5 wt% U^{235}	All assemblies of the 6x6 array centered in the rack cell	0.9186	0.0001	-0.0011
1	5 wt% U^{235}	All 18 assemblies moved as far as possible to the lower right side of the cell in a 6x6 array.	0.9194	0.0001	-0.0004
1	5 wt% U^{235}	4x6 eccentric array (12 assemblies) in the center of a 6x8 array (Outer row assemblies are centered in cell)	0.9197	0.00005	0.0000
1	5 wt% U^{235}	5x5 eccentric array (12 assemblies) in the center of a 6x6 array (one row centered between asymmetric areas)	0.9198	0.00005	0.0000
2	1.9 wt% U^{235}	4x4 eccentric array (16 assemblies) in the center of a 6x6 array (Outer row assemblies are centered in cell)	0.9577	0.00006	
2	1.9 wt% U^{235}	All assemblies of the 6x6 array centered in the rack cell	0.9537	0.00006	-0.0041
2	1.9 wt% U^{235}	All 36 assemblies moved as far as possible to the lower right side of the cell in a 6x6 array.	0.9556	0.00006	-0.0022

9.2.4 Other Uncertainties and Biases

The remaining uncertainties are the code/cross section validation uncertainty from Section 6.3. For Region 1 the code/cross section validation uncertainty is 0.005 (from Table 6.6). The final uncertainty is the Monte Carlo uncertainty for the base case (2 sigma or 0.0002).

There are a few biases that need to be added in. They are a validation bias, a temperature bias, a grid bias, and a margin for NRC review bias. The code/cross section validation bias is 0.0035 (from Table 6.6). The minimum size Zircaloy grid bias is shown in Table 9.1 and is 0.0016.

All uncertainty and bias cases except temperature bias are performed with 0 ppm soluble boron, 293 K (68 °F) water temperature (0.9982 g/cc water density). In order to determine if there is a temperature bias the base case was run with a range of temperatures. The maximum normal spent fuel pool temperature is 140 °F. Table 9.4 shows the results of the analysis. As the water

density increases, the calculated k increases and as the temperature increases the small temperature bias from the critical experiments increases (See Section 6.3.3). A small temperature bias of 0.0008 covers the range of temperatures.

Table 9.4: Change in k with Temperature for Region 1

Temperature (°F)	Water Density (g/cc)	k	Sigma	Max Delta k	Validation Bias	Total Bias
68	0.9982	0.9198	0.00010	N/A	0	
32	0.9999	0.9201	0.00011	0.0006	0	0.0006
39	1.0000	0.9203	0.00006	0.0008	0	0.0008
120	0.9886	0.9197	0.00010	0.0003	0.0005	0.0008
140	0.9832	0.9191	0.00010	-0.0004	0.0007	0.0003

The final bias is the "Margin for NRC Review." This bias is margin provided to the NRC to be used to offset any concerns with the methods used in this analysis. Margin to the regulatory limit in excess of this 1% NRC margin may be used by Dominion in 10CFR50.59 analysis for future requirements.

9.3 Meeting Acceptance Requirements for Region 1

Table 9.5 shows the analyzed k for Region 1 and the uncertainties and biases needed to meet the acceptance criteria for the analysis without soluble boron. The acceptance criteria is that k is less than 1.0 with a 95/95 probability and confidence level. The $k_{95/95}$ is 0.9420 which leaves 0.058 margin which may be applied to resolve using 10CFR50.59 future criticality issues.

Table 9.5: Region 1 Rack up of Biases and Uncertainties for the 0 Soluble Boron Analysis

Enrichment (wt% U-235)	**5.00**
Burnup (GWd/MTU)	**0**
Reference Case k	**0.9198**
Uncertainty in the Fuel Stack Density	0.0009
Uncertainty in the Pellet OD	0.0007
Uncertainty in the Fuel Active Length	0.0003
Uncertainty in the Fuel Stack Position	0.0003
Uncertainty in the Clad ID	0.0004
Uncertainty in the Clad OD	0.0026
Uncertainty in the Guide Tube ID	0.0005
Uncertainty in the Guide Tube OD	0.0006
Uncertainty in the Pin Pitch	0.0003
Uncertainty in the Cell Wall Thickness	0.0016
Uncertainty in the Cell Pitch	0.0007
Uncertainty in the Wrapper thickness	0.0014
Uncertainty in the Tie plates thickness	0.0004
Monte Carlo uncertainty in the Reference Case	0.0002
Validation uncertainty	0.0050
Statistically Combined Uncertainties	**0.0063**
Bias from Code and Cross Section Library Validation	0.0035
Bias to the most reactive temperature	0.0008
Bias to the most reactive grid volume	0.0016
Sum of Biases	**0.0059**
Margin for NRC review	**0.0100**
k-eff with 95/95 probability and confidence	**0.9420**
Acceptance criteria	1.0
Dominion held Margin	**0.0580**

Table 9.6 shows the analysis of Region 1 taking credit for soluble boron. This analysis credits a soluble boron concentration of 900 ppm for normal operation. The boron dilution analysis of record showed that dilution below 1200 ppm would be prevented due to the large water volume required, the dilution time, and administrative controls including spent fuel pool level monitoring. [46] The previous criticality analysis used only 900 ppm soluble boron credit in the analysis approved with an NRC SER. [47] This analysis likewise provides a 300 ppm margin to the 1200 ppm minimum soluble boron concentration. As a note of further conservatism, the analysis supporting 1200 ppm used an initial boron concentration of 2300 ppm. North Anna Technical Specification 3.7.17 requires spent fuel pool soluble boron ≥2600 ppm when fuel is store in the spent fuel pool.

The manufacturing uncertainties and grid volume bias used on Table 9.6 were performed at the 0 ppm condition and therefore are approximations for the 900 ppm boron condition. A Millstone Unit 2 analysis of a similar rack design (Region 1 Boraflex flux trap design with no Boraflex credit, no burnup credit, and 2 out of 4 checkerboard storage) showed that total uncertainty was the same at 0 and 2000 ppm soluble boron. Temperature bias decreased slightly at the higher boron concentration. [9] Similarly, the EPRI analysis of the change in uncertainties with the change in soluble boron showed that it was conservative to use the unborated uncertainties for all Region 1 analysis. [30] The rack cell inside dimension tolerance was omitted from Tables 9.5 and 9.6. If included, the indicated combined uncertainty would not change.

The temperature bias was calculated for the 900 ppm case and is included on Table 9.6. The most reactive condition was for the lowest temperature rather than the highest temperature. This may be because at 900 ppm soluble boron and checkerboard storage the assemblies are neutronically isolated and the most reactive condition occurs with the most moderator in the pin lattice.

Because there is significant margin available and because tolerances were not recalculated with 900 ppm soluble boron, the margin for NRC review has been raised from 1% to 2% to cover any concerns over the estimated uncertainties. Notice that the validation bias and uncertainty did not need to be increased since the EALF for the borated base case is 0.34 eV.

Table 9.6: Region 1 Rack up of Biases and Uncertainties for the 900 ppm Soluble Boron Credit Analysis

Enrichment (wt% U-235)	**5.00**
Burnup (GWd/MTU)	**0**
Reference Case k	**0.8000**
Uncertainty in the Fuel Stack Density[a]	0.0009
Uncertainty in the Pellet OD[a]	0.0007
Uncertainty in the Fuel active length[a]	0.0003
Uncertainty in the Fuel Stack position[a]	0.0003
Uncertainty in the Clad ID[a]	0.0004
Uncertainty in the Clad OD[a]	0.0026
Uncertainty in the Guide Tube ID[a]	0.0005
Uncertainty in the Guide Tube OD[a]	0.0006
Uncertainty in the Pin Pitch[a]	0.0003
Uncertainty in the Cell wall thickness[a]	0.0016
Uncertainty in the Cell pitch[a]	0.0007
Uncertainty in the Wrapper thickness[a]	0.0014
Uncertainty in the Tie plates thickness[a]	0.0004
Monte Carlo Uncertainty in the Reference Case	0.0002
Validation Uncertainty	0.0050
Statistically Combined Uncertainties	**0.0063**
Bias from Code and Cross Section Library Validation	0.0035
Bias to the Most Reactive Temperature	0.0006
Bias to the Most Reactive Grid Volume[a]	0.0016
Sum of Biases	**0.0057**
Margin for NRC review	**0.0200**
k-eff with 95/95 probability and confidence	**0.8320**
Acceptance criteria	0.95
Dominion held Margin	**0.1180**

[a]Due to the large margin the unborated uncertainties and bias were used for these parameters

9.4 Non-Standard Fuel Allowances

The fuel rod storage rack is shown in Section 10.8 to be less reactive than Region 2 fuel and is therefore acceptable for storage in a Region 1 fuel cell. There currently are no other fuel containers in the North Anna spent fuel pool cells. Section 12.5 discusses reconstitution of fuel assemblies. Section 12.5 concludes that reconstituted fuel is allowed in Region 1.

9.5 Non-Fuel Component Location Restrictions

Non-fuel components may be placed in any cell where fuel is allowed since they are less reactive than fuel. Non-fuel can also be placed in the guide tubes of any fuel assembly. This is because the fuel lattice is under moderated. This can be seen by the guide tube tolerance calculations. However, to confirm this, calculations were performed where voided zirconium tubes were placed in the guide tubes. For Region 1 and Region 2 with high and low enrichments the k decreased more than 1% in k. This analysis was done without soluble boron. A case was also run at 2600 ppm with the voided zirconium tubes (as part of the multiple misload analysis described in Section 13.2) and k still decreased by 0.3% in k.

The empty cells credited for Region 1 may not contain any item with the exception of a control rod. Control rods may be stored in the empty cells because they are by design much stronger neutron absorbers than borated or unborated water of the same volume. Currently at North Anna, there are stainless steel cell blockers which can hold control rods. These may be used as well, because they are above the active fuel region.

9.6 Summary of the Loading Restrictions for Region 1

Region 1 blocks can be anywhere in the pool as long as they meet the following four requirements:

1) Region 1 blocks must have empty cells at the outer corners.

2) At least two Region 2 rows must exist between Region 1 blocks.

3) Each Region 1 block shall be fully contained in a single rack module where a rack module is adjacent to another rack module. This requirement eliminates the need to perform an analysis postulating rack-to-rack misalignment (seismic event or installation) such that part of the checkerboard would not be properly aligned.

4) The spent fuel cells AA21, AA22, BB21, BB22, CC21, and CC22 may not be part of a Region 1 block due to the new fuel elevator. (See Figure 9.7 for location of these cells.)

All of the fuel types at North Anna (see Section 4) can be loaded into Region 1 with no required burnup. Fuel enrichments up to and including 5 wt% U-235 have been shown to meet the criticality safety requirements. The criticality analysis does not credit any burnable absorbers or control rods so any or no non-fuel insert may be contained in the guide tubes. Any fuel bearing item shown acceptable for placement in Region 2 is also acceptable for placement in a Region 1 location that can be loaded with fuel, because the Region 1 checkerboard storage allows much higher fuel reactivity than Region 2 all-cell storage.

All present and anticipated future reconstituted or damaged fuel can be placed in Region 1 (See Section 12.5).

The Region 1 empty cells may contain full length or part length control rods with or without cell blockers but otherwise must be empty in the active fuel elevations. Cell blockers are above the active fuel and are acceptable.

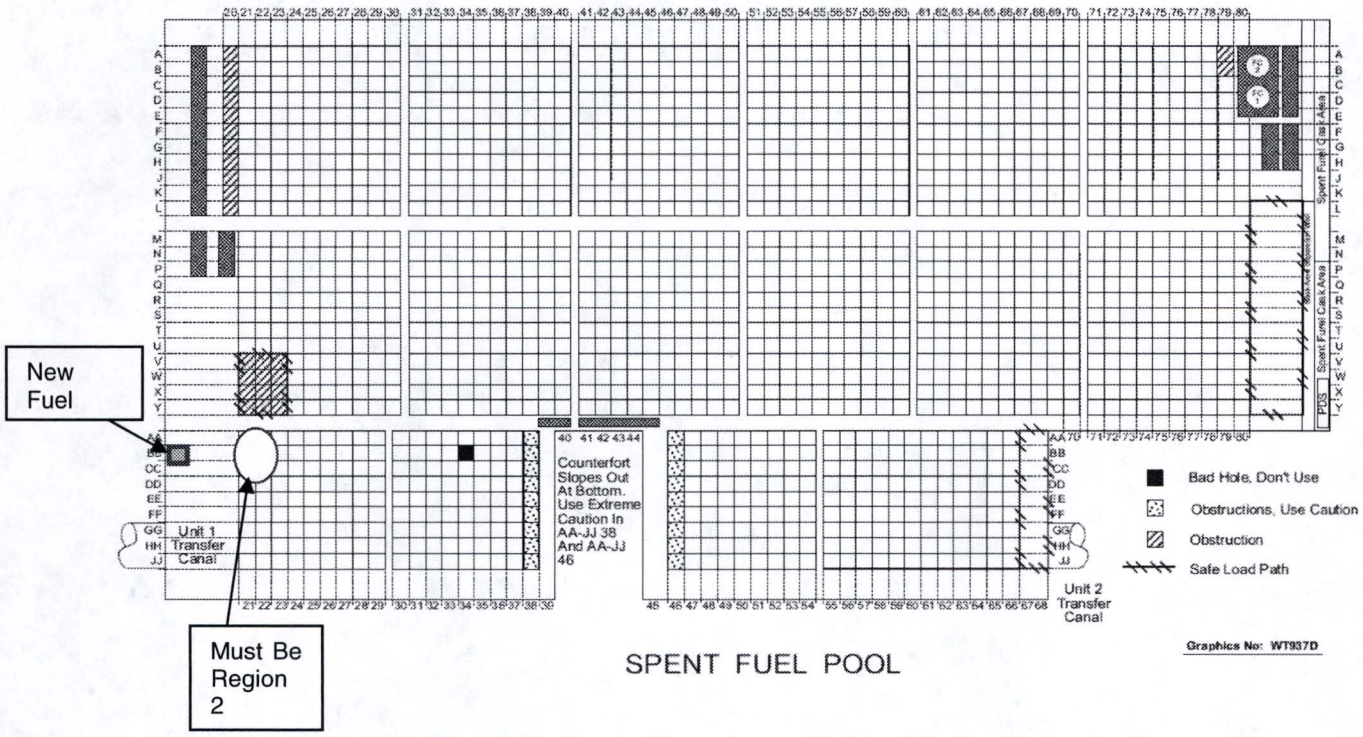

Figure 9.7: North Anna Spent Fuel Pool Rack Cell Coordinates

10 Region 2 Analysis

All of the North Anna spent fuel pool racks have the same storage cell design (flux trap Boraflex racks) and fuel assembly pitch. No credit is taken for Boraflex, which is modeled as water. Region 1 and Region 2 both utilize these rack modules. The difference is Region 1 requires checker boarding with empty cells while Region 2 allows the loading of every cell. Also, Region 1 does not require burnup, but Region 2 has minimum burnup requirements.

10.1 Rack Model

The rack model for Region 2 is the same as Region 1 (see Section 9.1) except there are 18 axial fuel zones to accommodate the axial variation in fuel burnup and all cells contain fuel. The model is a 6x6 array with the central 4x4 with asymmetric placement of the fuel in the cell. (See Section 9.2.3) Figure 10.1 is a top view of the Region 2 model. Figure 10.2 is a side view of the Region 2 model cut though the center.

Section 8 presented the depletion analysis needed to get the atom densities for the 18 axial nodes. Table 10.1 shows the enrichment and burnup combinations of the atom density sets used for developing the loading curve of the 5 day decay analysis. (Additional sets for single nodes were created to address some sensitivities.) Calculations with the uniform axial burnup distribution and with the NUREG/CR-6801 distributions for 10, 20, and 30 GWd/MTU were performed. For burnups of 20 GWd/MTU and up the NUREG shapes yielded higher ks. For 10 GWd/MTU the uniform shape was most limiting. For the rest of this report all 10 GWd/MTU calculated ks used the uniform shape and all other calculated ks used the appropriate NUREG shape.

Most Region 2 KENO cases use 9000 generations, 1000 generations skipped, and 16000 neutrons per generation. In order to reduce computer run time, most sensitivity cases are run using a reduced set of isotopes (28 plus oxygen).

Table 10.1: Atom Density Sets Used in the Analysis

Enrichment (wt% U-235)	Burnup (GWd/MTU)	Axial Shape (Group # from Table 8.4)
2.45*	10	Uniform
2.5	10	11 and Uniform
3.05*	20	8
3.075	20	8
3.10	20	8 and Uniform
3.8*	30	5 and Uniform
3.85	30	5
4.4	38	3
4.5	38	3
4.95	44	2
5.0*	44	2

*For these enrichments and burnups an additional atom density set was calculated where the grid was expanded, the clad outer diameter was decreased due to creep and the power was reduced to 50% for the last 40 days of the depletion.

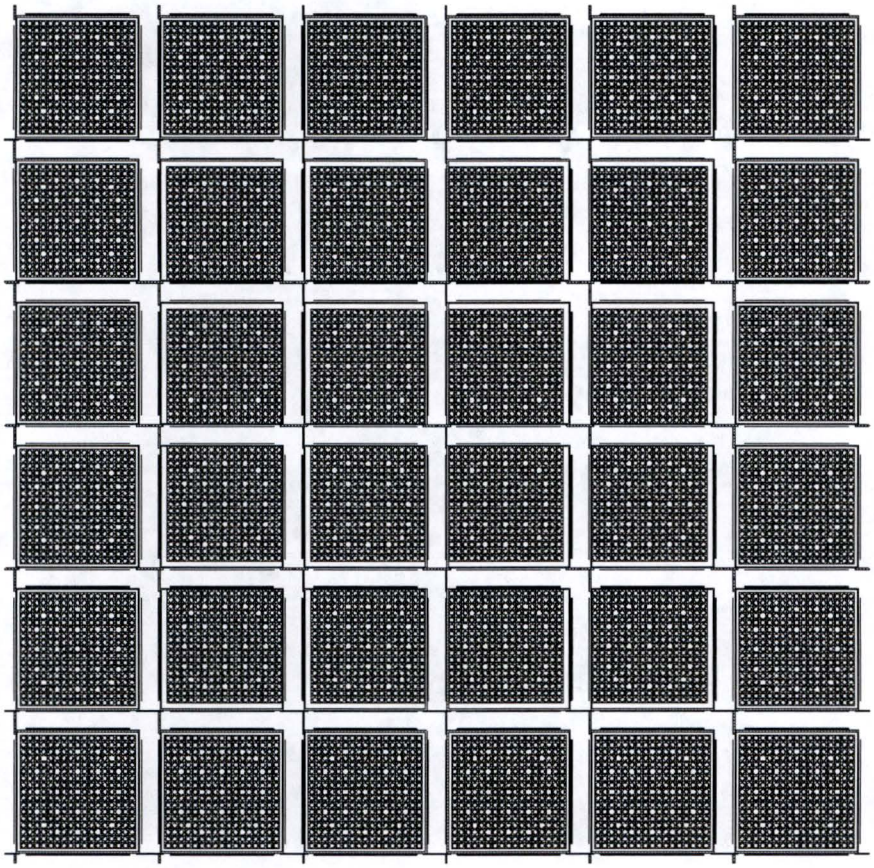

Figure 10.1: Top View of the Region 2 model

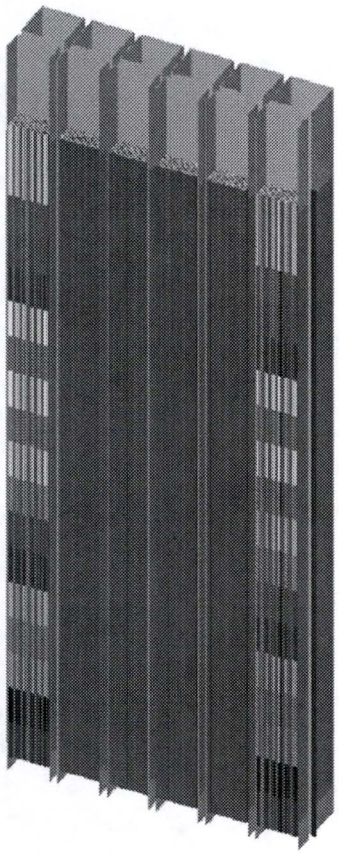

(Note that the middle assemblies do not show 18 fuel nodes like the outside assemblies because they are asymmetrically shifted which caused the picture to only show its fuel cladding)

Figure 10.2: Side View of the Region 2 Model Cut Though the Center

10.1.1 Horizontal Burnup Gradient

The models assume the same burnup for every pin. An assessment of the reactivity effect of a horizontal tilt in the burnup has been made for the North Anna spent fuel pool. NUREG/CR-6800 [48] addresses the effect of horizontal burnup tilts for spent fuel pool storage in casks. Horizontal tilt is defined as increased burnup in one half of an assembly and reduced burnup in the other. The quantity of the tilt (%) is (1 – low burnup/assembly average burnup) x 100. Figure 22 of reference 48 indicates that for burnup modeling with actinides and fission products in a cask model the effect of ≤20% horizontal tilt at ≤20 GWd/MTU is negative (reduces k).

Similarly, the effect of ≤10% tilt at ≤40 GWd/MTU is zero or less within the uncertainty of the calculation.

End of cycle horizontal burnup tilts were calculated for fuel in cycles North Anna Unit 1 cycles 20 through 24 and Unit 2 cycles 20 through 23. Figure 10.3 shows that less than 5% of the North Anna horizontal burnup tilts exceed 20% at or near 20 GWd/MTU and less than 5% exceed 10% at or near 40 GWd/MTU.

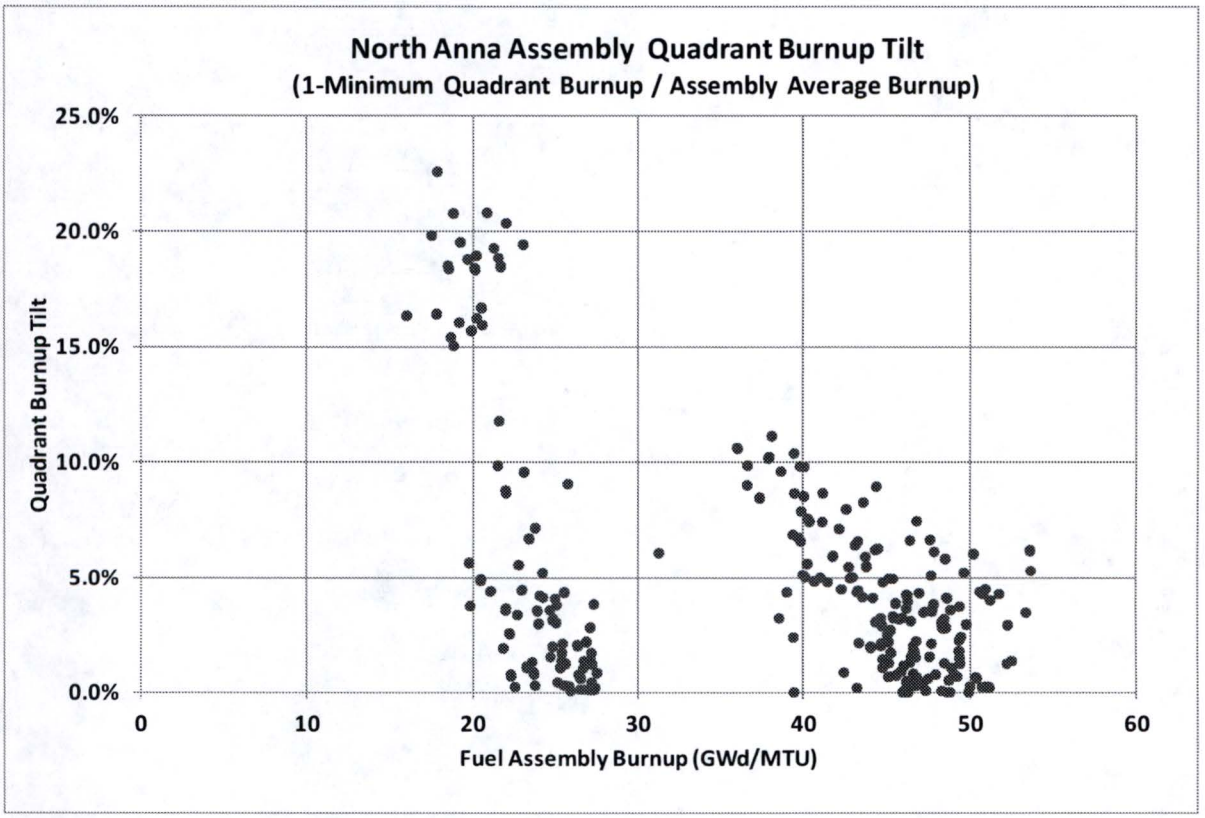

Figure 10.3: North Anna Assembly Quadrant Burnup Tilt

In order to estimate the potential effect of the horizontal tilt, North Anna Region 2 KENO cases were run with a reflected assembly model with a diagonal burnup asymmetry. Figure 10.4 shows the image of the KENO model. A diagonal gradient with reflected boundary conditions places the four low burnup quadrants in closest proximity to maximize the effect while maintaining quadrant average burnups. Two enrichment / burnup combinations providing reasonable ks were used (3.1 w/o with 20 GWd/MTU and 4.7 w/o at 40 GWd/MTU). A uniform

axial burnup was used. This is acceptable because the intent of this calculation is to estimated the magnitude of the horizontal burnup effect. The top few nodes typically dominate PWR spent fuel pool calculations with depleted fuel. Node 16 depletion conditions were chosen for this comparison.

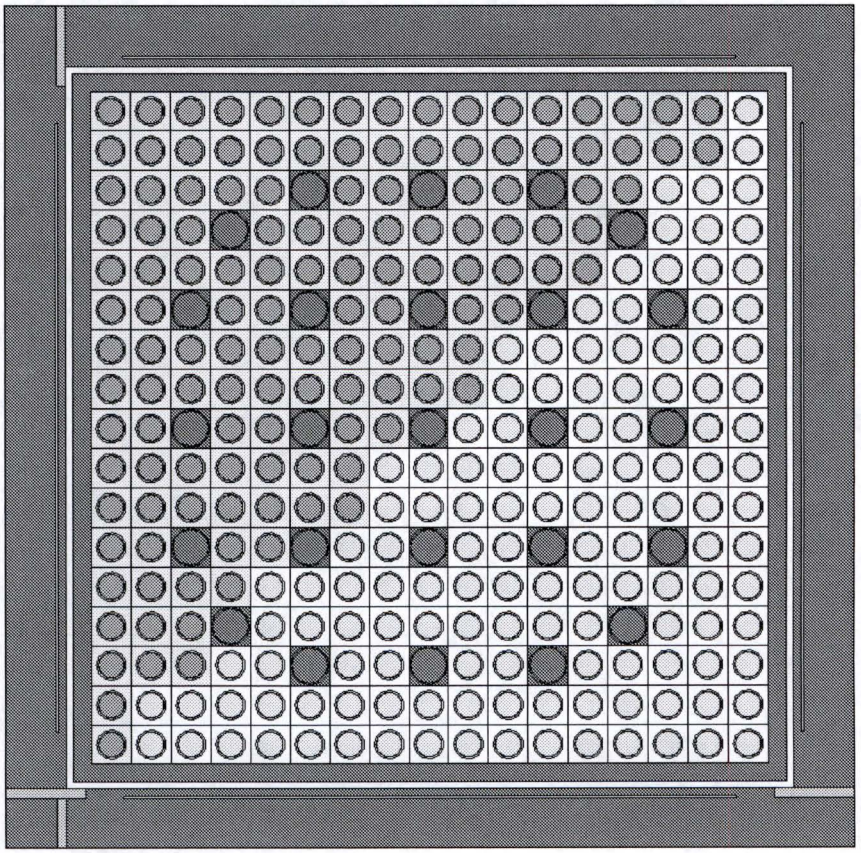

Figure 10.4: KENO Horizontal Burnup Tilt Model

For each burnup, two cases were run:

1) Uniform average burnup

2) Diagonal tilt with higher than average and lower than average burnups.

Table 10.2 provides the results of the burnup tilt cases. Based on these results, a bias of 0.0013 Δk is reasonable to account for horizontal burnup tilt effects.

Table 10.2: Effect of Horizontal Burnup Tilt

Enrichment (wt% U-235)	Burnup (GWd/MTU)	Tilt	k-eff	sigma	Max Delta k
3.1	20	0	0.9464	0.00008	-
3.1	20	20%	0.9475	0.00008	0.0013
4.7	40	0	0.9381	0.00008	
4.7	40	10%	0.9389	0.00008	0.0010

10.2 Dimensional Changes with Burnup

With burnup there are a number of physical changes. The fuel pellet initially densifies and then expands, the clad can creep down toward the fuel pellet and the grids may grow. The reactivity effect of the fuel pellet changes is small because there is no change to the fuel mass and therefore no change to the fuel to moderator ratio. Note that even though the fuel pellet OD tolerance in Section 10.4 increases the amount of fuel, the reactivity change is very small. This small reactivity effect is ignored. Grid growth and clad creep, however, increase reactivity due to increasing the moderation in the fuel assembly and will be handled as a bias. The next two subsections describe the modeling for these effects.

10.2.1 Grid Growth

Zircaloy based grids tend to grow with increasing fuel burnup. Grid growth increases fuel pin pitch, which can increase fuel reactivity in the spent fuel pool. Inconel grids used at the bottom of the fuel stack and above the active fuel in current designs are ignored for this calculation because Inconel is a strong neutron absorber. In addition, for current fuel designs, Inconel grids are in neutronically unimportant parts of the depleted fuel assembly. Inconel grids were used throughout the fuel stack for the fresh fuel batches initially loaded in cycles 1 through 11 for Unit 1 and cycles 1 through 12 for Unit 2. Grid expansion is ignored for those non-limiting designs because neutron absorption by the Inconel would offset the reactivity increase due to expansion, fuel density in those fuel batches (Table 8.7) was ~1% less than assumed in the

spent fuel pool model, and because those assemblies have been cooling for ~20 years all provide additional margin.

Zircaloy-4 grids were used for the fresh fuel batches loaded in North Anna Unit 1 cycles 9 and 10 and Unit2 cycles 8, 9, and 10. For the last 15 cycles (22 years), Zircaloy-4 has not been used for grids in fresh fuel, rather M5 and Zirlo have been used. (Four lead test assemblies inserted in Cycle 13 in Unit 1 had Zircaloy-4 grids. These assemblies were burned to high burnup such that they are not limiting assemblies.)

Zircaloy-4 Grid Growth:

Zircaloy-4 grid growth has been measured for numerous assemblies. Figure 10.5 shows grid 2 (the grid at 15 inches from top of fuel) data collected by FRAMATOME. [49] This plot includes only the grid 2 measurements taken on North Anna assemblies NJ092P, NJ092T and NJ092V. The North Anna assembly data for all the grids is given on Table 10.3. As can be seen from the data on Table 10.3 there is a strong dependence on height in the core with those grids closest to the top growing more. This has been seen with all the data which suggests a strong dependence on temperature. Note the top of the assembly actually has lower burnup so this axial trend is counter to the burnup trend.

The bias for grid growth used in this criticality analysis is based on Zirlo grid growth because Zircaloy-4 grids will no longer be used at North Anna and Zircaloy-4 was used in only 5 fuel batches. The burnups of all the historical Zircaloy-4 assemblies have been compared to the minimum burnup requirements and all but two assemblies have greater than 6 GWd/MTU excess burnup. This excess burnup is worth at least 2% in k which is much greater than the grid growth effect. Even though these assemblies have a large burnup margin, the grid expansion assumption based on Zirlo may be sufficient. Since the highest enrichment for theses assemblies is 4.2 wt%, the burnup requirement is only 33.5 GWd/MTU. The assumed grid growth from the Zirlo data for 33.5 GWd/MTU is [ ]^{a,c}. This is marked on Figure 10.5 by the red block. The red block shows that the grid expansion based on the Zirlo data is close to the expected grid expansion at that burnup. Based on pin pitch tolerance cases (Table 10.4), the reactivity effect of grid growth is on the order of 0.01 Δk / % grid expansion which means the reactivity of 0.2% grid expansion is on the order of [ ]^{a,c}. This is [ ]^{a,c}

lower than the excess depletion reactivity. Also this limited number of assemblies has less limiting burnable absorbers than assumed and are cooled at least 15 years which provides additional margin to cover this historical fuel design.

The remaining two assemblies are under burned (total burnup 24 and 27 GWd/MTU). Grid expansion is not a concern at low burnup. In addition, because of the low burnup these two assemblies will be treated as fresh fuel.

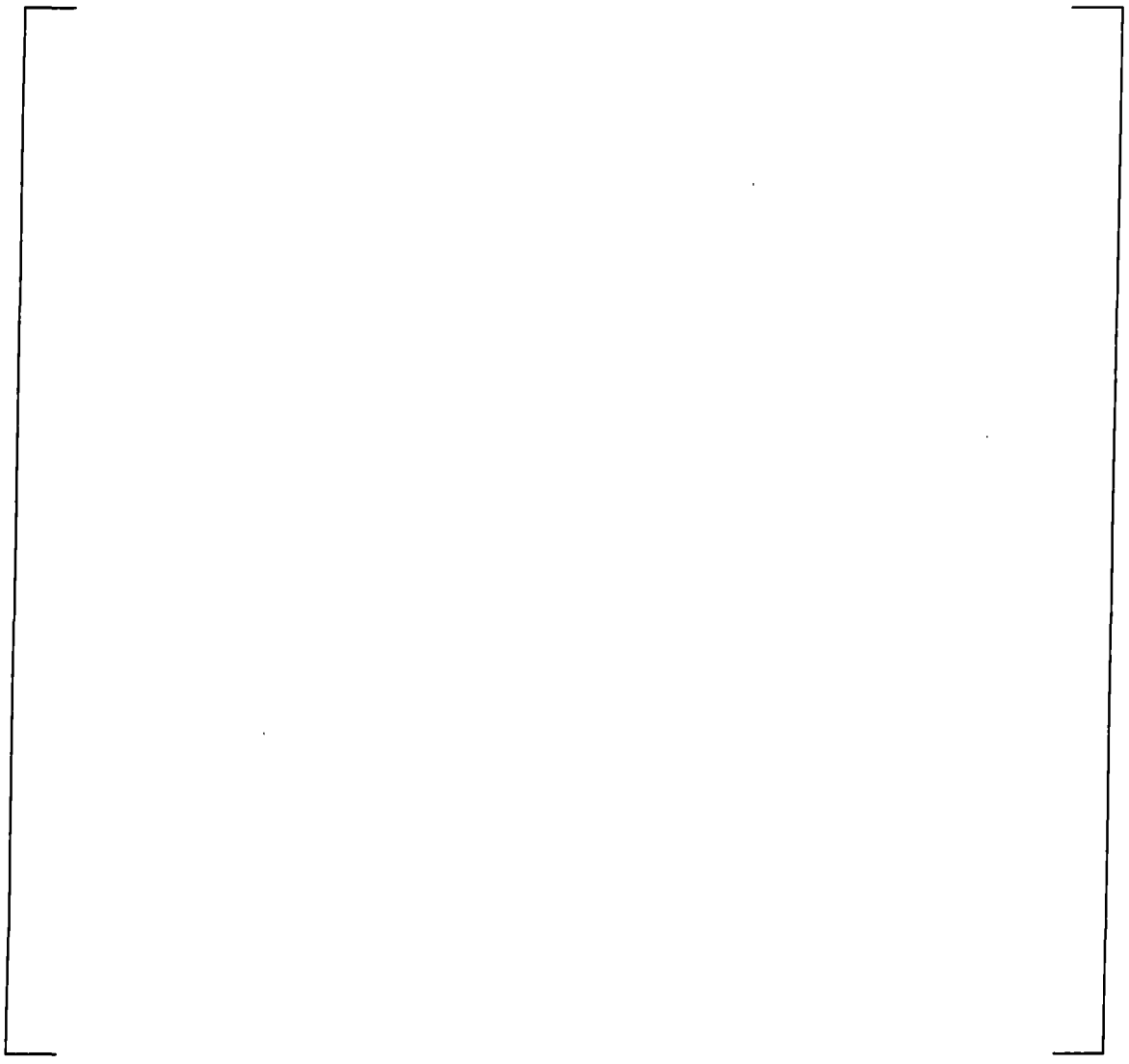

A

Table 10.3: Grid Growth Measurements at North Anna [49]

Assembly ID	Grid Location From Top of Fuel (inches)	Burnup (GWd/MTU)	% Grid Growth
[ ]A	[ ]A	[ ]A	[ ]A
	[ ]A	[ ]A	[ ]A
	[ ]A	[ ]A	[ ]A
	[ ]A	[ ]A	[ ]A
	[ ]A	[ ]A	[ ]A
	[ ]A	[ ]A	[ ]A
	[ ]A	[ ]A	[ ]A
	[ ]A	[ ]A	[ ]A
[ ]A	[ ]A	[ ]A	[ ]A
	[ ]A	[ ]A	[ ]A
	[ ]A	[ ]A	[ ]A
	[ ]A	[ ]A	[ ]A
	[ ]A	[ ]A	[ ]A
[ ]A	[ ]A	[ ]A	[ ]A
	[ ]A	[ ]A	[ ]A
	[ ]A	[ ]A	[ ]A
	[ ]A	[ ]A	[ ]A

ZIRLO Grid Growth

M5 and ZIRLO are more advanced materials intended to reduce growth at high burnup relative to Zircaloy-4. Figure 10.6 shows the ZIRLO grid growth using data from 5 plants. [50] Additional data was obtained from a few more plants and is plotted on Figure 10.7.

This criticality analysis only takes credit up to 44 GWd/MTU. The red dashed lines on Figures 10.6 and 10.7 show the grid growth assumed in this analysis for all axial elevations. Notice that up to 44 GWd/MTU the line covers all the available data.

a.c

a.c

M5 Grid Growth

Figure 10.8 shows the M5 grid growth data from four different plants (three lattice sizes). [52] The red dashed line added to Figure 10.8 shows the grid growth assumed in this analysis for all axial elevations. The assumed grid growth is conservative for burnups between 15 GWd/MTU and the maximum credited burnup of 44 GWd/MTU. At the low burnups the data exceeds the growth assumption by less than 0.02% which has a negligible reactivity effect. Further, in order to load fuel with burnups that low in Region 2 the initial enrichment would have to be less than 2.8 wt% U-235 which is less than would be ordered for contemporary fuel management. Use of the same grid expansion for all elevations introduces additional conservatism, particularly at low burnups at which uniform axial burnup is limiting.

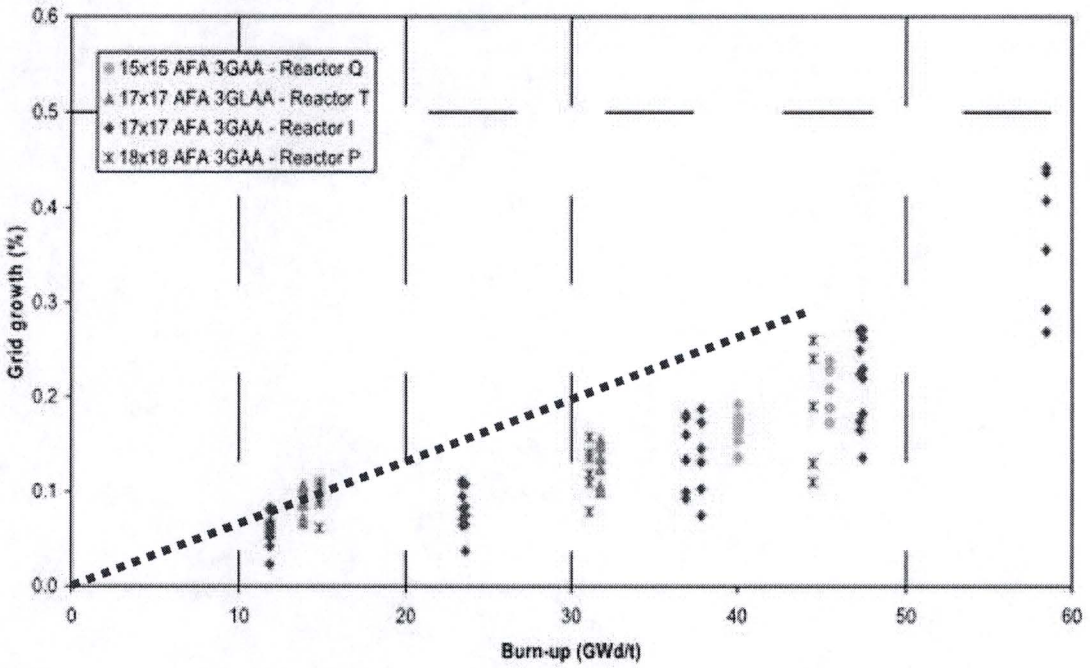

Figure 10.8: Grid Growth for M5 Grids [52]

Grid Growth Modeling

To cover grid growth, analysis is performed to determine a bias. The analysis models the grid growth during depletion by assuming a constant larger pitch consistent with the average grid growth over the depletion from fresh fuel to a given burnup. It is assumed that the grid grows linearly during depletion from [

]^{a,c}. In the final calculation of k the atom densities taken from the average expanded grid depletion are input into a KENO calculation where the pitch is expanded to the nominal pitch times (1+BU*.003/50) where BU is the burnup in GWd/MTU. Since there are three bias components that require depletion analysis, the bias for the grid growth, clad creep, and low power near end of life are done together. Unfortunately, this means that the bias due to just the grid growth is never individually determined. However, based on pin pitch tolerance cases (Table 10.4), the effect is on the order of 0.01 Δk / % grid expansion. The grid growth modeling is conservative since it assumes the full length pitch of the fuel rods expands consistent with the largest expansion of a grid.

10.2.2 Clad Creep

Spent fuel pool k increases with reduced clad outer diameter (OD) with no soluble boron (See Section 10.4). Clad behavior with burnup is a complex function of many variables. A simple and conservative approach is needed for spent fuel pool criticality calculations.

The zirconium alloys Zircaloy-4, M5, and ZIRLO have been used for cladding at North Anna. Reference 53 shows maximum fuel clad diameter reduction for Zircaloy-4 of about 70 microns (approximately 0.7% using the North Anna fuel clad OD).

An evaluation of four M5 clad fuel rods with average burnup 72 GWd/MTU (Ref. 55) depleted at North Anna found essentially zero rod average diameter change and maximum creep down of about [ ]^{A,E} on the low burnup portion of the rod.

[

]^{a,c}.

Fuel clad creep down will be evaluated as a bias. There are two components of this evaluation: (1) Depletion using the burnup averaged clad OD, which may partially offset the growth bias via a softer depletion spectrum, and (2) use of the clad OD vs burnup function to determine fuel clad OD vs burnup for the spent fuel pool rack k calculation. Although models and measurements confirm that clad OD rebounds after reaching a maximum reduction, a conservative two segment linear function will be used. The clad OD will be assumed to decrease linearly by [ ]^{a,c} at 20 GWd/MTU and then remain at this minimum OD through the rest of the burnup range.

10.3 Enrichment/Burnup Requirements

Region 2 features 4 out of 4 storage of fuel with an acceptable combination of enrichment, burnup and decay time. Fuel that is un-acceptable for Region 2 storage must be stored in Region 1 unless it contains a control rod (See Section 10.7). Determination of acceptable

combinations of these three variables for the 0 ppm soluble boron normal storage condition is an iterative process. First, an enrichment/burnup/cooling time is selected and the depletion analysis is performed. The atom densities from this depletion are used in a calculation of the Region 2 k. An estimate of the total bias and uncertainty is applied to this calculated k and the resulting k is compared to 1.0. If the margin to 1.0 is acceptable (not too large or small) then final calculations of the bias and uncertainty are done to determine the final k. If the margin is not acceptable, the process is repeated using another enrichment/burnup/cooling time. This process is done enough times to cover the enrichments that need burnup up to 5 wt% U-235 fuel. In final setting of the enrichment/burnup/cooling time, very small adjustments to the enrichment can be made to provide consistent margin at different enrichment/burnup/cooling time combinations. For example, depletions to 44 GWd/MTU were done at 4.95 wt% and 5.0 wt% U-235, but the final loading criteria for 44 GWd/MTU burnup was set at 44 GWd/MTU at 4.98 wt% U-235.

Only two decay times will be evaluated. Table 6.4 confirms that five days decay maximizes spent fuel reactivity; therefore, the primary burnup credit curve (acceptable minimum fuel burnup versus initial fuel enrichment) will be for five days decay. A decay time of three years provides significant reduction in required burnup for storage in Region 2 and matches well with normal fuel movements in the spent fuel pool. This analysis does not support any extrapolation and interpolation of the cooling time.

Figure 10.9 shows the minimum burnup requirements for Region 2 without credit for cooling. The curve fit is constructed to match or exceed the burnup of all of the calculated burnup / enrichment points. Also shown for reference are the enrichment / burnup points representing fuel in the North Anna Spent Fuel Pool as of 10/1/2015. The pool content is provided to put the burnup credit curve in context but has not been used as input to this criticality safety analysis. Figure 10.10 provides the Region 2 loading requirements for assemblies that have not been at power for more than 3 years.

Required Minimum Burnup (MWd/MTU) = $372.1x^3 - 5304.4x^2 + 36688x - 53110$

where x is enrichment in wt% U-235

(No Cooling Time Required)

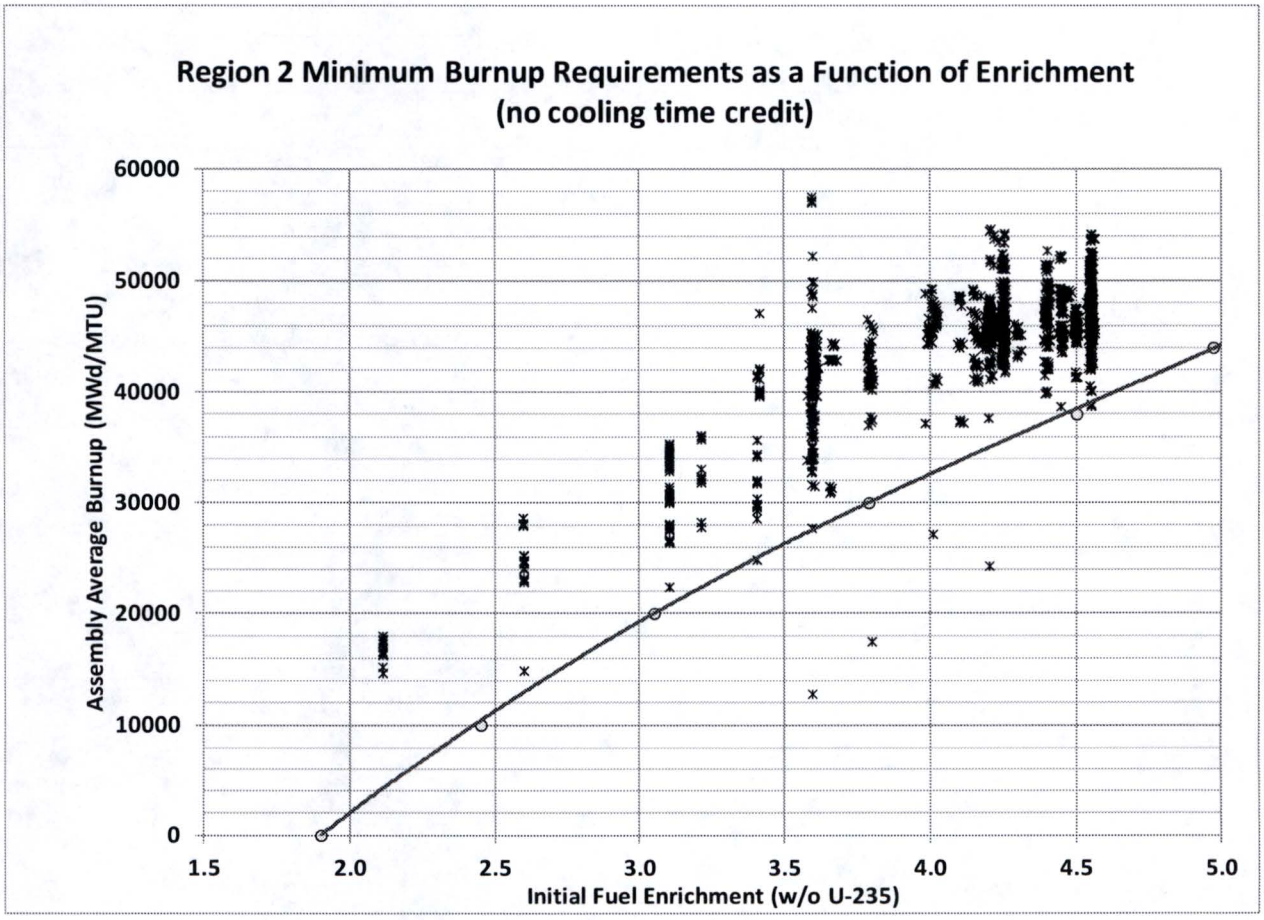

Figure 10.9: Region 2 Minimum Burnup Requirements as a Function of Enrichment (no cooling time credit)

Required Minimum Burnup (MWd/MTU) = $404.2x^3 - 5538.2x^2 + 36520x - 52167$

where x is enrichment in wt% U-235

and the Fuel is Cooled 3 Years or More

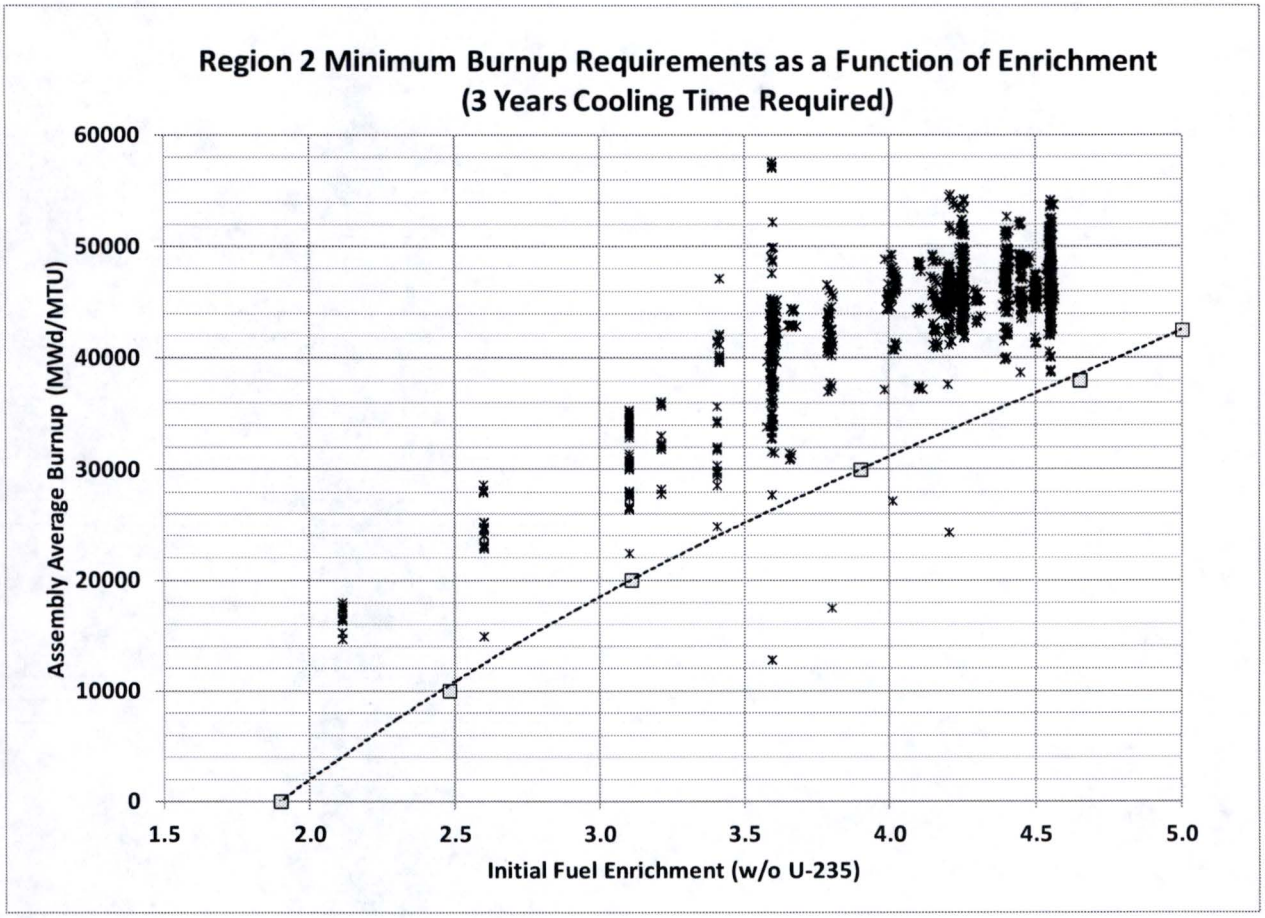

Figure 10.10: Region 2 Minimum Burnup Requirements as a Function of Enrichment (3 Years Cooling Time Required)

The yellow dots along the curves on Figures 10.9 and 10.10 are the burnup/enrichment pairs that were calculated to confirm the minimum burnup requirements. For those points a k is calculated followed by the addition of the biases and the statistically combined uncertainties. This total is then shown not to exceed the 1.0. The biases and uncertainties are presented in the next section.

10.4 Uncertainties and Biases

This section calculates the uncertainties associated with the fuel and rack manufacturing tolerances. This is followed by uncertainty and biases due to the modeling, burnup, and validation.

10.4.1 Fuel Assembly Tolerances

The fuel assembly tolerances were previously given on Table 4.2. Table 10.4 provides the results of the analysis of the reactivity of the fuel tolerances for Region 2. The reactivity due to most of the fuel tolerances is small so in order to save time these small reactivities were calculated using the maximum enrichment fresh fuel allowed in Region 2, 1.9 wt% U-235.

The maximum delta k given on Table 10.4 is the delta k from the base case plus 2 times the square root of the sum of the squares of the Monte Carlo uncertainty. The grid reactivity on Table 10.4 is considered a bias rather than an uncertainty since it represents the low grid volume fuel in the pool.

Table 10.4: Reactivity Associated with Fuel Assembly Tolerances in Region 2

Enrichment (wt% U^{235})	Burnup (GWd/MTU)	Item	Change	k (σ=6E-5)	Max Delta k
1.9	0	Base	N/A	0.9577	N/A
1.9	0	Fuel Stack Density	95.5% increased by the theoretical density tolerance	0.9588	0.0012
1.9	0	Pellet OD	0.8192 cm increased by the tolerance	0.9582	0.0006
1.9	0	Fuel active length	Increase 1 cm	0.9578	0.0002
1.9	0	Fuel Stack position	Lower fuel 1 cm exposing more fuel below wrapper	0.9578	0.0002
1.9	0	Clad ID	0.836 cm increased by the tolerance	0.9581	0.0005
1.9	0	Clad OD	0.95 cm decreased by the tolerance	0.9589	0.0013
1.9	0	Guide Tube ID	1.143 cm increased by the tolerance	0.9580	0.0004
1.9	0	Guide Tube OD	1.224 cm decreased by the tolerance	0.9579	0.0003
1.9	0	Pin Pitch	1.26 cm increased by the tolerance	0.9592	0.0016
1.9	0	Grid	1/3 less grid volume	0.9584	0.0008
1.95	0	Enrichment	Increased 0.05 wt%	0.9655	0.0079
2.45	10U	Base	N/A	0.9549	N/A
2.5	10U	Enrichment	Increased 0.05 wt%	0.9594	0.0046
2.45	10U	Base using 28 Isotopes	N/A	0.9658	N/A
2.45	10U	Pin Pitch	1.26 cm increased by the tolerance	0.9674	0.0017
2.45	10U	Fuel Stack position	Lower fuel 1 cm exposing more fuel below wrapper	0.9659	0.0002
2.45	10U	Grid	1/3 less grid volume	0.9664	0.0008
3.05	20	Base	N/A	0.9527	N/A
3.10	20	Enrichment	Increased 0.05 wt%	0.9562	0.0037
3.075	20	Base using 28 Isotopes	N/A	0.9679	N/A
3.075	20	Pin Pitch	1.26 cm increased by the tolerance	0.9698	0.0020
3.075	20	Fuel Stack position	Raised fuel 1 cm exposing more fuel above wrapper	0.9681	0.0004
3.075	20	Grid	1/3 less grid volume	0.9687	0.0010
3.80	30	Base	N/A	0.9502	N/A
3.85	30	Enrichment	Increased 0.05 wt%	0.9530	0.0029
3.80	30	Base using 28 Isotopes	N/A	0.9681	N/A
3.80	30	Pin Pitch	1.26 cm increased by the tolerance	0.9698	0.0019
3.80	30	Fuel Stack position	Raised fuel 1 cm exposing more fuel above wrapper	0.9683	0.0004
3.80	30	Grid	1/3 less grid volume	0.9688	0.0009
4.50	38	Base	N/A	0.9457	N/A

Enrichment (wt% U^{235})	Burnup (GWd/MTU)	Item	Change	k (σ=6E-5)	Max Delta k
4.40	38	Enrichment	Increased 0.1 wt% delta k divided by 2	0.9407	0.0026
4.50	38	Base using 28 Isotopes	N/A	0.9673	N/A
4.50	38	Pin Pitch	1.26 cm increased by the tolerance	0.9690	0.0019
4.50	38	Fuel Stack position	Raised fuel 1 cm exposing more fuel above wrapper	0.9674	0.0003
4.50	38	Grid	1/3 less grid volume	0.9681	0.0010
5.00	44	Base	N/A	0.9466	N/A
4.95	44	Enrichment	Decrease 0.05 wt% delta k multiplied by -1	0.9443	0.0024
5.00	44	Base using 28 Isotopes	N/A	0.9693	N/A
5.00	44	Pin Pitch	1.26 cm increased by the tolerance	0.9710	0.0019
5.00	44	Fuel Stack position	Raised fuel 1 cm exposing more fuel above wrapper	0.9693	0.0001
5.00	44	Grid	1/3 less grid volume	0.9700	0.0009

10.4.2 Rack Manufacturing Tolerances

Table 10.5 shows the reactivity impact of the rack manufacturing tolerances. Adding more water to the array and reducing stainless steel by making the cell wall or wrapper thinner increases k. Decreasing the cell separation increases k. The reactivity of each of these three tolerance uncertainties is larger than the reactivity of any of the tolerance uncertainties associated with the fuel manufacturing except the enrichment tolerance. The reactivity associated with the uncertainty in tie plate dimensions is very small.

Table 10.5: Reactivity Associated with Rack Manufacturing Tolerances in Region 2

Enrichment (wt% U^{235})	Burnup (GWd/MTU)	Item	Change	k (σ=6E-5)	Max Delta k
1.9	0	Base	N/A	0.9577	N/A
1.9	0	Cell wall thickness	From 0.229 cm to 0.2163 cm	0.9601	0.0026
1.9	0	Cell pitch	From 26.83 cm to 26.7665 cm	0.9605	0.0029
1.9	0	Cell ID	From 22.54 to 22.66 cm	0.9586	0.0010
1.9	0	Wrapper thickness	From 0.074 to 0.0617 cm	0.9600	0.0024
1.9	0	Tie plates thickness*	From 0.305 to 0.287 cm	0.9579	0.0003
2.45	10U	Base using 28 Isotopes	N/A	0.9658	N/A
2.45	10U	Cell wall thickness	From 0.229 cm to 0.2163 cm	0.9680	0.0023
2.45	10U	Cell pitch	From 26.83 cm to 26.7665 cm	0.9686	0.0029
2.45	10U	Wrapper thickness	From 0.074 to 0.0617 cm	0.9681	0.0024
2.45	10U	Tie plates thickness*	From 0.305 to 0.287 cm	0.9659	0.0002
3.075	20	Base using 28 Isotopes	N/A	0.9679	N/A
3.075	20	Cell wall thickness	From 0.229 cm to 0.2163 cm	0.9701	0.0023
3.075	20	Cell pitch	From 26.83 cm to 26.7665 cm	0.9708	0.0031
3.075	20	Wrapper thickness	From 0.074 to 0.0617 cm	0.9702	0.0024
3.075	20	Tie plates thickness*	From 0.305 to 0.287 cm	0.9682	0.0005
3.80	30	Base using 28 Isotopes	N/A	0.9681	N/A
3.80	30	Cell wall thickness	From 0.229 cm to 0.2163 cm	0.9702	0.0023
3.80	30	Cell pitch	From 26.83 cm to 26.7665 cm	0.9708	0.0028
3.80	30	Wrapper thickness	From 0.074 to 0.0617 cm	0.9701	0.0022
3.80	30	Tie plates thickness*	From 0.305 to 0.287 cm	0.9683	0.0004
4.50	38	Base using 28 Isotopes	N/A	0.9673	N/A
4.50	38	Cell wall thickness	From 0.229 cm to 0.2163 cm	0.9694	0.0024
4.50	38	Cell pitch	From 26.83 cm to 26.7665 cm	0.9700	0.0029
4.50	38	Wrapper thickness	From 0.074 to 0.0617 cm	0.9694	0.0023
4.50	38	Tie plates thickness*	From 0.305 to 0.287 cm	0.9674	0.0004
5.00	44	Base using 28 Isotopes	N/A	0.9693	N/A
5.00	44	Cell wall thickness	From 0.229 cm to 0.2163 cm	0.9712	0.0021
5.00	44	Cell pitch	From 26.83 cm to 26.7665 cm	0.9718	0.0026
5.00	44	Wrapper thickness	From 0.074 to 0.0617 cm	0.9712	0.0021
5.00	44	Tie plates thickness*	From 0.305 to 0.287 cm	0.9693	0.0002

*Tie plate width and thickness tolerance has been conservatively combined and modeled by reducing the thickness 6%.

10.4.3 Eccentric Positioning

The base model uses a 4x4 set of eccentric assemblies to bound the degree of asymmetry expected over the life of the spent fuel pool (Section 9.2.3). Table 9.3 showed that the 4x4 asymmetry increased k in Region 2 by 0.0041 in delta k. Table 9.3 also showed that moving all the assemblies as far as possible in a single direction was less reactive than the 4x4 asymmetric grouping found in the base model. Since conservatism was used in the base model no bias is needed for eccentric positioning.

10.4.4 Temperature Bias

All cases are performed with 0 ppm soluble boron, 293 K (68 °F) water temperature (0.9982 g/cc water density). In order to determine the appropriate temperature bias, the base cases were run with a range of temperatures (with associated densities). Table 10.6 shows the results of the analysis. For Region 2 as the water density decreases the calculated k increases. In addition to the k increase there is a bias from the results of the critical experiments (See Section 6.3.3) which has been added to produce the total temperature bias. The upper bound on spent fuel pool temperature for criticality analysis of normal fuel storage in the North Anna spent fuel pool is 140 °F. The depleted fuel temperature bias is about 0.0068. All of the calculated temperature biases are used in the final analysis.

Table 10.6: Change in k with Temperature for Region 2

Enrichment (wt% U^{235})	Burnup (GWd/MTU)	Temperature (°F)	k (σ=6E-5)	Max Delta k	Validation Bias	Total Bias
1.9	0	68	0.9577	N/A	N/A	N/A
1.9	0	32	0.9576	0.0001	0	0.0001
1.9	0	120	0.9611	0.0035	0.0005	0.0040
1.9	0	140	0.9624	0.0048	0.0007	**0.0055**
2.45	10U	68	0.9549	N/A	N/A	N/A
2.45	10U	140	0.9654	0.0061	0.0007	**0.0068**
3.075	20	68	0.9544	N/A	N/A	N/A
3.075	20	140	0.9601	0.0059	0.0007	**0.0066**
3.80	30	68	0.9502	N/A	N/A	N/A
3.80	30	140	0.9560	0.0060	0.0007	**0.0067**
4.50	38	68	0.9457	N/A	N/A	N/A
4.50	38	140	0.9517	0.0061	0.0007	**0.0068**
5.00	44	68	0.9466	N/A	N/A	N/A
5.00	44	140	0.9525	0.0061	0.0007	**0.0068**

10.4.5 Validation Bias and Uncertainty

Section 6 of this report provides the validation biases and uncertainty. There are three components of this validation and all three depend on the actual analysis of the rack. The three components are: the depletion uncertainty, the major actinides and structural materials bias and uncertainty, and the fission product and minor actinide bias.

The depletion uncertainty is 5% of the delta of depletion. This 5% of the delta k of depletion has been accepted by the NRC via the Interim Staff Guidance, DSS-ISG-2010-01. [4] Table 10.7 shows the calculated delta k of depletion. In both the zero burnup and burned cases no burnable absorbers are included in the calculation. The delta k of depletion is the maximum delta k since it includes 2 times the square root of the sum of the squares of the Monte Carlo uncertainties. The depletion uncertainty found on the table is 5% of the delta k of depletion.

The bias and uncertainty from the validation of the major actinides and structural materials was developed in Section 6.3.1 and comes from Table 6.6. Section 6.3.1 specifies that the bias and uncertainty based on the MOX experiments and the bias and uncertainty based on the UO2 experiments need to be applied separately and the most limiting set is used in the final analysis. The fresh fuel Region 2 case (1.9 wt% U-235) uses only the UO2 experiments. At low burnups the total uncertainties are low so the MOX experiments which have a low bias and a high uncertainty dominate (bias = 0.0020, uncertainty = 0.0089). However, at high burnups the statistical combination of uncertainties makes the impact of the high MOX uncertainty less important so the bias and uncertainty from the UO2 experiments (bias = 0.0035, uncertainty = 0.0050) produces the highest final k. The change in which bias/uncertainty pair dominates occurs at 38 GWd/MTU. All of the 0 ppm cases have an Energy of the Average Lethargy of neutrons causing Fission (EALF) of well less than 0.4 eV. (The harder spectra only appear in borated cases and optimum moderation of the new fuel storage area.)

The fission product and minor actinides bias and uncertainty is handled as a bias of 1.5% of the delta k of the fission products and minor actinides. (See Section 6.3.2) Table 10.7 provides the worth and the bias that results from the product of the worth times 0.015. As in all reactivities and worths the reactivity on the table includes the uncertainties in the Monte Carlo analyses.

Table 10.7: Depletion Reactivity and Fission Product and Minor Actinide Worth

Enrichment (wt% U^{235})	Burnup (GWd/MTU)	Item	k (σ=6E-5 to 7E-5	Max Delta k	Depletion Uncertainty	Minor Actinide and FP Bias	Burnup Uncertainty
2.45	10U	Base	0.9549	N/A			
2.45	0	Depletion Reactivity	1.0304	0.0756	0.0038		0.0030
2.45	10U	Only Major Actinides	1.0065	0.0518		0.0008	
3.075	20	Base	0.9544	N/A			
3.075	0	Depletion Reactivity	1.0898	0.1356	0.0068		0.0054
3.075	20	Only Major Actinides	1.0226	0.0684		0.0010	
3.80	30	Base	0.9502	N/A			
3.80	0	Depletion Reactivity	1.1398	0.1898	0.0095		0.0076
3.80	30	Only Major Actinides	1.0382	0.0882		0.0013	
4.50	38	Base	0.9457	N/A			
4.50	0	Depletion Reactivity	1.1761	0.2306	0.0115		0.0092
4.50	38	Only Major Actinides	1.0507	0.1053		0.0016	
5.00	44	Base	0.9466	N/A			
5.00	0	Depletion Reactivity	1.1974	0.2510	0.0125		0.0100
5.00	44	Only Major Actinides	1.0580	0.1116		0.0017	

10.4.6 Uncertainty in the Declared Burnup

The uncertainty in the burnup used by North Anna to compare to the minimum burnup requirements is a combination of assembly relative power measurement uncertainty, calorimetric power uncertainty, fuel assembly loading uncertainty, and uncertainty due to time integration of measured power (performed approximately monthly, nominally 18 times per cycle).

Relative power measurement uncertainty is part of the station safety analysis and includes uncertainty in flux measurements, uncertainty associated with inferring assembly power from flux measurements and uncertainty in assembly average power inferred for non-instrumented assemblies. [57] For North Anna cycles using CASMO-4 and SIMULATE-3 core design models, a nuclear uncertainty factor for predicted assembly peak pin power was determined to be 1.03 (3% uncertainty; Ref. 57). This value assumes that all of the difference between measured and predicted in-core detector reaction rate integrals is mis-prediction. No method was proposed to estimate the relative contribution of measurement and predictive uncertainty. The 3% value is equally applicable as a conservative estimate of measured peak pin uncertainty, because the contribution of predicted uncertainty to this value is assumed to be zero. Measured peak pin uncertainty is larger than measured assembly power uncertainty because individual pin power is less accurately known than the average power of all pins in a fuel assembly.

The total North Anna calorimetric uncertainty using venturi flow measurement at HFP is estimated to be ~1.4% of the Rated Total Power (RTP). A bounding estimate of calorimetric uncertainty using ultrasonic flow meters is ~0.4% RTP.

Fuel assembly uranium loading variation within each batch is small. For example, for North Anna Unit 1 Batch 27A the standard deviation of assembly UO2 weight is less than 0.2%.

Fuel assembly relative power changes gradually through the cycle during which approximately 18 power distribution measurements are obtained. Integration of the assembly power over burnup using an 18 point approximation assuming constant power between points introduces relatively little uncertainty. A test of this for North Anna Unit 2 Cycle 24, using adverse assumptions that a map is obtained at the beginning of the integration period and that the

assembly power is assumed to be constant over the forward interval, the average burnup increase error over the cycle is less than 0.1%. The standard deviation of burnup increase differences is less than 0.6%. Considering that burnup sufficient to meet the storage requirement for Region 2 is accumulated over more than one cycle representing a 36 point (or more) approximation to the power vs burnup curve, a burnup integration uncertainty allowance of 1% is expected to bound actual integration uncertainty.

Assuming these uncertainty contributors are independent, they may be combined by root sum square to obtain a burnup measurement uncertainty estimate, The RSS of 3%, 1.4%, 0.2%, and 1% is 3.5%. 4% of the burnup is used to cover the uncertainty in the burnup used to compare to the burnup requirements.

The burnup uncertainty is found on Table 10.7 and was obtained by multiplying the depletion reactivity by 0.04. For a given % uncertainty, this method of calculating burnup uncertainty is conservative. A more accurate burnup uncertainty reactivity is the change in reactivity due to a 4% reduction in burnup. Since the slope of the depletion reactivity as a function of burnup (Figure 12.6) decreases with burnup, using the average slope over the entire burnup is conservative as compared to the slope at the endpoint burnup. The simple method (4% of burnup worth) is conservative at 44 GWd/MTU by about 0.003 in k.

10.4.7 Bias for Grid Growth, Clad Creep, and Low Power at End of Life

The bias for the grid growth, clad creep, and low power at end of cycle all require depletion analysis. In order to be more time efficient these three effects were calculated together. See Section 8.7 and 10.2 for model assumptions. Table 10.8 shows the calculated k's with the atom densities from the new depletions and dimensions changed in the KENO analysis of Region 2. Also shown on Table 10.8 is the resulting bias which includes the Monte Carlo uncertainties from the cases. One case is included that shows the effect of low power near EOL only.

One out of five bias values accounting for the combined grid growth, creep, and low specific power at EOL effect was obtained by interpolation versus burnup based on the observed (nearly linear) trend of the other four calculated values.

When the conservative clad creep model is being used the manufacturing tolerance uncertainty in reactivity due to the clad OD is set to zero.

Table 10.8: Bias Due to Grid Growth, Clad Creep, and Low Power at End of Life

Enrichment (wt% U^{235})	Burnup (GWd/MTU)	Item	k (σ=6E-5)	Max Delta k
2.45	10U	Base	0.9549	N/A
2.45	10U	Grid Growth, Clad Creep Down, and 50% Power at EOL	0.9591	0.0043
2.45	10U	50% Power at EOL	0.9581	0.0034
3.05	20	Base	0.9527	N/A
3.05	20	Grid Growth, Clad Creep Down, and 50% Power at EOL	0.9571	0.0046
3.80	30	Base	0.9502	N/A
3.80	30	Grid Growth, Clad Creep Down, and 50% Power at EOL	0.9552	0.0052
4.50	38	Base	0.9457	N/A
4.50	38	Grid Growth, Clad Creep Down, and 50% Power at EOL		0.0056*
5.00	44	Base	0.9466	N/A
5.00	44	Grid Growth, Clad Creep Down, and 50% Power at EOL	0.9523	0.0059

*This bias was interpolated from the other calculated biases.

10.4.8 Other Uncertainties and Biases

The only uncertainty not mentioned in the previous subsections is the Monte Carlo uncertainty in the final calculation of k. The sigma for those runs is 0.00006. Multiplied by 2 and rounded makes this uncertainty 0.0001.

There are two biases that were presented in the other sections. A bias of 0.0013 is applied to cover the reactivity of a horizontal gradient in the assembly burnup. (See Section 10.1.1) There is also a bias of 0.0006 applied to cover the reactivity effect of the water displacement due to the incore flux detectors. (See Section 8.9.4)

Although given in Section 10.4.1 with the fuel assembly tolerances, since there is a variation in the grid volume between assembly designs, a bias is taken for grids that are lower in volume. These biases are found on Table 10.4.

Finally, the last bias is the "Margin for NRC Review." This bias is margin provided to the NRC to be used to offset any concerns with the methods used in this analysis. Margin in excess of this 1% NRC margin may be used by Dominion in 10CFR50.59 analysis for future requirements.

10.5 Final $k_{59/95}$ For Region 2 No Cooling Time Credit

Table 10.9 contains the calculation of total uncertainty, bias, and margin to the k<1.0 limit for the 0 ppm normal storage condition with 5 days cooling time. There is significant margin to the limit in addition to the 1% Δa margin for NRC review allowance. No credit has been taken for U-234, integral absorbers, or installed neutron absorbers (Boraflex) in the spent fuel pool racks. The rack cell inside dimension was omitted from Table 10.9. If included, the indicated combined uncertainty would increase by less than 0.0001

Table 10.9: Region 2 Rack up of Biases and Uncertainties for the 0 Soluble Boron Analysis and No Cooling Time Credit

Enrichment (wt% U-235)	**1.9**	**2.45**	**3.05**	**3.79**	**4.50**	**4.98***
Burnup (GWd/MTU)	**0**	**10**	**20**	**30**	**38**	**44**
Reference Case k	0.9577	0.9549	0.9527	0.9497**	0.9457	0.9457***
Uncertainty in the Fuel Stack Density	0.0012	0.0012	0.0012	0.0012	0.0012	0.0012
Uncertainty in the Pellet OD	0.0006	0.0006	0.0006	0.0006	0.0006	0.0006
Uncertainty in the Fuel active length	0.0002	0.0002	0.0002	0.0002	0.0002	0.0002
Uncertainty in the Fuel Stack position	0.0002	0.0002	0.0004	0.0004	0.0003	0.0001
Uncertainty in the Clad ID	0.0005	0.0005	0.0005	0.0005	0.0005	0.0005
Uncertainty in the Clad OD****	0.0013	0.0000	0.0000	0.0000	0.0000	0.0000
Uncertainty in the Guide Tube ID	0.0004	0.0004	0.0004	0.0004	0.0004	0.0004
Uncertainty in the Guide Tube OD	0.0003	0.0003	0.0003	0.0003	0.0003	0.0003
Uncertainty in the Pin Pitch	0.0016	0.0017	0.0020	0.0019	0.0019	0.0019
Uncertainty in the Enrichment	0.0079	0.0046	0.0037	0.0029	0.0026	0.0024
Uncertainty in the Cell wall thickness	0.0026	0.0023	0.0023	0.0023	0.0024	0.0021
Uncertainty in the Cell pitch	0.0029	0.0029	0.0031	0.0028	0.0029	0.0026
Uncertainty in the Wrapper thickness	0.0024	0.0024	0.0024	0.0021	0.0023	0.0021
Uncertainty in the Tie plates thickness	0.0003	0.0002	0.0005	0.0004	0.0004	0.0002
Uncertainty in Atom Densities (Depletion Uncertainty)	0.0000	0.0038	0.0068	0.0095	0.0115	0.0125
Uncertainty in Declared Burnup (Burnup Measurement Uncertainty)	0.0000	0.0030	0.0054	0.0076	0.0092	0.0100
Uncertainty from Validation of Major Actinides and Structural Materials	0.0050	0.0089	0.0089	0.0089	0.0050	0.0050
Monte Carlo Uncertainty in Final k calculation	0.0001	0.0001	0.0001	0.0001	0.0001	0.0001
Statistically Combined Uncertainties	**0.0107**	**0.0122**	**0.0140**	**0.0161**	**0.0166**	**0.0176**
Bias to the most reactive temperature	0.0055	0.0068	0.0066	0.0067	0.0068	0.0067
Bias for Minor Actinides and Fission Products	0.0000	0.0008	0.0010	0.0013	0.0016	0.0017
Bias from Validation of Major Actinides and Structure Materials	0.0035	0.0020	0.0020	0.0020	0.0035	0.0035
Bias to Cover Dimensional Changes with Burnup & Low Power Operation at EOL	0.0000	0.0043	0.0046	0.0052	0.0056	0.0059
Bias to the most reactive grid volume	0.0008	0.0008	0.0010	0.0009	0.0010	0.0009
Bias to Cover Horizontal Burnup Gradient	0.0000	0.0013	0.0013	0.0013	0.0013	0.0013
Bias to Cover Incore Thimble Water Displacement	0.0000	0.0006	0.0006	0.0006	0.0006	0.0006
Sum of Biases	**0.0098**	**0.0166**	**0.0171**	**0.0179**	**0.0204**	**0.0206**
Margin for NRC review	**0.0100**	**0.0100**	**0.0100**	**0.0100**	**0.0100**	**0.0100**
k-eff with 95/95 probability and confidence	**0.9883**	**0.9937**	**0.9937**	**0.9937**	**0.9926**	**0.9939**
Acceptance criteria	1.0	1.0	1.0	1.0	1.0	1.0
Dominion held Margin	**0.0117**	**0.0063**	**0.0063**	**0.0063**	**0.0074**	**0.0061**

*The highest enrichment allowed is 5.0 but the analysis was performed 44 GWd/MTU burnup which corresponds to 4.98 wt% U-235. A small extrapolation of the loading curve (Figure 10.9) to 5 wt% fuel gives a burnup requirement of 44.233 GWd/MTU.

**This k was interpolated for a different enrichment using the calculated k's for 3.8 wt% (0.95021) and 3.85 wt% (0.95021).

***This k was interpolated for a different enrichment using the calculated k's for 4.95wt% (0.94433) and 5.00 wt% (0.94659).

****The clad OD uncertainty for burned fuel is replaced by the dimensional changes with burnup bias.

10.6 Credit for 3 Years or More Cooling

Fuel assemblies are stored in the spent fuel pool at least until the assembly decay heat has declined below the maximum cask storage heat load (on the order of 7 years). Decay time credit of 3 years provides a reduced burnup credit requirement such that an assembly with slightly inadequate burnup for storage in Region 2 (must be stored in Region 1 as fresh fuel) could be moved to Region 2 after 3 years in the spent fuel pool (2 cycles).

The analysis required for decay time is the same as for the no cooling credit burnup curve, except 3 years decay is used at the end of the TRITON depletions rather than 5 days. In order for these cases to reflect only the effect of additional decay time, the same burnup shapes are used for corresponding points on each burnup curve. Fuel enrichment will be increased from the base burnup curve to obtain the 3 year decay time burnup curve. The decay time curve has similar margin to the limit as the corresponding points on the primary burnup curve.

The total uncertainty for the depleted fuel cases is dominated by three terms; the depletion uncertainty, the burnup uncertainty, and the validation uncertainty. These three uncertainties account for 83% at low burnups to 95% at the high burnup of the total uncertainty. Since the change in the manufacturing uncertainties with burnup/enrichment is modest, the manufacturing uncertainties from the no cooling credit are used for the 3 year cooling credit analysis.

The largest bias is the temperature bias so new temperature biases are calculated for the 3 years cooling analysis. The second largest bias is the lumped bias for dimensional changes with burnup and low power at end of life. The highest burnup case (depletion plus pool k calculation) was analyzed for the lumped bias and the result was within round off of the 5 day decay time result, so the other burnup values were taken from the no cooling credit analysis. The grid variation bias from the no cooling credit analysis was also assumed to be the same for the three years cooling (This is a small bias that is essentially the same for all enrichment/burnup points)). Table 10.10 provides the calculations for the bias and uncertainty for 3 years cooled fuel.

Table 10.11 shows the 3 year cooling rack up of biases and uncertainties to determine the $k_{95/95}$. As can be seen at the bottom of the table the criticality criterion is met and there is significant margin. The rack cell inside dimension was omitted from Table 10.11. If included, the indicated combined uncertainty would increase by less than 0.0001.

Table 10.10: Uncertainty and Bias Calculations for 3 Years Cooled Fuel

Enrichment (wt% U^{235})	Burnup (GWd/MTU)	Item	k (σ=6E-5 to 7E-5)	Max Delta k	Depletion Uncertainty	Minor Actinide and FP Bias	Burnup Uncertainty
2.48	10U	Base	0.9538	N/A			
2.48	0	Depletion Reactivity	1.0337	0.0800	0.0040		0.0032
2.48	10U	Only Major Actinides	1.0065	0.0529		0.0008	
2.48	10U	140 F	0.9595	0.0066			
3.11	20	Base	0.9520	N/A			
3.11	0	Depletion Reactivity	1.0925	0.1407	0.0070		0.0056
3.11	20	Only Major Actinides	1.0188	0.0669		0.0010	
3.11	20	140 F	0.9577	0.0066			
3.90	30	Base	0.9491	N/A			
3.90	0	Depletion Reactivity	1.1456	0.1967	0.0098		0.0079
3.90	30	Only Major Actinides	1.0353	0.0864		0.0013	
3.90	30	140 F	0.9550	0.0067			
4.65	38	Base	0.9447	N/A			
4.65	0	Depletion Reactivity	1.1829	0.2384	0.0119		0.0095
4.65	38	Only Major Actinides	1.0479	0.1034		0.0016	
4.65	38	140 F	0.9507	0.0068			
5.00	42.5	Base	0.9440	N/A			
5.00	0	Depletion Reactivity	1.1974	0.2536	0.0127		0.0101
5.00	42.5	Only Major Actinides	1.0511	0.1073		0.0016	
5.00	42.5	140 F	0.9500	0.0069			

Table 10.11: Region 2 Rack up of Biases and Uncertainties for the 0 Soluble Boron Analysis and 3 Years Cooling Time Credit

Enrichment (wt% U-235)	**1.9**	**2.48**	**3.11**	**3.9**	**4.65**	**5.00**
Burnup (GWd/MTU)	**0**	**10**	**20**	**30**	**38**	**42.5**
Reference Case k	**0.9577**	**0.9538**	**0.9520**	**0.9491**	**0.9447**	**0.9440**
Uncertainty in the Fuel Stack Density	0.0012	0.0012	0.0012	0.0012	0.0012	0.0012
Uncertainty in the Pellet OD	0.0006	0.0006	0.0006	0.0006	0.0006	0.0006
Uncertainty in the Fuel active length	0.0002	0.0002	0.0002	0.0002	0.0002	0.0002
Uncertainty in the Fuel Stack position	0.0002	0.0002	0.0004	0.0004	0.0003	0.0001
Uncertainty in the Clad ID	0.0005	0.0005	0.0005	0.0005	0.0005	0.0005
Uncertainty in the Clad OD*	0.0013	0.0000	0.0000	0.0000	0.0000	0.0000
Uncertainty in the Guide Tube ID	0.0004	0.0004	0.0004	0.0004	0.0004	0.0004
Uncertainty in the Guide Tube OD	0.0003	0.0003	0.0003	0.0003	0.0003	0.0003
Uncertainty in the Pin Pitch	0.0016	0.0017	0.0020	0.0019	0.0019	0.0019
Uncertainty in the Enrichment	0.0079	0.0046	0.0037	0.0029	0.0026	0.0024
Uncertainty in the Cell wall thickness	0.0026	0.0023	0.0023	0.0023	0.0024	0.0021
Uncertainty in the Cell pitch	0.0029	0.0029	0.0031	0.0028	0.0029	0.0026
Uncertainty in the Wrapper thickness	0.0024	0.0024	0.0024	0.0021	0.0023	0.0021
Uncertainty in the Tie plates thickness	0.0003	0.0002	0.0005	0.0004	0.0004	0.0002
Uncertainty in Atom Densities (Depletion Uncertainty)	0.0000	0.0040	0.0070	0.0098	0.0119	0.0127
Uncertainty in Declared Burnup (Burnup Measurement Uncertainty)	0.0000	0.0032	0.0056	0.0079	0.0095	0.0101
Uncertainty from Validation of Major Actinides and Structural Materials	0.0050	0.0089	0.0089	0.0089	0.0050	0.0050
Monte Carlo Uncertainty in Final k calculation	0.0001	0.0001	0.0001	0.0001	0.0001	0.0001
Statistically Combined Uncertainties	**0.0107**	**0.0123**	**0.0142**	**0.0164**	**0.0170**	**0.0178**
Bias to the most reactive temperature	0.0055	0.0066	0.0066	0.0067	0.0068	0.0069
Bias for Minor Actinides and Fission Products	0.0000	0.0008	0.0010	0.0013	0.0016	0.0016
Bias from Validation of Major Actinides and Structure Materials	0.0035	0.0020	0.0020	0.0020	0.0035	0.0035
Bias to Cover Dimensional Changes with Burnup & Low Power Operation at EOL	0.0000	0.0043	0.0046	0.0052	0.0056	0.0058
Bias to the most reactive grid volume	0.0008	0.0008	0.0010	0.0009	0.0010	0.0009
Bias to Cover Horizontal Burnup Gradient	0.0000	0.0013	0.0013	0.0013	0.0013	0.0013
Bias to Cover Incore Thimble Water Displacement	0.0000	0.0006	0.0006	0.0006	0.0006	0.0006
Sum Of Biases	**0.0098**	**0.0163**	**0.0170**	**0.0179**	**0.0204**	**0.0205**
Margin for NRC review	**0.0100**	**0.0100**	**0.0100**	**0.0100**	**0.0100**	**0.0100**
k-eff with 95/95 probability and confidence	**0.9883**	**0.9925**	**0.9932**	**0.9935**	**0.9921**	**0.9923**
Acceptance criteria	1.0	1.0	1.0	1.0	1.0	1.0
Dominion held Margin	**0.0117**	**0.0075**	**0.0068**	**0.0065**	**0.0079**	**0.0077**

*The clad OD uncertainty for depleted fuel is replaced by the dimensional changes with burnup bias.

10.7 Control Rod Credit

The North Anna spent fuel pool contains numerous used control rods (RCCAs). These control rods were removed from service for mechanical wear limits and neutronically are essentially new control rods. A conservative depletion analysis will be used to determine the RCCA absorber content. These control rods allow any assembly to be placed in Region 2 without burnup credit. This is useful for under-burned assemblies and could be helpful if an unexpected full core offload is necessary.

There are two batches of discharged RCCAs in the North Anna spent fuel pool that are of similar but not identical design. The design of the control rods in current use and the control rods of the 1995 to 2010 vintage differ only slightly from the original design. Of interest for criticality, [

]^{a,c}. A very thin hard chrome plating on the outside of the clad was also added. This plating is intended only for wear control and is too thin to have a significant effect of the control rod worth and is ignored. Because the reduced absorber diameter could slightly reduce RCCA worth, it is conservative to use the newer design in the evaluation of control rod credit.

The dimensions of the North Anna RCCA is given on Table 4.4

RCCAs are shuffled each cycle so that no single RCCA resides in the lead control position more than three cycles over its lifetime. This practice limits wear but also limits the depletion time for the portion of the RCCA that is in the active fuel region during at-power reactor operation. North Anna tends to operate with RCCAs nearly fully withdrawn (See Table 8.12). The largest cycle average insertion for the lead bank was found to be 1.7 steps (~1 inch). RCCA depletion was performed to conservatively bound that insertion by depleting the entire 12 inch reduced diameter lead section of all North Anna RCCAs for three full cycles (51 months of depletion).

The RCCA depletion used the North Anna Node 18 burnup credit TRITON fuel depletion model (RCCA depleted using the flux depletion option). Node 18 represents the uppermost 8 inches of fuel. Typical depletion conditions are represented using 4.0 w/o fuel and the 30 GWd/MTU NUREG axial burnup shape used for the development of the Region 2 burnup credit curve. Bounding high assembly power was used, which will maximize control rod depletion. The

remainder of the control rod absorber is neutronically far from the fluence levels found in the core and are not depleted. Table 10.12 provides the atom densities of the fresh and depleted control rods. The depleted control rod model actually used all the isotopes created by TRITON which consisted of 37 isotopes but only the isotopes with significant atom densities or absorption are on Table 10.12.

Table 10.12: Control Rod Atom Densities

Isotope	Fresh Atom Density (atoms/barn-cm)	Depleted Atom Density (atoms/barn-cm)
Ag-107	2.352E-02	2.244E-02
Ag-109	2.185E-02	1.935E-02
Cd-106	3.466E-05	3.420E-05
Cd-108	2.268E-05	1.118E-03
Cd-110	3.396E-04	2.813E-03
Cd-111	3.475E-04	3.778E-04
Cd-112	6.561E-04	6.664E-04
Cd-113	3.306E-04	2.873E-07
Cd-114	7.842E-04	1.115E-03
Cd-116	2.059E-04	2.052E-04
In-113	3.414E-04	2.798E-04
In-115	7.651E-03	5.664E-03
Sn-114	0	5.563E-05
Sn-116	0	1.984E-03
Sn-117	0	1.743E-05
Pd-108	0	2.820E-05

Figure 10.11 is a KENO3D representation of the Region 2 KENO spent fuel pool rack model with RCCAs inserted.

The RCCA credit KENO rack models include a 5 inch unpoisoned fuel length at the bottom of the fuel assembly, which conservatively bounds the most limiting fuel design. The current designs have less than 5 inches covered by over 0.6 inches which easily bounds any of the uncertainties in position. Further, the model does not include the control rod end plug. An analysis with the end plug modeled showed that ignoring the end plug is conservative. Due to this margin the uncertainty of the fuel stack position relative to the wrapper plates was not

recalculated, rather the highest uncertainty from all the calculations (0.0004) for Regions 1 or 2 was used (having no impact on the final statistically combined uncertainty).

Two additional check calculations were performed. Two cases were run where the control rodded assemblies placed in Region 2 models with burned fuel. One case placed four 5wt% U-235 assemblies with control rods in model with 2.45 wt% U-235 fuel burned to 10 GWd/MTU. The axial burnup distribution for this case was uniform. Although the k of control rodded assemblies is higher than the burned 2.45 wt% assemblies the k of the mixed system was lower than the k of burned 2.45 wt% reference case. This was likely because the k of the control rodded cases is dominated by the reactivity from the bottom 5 inches of the fuel which is below the bottom of the control rods. The burned 2.45 wt% fuel reactivity is slightly top peaked since the higher temperature depletion makes the top of the fuel more reactive. (Note that although the burnup is assumed to be uniform up the fuel, each node has its own depletion parameters.) This conflict in axial distribution of reactivity results in lower k's. Figure 10.12 shows the model used. Table 10.13 shows the calculated k's of the mixed models. The second mixed model case used high burned fuel and as expected the k of the mixed model decreases even more.

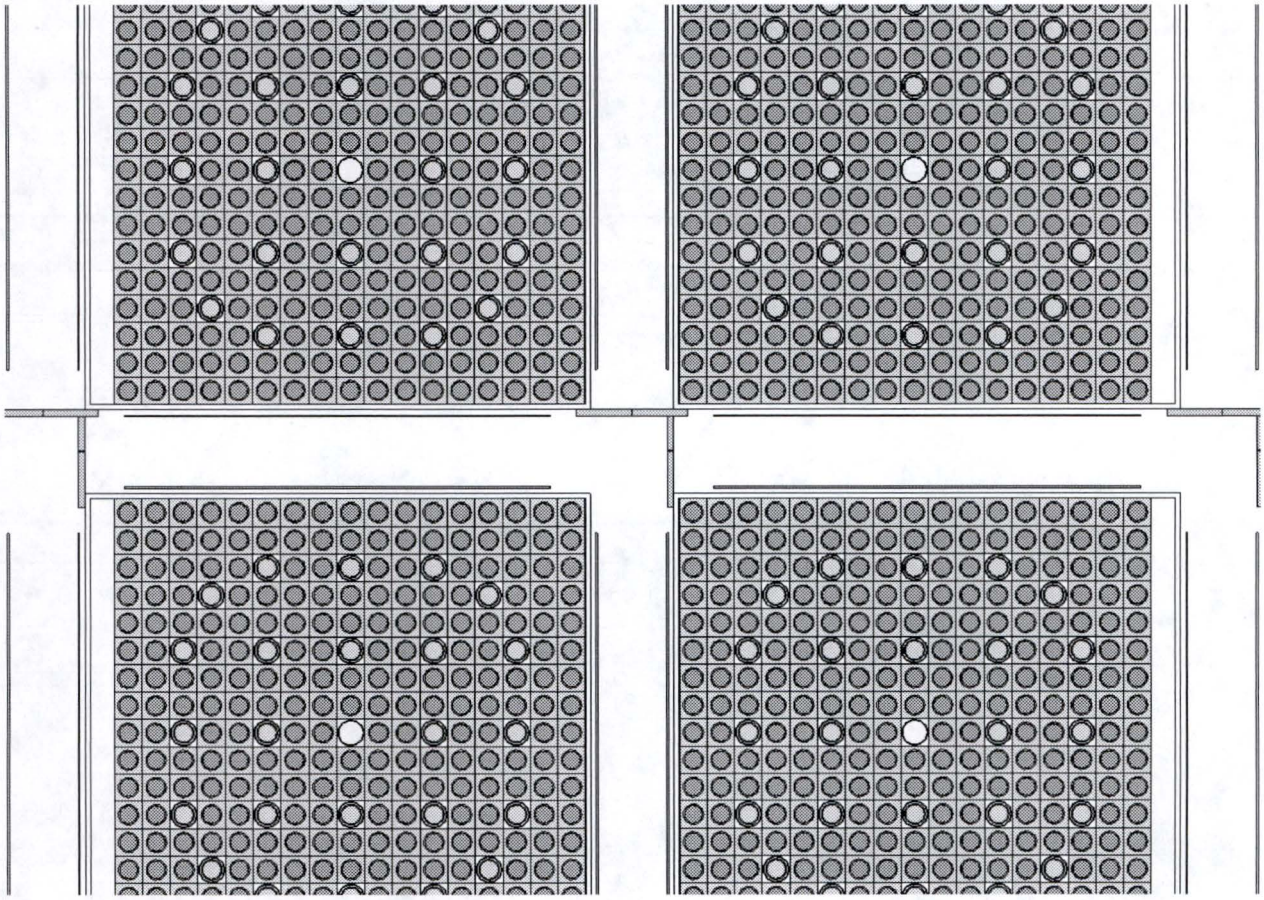

Figure 10.11: KENO Region 2 Control Rod Credit Model (close-up portion of 6x6)

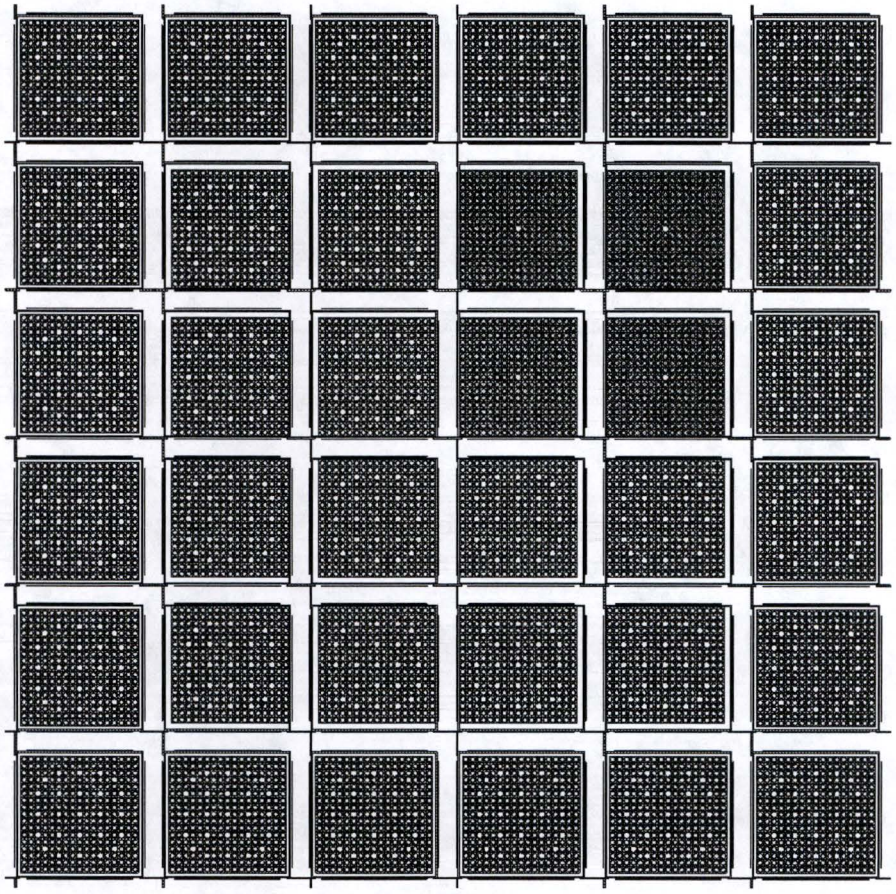

Figure 10.12: KENO Region 2 Mix Control Rod Credit and Burnup Credit Model

Table 10.13: Calculated k's for the Mixed Control Rod/Burnup Credit Models

Enrichment (wt% U-235)	Burnup (GWD/MTU)	Case	k-eff	Sigma	Max Delta k
2.45	10U / 0	Reg 2 base	0.9549	0.00006	N/A
2.45 / 5.0	10U / 0	Mixed Reg 2	0.9542	0.00006	-0.0006
5.00	44	Reg 2 base	0.9466	0.00006	N/A
5.0 / 5.0	44 / 0	Mixed Reg 2	0.9436	0.00006	-0.0028

Region 2 bias and uncertainty calculation results for the Region 2 control rod credit model with 5.0 w/o fresh fuel are presented in Table 10.14.

Table 10.15 adds the statistically combined uncertainty and the biases to the calculated k and shows that the criterion that $k_{95/95}$ is less than 1.0 with no credit for soluble boron is met. The margin to the criticality limit is similar to that for the burnup credit cases for Region 2. The rack cell inside dimension was omitted from Table 10.15. If included, the indicated combined uncertainty would increase by less than 0.0001.

Table 10.14: Bias and Uncertainty Calculations for 5 wt% U-235 Fuel with No Burnup and a Control Rod Inserted

Item	Change	k	Sigma	Max Delta k
Base	N/A	0.9652	0.00007	N/A
Fuel Stack Density	95.5% increased by the theoretical density tolerance	0.9658	0.00008	0.0009
Pellet OD	0.8192 cm increased by the tolerance	0.9655	0.00006	0.0005
Fuel Active Length	Increase 1 cm	0.9650	0.00006	0.0000
Clad ID	0.836 cm increased by the tolerance	0.9652	0.00007	0.0002
Clad OD	0.95 cm decreased by the tolerance	0.9664	0.00007	0.0014
Guide Tube ID	1.143 cm increased by the tolerance	0.9652	0.00007	0.0002
Guide Tube OD	1.224 cm decreased by the tolerance	0.9653	0.00006	0.0003
Pin Pitch	1.26 cm increased by the tolerance	0.9670	0.00006	0.0020
Control Absorber Material OD	Decreased by the tolerance	0.9655	0.00007	0.0005
Control Rod Clad OD	Increased by the tolerance	0.9652	0.00007	0.0002
Cell Wall Thickness	From 0.229 cm to 0.2163 cm	0.9676	0.00007	0.0026
Cell Pitch	From 26.83 cm to 26.7665 cm	0.9679	0.00006	0.0029
Wrapper Thickness	From 0.074 to 0.0617 cm	0.9674	0.00007	0.0024
Tie plates Thickness	From 0.305 to 0.287 cm	0.9652	0.00006	0.0002
Grid	1/3 less grid volume	0.9659	0.00006	0.0009
Temperature	From 68 F to 140 F	0.9712	0.00007	0.0069

Table 10.15: Region 2 Rack up of Biases and Uncertainties for the 0 Soluble Boron Analysis 5 wt% Fuel with Control Rods

Enrichment (wt% U-235)	**5.0**
Burnup (GWd/MTU)	**0**
Reference Case k	**0.9652**
Uncertainty in the Fuel Stack Density	0.0009
Uncertainty in the Pellet OD	0.0005
Uncertainty in the Fuel Active Length	0.0000
Uncertainty in the Fuel Stack Position	0.0004
Uncertainty in the Clad ID	0.0002
Uncertainty in the Clad OD	0.0014
Uncertainty in the Guide Tube ID	0.0002
Uncertainty in the Guide Tube OD	0.0003
Uncertainty in the Pin Pitch	0.0020
Uncertainty in the Control Absorber Material OD	0.0005
Uncertainty in the Control Rod Clad OD	0.0002
Uncertainty in the Cell wall thickness	0.0026
Uncertainty in the Cell pitch	0.0029
Uncertainty in the Wrapper thickness	0.0024
Uncertainty in the Tie plates thickness	0.0002
Monte Carlo uncertainty in the Reference Case	0.0001
Validation uncertainty	0.0050
Statistically Combined Uncertainties	**0.0073**
Bias from Code and Cross Section Library Validation	0.0035
Bias to the most reactive temperature	0.0069
Bias to the most reactive grid volume	0.0009
Sum of Biases	**0.0113**
Margin for NRC review	**0.0100**
k-eff with 95/95 probability and confidence	**0.9938**
Acceptance criteria	1.0
Dominion held Margin	**0.0062**

10.8 Meeting Region 2 Soluble Boron Credit Criterion

With boron credit, $k_{95/95}$ must be less than 0.95. The boron dilution analysis of record showed that dilution below 1200 ppm would be prevented even with the largest flow rate of pure water due to the large dilution time. [46] The previous criticality analysis used only 900 ppm in the analysis approved with an NRC SER. [47] For this analysis 900 ppm boron credit is used.

Table 10.16 shows the $k_{95/95}$ values for Region 2 with 900 ppm. The rack cell inside dimension was omitted from Table 10.9. If included, the indicated combined uncertainty would increase by less than 0.0001

Due to the large margin for the borated cases the uncertainties and biases are taken from the zero boron cases. A Millstone 2 analysis showed that the uncertainties decreased under the borated condition, primarily due to a substantial decrease in depletion reactivity that dominates the depleted fuel uncertainty. [9] For that analysis, the temperature bias and asymmetric placement bias increased with boron. However, the asymmetric condition is part of the rack model for the North Anna analysis, and the temperature bias is calculated for the zero burnup and high burnup cases. The EPRI analysis [30] of the change in uncertainties with the change in boration showed that for Region 2 type analysis, the maximum non-conservatism from using the unborated uncertainties and no grids was about 0.0035 in k (Table 5-16, Reference 30).

The temperature bias with soluble boron present decreased for both cases, so the temperature bias used for the total bias calculation is from the 0 ppm cases except for the three calculated values (RCCA credit case, fresh fuel case, and maximum burnup case).

Although the cases analyzed have 900 ppm soluble boron the EALF's for all the cases are less than 0.4 eV so increased validation bias and uncertainty is not needed.

Since there is significant margin available, the margin for NRC review has been raised from 1% to 2% to cover any concerns over the estimated uncertainties. Note that this additional margin is much larger than the maximum increase calculated in the EPRI and Millstone Unit 2 analyses. No credit has been taken for the reduction in depletion reactivity at higher soluble boron. The Table 10.16 $k_{95/95}$ values are lower than 0.95 so the soluble boron credit criterion is met.

The three years cooled conditions are similar to the no cooling analysis and again due to the large margin no calculations are needed to confirm that the 0.95 $k_{59/95}$ criteria are met.

Table 10.16: Region 2 Rack up of Biases and Uncertainties for the 900 ppm Soluble Boron Credit Analysis and No Cooling Time Credit

Enrichment (wt% U-235)	**1.9**	**2.45**	**3.05**	**3.79**	**4.50**	**4.98***	**5.0**
Burnup (GWd/MTU)	**0**	**10**	**20**	**30**	**38**	**44**	**0+CR*** **
Reference Case k	0.7565	0.7843	0.7932	0.8001**	0.8020	0.8062**	0.8210
Uncertainties:							
Fuel Stack Density[c]	0.0012	0.0012	0.0012	0.0012	0.0012	0.0012	0.0009
Pellet OD[c]	0.0006	0.0006	0.0006	0.0006	0.0006	0.0006	0.0005
Fuel Active Length[c]	0.0002	0.0002	0.0002	0.0002	0.0002	0.0002	0.0000
Fuel Stack Position[c]	0.0002	0.0002	0.0004	0.0004	0.0003	0.0001	0.0004
Clad ID[c]	0.0005	0.0005	0.0005	0.0005	0.0005	0.0005	0.0002
Clad OD	0.0013	0.0000	0.0000	0.0000	0.0000	0.0000	0.0014
Guide Tube ID[c]	0.0004	0.0004	0.0004	0.0004	0.0004	0.0004	0.0002
Guide Tube OD[c]	0.0003	0.0003	0.0003	0.0003	0.0003	0.0003	0.0003
Pin Pitch[c]	0.0016	0.0017	0.0020	0.0019	0.0019	0.0019	0.0020
Enrichment[c]	0.0079	0.0046	0.0037	0.0029	0.0026	0.0024	0.0
Cell Wall Thickness[c]	0.0026	0.0023	0.0023	0.0023	0.0024	0.0021	0.0026
Cell Pitch[c]	0.0029	0.0029	0.0031	0.0028	0.0029	0.0026	0.0029
Wrapper Thickness[c]	0.0024	0.0024	0.0024	0.0021	0.0023	0.0021	0.0024
Tie Plates Thickness[c]	0.0003	0.0002	0.0005	0.0004	0.0004	0.0002	0.0002
Depletion Uncertainty[c]	0.0000	0.0038	0.0068	0.0095	0.0115	0.0125	0.0005[a]
Declared Burnup Uncertainty[c]	0.0000	0.0030	0.0054	0.0076	0.0092	0.0100	0.0002[b]
Validation From Crits	0.0050	0.0089	0.0089	0.0089	0.0050	0.0050	0.0050
Monte Carlo Uncertainty	0.0001	0.0001	0.0001	0.0001	0.0001	0.0001	0.0002
Statistically Combined Uncertainties	**0.0107**	**0.0122**	**0.0140**	**0.0161**	**0.0166**	**0.0176**	**0.0073**
Biases							
Temperature	0.0041	0.0068[c]	0.0066[c]	0.0067[c]	0.0068[c]	0.0059	0.0049
Minor Actinides and FP [c]	0.0000	0.0008	0.0010	0.0013	0.0016	0.0017	0.0
Validation From Crits	0.0035	0.0020	0.0020	0.0020	0.0035	0.0035	0.0035
Dimensional Changes with Burnup & Low Power EOL[c]	0.0000	0.0043	0.0046	0.0052	0.0056	0.0059	0.0
Most Reactive Grid Volume[c]	0.0008	0.0008	0.0010	0.0009	0.0010	0.0009	0.0009

Horizontal Burnup Gradient[c]	0.0000	0.0013	0.0013	0.0013	0.0013	0.0013	0.0
Incore Thimble Hardening[c]	0.0000	0.0006	0.0006	0.0006	0.0006	0.0006	0.0
Sum Of Biases	**0.0084**	**0.0166**	**0.0171**	**0.0180**	**0.0204**	**0.0198**	**0.0093**
Margin for NRC review	**0.0200**	**0.0200**	**0.0200**	**0.0200**	**0.0200**	**0.0200**	**0.0200**
k-eff with 95/95 probability and confidence	**0.7947**	**0.8330**	**0.8442**	**0.8542**	**0.8590**	**0.8636**	**0.8577**
Acceptance criteria	0.95	0.95	0.95	0.95	0.95	0.95	0.95
Dominion held Margin	**0.1553**	**0.1170**	**0.1058**	**0.0958**	**0.0910**	**0.0864**	**0.0923**

*The highest enrichment allowed, 5.0, requires 44.233 GWd/MTU. The analysis was performed at 44 GWd/MTU burnup which corresponds to a maximum enrichment of 4.98 wt% U-235.

**This k was conservatively calculated using the enrichment rounded up to the nearest 0.1 in enrichment (i.e. 3.8 and 5.0).

*** This case has control rods inserted in the assembly.

[a] Uncertainty in the Control Absorber Material OD

[b] Uncertainty in the Control Rod Clad OD

[c] Due to the large margin the unborated uncertainties and bias were used for these parameters.

10.9 Non-Standard Fuel Allowances

There are two types of non-standard fuel, a fuel assembly that has been reconstituted and a container for fuel rods or pieces. Reconstituted fuel will be handled in Section 12.5. The only fuel bearing container is the "Fuel Rod Storage Racks" (FRSR). There are two of these containers in the North Anna spent fuel pool. Although the drawing calls these racks, they are containers open to the water for storage of 52 individual fuel rods that are to be placed in a spent fuel pool rack cell. Figure 4.3 (Section 4 describes all items in the pool) shows a picture of one of them.

Analysis of the FRSR is needed to determine if any restrictions on loading the FRSR are required. A KENO model of the North Anna spent fuel pool rack with the FRSR was made to determine the reactivity of a full FRSR in the rack. A few conservative assumptions were made:

- A fresh, 5.0 wt% fuel pin is placed in every FRSR tube. This is conservative because failed fuel pins have burnup.

- It is unclear what the axial position of the fuel stack would be when a fuel pin is placed into the FRSR. Therefore, the axial position of the active fuel is conservatively assumed to be the same axial positioning of the active fuel in the rest of the pool.

- The tubes will be conservatively modeled as water instead of a metal, therefore the tube dimensions are not used.

- The FRSR is conservatively modeled without the corner braces or grids. Figure 10.13 is a side view of the FRSR showing the top grid and corner braces. To account for the possibility that the FRSR lattice is over moderated, the optimum void fraction was determined. The results of this analysis (See Table 10.17) shows that the max k was achieved with full density water.

If a Fuel Rod Storage Rack was placed in every cell in North Anna spent fuel pool the maximum k would be 0.8012. This is more than 10% in k lower than the calculated k's for the loading requirements for Region 1 or 2. To confirm that there is no interaction between the FRSR and the fuel assemblies in the normally loaded rack, a few cases were run with an FRSR in several locations of the normal Region 1 and Region 2 models. In all cases k decreased. Since the standard models contain 36 assemblies for Region 2 and 18 assemblies for Region 1, a single FRSR did not depress k much due to its relatively small volume. However, when the FRSR was placed in the highest worth asymmetry positions it decreased k more.

Since when fully loaded with 5 wt% U-235 rods the Fuel Rod Storage Rack has a lower reactivity than a loading requirements for Region 1 or Region 2, there are no restrictions on the placement of the two Fuel Rod Storage Racks.

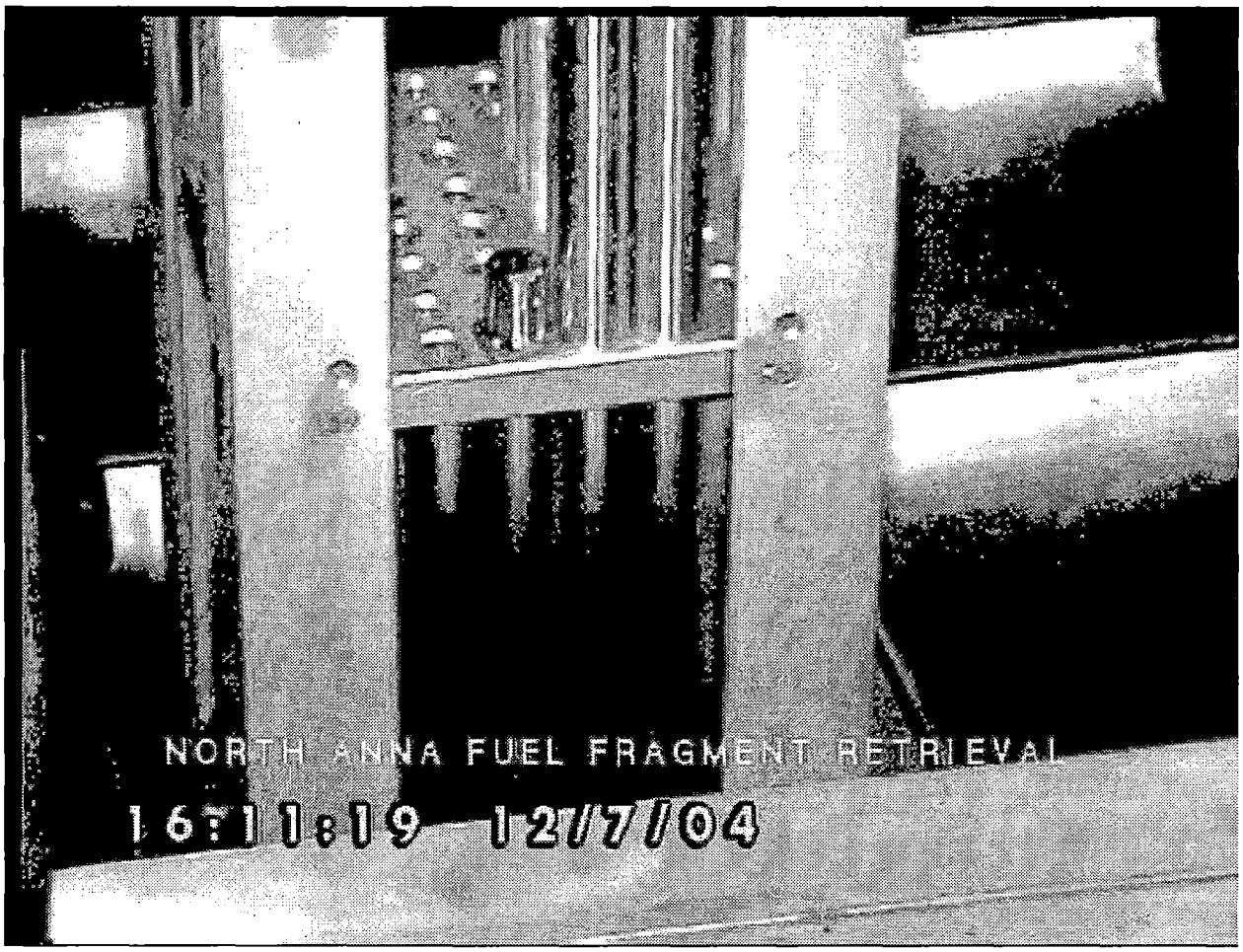

Figure 10.13: Side View of the Fuel Rod Storage Rack

Table 10.17: KENO Results for a Fuel Rod Storage Rack Analysis

Case Scenario	k-eff
Fuel Rod Storage Rack in every cell, 0.0% Void Fraction	0.8012 ± 0.00010
Fuel Rod Storage Rack in every cell, 0.5% Void Fraction	0.8008 ± 0.00010
Fuel Rod Storage Rack in every cell, 1.0% Void Fraction	0.8006 ± 0.00010
Fuel Rod Storage Rack in every cell, 1.5% Void Fraction	0.7800 ± 0.00011
Fuel Rod Storage Rack in every cell, 2.0% Void Fraction	0.7997 ± 0.00010
Fuel Rod Storage Rack in every cell, 3.0% Void Fraction	0.7985 ± 0.00010
Fuel Rod Storage Rack in every cell, 5.0% Void Fraction	0.7967 ± 0.00011

10.10Non-Fuel Component Location Restrictions

Non-fuel components may be placed in any cell where fuel is allowed since it is less reactive than fuel. Non-fuel can also be placed in the guide tubes of any fuel assembly. This is because the fuel lattice is under moderated. This can be seen by the guide tube tolerance calculations. As stated in Section 9.5 this has been confirmed by calculation.

11 Interface Analysis

Only one rack design is used in the North Anna Spent Fuel Pool. The two regions are actually only two different configurations for arrangements of the fuel in the racks. Region 1 is a checkerboard configuration and Region 2 is a fully loaded configuration. The geometry restrictions for the interface to remain applicable are summarized as follows:

1) The corners of Region 1 must be empty cells

2) Region 1 may not cross a rack boundary (avoids a possible seismic rack alignment issue)

3) At least two rows of Region 2 fuel must exist between separate Region 1 groupings.

4) The spent fuel cells AA21, AA22, BB21, BB22, CC21, and CC22 may not be part of a Region 1 block due to the new fuel elevator. (See Figure 9.7 for location of these cells.)

Region 1 and Region 2 analyses are performed using infinite lattice regions. To verify that the interface where Regions 1 and 2 adjoin does not cause k margin for the combined regions to be less than determined for the two regions individually, three models will be used. A 5x5 model will be used in which Region 1 will occupy a 3x3 with the remaining cells containing Region 2 fuel. A 7x7 model will be used in which Region 1 will occupy a 3x3 with the remaining cells containing Region 2 fuel. A 7x7 model will be used in which Region 1 will occupy a 5x5 with the remaining cells containing Region 2 fuel.

In each model, a 4x4 grouping of cells (2 rows and columns on each side of the Region interface) will be asymmetrically loaded with fuel toward the center of the 4x4 Region, consistent with the asymmetric modeling of the infinite lattice models. Region 1 fuel is 5 w/o U-235 fresh with no burnable absorber. Region 2 fuel will include fresh 1.9 w/o fuel, 2.45 or 2.5 w/o fuel with 10 GWd/MTU assembly burnup (uniform and NUREG axial burnup shapes considered), and 5.0 w/o fuel with 44 GWd/MTU assembly burnup.

Figure 11.1 illustrates the 5x5 Region 1 in 7x7 Region 2 KENO model. Periodic boundary conditions ensure that different Region 1 groupings are separated by at least two rows of Region 2 fuel. Fewer rows of separation would allow fresh 5.0 w/o Region 1 assemblies to be

closer together, which would increase k. Margin to the regulatory limit is determined as with the individual regions, except that the largest total bias and uncertainty of either Region will be added to the combined region model k. This is the approach described in Reference 4:

> *Absent a determination of a set of biases and uncertainties specifically for the combined interface model, use of the maximum biases and uncertainties from the individual storage configurations should be acceptable in determining whether the keff of the combined interface model meets the regulatory requirements.*

Table 11.1 summarizes the results of the interface cases. For fresh fuel and depleted fuel (uniform and non-uniform axial burnup shapes, 10 Gwd/MTU and 44 GWd/MTU), the interface model k is lower than the Region 2 k. Region 2 has a larger total bias and uncertainty than Region 1. Use of the Region 2 total bias and uncertainty with the interface model is bounded by the Region 2 infinite lattice analysis. Region 1 k is much lower than the interface model k and is bounded by the interface model and the Region 2 model. Therefore, the interface analysis demonstrates margin to the k limit that is larger than the Region 2 margin using the approach endorsed in DSS-ISG-2010-01 Rev. 0.

Additional interface model cases with reflective boundary conditions were run to evaluate interface effects where storage rack modules were adjacent to the SFP wall. Region 2 wall interface cases considered varying distance from the SFP wall (0-10 cm), concrete thickness (20 and 40 cm), and concrete composition (SCALE regulatory concrete, EPRI dry concrete, and water). K-eff sensitivity to these parameters is very small (0.0003 dk range of variation). K-eff of the Region 2 wall interface model is 0.004 dK lower than the Region 2 infinite lattice model.

SFP wall boundary cases were also run with a Region 1 block contained in the Region 2 wall interface model. The position of the Region 1 block within the Region 2 area was varied to include interior locations, locations at the SFP wall, and cases in which the Region 1 block within the rack at the SFP wall was incomplete (effectively projecting the normal block configuration into the SFP wall area). All of the mixed Region wall boundary cases were bounded by the k-eff of the all Region 2 wall boundary model.

The results of the SFP wall boundary cases indicate the following:

1) Spacing between the rack and the pool wall, concrete composition, and concrete thickness had very little influence on the results
2) The Region 2 infinite lattice analysis is bounding for the SFP wall interface
3) Configurations with full or partial Region 1 blocks adjacent to the SFP wall are bounded by configurations with all Region 2 fuel

The Region 1 infinite lattice analysis established requirements for Region 1 blocks including a) Region 1 must be contained within a rack module and b) Region 1 corner cells must be empty. The first requirement is intended to prevent extending the Region 1 checkerboard configuration across adjacent rack modules so that a seismic event that shifts the rack modules would not change the checkerboard fuel pattern. That requirement is not relevant at the SFP wall because no fuel pattern exists beyond the rack at the SFP wall. Results of the partial Region 1 cases at the SFP wall confirm that the empty corner cell requirement is only necessary for the portion of the Region 1 block that is actually in the rack. Rack modules that are adjacent to the spent fuel pool wall may credit the wall region as empty cells for the purposes of meeting the Region 1 requirements.

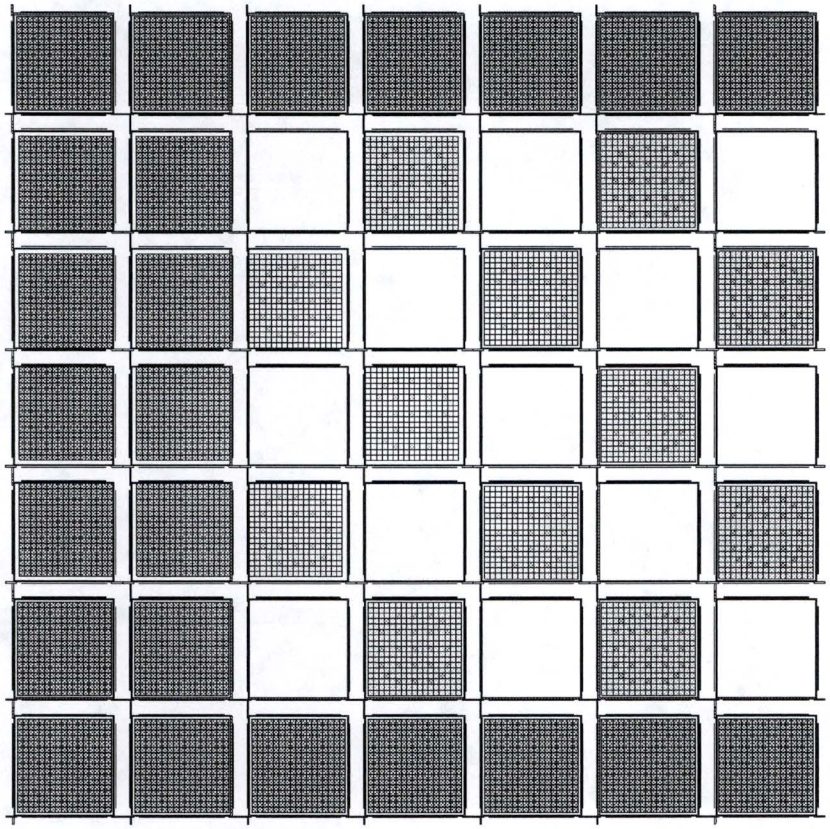

Figure 11.1: KENO 7x7 Interface Model with Embedded 5x5 Region 1

Table 11.1: KENO Interface Model Results

Enrichment	Burnup (GWd/MTU)	Buffer Rows	Notes	K-eff	Uncert.	Interface Δk
5.0	0	N/A	Reference 6x6 Reg 1	0.9198	0.00010	N/A
1.9	0	N/A	Reference 6x6 Reg 2	0.9577	0.00006	N/A
5.0/1.9	0/0	2	3x3 Reg 1 in 5x5 model	0.9533	0.00007	-0.0044
5.0/1.9	0/0	2	5x5 Reg 1 in 7x7 model	0.9538	0.00007	-0.0039
5.0/1.9	0/0	4	3x3 Reg 1 in 7x7 model	0.9532	0.00006	-0.0045
2.45	10U*	N/A	Reference 6x6 Reg 2	0.9549	0.00006	N/A
5.0/2.45	0/10U	2	3x3 Reg 1 in 5x5	0.9522	0.00008	-0.0027
5.0/2.45	0/10U	2	5x5 Reg 1 in 7x7	0.9527	0.00008	-0.0023
2.5	10	N/A	Reference 6x6 Reg 2	0.9557	0.00006	N/A
5.0/2.5	0/10	2	5x5 Reg 1 in 7x7	0.9528	0.00008	-0.0030
5.0	44	N/A	Reference 6x6 Reg 2	0.9466	0.00006	N/A
5.0/5.0	0/44	2	5x5 Reg 1 in 7x7	0.9422	0.00007	-0.0044

*U indicates uniform axial burnup shape.

12 Normal Conditions

This section reviews the normal operations in the North Anna Spent Fuel Pool. As part of normal operations the fuel is:

1. Placed on the new fuel elevator at the top of pool,
2. Lowered down to the bottom of the pool using the new fuel elevator,
3. Lifted out of the new fuel elevator to above the rack height and moved to a Region 1 cell,
4. Lowered into a Region 1 cell,
5. Lifted out of the Region 1 cell and moved through the fuel transfer canal to the upender,
6. Laid down to horizontal by the upender and transferred by the trolley through the transfer tube into the containment,
7. Upended in the containment and loaded into the core,
8. Returned to the spent fuel pool by reversing steps 5 through 7,
9. Lifted out of the spent fuel racks and moved to a spent fuel cask.

In addition to these steps the assembly can be placed in the Failed Fuel Storage cans or inspected. There are no other locations allowed for fuel assemblies. The inspections can occur in a rack cell or while the assembly is hanging from the Fuel Building Movable Platform Crane (FBMPC) over the spent fuel rack or over the floor of the cask loading pit.

In order to help visualize the operation Figure 12.1 is provided which shows the fuel building and the containment buildings.

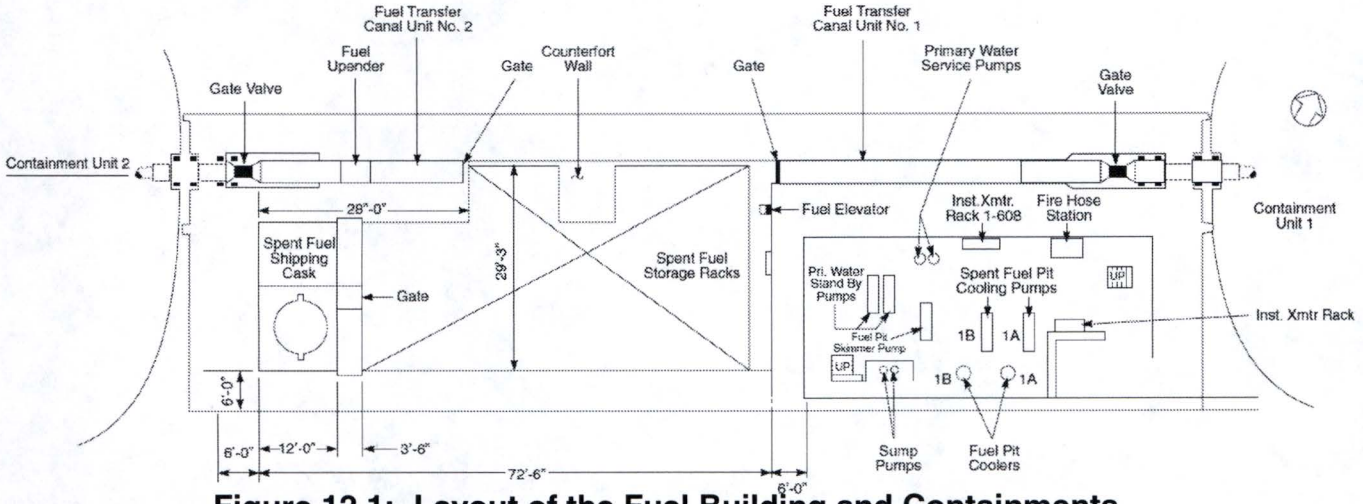

Figure 12.1: Layout of the Fuel Building and Containments

Normal operations allow the fuel to rotate in any direction. This was considered with the horizontal burnup gradient bias developed in Section 10.1.1. The pool water temperature ranges up to 140 F. This is covered by temperature biases used in Sections 9 and 10. The criticality analysis does not credit spent burnable absorbers or source rods. Inserting these in the assembly decrease k. Guide tube tolerance calculations reducing water in the guide tubes lowers k, so the normal operation of moving these inserts is acceptable. A single assembly of the maximum enrichment if isolated in water meets the criticality acceptance criteria as do 2 assemblies 12 inches (30.48 cm) apart (See Figure 12.3).

Historically, the RCCAs were moved between assemblies using an RCCA exchange station in the containment that consists of an RCCA holding cell and a place for an assembly on either side of the holding cell. This area supported two fuel assemblies that were separated from each other by more than 21 cm of water. Although it is no longer permitted to use the RCCA exchange station in the containment it is subcritical even at 0 ppm (See Figure 12.3) and during refueling the core would be the criticality limiting area in the containment.

12.1 New Fuel Elevator

The new fuel elevator may be operated at the same time as the fuel building movable platform crane (FBMPC) is moving an assembly. The new fuel elevator is simply a rectangular stainless steel tube that is hoisted up and down using tracks placed on the pool wall. There is no absorbing material on the elevator tube and FBMPC can move an assembly next to the new fuel elevator. Such a movement of fuel next to the new fuel elevator is not a likely event, but in order to eliminate future concerns a new constraint will be added to the fuel handling procedures to preclude such operation. This new procedural constraint will be in place prior to implementing this new criticality safety analysis. The procedural constraint will require that fuel assemblies being moved via the FBMPC must never be closer than 12 inches (30.48 cm) from any assembly not in the spent fuel pool rack or cask (e.g., the New Fuel Elevator, either Upender).

In order to confirm 12 inches of water this is enough water to isolate the assemblies, two fresh 5.0 wt% assemblies were modeled in KENO submerged in unborated water with varying distances between them. Figure 12.2 shows the KENO model. Figure 12.3 shows that two fresh 5 wt% U-235 fuel assemblies with no burnable absorbers can go critical if they are moved

within ~7 cm from each other. However, if separated by 12 inches (30.48 cm) the two assemblies are well subcritical. EPRI, when it performed an analysis for separation leading to isolation using Westinghouse 17X17 fuel, concluded that 10 inches of separation isolates the assemblies. [30].

When the fresh fuel assembly is at the rack level there is insufficient separation between that assembly and the rack for isolation. If there were a Region 1 arrangement of fuel next to the new fuel elevator it would be possible for two 5 wt% fuel assemblies to be closer than 12 inches apart. Therefore, it is required that cells in the two rows adjacent to the new fuel elevator the rack arrangement must be Region 2. The separation between the new fuel elevator and the rack is greater than the fuel separation in the rack cells so this condition is covered by the Region 1/Region 2 interface analysis.

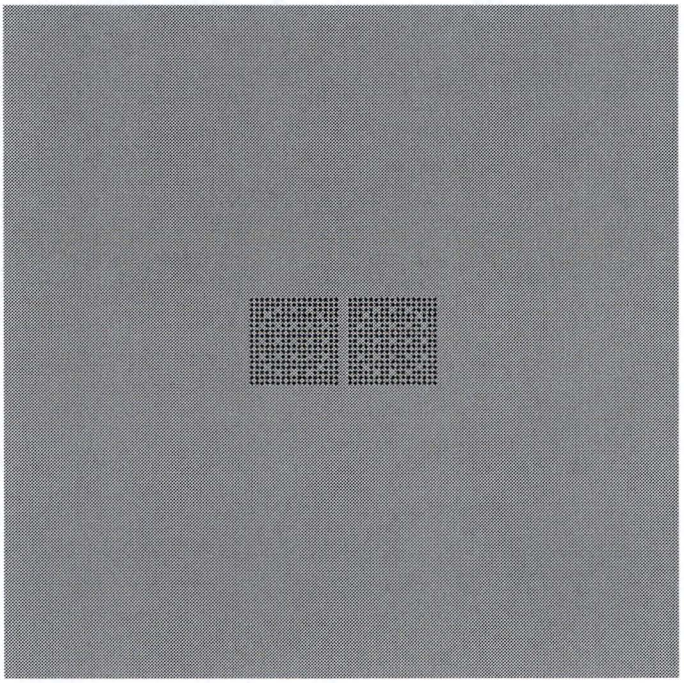

Figure 12.2: KENO Model of Two Assemblies Submerged in Water

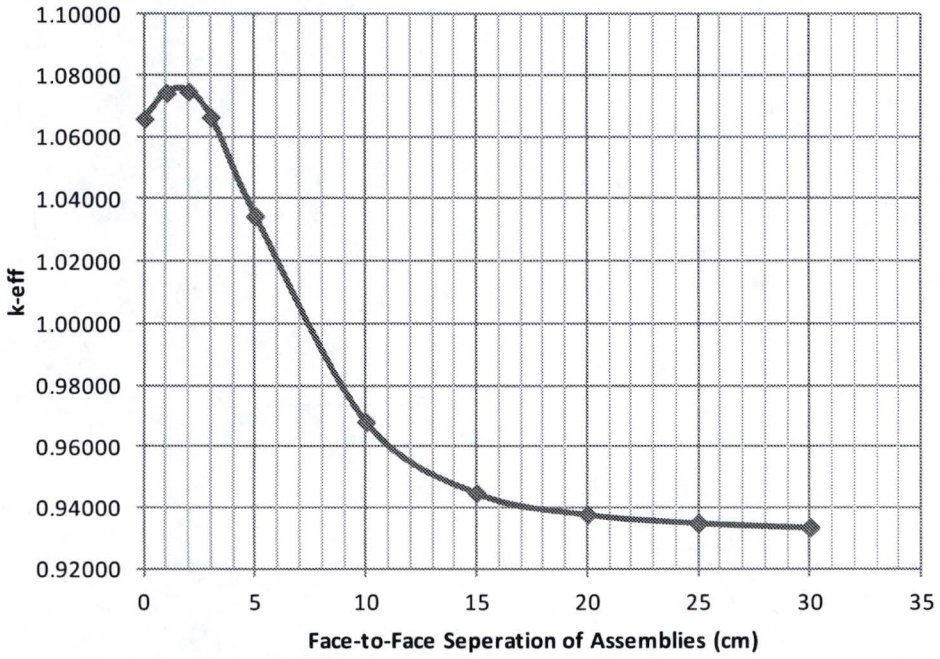

Figure 12.3: k of Two Fresh, 5 wt% Fuel Assemblies in Unborated Water

12.2 Fuel Upenders

Fuel can be placed in the upenders and it would be possible to bring another fuel assembly into the transfer canal and have the two assemblies in close proximity. In the previous section it was shown that 12 inches of water isolates the assemblies from each other. Although there currently is not a procedural constraint to prevent close proximity between assemblies, a 12 inch mandatory separation will be added to the procedures prior to implementing this new criticality analysis. Normally, there are not two assemblies in the transfer canal at the same time so the new procedural requirements will not affect the planned approach to refueling. It will however assure that a criticality concern would not be added if there is a problem with the upender.

There is no place out of the spent fuel pool to store depleted fuel assemblies (e.g., no extra racks in the fuel transfer canal, the containment building, or the cask loading pit).

12.3 Failed Fuel Storage Cans

There are two Failed Fuel Storage Cans (FFSC) in the corner of the spent fuel pool that do not contain fuel and there are no plans for placement of fuel in the cans in the future. Figure 12.4 shows their location relative to the racks. Figure 12.5 is a top view showing that if assemblies are placed in the FFSC they are further apart from other assemblies than the normal Region 2 separation. An assembly meeting Region 2 requirements can be placed in the FFSC. However, if that area of the rack was configured as Region 1, placing a Region 1 assembly in the FFSC would not meet the criticality constraints. Rather than establish special rules to allow more reactive fuel to be placed in the FFSC, the FFSC is restricted to assemblies that meet the requirements for Region 2. Since these cans are being treated as exclusively Region 2 there is no restriction on non-fuel items being placed in the FFSC.

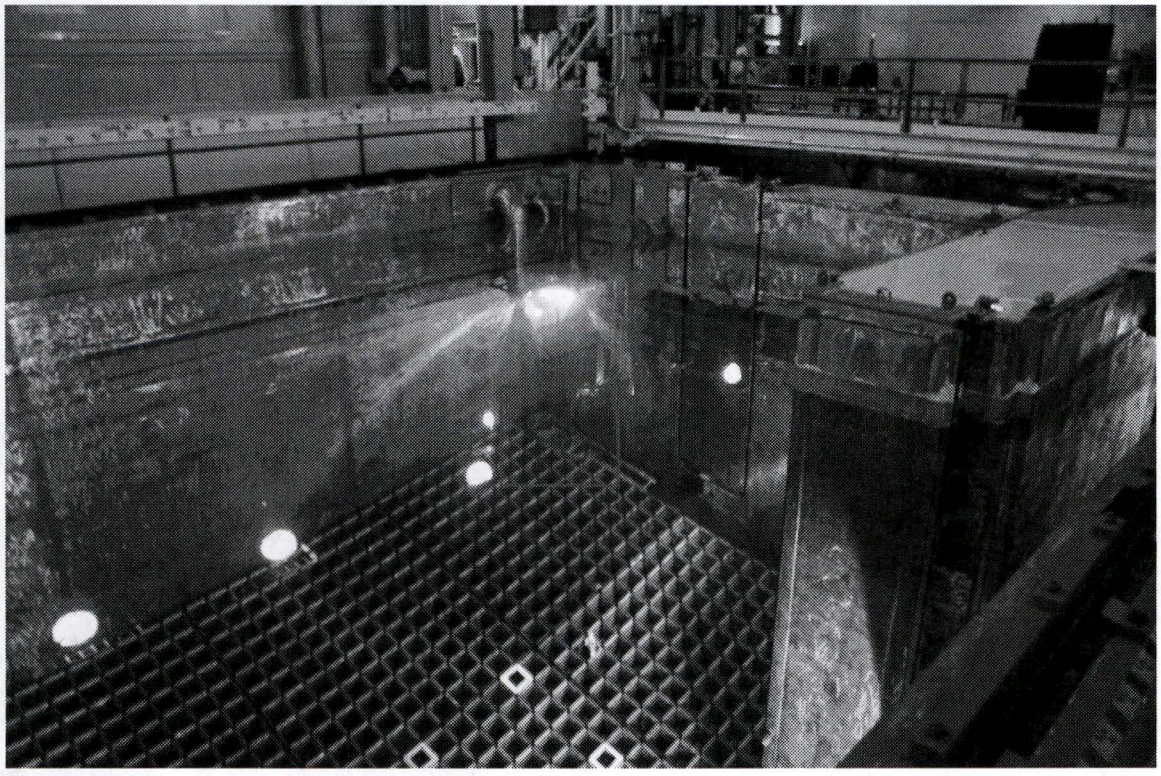

Figure 12.4: Failed Fuel Storage Cans

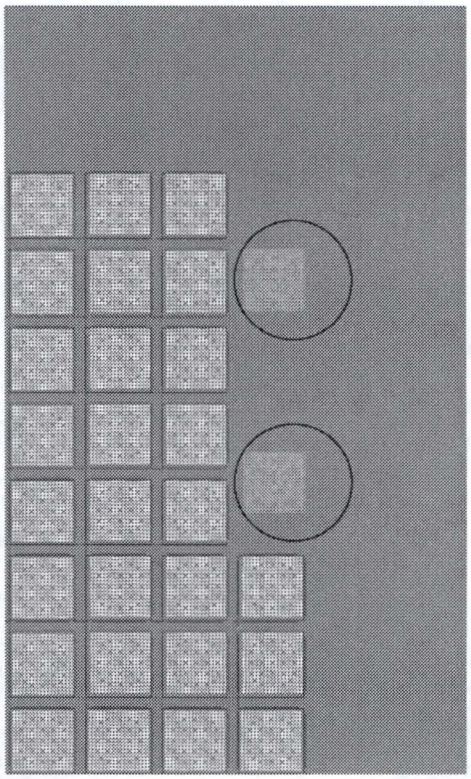

Figure 12.5: KENO Model of the Failed Fuel Storage Cans

12.4 Inspections

Fuel inspections occur while being held by the Fuel Building Movable Platform Crane. Since there is only one of these cranes at North Anna the inspections are criticality safe since the fuel assembly is isolated. Inspections include ultrasonic testing for fuel rod failure and visual inspections with a camera.

12.5 Reconstitution

Due to failed fuel pins or examinations for test fuel designs, the fuel pins have been removed from several assemblies. (In most cases the fuel pin is replaced. This process (reconstitution) can result in a fuel reactivity increase. ORNL performed a study for the NRC (NUREG/CR-6835) for spent fuel casks where they investigated how k can change with the removal of fuel pins. [63] In this study (which used Westinghouse 17x17 fuel like in North Anna) they found the maximum increase in k due to removing fuel rods was 0.015 with guide tubes present. In addition, removal of rods near an assembly center in a diagonal orientation with guide tubes (or

water holes) was found to have the largest positive effect on k. The last sentence of Section 2.2.1.2 of NUREG/CR-6835 states:

> *"The most reactive configurations involved missing pins (~10% of total) in the inner regions of the assemblies [i.e., central (N-2) x (N-2) positions] oriented in alternating diagonal rows of missing rods with guide tubes/water holes and fuel rods."*

Spent fuel pool casks typically include strong neutron poisons in the design. The North Anna spent fuel pool racks are modeled as un-poisoned (no credit for Boraflex) so a similar study was done for the North Anna fuel and racks and Table 12.1 shows the results. Fuel rods were removed sequentially and symmetrically beginning in the center of the fuel assembly and proceeding outward maintaining diagonal orientation to guide tubes or water holes. North Anna calculations agree with the NUREG results and so the maximum positive worth due to removing fuel pins is less than 0.015 in k.

Table 12.1: Maximum Fuel Pin Removal Effect (Region 2, Fresh 5.0 w/o Fuel)

Pins Removed	k	Sigma	Δk
0	1.1974	0.00006	0
4	1.2005	0.00007	0.0031
8	1.2028	0.00007	0.0055
16	1.2075	0.00011	0.0101
20	1.2097	0.00011	0.0123
24	1.2104	0.00011	0.0130
28	1.2122	0.00013	**0.0148**
32	1.2121	0.00011	0.0147
36	1.2121	0.00012	0.0147
40	1.2120	0.00012	0.0146
44	1.2114	0.00012	0.0140

In order to confirm that the maximum change in worth is for the most reactive fuel pins, the analysis was repeated using 1.9 wt% U-235 fuel. Table 12.2 shows that the pin worth for low enrichment fuel is much less than for high enrichment, therefore the 0.015 delta k is bounding.

Table 12.2: Maximum Fuel Pin Removal Effect (Region 2, Fresh 1.9 w/o Fuel)

Pins Removed	k	Sigma	Δk
0	0.9577	0.00006	0
4	0.9590	0.00006	0.0012
8	0.9590	0.00006	0.0013
16	0.9596	0.00010	0.0018
20	0.9594	0.00010	0.0017
24	0.9584	0.00010	0.0006
28	0.9577	0.00010	-0.0001
32	0.9556	0.00010	-0.0022
36	0.9531	0.00010	-0.0046

Reconstitution cannot challenge a criticality limit as long as the reconstitution location has at a minimum an empty cell on all 4 face adjacent sides. This is because Region 1 has >0.05 margin in k which is much greater than the maximum worth of 0.015 that could be required In addition, this assessment is very conservative since it ignores any fuel burnup. Fuel is reconstituted due to post irradiation fuel failure or to support post-irradiation fuel inspection. There is no known reason to reconstitute a fresh fuel assembly in the pool.

After reconstitution the fuel assembly can be more reactive that a standard assembly so a set of rules for placement of reconstituted assemblies is needed.

The most common and preferred reconstitution is to replace a removed fuel rod with a stainless steel rod of the same outside diameter. This always lowers k as shown on Table 12.3. The analysis shown on Table 12.3 started with the reference model from a previous section and replaced one fuel rod with a stainless steel rod. The fuel rod selected for replacement was either in the outer row of fuel rods or in the center of the fuel assembly corner adjacent to the instrument tube. Since the reactivity for the assembly decreases when the fuel rod is replaced with a stainless steel rod, the assembly storage constraints are the same as fuel which has not been reconstituted.

Table 12.3: KENO Results for Replacing Fuel Pins with Stainless Steel Pins

Case Scenario	k-eff	Δk
Region 1 Reference Case	0.9198 ± 0.00010	N/A
Region 1, 1 SS Inner Pin	0.9172 ± 0.00010	-0.0026
Region 1, 1 SS Outer Pin	0.9183 ± 0.00010	-0.0014
Region 2, 2.45 wt%, 10 GWD/MTU Reference Case	0.9549 ± 0.00006	N/A
Region 2, 2.45 wt%, 10 GWD/MTU, 1 SS Inner Pin	0.9527 ± 0.00005	-0.0022
Region 2, 2.45 wt%, 10 GWD/MTU, 1 SS Outer Pin	0.9521 ± 0.00006	-0.0028
Region 2, 5.00 wt%, 44 GWD/MTU Reference Case	0.9466 ± 0.00006	N/A
Region 2, 5.00 wt%, 44 GWD/MTU, 1 SS Inner Pin	0.9453 ± 0.00006	-0.0013
Region 2, 5.00 wt%, 44 GWD/MTU, 1 SS Outer Pin	0.9443 ± 0.00006	-0.0023

A removed fuel pin can also be replaced by a lower enriched fuel pin. Region 2 requires no burnup for enrichments less than 1.9 wt% U-235. Since the 1.9 wt% U-235 analysis uses fresh fuel bias and uncertainties, the maximum fresh fuel enrichment allowed using the largest bias and uncertainty from the burned fuel was determined. Fresh fuel of 1.75 wt% in Region 2 produces a k of 0.9440 which matches the lowest base k of Tables 10.9 and 10.11. Therefore, replacing a fuel pin with ≤1.75 wt% U-235 enrichment allows the reconstituted assembly to be stored with the same constraints as an assembly that has not been reconstituted. The fuel enrichment and burnup used for comparison to the burnup requirement are the assembly average values (highest planar average enrichment if axial blankets are present) ignoring the low enrichment replacement rods.

Sometimes the removed fuel pin is not replaced with any rod. If the missing fuel rod is on the outer two rows of the fuel assembly, the reactivity of the assembly decreases. This has been confirmed by analysis and is consistent with Reference 65. Assemblies with missing fuel pins only on the outside two rows of pins may be placed consistent with the restrictions of a normal fuel assembly.

If the failed or removed fuel pin leaves an empty pin lattice position inside the fuel assembly the assembly may be treated as a fresh fuel assembly and placed in Region 1 or in Region 2 with a control rod. Alternatively, if the assembly has burnup in excess of the minimum burnup requirements for Region 2 some of this excess burnup may be used to allow an assembly with missing interior fuel rods to be placed in Region 2 without a control rod. It is assumed that the full 0.015 in k reactivity (the maximum reactivity for any number of fuel pins removed) must be

compensated with additional burnup. Figures 12.6 and 12.7 show the 5 day and 3 year decay time burnup worth from Tables 10.7 and 10.10 including a quadratic fit of the data. Table 12.4 shows the worth of an additional 5 GWd/MTU obtained using the fit line. The smallest magnitude reduction in k attributable to an additional 5 GWd/MTU burnup is 0.017. Therefore, any assembly with removed fuel pins may be placed in Region 2 if it exceeds the minimum burnup requirement by 5 GWd/MTU or more.

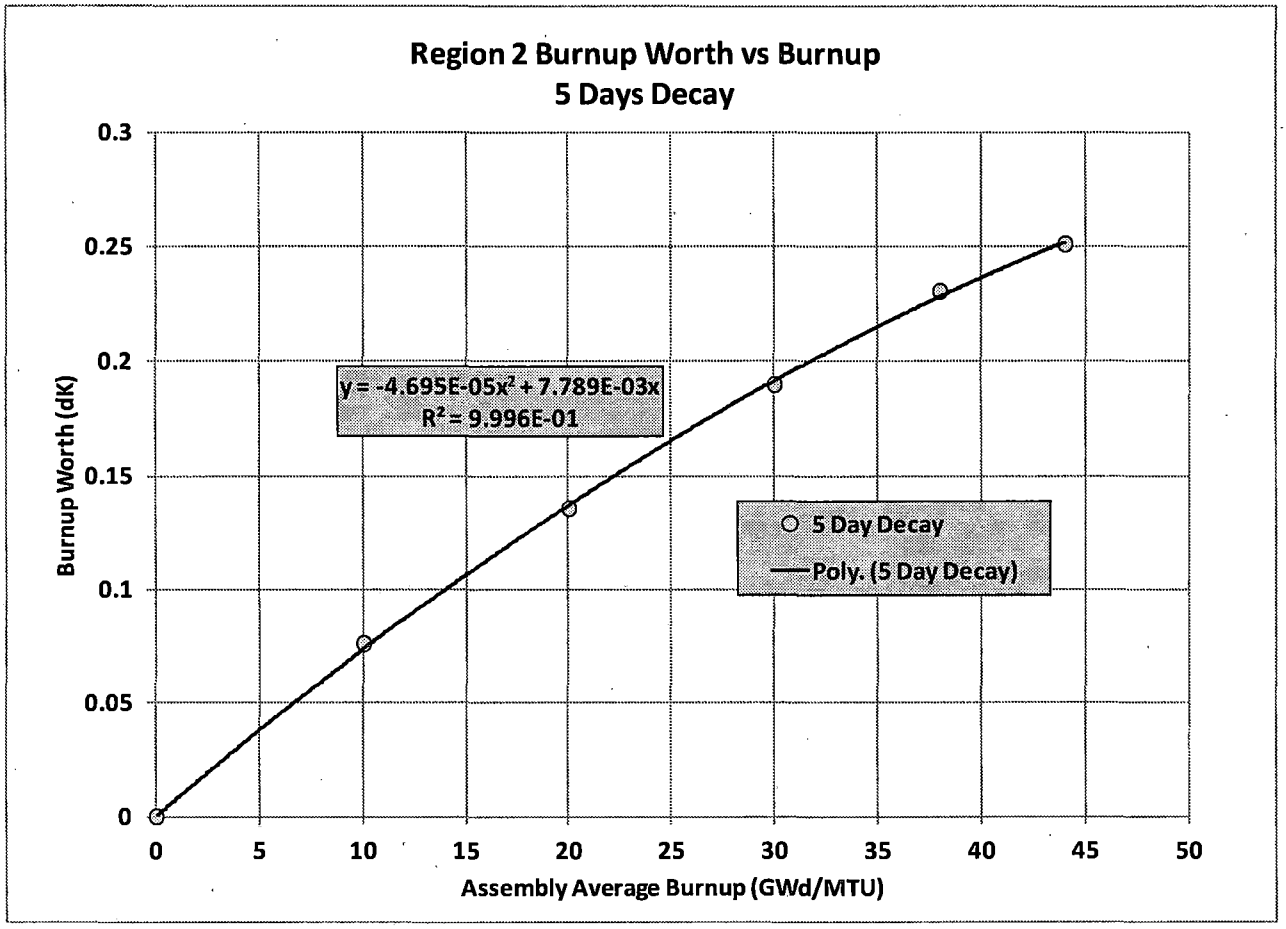

Figure 12.6: Region 2 Burnup Worth, 5 Days Decay

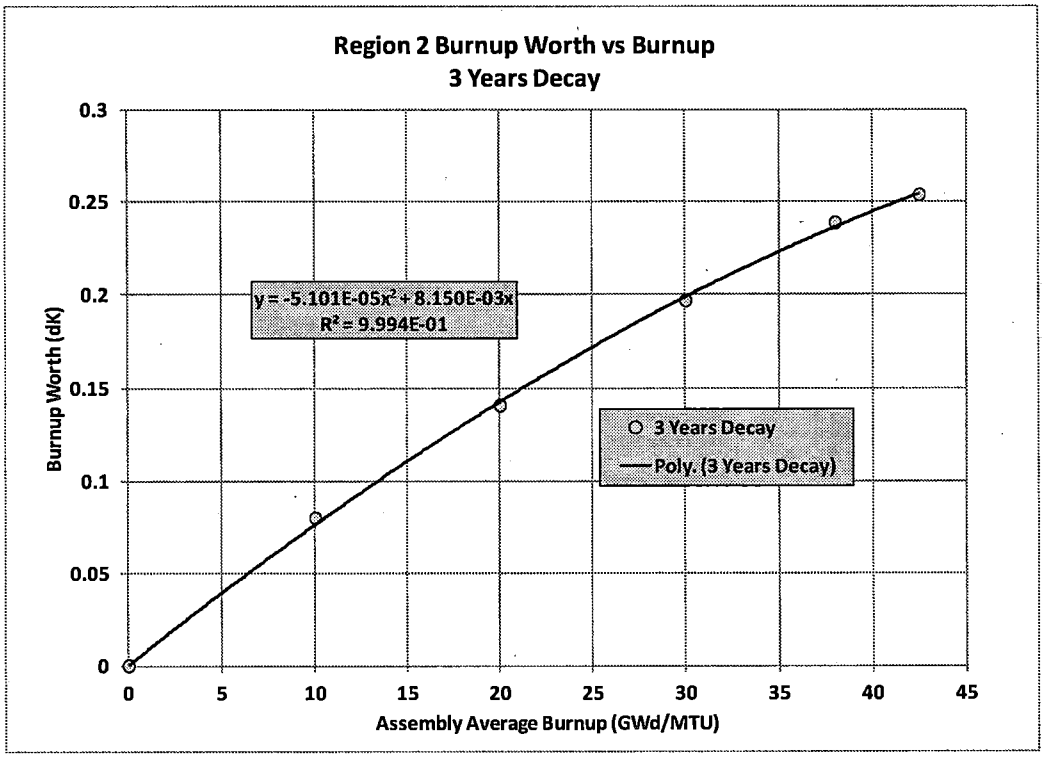

Figure 12.7: Region 2 Burnup Worth, 3 Years Decay

Table 12.4: Burnup Worth of 5 GWd/MTU

Burnup (GWd/MTU)	5 Day Decay: Worth of 5 Additional GWd/MTU (Δk)	3 Year Decay: Worth of 5 Additional GWd/MTU (Δk)
0	0.0378	0.0395
10	0.0331	0.0344
20	0.0284	0.0293
30	0.0237	0.0242
38	0.0199	0.0201
42.5	0.0178	0.0178
44	0.0171	0.0170

The final type of reconstitution that requires placement rules is reconstitution where fuel rods that are either from a different fuel assembly or have been depleted in a different number of cycles are inserted into the fuel assembly. This form of reconstitution is infrequently used for a special demonstration or testing program. This fuel may be stored in Region 1 or in Region 2 with an RCCA inserted. Alternatively, it can be placed in Region 2 using the following method to determine if it meets the burnup requirements if the replacement rods have been depleted at least one cycle. First, the enrichment to be used for the determination should be the highest enrichment in the assembly. Next, the burnup must be conservatively determined using the following steps:

a) Assume 0 burnup for the replacement fuel rods. This is the main conservatism of the method.

b) Calculate the modified assembly average burnup as the average of all fuel rod burnups.

c) Compare the modified assembly average burnup to the loading curve requirement for Region 2 for the highest enrichment in the assembly.

If the modified burnup is greater than the normal fuel burnup requirement, then the fuel may be stored in Region 2.

12.6 Disposition of Non-Standard Fuel Assemblies

There are currently a number of assemblies in the North Anna spent fuel pool that do not have a standard configuration. In order to disposition these assemblies they are lumped into the following five non-standard fuel categories:

1 – Damaged assembly with no change to fuel rod lattice (store as normal fuel)

2 – Normal reconstitution with inert or low enrichment rods (store as normal fuel)

3 – Interior fuel rod(s) missing (store in Region1, store in Region 2 with an RCCA, or store in Region 2 with no RCCA if the assembly burnup exceeds the requirement by at least 5 GWd/MTU)

4 – Contains rods from a different fuel assembly or rods from the same assembly that have different depletion history (store in Region1, store in Region 2 with an RCCA, or store in Region 2 if the calculated conservative burnup exceeds the Region 2 minimum burnup requirement evaluated at the highest enrichment of the fuel in the assembly). Different depletion history means fuel rods were removed from the assembly and re-inserted such that the depletion history of the rest of the assembly is different from the depletion history of the re-inserted rods.

5 – Missing fuel rod(s) on outer two rows of FA (reduces reactivity, store as normal fuel)

Table 12.5 describes the current inventory of non-standard fuel assemblies in the North Anna spent fuel pool.

Table 12.5: North Anna SFP Non-Standard Fuel Assembly Inventory

#	FA ID	Description	Enrichment (w/o U-235)	Burnup (MWd/MTU)	Category	Region 2 Storage Without RCCA?
1	1A9	An interior fuel rod on Face 1 is missing a section of rod (severed during recon)	4.0	27581	3	No
2	4Z9	Baffle Jetting FA, damaged rods missing pellets on assembly face	4.45	47313	5	Yes
3	5K9	Broken rod G6-Bottom 79-80" section of rod remains in the assembly	4.55	49153	3	Yes
4	5L4	Most of fuel rod B10 removed, small piece remains in Grid 4 (no replacement rod)	4.21	24667	3	No
5	65N	Armored FA, built with steel dummy rods in locations A17 thru A12 and B17	1.5	0	2	Yes
6	Y48	Missing a 3 inch section of rod 3, face 3, span 6.	4.21	45328	5	Yes
7	30A	Removed rods (DOE) (Dummy rods in place)	4.55	52020	2	Yes
8	3A1	Removed rods (DOE) (Dummy rods in place)	4.00	50012	2	Yes
9	3D8	Removed rods (DOE) (Dummy rods in place)	4.2	54952	2	Yes
10	3F9	Removed rods (DOE) (Dummy rods in place)	4.25	52280	2	Yes
11	6U3	Removed rods (DOE) (Dummy rods in place)	4.45	52728	2	Yes
12	6K1	Removed rods (DOE) (Dummy rods in place)	4.55	49135	2	Yes

13	FM3	Top 28" of guide tube has been removed from location D14, contains 4 SS dummy rods	4.2	67725	3	Yes
14	5K7	Removed rods (4) (DOE) (Dummy rods in place)	4.55	53335	2	Yes
15	6B0	Contains one rod from 2M7 (4.01 w/o)	4.21	47755	4	Yes
16	AM2	Contains 27 AM2 rods with reduced burnup	3.99	51707	4	Yes
17	F25	Recon (contains dummy rods)	3.59	38457	2	Yes
18	F35	Recon (contains dummy rods)	3.59	57909	2	Yes
19	F54	Recon (contains dummy rods)	3.59	37689	2	Yes
20	F55	Recon (contains dummy rods)	3.59	38629	2	Yes
21	F62	Recon (contains dummy rods)	3.59	38209	2	Yes
22	T62	Recon (contains dummy rods)	3.60	44995	2	Yes
23	3A4	Contains one SS rod and 8 rods irradiated one cycle	4.20	45778	4	Yes
24	4C3	Recon (contains dummy rods)	4.21	44972	2	Yes
25	1C6	Contains one rod from 2M7 (4.01 w/o)	4.01	41792	4	Yes
26	3C3	Contains 3 rods from 2M7 (4.01 w/o)	4.21	45133	4	Yes
27	5C4	Recon (contains dummy rods)	4.21	42160	2	Yes
28	5C7	Contains one rod from 2M7 (4.01 w/o)	4.21	43851	4	Yes
29	2R6	Recon (contains dummy rods)	4.10	37796	2	Yes
30	55L	Recon (contains dummy rods)	4.49	20067	2	Yes
31	T52	2 inch section of flattened rod on assembly face near bottom of rod	3.60	37254	5	Yes

13 Accident Analysis

The Technical Specifications minimum soluble boron requirement is 2600 ppm, which is shown to be more than sufficient to offset the reactivity increase for all postulated non-dilution accidents. The boron dilution analysis of record has been reviewed and found to remain applicable for the dilution accident with large margin to the criticality limit.

13.1 Boron Dilution Accident

As stated in Sections 9.3 and 10.8, the boron dilution analysis of record shows that dilution below 1200 ppm would be prevented due to the large water volume required, the dilution time, and administrative controls including spent fuel pool level monitoring. [46] The previous criticality analysis utilized only 900 ppm soluble boron credit in the analysis approved with an NRC SER. [47] This analysis likewise provides a 300 ppm margin to the 1200 ppm minimum soluble boron concentration. As a note of further conservatism, the analysis supporting 1200 ppm used an initial boron concentration of 2300 ppm. North Anna Technical Specification 3.7.17 requires spent fuel pool soluble boron ≥2600 ppm when fuel is stored in the spent fuel pool. Accounting for the actual starting and ending boron concentration (2600 ppm and 900 ppm, respectively) increases the minimum dilution time to 18 hours rather than the 11 hours in the analysis of record and would result in much more water overflowing the pool.

The analyses in Section 9 and 10 show that for normal storage, $k_{95/95}$ is less than 0.95 using 900 ppm soluble boron. Those analyses are consistent with the boron dilution analysis assumptions, therefore criticality limits will be met in the event of a boron dilution accident.

13.2 Multiple Misload Accident

The multiple misload accident assumes that all the safeguards, procedures and human performance tools fail to prevent fresh 5.0 wt% fuel being placed in every rack cell. Since this is an accident scenario, the spent fuel pool water was modeled with a boron concentration of 2600 ppm. The multiple misload accident is the limiting accident of the North Anna spent fuel pool criticality analysis. A KENO analysis using the standard 6x6 array with 4x4 asymmetric assemblies, was performed assuming all assemblies are fresh 5 wt% U-235 fuel and the soluble boron concentration was 2600 ppm. Since this case could have a larger temperature bias, the case was run at 140 F as well as the reference 68 F to determine a temperature bias. Since

there is a significant margin in the final results, the fuel and rack tolerance uncertainties were assumed to be the same as the Region 2 control rod case (See Table 10.1). Since the EALF for this case is 0.44 eV, the higher bias and uncertainty from Table 6.6 is used. Table 13.1 shows the calculation of $k_{95/95}$ to compare to the 0.95 criterion. As in the other cases the tolerance uncertainties were not recalculated and the margin for NRC review was raised from 1% to 2% Δk.

Table 13.1: Determination of $k_{95/95}$ For a Multiple Misload with All Cells Fresh 5 wt% U^{235} Fuel and 2600 ppm

Enrichment (wt% U-235)	**5.00**
Burnup (GWd/MTU)	**0**
Reference Case k	**0.8291**
Uncertainty in the Fuel Stack Density*	0.0009
Uncertainty in the Pellet OD*	0.0005
Uncertainty in the Fuel active length*	0.0000
Uncertainty in the Fuel Stack position*	0.0004
Uncertainty in the Clad ID*	0.0002
Uncertainty in the Clad OD*	0.0014
Uncertainty in the Guide Tube ID*	0.0002
Uncertainty in the Guide Tube OD*	0.0003
Uncertainty in the Pin Pitch*	0.0020
Uncertainty in the Cell wall thickness*	0.0026
Uncertainty in the Cell pitch*	0.0029
Uncertainty in the Wrapper thickness*	0.0024
Uncertainty in the Tie plates thickness*	0.0002
Monte Carlo uncertainty in the Reference Case	0.0002
Validation uncertainty	0.0060
Statistically Combined Uncertainties	**0.0080**
Bias from Code and Cross Section Library Validation	0.0060
Bias to the most reactive temperature	0.0058
Bias to the most reactive grid volume*	0.0009
Sum of Biases	**0.0127**
Margin for NRC review	**0.0200**
k-eff with 95/95 probability and confidence	**0.8698**
Acceptance criteria	0.95
Dominion held Margin	**0.0802**

*Due to the large margin the unborated uncertainties and bias were used for these parameters

13.3 Assemblies Within Twelve Inches from Each Other Accident

A failure to adhere to fuel handling procedures could result in two fresh 5 wt% U-235 assemblies being next to each other due to a fresh assembly being in the new fuel elevator or one of the upenders. This event is more than offset by the Tech Spec minimum 2600 ppm. This accident was modeled in KENO as two assemblies submerged in water borated to 2600 ppm with varying distances between them. Figure 13.1 shows that this accident is significantly more benign than the multiple misload accident which had a calculated k of 0.8291.

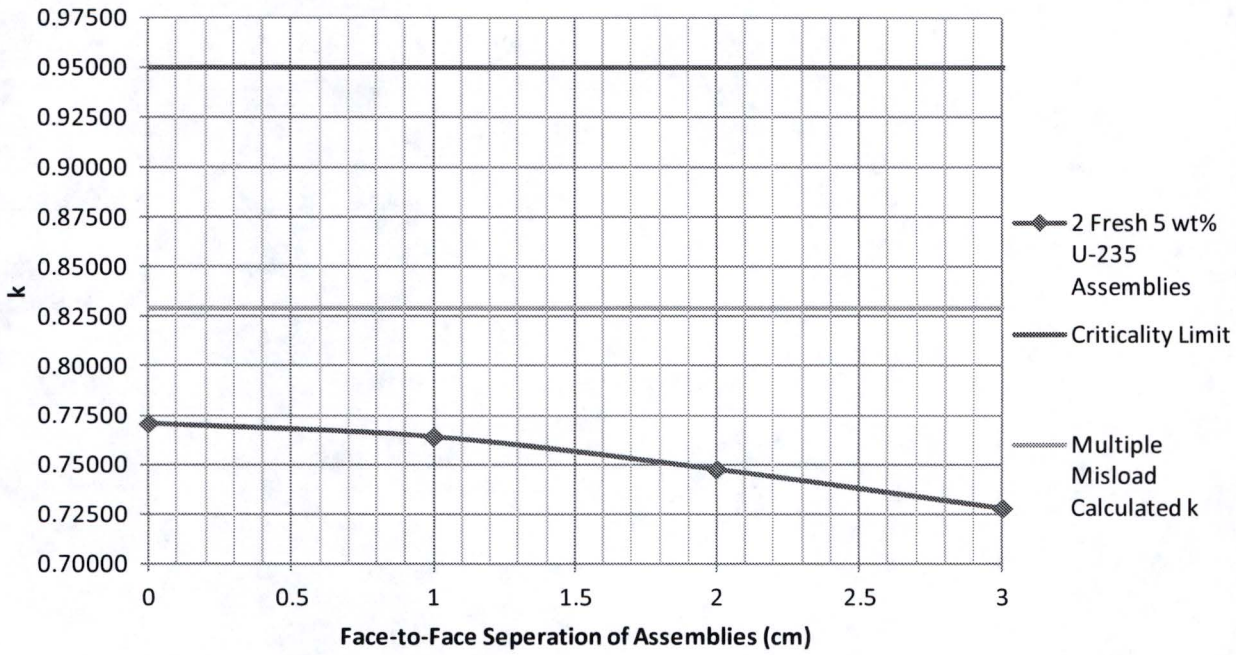

Figure 13.1: k of Two Fresh 5 wt% Fuel Assemblies in 2600 ppm Borated Water

13.4 Dropped and Misplaced Assembly Accident

This section will cover accident scenarios that involve dropping or misplacing an assembly. An assembly could be 1) dropped or misplaced in the wrong rack cell, 2) misplaced or dropped outside of the fuel racks, 3) dropped on top of another fuel assembly, or 4) dropped and falling over on top of the racks.

The dropped/misplaced assembly analysis includes a conservative representation of the dropped fuel assembly in a rack model with 2600 ppm soluble boron. To cover potential damage to the fuel assembly in the dropped event it is conservatively assumed that the grids fail and the fuel pin pitch increases. The cell wall and wrappers for the cell where the assembly was dropped are removed to allow the pin pitch to increase to 1.25 times the nominal pin pitch. The fresh 5 wt% U-235 dropped assembly is assumed to occur in a required empty cell in Region 1 and at the Region 1 Region 2 interface. Figures 13.2 and 13.3 show the models. No credit for burnable absorbers is included. Table 13.2 shows the calculated ks. The multiple misload calculated k is 0.8291. All the dropped / misplaced assembly calculated k's are much lower than the multiple misload case so this accident is not limiting.

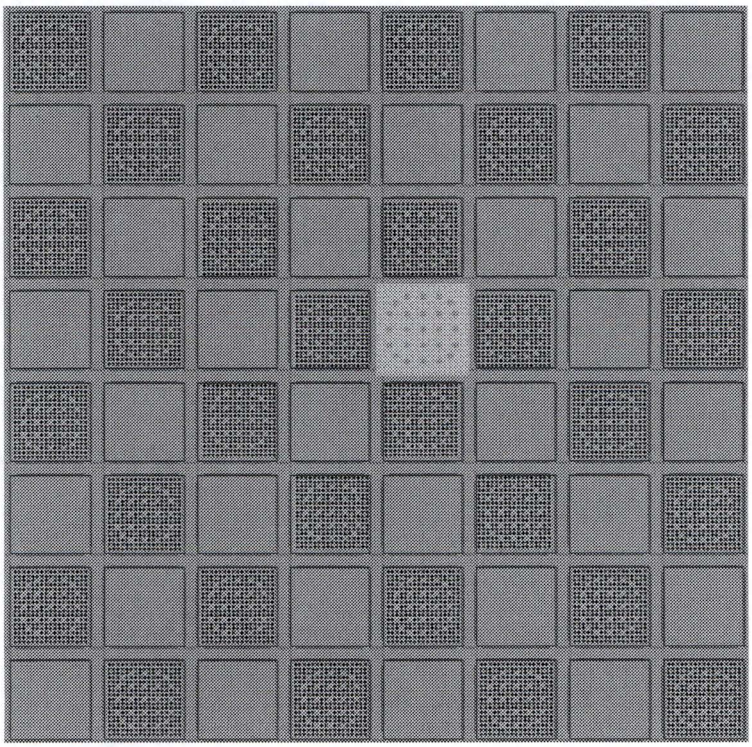

Figure 13.2: Region 1 KENO Model of Dropped Assembly Accident

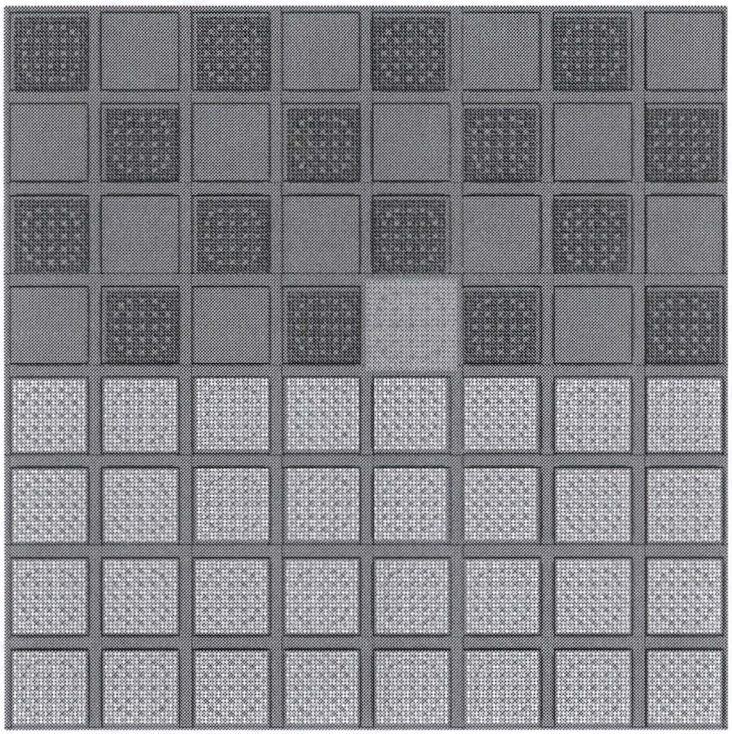

Figure 13.3: Region Interface KENO Model of Dropped Assembly Accident

Table 13.2: KENO Results for the Dropped Assembly Accident

Case Scenario	k-eff
Region 1, Dropped Assembly, +0% Pin Pitch	0.7531 ± 0.00009
Region 1, Dropped Assembly, +5% Pin Pitch	0.7659 ± 0.00009
Region 1, Dropped Assembly, +10% Pin Pitch	0.7755 ± 0.00009
Region 1, Dropped Assembly, +15% Pin Pitch	0.7827 ± 0.00008
Region 1, Dropped Assembly, +20% Pin Pitch	0.7872 ± 0.00009
Region 1, Dropped Assembly, +25% Pin Pitch	0.7900 ± 0.00009
Region Interface, Dropped Assembly, +25% Pin Pitch	0.7865 ± 0.00010
Region 2, Dropped Assembly, +25% Pin Pitch	0.7390 ± 0.00010

This model of a dropped assembly in Region 1 also conservatively bounds the other dropped/misplaced accident scenarios.

The most reactive location that an assembly could be dropped or misplaced outside of the rack would be on the inside corner between a Region 2 rack module and Region 1 rack module. This means that one face of the assembly would be adjacent to a Region 1 assembly, once face

would be adjacent to a Region 2 assembly and the remaining two faces would be adjacent to open water. The region interface model has a dropped assembly facing three Region 1 assemblies and one Region 2 assembly. This is obviously conservative for the scenario of an assembly misplaced or dropped outside of the rack.

If an assembly is dropped on top of another assembly, then the bottom assembly could be damaged but would still be contained by the rack cell wall and would be less reactive than the dropped assembly model. The active fuel region of the assembly on top of the crushed assembly is isolated from the fuel in the racks due to the assembly structure above and below each fuel assembly and does not need to be considered.

Finally, an assembly could be dropped on top of the racks and then tip over to lie across the top of the racks. There is about 50 cm between the active fuel and the top of the racks. Figure 12.3 shows that by 25 cm of water the assembly on top of the rack would be isolated from the other assemblies in the rack. Therefore, this accident less limiting than the other dropped assembly accidents.

A heavy load (non-fuel) drop accident was not analyzed because heavy load movements are restricted by procedure. A fuel building bridge and trolley crane operating procedure, restricts movement of items >2000 lbs (note that the weight of a fuel assembly with a control rod is about 1700 lbs). Movement of any items >2000 lbs requires the use of two safety cables to ensure that the movement is single-failure-proof.

13.5 Over-Temperature Accident

The highest normal operating temperature of the spent fuel pool is 140°F. Region 1 at 900 ppm showed a decrease in reactivity with increasing temperature. To ensure that the pool can handle a heat up accident, a few calculations for elevated temperatures were performed. The KENO cases were run at 212°F and with and without a void fraction of 20% to simulate boiling. Region 1 fresh 5 wt% fuel and Region 2, 5.00 wt%, 44 GWD/MTU fuel were modeled. The calculated k's with 2600 ppm are very low showing that increasing reactivity with increasing temperature does not challenge the criticality safety. The results of the analysis are found on Table 13.3.

In reality, the boiling point of the water in the active fuel region would be higher than 212°F because the middle of the fuel is under ~35 feet of water. A depth of 35 feet results in a pressure of ~30 psia. The saturation temperature of water at 30 psia is 250°F. The Region 1 temperature bias is negative so it is conservative to disregard the increased temperature. Extrapolating the Region 2 temperature bias to 250°F results in a 0.003 Δk reactivity increase which is negligible when compared to the margin to the limit.

Table 13.3: KENO Results for a Heat Up Accident

Region	Enrichment (wt% U^{235})	Burnup (GWd/MTU)	Temperature (F)	Void	k-eff	sigma
1	5	0	68	0	0.6675	0.00009
1	5	0	212	0	0.6639	0.00012
1	5	0	212	20%	0.6301	0.00009
2	5	44	68	0	0.6633	0.00005
2	5	44	212	0	0.6739	0.00005
2	5	44	212	20%	0.6947	0.00005

13.6 Seismic Accident

North Anna experienced a seismic even on August 23, 2011 which resulted in ground motion exceeding the North Anna's Safe Shutdown/Design Basis Earthquake. As an immediate response, the spent fuel racks were examined by video. In the inspection report it was concluded that the fuel racks showed "no discernible signs of earthquake induced degradation or deformation that could challenge the ability of the spent fuel racks to perform their design functions".

In response to the August 23, 2011 earthquake, the NRC issued a Confirmatory Action Letter (CAL) listing 10 commitments required by Dominion. Dominion satisfactorily completed these commitments and the NRC closed its Confirmatory Action Letter in December of 2015 [64]. The closure of the CAL signifies that North Anna's safety systems, structures and components, including the spent fuel pool, are seismically safe to operate now and in the future.

Increasing North Anna's enrichment limit will not increase the weight of the individual fuel assembly. Instead, the enrichment increase will decrease the load on the fuel racks and pool floor since the design of Region 1 requires more open rack cells than the current configuration.

Since the change in enrichment does not adversely affect the seismic analysis, no further assessment of seismic margins will be necessary.

The North Anna spent fuel pool racks are installed such that there is at minimum 1.5 inch spacing between racks measured at the cell lead-in flare at the top of the rack. As installed, the effective minimum rack cell pitch at each rack-to-rack interface is more than an inch larger than the nominal in-rack cell pitch. Rack tolerance cases in Sections 9.3, 10.5, and 10.6 demonstrate that increased cell pitch reduces k. No credit has been taken for this rack spacing.

Displacement of the racks during a seismic event could change the rack interface spacing. The minimum spacing allowable by the rack design if adjacent rack baseplates are in full contact with each other is only 1/16 inch less than the nominal cell pitch (one half of the rack cell pitch tolerance). Therefore the effect on k of a hypothetical reduction in the rack interface cell pitch dues to a seismic event is very small and easily bounded by other accidents. Increasing the rack interface pitch would result in a lower k. Rack tolerance cases indicate reducing cell pitch increases k. Figure 12.3 shows that increased fuel assembly separation reduces k monotonically if the assembly spacing is greater than 2 cm. The minimum spacing between asymmetrically loaded fuel assemblies with nominal rack cell pitch is more than 4 cm. Therefore, the increased rack interface spacing k is bounded by the base case analysis k.

In summary, a seismic event can have several effects on the spent fuel pool, but it will not cause a criticality event. An earthquake can cause individual rack modules to slide. This scenario is covered because Region 1 blocks cannot cross rack module boundaries so there is no risk of two fresh 5.0 wt% assemblies ending up next to each other. A change to the spacing between racks can only cause a very small increase in k or a reduction in k as compare to the base case analysis, therefore rack interface changes are bounded by other accidents. An earthquake can cause fuel assemblies to shift around within their rack cell. This scenario is covered by the asymmetric bias included the base cases. An earthquake can cause a dropped assembly. This scenario is covered by Section 13.4. Finally, the analyses done in response to the Confirmatory Action Letter [64] confirm that the fuel building, spent fuel pool and spent fuel pool racks can withstand an earthquake now and in the future.

14 Summary and Conclusions

This section summarizes the new criticality safety analysis done for the North Anna spent fuel pool. The new analysis was done to permit a higher enrichment of up to 5.0 wt% U-235 to improve fuel cycle economics. The spent fuel pool uses one rack module design that contains Boraflex for criticality control. Credit for the Boraflex was removed in a prior criticality analysis and it is not credited here. This analysis uses two configurations in the racks labeled Region 1 and Region 2. Region 1 employs a checkerboard arrangement of the fuel and empty cells that is intended for storage of fresh and once burned fuel. Region 2 is a full loading of every cell and requires burnup consistent with at least two cycles of fuel use.

This summary includes a review of the limits on placement of Region 1 (Section 14.1) followed by a review of bounding assembly design values (Section 14.2). Section 14.3 reviews key depletion condition input used in this analysis. Finally, Section 14.4 provides the final loading constraints. The new fuel storage area is only constrained by the fuel design limits provided in Section 14.2 which are not repeated in Section 14.4.

14.1 Region 1 Placement Constraints

Region 1 blocks can be anywhere in the pool as long as they meet the following four requirements:

1) Region 1 blocks must have empty cells at the outer corners.

2) At least two Region 2 rows must exist between Region 1 blocks.

3) Each Region 1 block shall be fully contained in a single rack module where a rack module is adjacent to another rack module.

4) The spent fuel cells AA21, AA22, BB21, BB22, CC21, and CC22 may not be part of a Region 1 block due to the new fuel elevator. (See Figure 9.7 for location of these cells.)

14.2 Bounding Fuel Design Values

Table 14.1 summarizes the bounding fuel design used for this analysis.

Table 14.1: Bounding Fuel Design Values

Enrichment	≤ 5 wt% U-235
Pellet Diameter	0.3225 inch
Clad Inner Diameter	0.329 inch
Clad Outer Diameter	0.374 inch
Clad Material	zirconium alloy
Rod Pitch	0.496 inch
Grid Volume (per fuel assembly)	[ ]^{a,c} - [ ]^{A} cubic inches excluding Inconel grids
Grid Material	A low growth zirconium alloy such as ZIRLO or M5. Existing inventory of Zircaloy 4 is accommodated by the analysis.
Pellet Stack Net Theoretical Density	≤95.5%

Axial blankets and burnable absorbers are not credited in the analysis and are permitted as well as annular pellets. Burnable absorbers affect the depletion. Depletion related limits for burnable absorbers follow in the next section.

14.3 Bounding Depletion Condition Input

Depletion parameters were selected to cover past and anticipated future operation. Table 14.2 lists key depletion condition input selected to bound actual fuel depletion conditions. The temperature and soluble boron assumptions are averages over the total burnup (multi-cycle) for a given assembly.

Table 14.2: Depletion Conditions for Region 2 Burnup Credit

Parameter	Value	Notes
Maximum Burnup Averaged Soluble Boron	≤ 1100 ppm	This is an average for all cycles in which the assembly was depleted.
Maximum Average Fuel Exit Temperature	≤ 620.82 °F	This is not a value used directly in the analysis but is a proxy for the nodal moderator temperatures.
Maximum Burnup Averaged Relative Assembly Power	≤ Figure 8.1	0 to 30 GWd/MTU BARAP ≤1.44 Linearly decreases to 1.30 at 53 GWd/MTU Then linearly decreases to 1.0 at 60 GWd/MTU
Maximum Removable Burnable Absorbers with IFBA	≤ 8 fingered BPRA or WABA with up to [ ]^{a,c} IFBA, ≤ 24 fingered BPRA or WABA with no IFBA	Analysis assumed 200 Maximum loaded IFBA and used highest loaded removable burnable absorbers.

14.4 Summary of Loading Constraints

Spent Fuel Pool Region 1 and the New Fuel Storage Area can store fresh fuel assemblies enriched to 5.0 wt% U-235 or less with no credit for burnable absorbers or rack absorbers. The only requirement is the fuel design given in Section 14.2.

Region 2 has three loading criteria:

1) Burnup credit and no cooling credit
2) Burnup credit and 3 years cooling credit, and
3) Control Rod credit with no burnup required.

The loading curve for burnup credit and no cooling is shown on Figure 14.1 and the loading curve with three years cooling time credit is shown on Figure 14.2.

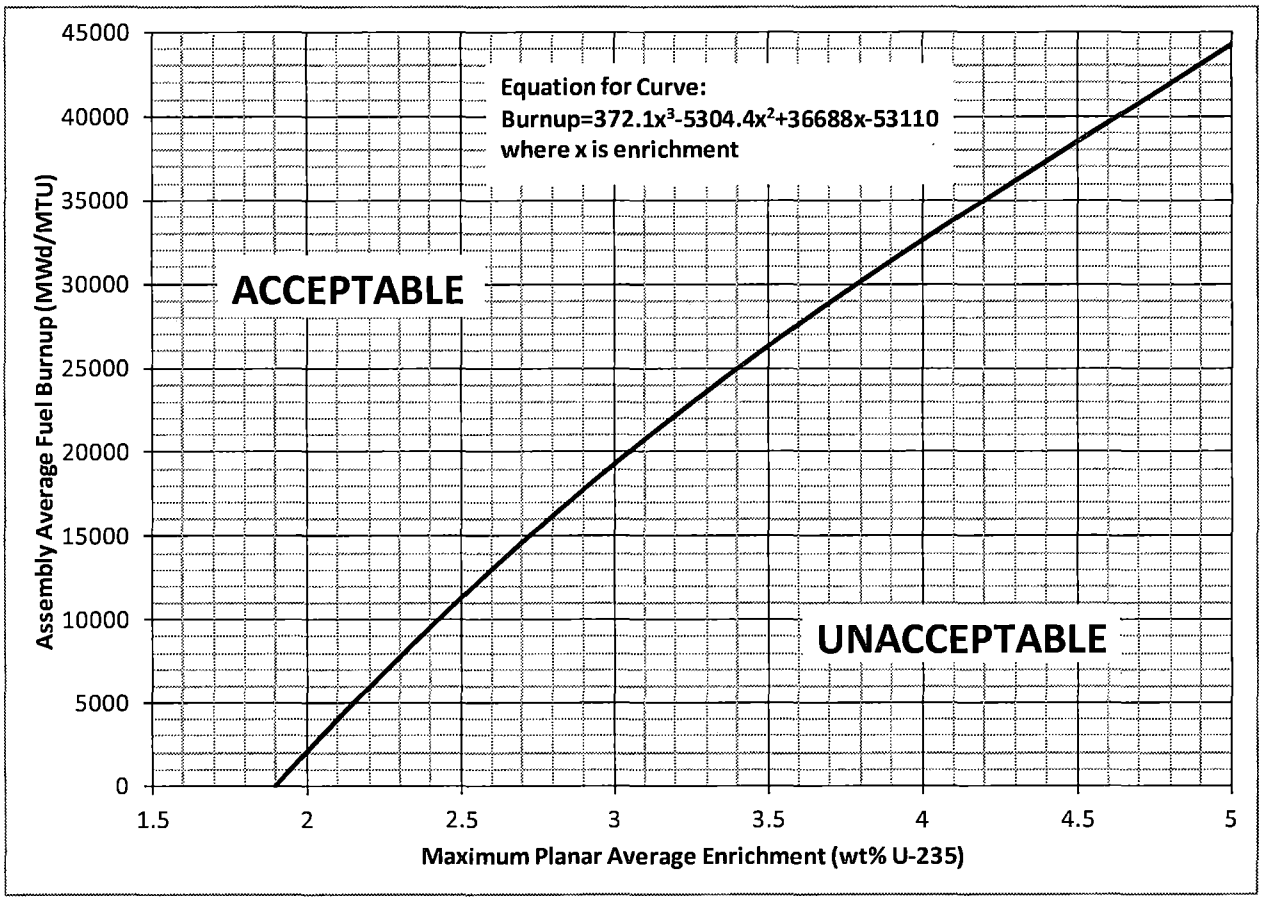

Figure 14.1 Minimum Burnup Requirements For Region 2 With No Credit For Cooling

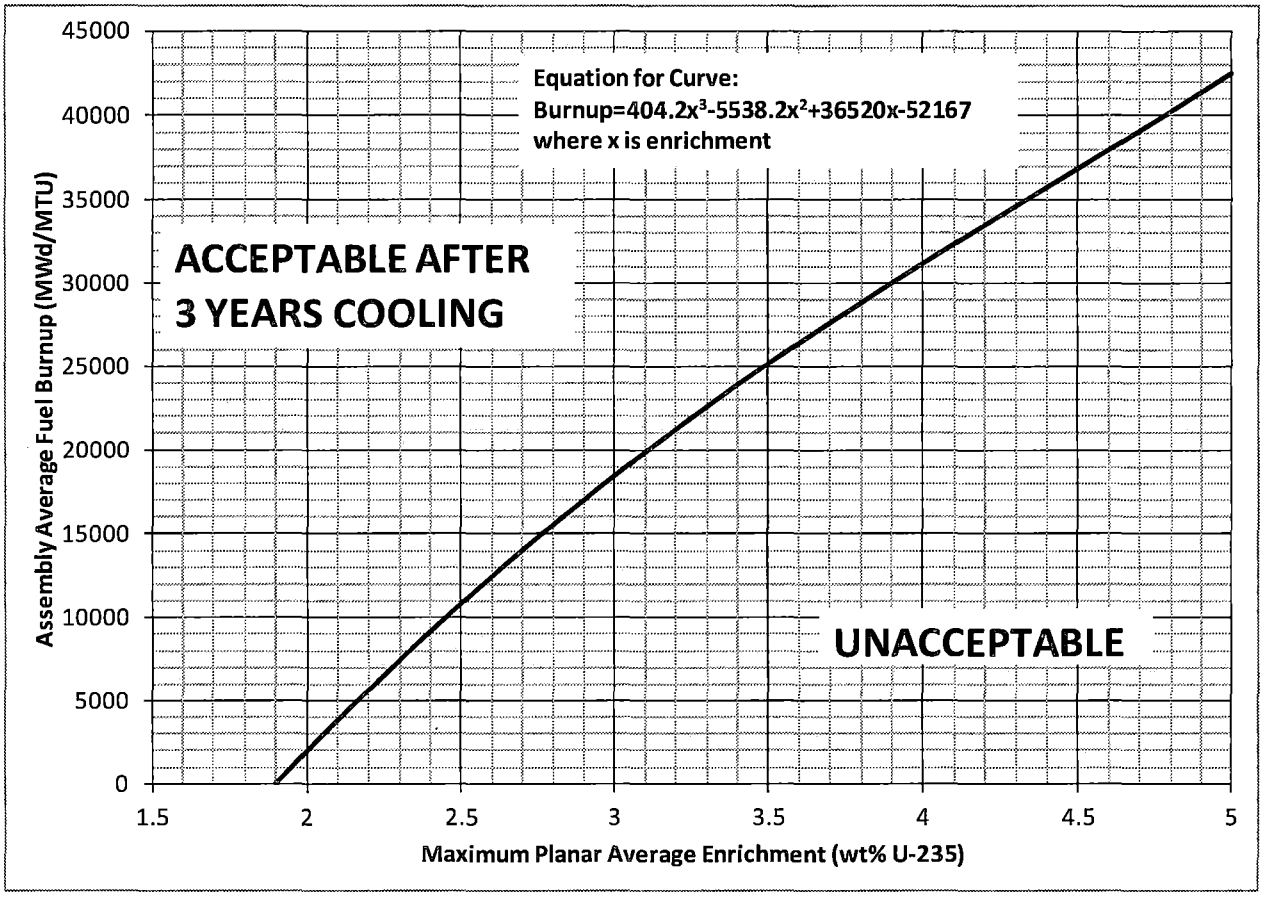

Figure 14.2: Minimum Burnup Requirements for Region 2 for Assemblies Cooled 3 Years or More

The burnup to be used in meeting the loading requirement is the plant measured burnup. No adjustment to the burnup is needed since the uncertainty in the burnup is included in setting the limit. The enrichment should be the as built enrichment for the assembly. If axial blankets are used, the highest radial average enrichment segment in the assembly should be used.

Assemblies reconstituted with stainless steel rods or new rods with enrichments of 1.75 wt% U-235 or less can be loaded using their burnup and enrichment just as any non-reconstituted assembly. Assemblies with a missing fuel rod in the outer two rows of fuel also can be handled the same way. Assemblies with one or more missing rods inside the outer two rows must be handled without burnup credit in Region 1 or Region 2 or exceed the Region 2 minimum burnup requirements by 5 GWd/MTU or more. The fuel rods storage rack (the basket for 52 individual fuel rods) may be stored in any fuel storage location. The Failed Fuel Rod Cans on the south west corner of the spent fuel pool racks are allowed to store a Region 2 qualifying assembly in each can. The empty cell locations in Region 1 are allowed to contain control rods but no other material in the active fuel elevations. Any non-fuel item is allowed in any location where fuel is to be stored. All fuel pins are to be in their initial location in the fuel assembly with the exceptions already mentioned in this paragraph. A few assemblies have not met this requirement. The analysis to support their placement in the pool is given in Section 12.6.

14.5 New Administrative Controls

A requirement that two fuel assemblies, while simultaneously in the spent fuel pool or canals must be at least 12 inches apart if they are not in the fuel racks or in a dry shielded container of the spent fuel pool will be added to the fuel handling procedures.

No other new administrative controls are required.

15 References

[1] Code of Federal Regulations, Title 10, Part 50, Section 68, "*Criticality Accident Requirements.*"

[2] Code of Federal Regulations, Title 10, Part 50, Appendix A, "*General Design Criteria for Nuclear Power Plants*," Criterion 62, "Prevention of Criticality in Fuel Storage and Handling."

[3] NUREG-0800, *Standard Review Plan for the Review of Safety Analysis Reports for Nuclear Power Plants*, Section 9.1.1 Revision 3 (Criticality Safety of Fresh and Spent Fuel Storage and Handling), U.S. Nuclear Regulatory Commission, Washington, DC, March 2007.

[4] *Final Division of Safety Systems Interim Staff Guidance, DSS-ISG-2010-01 Revision 0, Staff Guidance Regarding the Nuclear Criticality Safety Analysis for Spent Fuel Pools*," Nuclear Regulatory Commission, October 2011. (ADAMS Accession Number ML110620086.)

[5] VEPCO Drawing 11715-FS-27G-2, "Plan & Details SH.1; New Fuel Racks – Framing; Fuel Building."

[6] "*SCALE: A Modular Code System for Performing Standardized Computer Analyses for Licensing Evaluation*," ORNL/TM-2005/39, Version 6, Volumes 1-3, Oak Ridge National Laboratory, Oak Ridge, Tennessee, USA, January 2009.

[7] S. Goluoglu, N. F. Landers, L. M. Petrie, and D. F. Hollenbach,"*CSAS5: Control Module For Enhanced Criticality Safety Analysis Sequences with KENO V.A*," ORNL/TM-2005/39, Version 6, Vol. 1, Section C5, Oak Ridge National Laboratory, Oak Ridge, Tennessee, USA, January 2009.

[8] M. A. Jessee, and M. D. DeHart, "*TRITON: A Two-Dimensional Transport and Depletion Module for Characterization of Spent Nuclear Fuel*," ORNL/TM-2005/39, Version 6 Vol. 1, Section T1, Oak Ridge National Laboratory, Oak Ridge, Tennessee, USA, January 2009.

[9] Dominion Letter, "DOMINION NUCLEAR CONNECTICUT, INC.MILLSTONE POWER STATION UNIT 2 RESPONSE TO SECOND REQUEST FOR ADDITIONAL INFORMATION REGARDING PROPOSED TECHNICAL SPECIFICATION CHANGE FOR SPENT FUEL STORAGE", 7/21/15, ADAMS Accession Number ML15209A729.

[10] USNRC Reg. Guide 1.183, "*Alternative Radiological Source Terms for Evaluating Design Basis Accidents at Nuclear Power Reactors*", US Nuclear Regulatory Commission, Washington, DC, July 2000.

[11] C. E. Beyer, and P. M. Clifford, "*Update of Gap Release Fractions for Non-LOCA Events Utilizing the Revised ANS 5.4 Standard*", PNNL-18212 Rev. 1, Pacific Northwest National Laboratory, Richland, Washington, June 2011. ADAMS Accession Number ML112070118.

[12] G. Radulescu, I. C. Gauld, and G. Ilas, *SCALE 5.1 Predictions of PWR Spent Nuclear Fuel Isotopic Compositions*, ORNL/TM-2010/44, Oak Ridge National Laboratory, Oak Ridge, Tennessee, USA, March 2010.

[13] J. O. Barner, "*Characterization Of LWR Spent Fuel MCC - Approved Testing Material--ATM-101*," PNL-5109 Rev. 1, Pacific Northwest National Laboratory, Richland, Washington (1985).

[14] R. J. Guenther, et al, "*Characterization Of Spent Fuel Approved Testing Material--ATM-103*," PNL-5109-103, Pacific Northwest National Laboratory, Richland, Washington (1988).

[15] R. J. Guenther, et al, "*Characterization Of Spent Fuel Approved Testing Material--ATM-104*," PNL-5109-104, Pacific Northwest National Laboratory, Richland, Washington (1991).

[16] R. J. Guenther, et al, "*Characterization Of Spent Fuel Approved Testing Material--ATM-105*," PNL-5109-105, Pacific Northwest National Laboratory, Richland, Washington (1991).

[17] R. J. Guenther, et al, "*Characterization Of Spent Fuel Approved Testing Material--ATM-106*," PNL-5109-106, Pacific Northwest National Laboratory, Richland, Washington (1988).

[18] A. Simpson, T. Marlow, J. Franco, M. Clapham and A. Chesterman, "Operational Experience in Radiometric Instrumentation for Spent Fuel Monitoring," Proceedings of the Institute of Nuclear Materials Management: INMM 44th Annual Meeting, Phoenix, Arizona, July 13-17, 2003, Institute of Nuclear Materials Management, Oakbrook Terrace, IL (2003).

[19] D. B. Lancaster, *Utilization of the EPRI Depletion Benchmarks for Burnup Credit Validation*, EPRI, Palo Alto, CA, 1025203 (2012).

[20] G. Radulescu, I. C. Gauld, G. Ilas, and J. C. Wagner, *An Approach for Validating Actinide and Fission Product Burnup Credit Criticality Safety Analyses – Isotopic Composition Predictions*, NUREG/CR-7108, Office of Nuclear Regulatory Research, U.S. Nuclear Regulatory Commission, Washington, DC, USA, April 2012.

[21] K. S. Smith, et al., *Benchmarks for Quantifying Fuel Reactivity Depletion Uncertainty*, EPRI, Palo Alto, CA, Technical Report Number 1022909 (2011).

[22] R. Hall, et al, *Qualification of the Studsvik Core Management System Reactor Physics Methods for Application to North Anna and Surry Power Stations*, DOM-NAF-1-Rev. 0.0 – A, Nuclear Analysis and Fuel Department, Dominion Richmond, VA, June, 2003. (NRC Approved March 12, 2003) ADAMS Accession Number ML031690108.

[23] Skipped.

[24] Skipped.

[25] J.C. Dean and R.W. Tayloe, Jr., *Guide for Validation of Nuclear Criticality Safety Calculational Methodology*, NUREG/CR-6698, Nuclear Regulatory Commission, Washington, DC January 2001

[26] *International Handbook of Evaluated Criticality Safety Benchmark Experiments*, NEA/NSC/DOC(95)3, Volumes IV and VI, Nuclear Energy Agency, OECD, Paris, September, 2014.

[27] D. E. Mueller, K. R. Elam, and P. B. Fox, *Evaluation of the French Haut Taux de Combustion (HTC) Critical Experiment Data*, NUREG/CR-6979 (ORNL/TM-2007/083), prepared for the US Nuclear Regulatory Commission by Oak Ridge National Laboratory, Oak Ridge, Tenn., September 2008

[28] J. M. Scaglione, D. E. Mueller, J.C. Wagner and W. J. Marshall, *An Approach for Validating. Actinide and Fission Product Burnup Credit Criticality Safety Analyses—Criticality (keff) Predictions*, US Nuclear Regulatory Commission, NUREG/CR-7109, Oak Ridge National Laboratory, Oak Ridge, Tenn. (2012).

[29] U.S. Nuclear Regulatory Commission, *Spent Fuel Project Office Interim Staff Guidance – 8, Rev. 3 – Burnup Credit in the Criticality Safety Analyses of PWR Spent Fuel in Transport and Storage Casks*, U.S. Nuclear Regulatory Commission, April, 2012.

[30] D. Lancaster, *Sensitivity Analyses for Spent Fuel Pool Criticality*, Technical Report EPRI Doc No. 3002003073,December 2014.

[31] Letter from NRC, "Request for Additional Information Related to NEI 12-16, 'Guidance for Performing Criticality Analyses of Fuel Storage at Light Water Reactor Power Plants,'" November 2015. ADAMS Accession Number ML15273A056.

[32] Kontani, Osamu, Ichikawa, Yoshikazu, Ishizawa, Akihiro, Takizawa, Masayuki, & Sato, Osamu (2011). "Irradiation effects on concrete durability of nuclear power plant," Proceedings of ICAPP 2011, (p. 2851). France.

[33] K. William, Y. Xi, and D. Naus, *A Review of the Effects of Radiation on Microstructure and Properties of Concretes Used in Nuclear Power Plants,* NUREG/CR-7171, Office of Nuclear Regulatory Research, U.S. Nuclear Regulatory Commission, Washington, DC, USA, November 2013.

[34] H. K. Hilsdorf, (1967) "A Method to Estimate the Water Content of Concrete Shields," *Nuclear Engineering and Design*, 6, 251-263.

[35] Specification No. NAP-0050, Rev. 0, *Specification for Mixing and Delivery of Safety Related Concrete, North Anna Power Station Units 1 and 2*, September 25, 1992.

[36] Standard, ASTM A480/A480M, "Standard Specification for General Requirements for Flat-Rolled Stainless and Heat Resisting Plate, Sheet, and Strip," November 2013.

[37] *Benchmark on the KRITZ-2 LEU and MOX Critical Experiments*, NEA/NSC/DOC(2005)24 Nuclear Energy Agency, OECD, Paris, 2006.

[38] A. Tsiboulia, et al., "Water-Moderated U(4.92)O_2 Fuel Rods in 1.29, 1.09, and 1.01 cm Pitch Hexagonal Lattices at Different Temperatures," LEU-COMP-THERM-026, *International Handbook of Evaluated Criticality Safety Benchmark Experiments*, NEA/NSC/DOC(95)3, Volume IV, Nuclear Energy Agency, OECD, Paris, September, 2014.

[39] A. D. Santos, et al., "Critical Loading Configurations of the IPEN/MB-01 Reactor Considering Temperature Variation From 14° C to 85° C," LEU-COMP-THERM-046, *International Handbook of Evaluated Criticality Safety Benchmark Experiments*, NEA/NSC/DOC(95)3, Volume IV, Nuclear Energy Agency, OECD, Paris, September, 2014.

[40] J. C. Wagner, M. D. DeHart, and C. V. Parks, "*Recommendations for Addressing Axial Burnup in PWR Burnup Credit Analyses*," US Nuclear Regulatory Commission, NUREG/CR-6801 Oak Ridge National Laboratory, Oak Ridge, Tenn. (2003).

[41] C. V. Parks, M. D. DeHart, and J. C. Wagner, *"Review and Prioritization of Technical Issues Related to Burnup Credit for LWR Fuel,"* US Nuclear Regulatory Commission, NUREG/CR-6665, Oak Ridge National Laboratory, Oak Ridge, Tenn. (2000).

[42] J. C. Wagner and C. V. Parks, *"Parametric Study of the Effect of Burnable Poison Rods for PWR Burnup Credit,"* US Nuclear Regulatory Commission, NUREG/CR-6761, Oak Ridge National Laboratory, Oak Ridge, Tenn. (2002).

[43] Skipped.

[44] C. E. Sanders and J. C. Wagner, *"Study of the Effect of Integral Burnable Absorbers for PWR Burnup Credit,"* US Nuclear Regulatory Commission, NUREG/CR-6760, Oak Ridge National Laboratory, Oak Ridge, Tenn. (2002).

[45] D. Lancaster and C. T. Rombough, *Criticality Safety Analysis of the Indian Point Unit 2 Spent Fuel Pool with Credit for Inserted Neutron Absorber Panels*, NET-300067-01 Rev. 1, NETCO Segment of Scientech, Curtiss-Wright, Connecticut, Feb. 2015. NRC Adams Accession Number ML15062A200. NRC safety review is Accession Number ML15292A161.

[46] Hartz, Leslie, letter to the NRC titled, "VIRGINIA ELECTRIC AND POWER COMPANY NORTH ANNA POWER STATION UNITS I AND 2 PROPOSED TECHNICAL SPECIFICATION CHANGES INCREASED FUEL ENRICHMENT AND SPENT FUEL POOL SOLUBLE BORON AND FUEL BURNUP CREDIT," Appendix A, September 27, 2000. NRC Adams Accession Number ML003758403.

[47] Monarque, Stephen, letter from the NRC to David Christian titled, "NORTH ANNA POWER STATION UNITS I AND 2 - ISSUANCE OF AMENDMENTS RE: TECHNICAL SPECIFICATION CHANGES TO INCREASE FUEL ENRICHMENT AND SPENT FUEL POOL SOLUBLE BORON AND FUEL BURNUP CREDIT (TAC NOS. MB0197 AND MB0198)," June 15, 2001. NRC Adams Accession Number ML011700557.

[48] J. C. Wagner, and C. E. Sanders, *"Assessment of Reactivity Margins and Loading Curves for PWR Burnup-Credit Cask Designs,"* US Nuclear Regulatory Commission, NUREG/CR-6800, Oak Ridge National Laboratory, Oak Ridge, Tenn. (2003).

[49] BAW-2422P Rev. 01, "North Anna 1 Cycle 15 PIE of Mark-BW LTAs," June 2002

[50] EPRI Report 3002000692 "Hot-Cell Examination and Assessment Report for a Next Generation Fuel Skeleton Irradiated in Millstone-3" (June 2013).

[51] Westinghouse Letter NF-VP-16-10 Rev. 1, "Grid Growth Data for Westinghouse 17RFA and 15Upgrade Fuel, Revision 1," 4/11/16.

[52] "Zr-Alloys, the Nuclear Material for Water Reactor Fuel. A Survey and Update with Focus on Fuel for Pressurized Water Reactor Systems,"7th International Conference on WWER Fuel Performance, Modelling and Experimental Support, Albena, Bulgaria, September 2007.

[53] ZIRAT14 Special Topical Report, "In-Reactor Creep of Zirconium Alloys," September 2009, Advanced Nuclear Technology International.

[54] Skipped

[55] EPRI Report 1018642 "Post-Irradiation Examination of AREVA M5 Guide Tubes and Fuel Rods Irradiated in North Anna 1 and 2" (March 2009).

[56] WCAP-15063-P-A, Westinghouse Electric Company LLC., "Westinghouse Improved Performance Analysis and Design Model (PAD 4.0)", July 2000.

[57] Technical Report TR-NE-1367, Rev. 0, "Topical Report DOM-NAF-1, Qualification of the Studsvik Core Management System Reactor Physics Methods for Application to North Anna and Surry Power Stations".

[58] Skipped.

[59] Skipped

[60] B. P. Haugh, *Generic Application of the Studsvik Scandpower Core Management System to Pressurized Water Reactors*, SSP-14/P01-028-TR-NP, Studsvik Scandpower, Inc., Waltham, MA, December, 2015. NRC Adams Accession Number ML15355A285.

[61] NF-NEU-04-8, "Dominion Nuclear Connecticut Millstone Unit 3 Transmittal of Next Generation Fuel Lead Test Assembly Report", February 2004.

[62] BAW-10227PA, "Evaluation of Advanced Cladding and Structural Material (M5) in PWR Reactor Fuel," February 2000.

[63] K. R. Elam, J. C. Wagner, and C. V. Parks, *"Effects of Fuel Failure on Criticality Safety and Radiation Dose for Spent Fuel Casks,"* US Nuclear Regulatory Commission, NUREG/CR-6835, Oak Ridge National Laboratory, Oak Ridge, Tenn. (2003).

[64] NRC Correspondence, ADAMS Accession Number ML15015A575, "Closure of Confirmatory Action Letter Regarding North Anna Power Station, Units 1 and 2", December 2015.

Appendix A: Validation for Criticality Analysis Using Laboratory Critical Experiments

A.1. Overview

This appendix determines the computer code and cross-section library bias and uncertainty in the k's calculated for the North Anna spent fuel pool and new fuel storage area when using the CSAS5 module of SCALE 6.0 and the 238 Group ENDF/B-VII cross section library. [A.1] The CSAS5 module executes the CENTRM and BONAMI programs for the resonance self-shielding calculations and KENO V.a for the Monte Carlo calculation of k. All the computer runs use a large Monte Carlo sampling of at least 1500 generations and 6000 neutrons per generation. The bias and uncertainties determined in this Appendix covers the major actinides and structural materials.

This validation follows the direction of NUREG/CR-6698, "Guide for Validation of Nuclear Criticality Safety Calculational Methodology" [A.2]. The guide establishes the following steps for performing the validation:

1. Define operation/process to identify the range of parameters to be validated
2. Select critical experiment data
3. Model the experiments
4. Analyze the data
5. Define the area of applicability of the validation and limitations

It further defines the steps of "Analyze the data" as:

1. Determine the Bias and Bias Uncertainty
2. Identify Trends in Data, Including Discussion of Methods for Establishing Bias Trends
3. Test for Normal or Other Distributions
4. Select the Statistical Method for Treatment of Data
5. Identify and Support Subcritical Margin
6. Calculate the Upper Safety Limit

The validation consists of modeling 204 UO_2 and 117 MOX critical experiments for the determination of the bias and the uncertainty in the calculation of k for fresh fuel and spent fuel.

A.2. Definition of the Range of Parameters to Be Validated

The validation guidance document [A.2] states:

> *"Prior to the initiation of the validation activity, the operating conditions and parameters for which the validation is to apply must be identified. The fissile isotope, enrichment of fissile isotope, fuel density, fuel chemical form, types of neutron moderators and reflectors, range of moderator to fissile isotope, neutron absorbers, and physical configurations are among the parameters to specify. These parameters will come to define the area of applicability for the validation effort."*

The fuel is low enriched uranium dioxide (less than or equal to 5.0 wt% U-235). The fuel is in pellets with a density of greater than 94% of the theoretical density. The only significant neutron moderators are water and the oxygen in the fuel pellet. The neutron absorbers credited are boron (in solution or sometimes as rods) and Ag-In-Cd control rods which may be credited. The reflectors are water, steel, or concrete. The fuel is in assemblies with a rectangular pitch. The assemblies are arranged in cells with space between the cells. The assemblies and cells are in water with varying density and temperature.

A.3. Selection of the Critical Benchmark Experiments

A.3.1 Selection of the Fresh UO_2 Critical Benchmark Experiments

The UO2 benchmarks that were selected met the following criteria:

- Low enriched (5 wt% U-235 or less) UO2 to cover the principle isotopes of concern.
- Fuel in rods to assure that the heterogeneous analysis used in SCALE also is applied in the benchmark analysis.
- Square lattices to assure the lattice features of SCALE used in the rack analysis are also modeled in the critical benchmarks selected.

- Presence of soluble boron, boron bearing rods and Cd to cover most of the control rod absorption.

- No emphasis on a feature or material not of importance to the rack analysis such as lead or copper or borated absorber panels.

The OECD/NEA *International Handbook of Evaluated Criticality Safety Benchmarks Experiments* [A.3] is the appropriate reference for criticality safety benchmarks. This handbook has reviewed the available benchmarks and evaluated the uncertainties in the experiments. The appropriate modeling is presented. All of the experiments used in the UO_2 validation were taken from this handbook. Volume IV of the handbook is for low enriched uranium systems. The section of Volume IV of interest to this validation is the "Thermal Compound Systems." All of the experiments selected are numbered LEU-COMP-THERM-0XX. This validation will refer to the experiments LEU-COMP-THERM-0XX as just XX where any leading zero is not included. (Experiments are also referred to as LCT-XX.)

There are more critical experiments in the handbook that meet the requirements for this validation than would be necessary to use. However, most of the applicable available benchmarks were used. There are 92 sets of benchmarks in the September 2014 version of the handbook. 24 of these sets were eliminated, since they were for hexagonal arrays. 4 more sets were eliminated due to enrichments of 6.9 wt% U-235 or higher. 8 experimental sets were not for water moderated fuel rods. 5 experimental sets were eliminated due to high uncertainties. 8 experiment sets were eliminated due to features that are not in spent fuel pool racks such as copper tubes, Gd rods or solution, Titanium screens, lead reflectors, or borated panels (The spent fuel pool for this analysis does not credit borated panels and Boraflex panels are not in the models). This leaves 43 benchmark sets of which 25 sets were used for this validation. The 18 unused benchmark sets were reviewed to be sure that there was no feature of the experimental set that was missing in the selected 25 sets. LCT-COMP-THERM-46 is not one of the 25 sets but is used for the temperature bias. The analysis of LCT-COMP-THERM is covered in Section A.8.

The selected 25 benchmark sets include critical experiments from six different critical experiment facilities. The fuel was mainly clad in aluminum, but experiments with stainless steel and zirconium cladding were also in the set.

The critical benchmark sets generally contained multiple experiments, but not all cases from each critical benchmark set is used. In some sets there are experiments that emphasize features that are out of the scope of this validation, such as lead or copper reflectors. The 25 selected benchmark sets resulted in **204 experiments** that are used for the statistical analysis.

A later section will evaluate the area of applicability provided by this selection of critical benchmarks.

Table A.3.1 provides a summary of all the low enriched thermal experiments (non-U metal) from the OECD/NEA handbook [A.3] and why some experiments were not used.

Table A.3.1: Selection Review of OECD/NEA Criticality Benchmarks

(All Experiments Start With LEU-COMP-THERM-)

Benchmark Number	Description	Lab	Selected
1	WATER-MODERATED U(2.35)O_2 FUEL RODS IN 2.032-CM SQUARE-PITCHED ARRAYS	PNL	All 8
2	WATER-MODERATED U(4.31)O_2 FUEL RODS IN 2.54-CM SQUARE-PITCHED ARRAYS	PNL	All 5
3	WATER-MODERATED U(2.35)O_2 FUEL RODS IN 1.684-CM SQUARE-PITCHED ARRAYS (GADOLINIUM WATER IMPURITY)	PNL	None. Gd impurity not well known. Not benchmark quality.
4	WATER-MODERATED U(4.31)O_2 FUEL RODS IN 1.892-CM SQUARE-PITCHED ARRAYS (GADOLINIUM WATER IMPURITY)	PNL	None. Gd impurity not well known. Not benchmark quality.
5	CRITICAL EXPERIMENTS WITH LOW-ENRICHED URANIUM DIOXIDE FUEL RODS IN WATER CONTAINING DISSOLVED GADOLINIUM	PNL	None. No sample SCALE decks. Soluble Gd not used in pools.
6	CRITICAL ARRAYS OF LOW-ENRICHED UO_2 FUEL RODS WITH WATER-TO-FUEL VOLUME RATIOS RANGING FROM 1.5 TO 3.0	JAEA	All 18
7	WATER-REFLECTED 4.738-WT.%-ENRICHED URANIUM DIOXIDE FUEL-ROD ARRAYS	Valduc	Only 4 cases used rest are in hexagonal arrays.
8	CRITICAL LATTICES OF UO_2 FUEL RODS AND PERTURBING RODS IN BORATED WATER	B&W	All 17
9	WATER-MODERATED RECTANGULAR CLUSTERS OF U(4.31)O_2 FUEL RODS (2.54-CM PITCH) SEPARATED BY STEEL, BORAL, COPPER, CADMIUM, ALUMINUM, OR ZIRCALOY-4 PLATES	PNL	16 cases used. Did not include Copper or borated panel cases
10	WATER-MODERATED U(4.31)O_2 FUEL RODS REFLECTED BY TWO LEAD, URANIUM, OR STEEL WALLS	PNL	22 cases used. Did not use lead cases since no lead in pools.
11	CRITICAL EXPERIMENTS SUPPORTING CLOSE PROXIMITY WATER STORAGE OF POWER REACTOR FUEL (PART I - ABSORBER RODS)	B&W	All 15

Benchmark Number	Description	Lab	Selected
12	WATER-MODERATED RECTANGULAR CLUSTERS OF U(2.35)O_2 FUEL RODS(1.684-CM PITCH) SEPARATED BY STEEL, BORAL, BOROFLEX, CADMIUM,OR COPPER PLATES (GADOLINIUM WATER IMPURITY)	PNL	None. Gd impurity not well known. Not benchmark quality.
13	WATER-MODERATED RECTANGULAR CLUSTERS OF U(4.31)O_2 FUEL RODS (1.892-CM PITCH) SEPARATED BY STEEL, BORAL, BOROFLEX, CADMIUM, OR COPPER PLATES, WITH STEEL REFLECTING WALLS	PNL	2 cases used. Did not use the cases with copper or borated panels.
14	WATER-REFLECTED ARRAYS OF U(4.31)O_2 FUEL RODS (1.890-CM AND 1.715-CM SQUARE PITCH) IN BORATED WATER	PNL	None used. High boron content uncertainty. Not benchmark quality.
15	THE VVER EXPERIMENTS: REGULAR AND PERTURBED HEXAGONAL LATTICES OF LOW-ENRICHED UO_2 FUEL RODS IN LIGHT WATER	KFKI	None used due to hex arrays.
16	WATER-MODERATED RECTANGULAR CLUSTERS OF U(2.35)O_2 FUEL RODS (2.032-CM PITCH) SEPARATED BY STEEL, BORAL, COPPER, CADMIUM, ALUMINUM, OR ZIRCALOY-4 PLATES	PNL	19 cases used. Did not use the copper or borated panel cases
17	WATER-MODERATED U(2.35)O_2 FUEL RODS REFLECTED BY TWO LEAD, URANIUM, OR STEEL WALLS	PNL	23 cases used. Did not use the 6 cases with a lead reflector.
18	LIGHT WATER MODERATED AND REFLECTED LOW ENRICHED URANIUM DIOXIDE (7 WT.%) ROD LATTICE	Winfrith	None used. Only 1 case with no SCALE sample deck. Complex system.
19	WATER-MODERATED HEXAGONALLY PITCHED LATTICES OF U(5%)O_2 STAINLESS STEEL CLAD FUEL RODS	Kurchatov Institute	None used due to hex arrays.
20	WATER-MODERATED HEXAGONALLY PITCHED PARTIALLY FLOODED LATTICES OF U(5%)O_2 ZIRCONIUM CLAD FUEL RODS, 1.3-CM PITCH	Kurchatov Institute	None used due to hex arrays.
21	HEXAGONALLY PITCHED PARTIALLY FLOODED LATTICES OF U(5%)O_2 ZIRCONIUM CLAD FUEL RODS MODERATED BY WATER WITH BORIC ACID	Kurchatov Institute	None used due to hex arrays.

Benchmark Number	Description	Lab	Selected
22	UNIFORM WATER-MODERATED HEXAGONALLY PITCHED LATTICES OF RODS WITH U(10%)O_2 FUEL	Kurchatov Institute	None used due to hex arrays.
23	PARTIALLY FLOODED UNIFORM LATTICES OF RODS WITH U(10%)O_2 FUEL	Kurchatov Institute	None used due to hex arrays.
24	WATER-MODERATED SQUARE-PITCHED UNIFORM LATTICES OF RODS WITH U(10%)O_2 FUEL	Kurchatov Institute	Did not use either case due to 10 wt% U-235 enrichment
25	WATER-MODERATED HEXAGONALLY PITCHED LATTICES OF U(7.5%)O_2 STAINLESS-STEEL-CLAD FUEL RODS	Kurchatov Institute	None used due to hex arrays.
26	WATER-MODERATED U(4.92)O_2 FUEL RODS IN 1.29, 1.09, AND 1.01 CM PITCH HEXAGONAL LATTICES AT DIFFERENT TEMPERATURES	IPPE	None used due to hex arrays.
27	WATER-MODERATED AND LEAD-REFLECTED 4.738% ENRICHED URANIUM DIOXIDE ROD ARRAYS	Valduc	None used due to lead reflector.
28	WATER-MODERATED U(4.31)O_2 FUEL RODS IN TRIANGULAR LATTICES WITH BORON, CADMIUM AND GADOLINIUM AS SOLUBLE POISONS	PNL	None used due to hex arrays.
29	WATER MODERATED AND WATER REFLECTED 4.74% ENRICHED URANIUM DIOXIDE ROD ARRAYS SURROUNDED BY HAFNIUM PLATES	Valduc	None used. No SCALE sample decks. hf plates cases without hf have the same pitch and pin as benchmark 7 above. No significant additional value
30	VVER PHYSICS EXPERIMENTS: REGULAR HEXAGONAL (1.27-CM PITCH) LATTICES OF LOW-ENRICHED U(3.5 WT.% 235U)O_2 FUEL RODS IN LIGHT WATER AT DIFFERENT CORE CRITICAL DIMENSIONS	Kurchatov Institute	None used due to hex arrays.
31	WATER-MODERATED HEXAGONALLY PITCHED PARTIALLY FLOODED LATTICES OF U(5%)O_2 ZIRCONIUM-CLAD FUEL RODS, 0.8-CM PITCH	Kurchatov Institute	None used due to hex arrays.
32	UNIFORM WATER-MODERATED LATTICES OF RODS WITH U(10%)O_2 FUEL IN RANGE FROM 20°C TO 274°C	Kurchatov Institute	None used due to hex arrays.

Benchmark Number	Description	Lab	Selected
33	REFLECTED AND UNREFLECTED ASSEMBLIES OF 2 AND 3%-ENRICHED URANIUM FLUORIDE IN PARAFFIN	ORNL	None used. Not UO_2
34	FOUR 4.738-WT.%-ENRICHED URANIUM DIOXIDE ROD ASSEMBLIES CONTAINED IN CADMIUM, BORATED STAINLESS STEEL, OR BORAL SQUARE CANISTERS, WATER-MODERATED AND -REFLECTED	Valduc	None used due to borated plates and high uncertainties with Cd panel cases.
35	CRITICAL ARRAYS OF LOW-ENRICHED UO_2 FUEL RODS IN WATER WITH SOLUBLE GADOLINIUM OR BORON POISON	JAEA	Used 2 cases. Did not use the case with dissolved Gd. (not like pool).
36	THE VVER EXPERIMENTS: REGULAR AND PERTURBED HEXAGONAL LATTICES OF LOW-ENRICHED UO_2 FUEL RODS IN LIGHT WATER - Part 2	KFKI	None used due to hex arrays.
37	WATER-MODERATED AND PARTIALLY CONCRETE-REFLECTED 4.738-WT.%-ENRICHED URANIUM DIOXIDE ROD ARRAYS	Valduc	None used. No SCALE sample decks.
38	WATER-MODERATED 4.738-WT.%-ENRICHED URANIUM DIOXIDE ROD ARRAYS NEXT TO A BORATED CONCRETE SCREEN	Valduc	None used. No SCALE sample decks. Used a borated concrete reflector (not like pool).
39	INCOMPLETE ARRAYS OF WATER-REFLECTED 4.738-WT.%-ENRICHED URANIUM DIOXIDE FUEL-ROD ARRAYS	Valduc	Used all 17 cases.
40	FOUR 4.738-WT.%-ENRICHED URANIUM DIOXIDE ROD ASSEMBLIES CONTAINED IN BORATED STAINLESS STEEL OR BORAL SQUARE CANISTERS, WATER MODERATED AND REFLECTED BY LEAD OR STEEL	Valduc	None used due to borated panels. Did not use lead reflector cases.
41	STORAGE ARRAYS OF 3%-ENRICHED LWR ASSEMBLIES: THE CRISTO II EXPERIMENT IN THE EOLE REACTOR	Cadarache	Did not use the 5 cases due to complex geometry and no SCALE sample deck.
42	WATER-MODERATED RECTANGULAR CLUSTERS OF $U(2.35)O_2$ FUEL RODS (1.684-CM PITCH) SEPARATED BY STEEL, BORAL, BOROFLEX, CADMIUM, OR COPPER PLATES, WITH STEEL REFLECTING WALLS	PNL	Used 2 cases. Did not use copper or borated panel cases.

Benchmark Number	Description	Lab	Selected
43	CRITICAL LOADING CONFIGURATIONS OF THE IPEN/MB-01 REACTOR WITH A HEAVY SS-304 REFLECTOR	IPEN	None used due to Gd rods.
44	CRITICAL LOADING CONFIGURATIONS OF THE IPEN/MB-01 REACTOR WITH UO_2, STAINLESS STEEL AND COPPER RODS	IPEN	None used due to copper rods.
45	PLEXIGLAS OR CONCRETE-REFLECTED $U(4.46)_3O_8$ WITH H/U=0.77 AND INTERSTITIAL MODERATION	Rocky Flats	None used since not pin geometry.
46	CRITICAL LOADING CONFIGURATIONS OF THE IPEN/MB-01 REACTOR CONSIDERING TEMPERATURE VARIATION FROM 14°C TO 85°C	IPEN	Used only for temperature bias. See Reference 9.
47	FUEL TRANSPORT FLASK CRITICAL BENCHMARK EXPERIMENTS WITH LOW-ENRICHED URANIUM DIOXIDE FUEL	Winfrith	None used. 3 complex cases. No SCALE sample decks.
48	LIGHT WATER MODERATED AND REFLECTED LOW-ENRICHED (3 WT.% 235U) URANIUM DIOXIDE ROD LATTICES	Winfrith	All 5 cases used
49	MARACAS PROGRAMME: POLYTHENE-REFLECTED CRITICAL CONFIGURATIONS WITH LOW-ENRICHED AND LOW-MODERATED URANIUM DIOXIDE POWDER, $U(5)O_2$	Valduc	None used. Powder rather than pellets. Not similar to pools.
50	149SM SOLUTION TANK IN THE MIDDLE OF WATER-MODERATED 4.738-WT.%-ENRICHED URANIUM DIOXIDE ROD ARRAYS	Valduc	7 cases used. Did not use cases with dissolved Sm. This is not typical of pools.
51	CRITICAL EXPERIMENTS SUPPORTING CLOSE PROXIMITY WATER STORAGE OF POWER REACTOR FUEL (PART II - ISOLATING PLATES)	B&W	9 cases used. Did not use cases with the borated Al plates since primary source listed a high uncertainty in the boron content.
52	URANIUM DIOXIDE (4.738-WT.%-ENRICHED) FUEL ROD ARRAYS MODERATED AND REFLECTED BY GADOLINIUM NITRATE SOLUTION	Valduc	None used due to hex arrays.

Benchmark Number	Description	Lab	Selected
53	VVER PHYSICS EXPERIMENTS: REGULAR HEXAGONAL (1.27 CM PITCH) LATTICES OF LOW-ENRICHED U(4.4 WT.% 235U)O_2 FUEL RODS IN LIGHT WATER AT DIFFERENT CORE CRITICAL DIMENSIONS	Kurchatov Institute	None used due to hex arrays.
54	CRITICAL LOADING CONFIGURATIONS OF THE IPEN/MB-01 REACTOR WITH UO_2, AND UO_2-Gd_2O_3 RODS	IPEN	None used due to Gd rods.
55	LIGHT-WATER MODERATED AND REFLECTED LOW-ENRICHED URANIUM (3 wt.% 235U) DIOXIDE ROD LATTICES	Winfrith	Neither case used. Complex geometry no KENO-V.a sample deck
56	CRITICAL EXPERIMENT WITH BORAX-V BOILING WATER REACTOR TYPE FUEL ASSEMBLIES	INL	None used. No sample SCALE decks. Complex BWR geometry.
57	4.738-WT.%-ENRICHED URANIUM DIOXIDE FUEL ROD ARRAYS REFLECTED BY WATER IN A DRY STORAGE CONFIGURATION	Valduc	None used. No sample SCALE decks.
58	CRITICAL LOADING CONFIGURATIONS OF THE IPEN/MB-01 REACTOR WITH LARGE VOID IN THE REFLECTOR	IPEN	None used. No sample SCALE decks.
59	Not included in 2014 Handbook		
60	RBMK GRAPHITE REACTOR: UNIFORM CONFIGURATIONS OF U(1.8, 2.0, or 2.4% 235U)O_2 FUEL ASSEMBLIES, AND CONFIGURATIONS OF U(2.0% 235U)O_2 ASSEMBLIES WITH EMPTY CHANNELS, WATER COLUMNS, AND BORON OR THORIUM ABSORBERS, WITH OR WITHOUT WATER IN CHANNELS	Kurchatov Institute	None used. RBMK – not typical of LWRs
61	VVER PHYSICS EXPERIMENTS: HEXAGONAL (1.27-CM PITCH) LATTICES OF U(4.4 WT.% 235U)O_2 FUEL RODS IN LIGHT WATER, PERTURBED BY BORON, HAFNIUM, OR DYSPROSIUM ABSORBER RODS, OR BY WATER GAP WITH/WITHOUT EMPTY ALUMINIUM TUBES	Kurchatov Institute	None used due to hex arrays.
62	2.6%-ENRICHED UO_2 RODS IN LIGHT-WATER MODERATOR WITH BORATED STAINLESS STEEL PLATE: SINGLE ARRAYS	JAEA	None used. No SCALE sample decks.

Benchmark Number	Description	Lab	Selected
63	LIGHT-WATER MODERATED AND REFLECTED LOW-ENRICHED URANIUM (3 wt.% 235U) DIOXIDE ROD LATTICES WITH DISCRETE POISON-ROD ARRAYS	Winfrith	None used. No SCALE sample decks.
64	VVER PHYSICS EXPERIMENTS: REGULAR HEXAGONAL (1.27 CM PITCH) LATTICES OF LOW-ENRICHED U(2.4 WT.% 235U)O2 FUEL RODS IN LIGHT WATER AT DIFFERENT CORE CRITICAL DIMENSIONS	Kurchatov Institute	None used since hex geometry.
65	CRITICAL CONFIGURATIONS OF 2.6%-ENRICHED UO_2 ROD ARRAYS IN LIGHT-WATER MODERATOR WITH BORATED STAINLESS STEEL PLATE: COUPLED ARRAYS	JAEA	None used. No SCALE sample decks.
66	PLEXIGLAS-REFLECTED, CONCRETE-REFLECTED, OR THIN STEEL-REFLECTED $U(4.46)_3O_8$ WITH H/U=0.77 AND HEU DRIVERS	Rocky Flats	None used. Not an array of rods.
67	Not included in 2014 Handbook		
68	PLEXIGLAS-REFLECTED, CONCRETE-REFLECTED, OR THIN STEEL-REFLECTED $U(4.48)_3O_8$ WITH H/U=1.25 OR H/U=2.03 AND HEU DRIVERS	Rocky Flats	None used. Not an array of rods.
69	PLEXIGLAS-REFLECTED $U(4.48)_3O_8$ WITH H/U=1.25 OR H/U=2.03 AND INTERSTITIAL MODERATION	Rocky Flats	None used. Not an array of rods.
70	VVER PHYSICS EXPERIMENTS: REGULAR HEXAGONAL (1.10-CM PITCH) LATTICES OF LOW-ENRICHED U(6.5 WT.% 235U)O_2 FUEL RODS IN LIGHT WATER AT DIFFERENT CORE CRITICAL DIMENSIONS	Kurchatov Institute	None used due to hex arrays.
71	LOW MODERATED 4.738-WT.%-ENRICHED URANIUM DIOXIDE FUEL ROD ARRAYS	Valduc	All 4 cases used.
72	UNDER-MODERATED 4.738-WT.%-ENRICHED URANIUM DIOXIDE FUEL ROD ARRAYS REFLECTED BY WATER OR POLYETHYLENE	Valduc	Used 3 cases. Did not use Polyethylene reflector cases.
73	UNDER-MODERATED 4.738-WT.%-ENRICHED URANIUM DIOXIDE FUEL ROD ARRAYS REFLECTED BY WATER WITH HETEROGENEITIES	Valduc	None used. No SCALE sample decks.

Benchmark Number	Description	Lab	Selected
74	MIRTE PROGRAM FOUR 4.738-WT.%-ENRICHED URANIUM-DIOXIDE FUEL-ROD ARRAYS IN WATER SEPARATED BY A CROSS-SHAPED SCREEN OF TITANIUM (5 MM AND 10 MM THICK)	Valduc	Not used due to Titanium screens
75	VVER PHYSICS EXPERIMENTS: HEXAGONAL (1.10 CM PITCH) LATTICES OF LOW-ENRICHED U(6.5 WT.% 235U)O_2 FUEL RODS IN LIGHT WATER, PERTURBED BY BORON ABSORBER RODS AND WATER HOLES	Kurchatov Institute	None used due to hex arrays.
76	LIGHT WATER MODERATED AND REFLECTED LOW ENRICHED URANIUM (3 WT.% 235U) DIOXIDE ROD LATTICES WITH EX-CORE DETECTOR FEATURE	Winfrith	None used. No KENO Va sample decks.
77	CRITICAL LOADING CONFIGURATIONS OF THE IPEN/MB-01 REACTOR	IPEN	Only one case used. Rest of cases same materials with small modification of arrays. Not sufficiently independent.
78	WATER-MODERATED SQUARE-PITCHED U(6.90)O2 FUEL ROD LATTICES WITH 0.52 FUEL-TO-WATER VOLUME RATIO (0.855 CM PITCH)	SNL	Not used due to high enrichment.
79	WATER-MODERATED U(4.31)O_2 FUEL ROD LATTICES CONTAINING RHODIUM FOILS	SNL	None used due to hex arrays..
80	WATER-MODERATED SQUARE-PITCHED U(6.90)O2 FUEL ROD LATTICES WITH 0.67 FUEL TO WATER VOLUME RATIO	SNL	Not used due to high enrichment.
81	PWR TYPE UO_2 FUEL RODS WITH ENRICHMENTS OF 3.5 AND 6.6 WT.% WITH BURNABLE ABSORBER ("OTTO HAHN" NUCLEAR SHIP PROGRAM, SECOND CORE)	ANEX	Single case not use. No sample SCALE deck. Unusual case.
82	CRITICAL LOADING CONFIGURATIONS OF THE IPEN/MB-01 REACTOR WITH LOW ENRICHED FUEL AND BURNABLE POISON RODS	IPEN	Used only one case. Rest of cases were not significantly different.

Benchmark Number	Description	Lab	Selected
83	CRITICAL LOADING CONFIGURATIONS OF THE IPEN/MB-01 REACTOR WITH A BIG CENTRAL VOID	IPEN	Used only one case. Rest of cases were not significantly different.
84	CRITICAL LOADING CONFIGURATIONS OF THE IPEN/MB-01 REACTOR WITH A CENTRAL CRUCIFORM ROD	IPEN	Used the single case..
85	VVER PHYSICS EXPERIMENTS: REGULAR HEXAGONAL (1.27 CM PITCH) LATTICES OF LOW-ENRICHED U(6.5 WT.% 235U)O_2 FUEL RODS IN LIGHT WATER AT DIFFERENT CORE CRITICAL DIMENSIONS	Kurchatov Institute	None used due to hex arrays.
86	VVER PHYSICS EXPERIMENTS: HEXAGONAL LATTICES (1.275 CM PITCH) OF LOW ENRICHED U(3.6, 4.4 WT.% 235U)O_2 FUEL ASSEMBLIES IN LIGHT WATER WITH H3BO3	NRI	None used due to hex arrays.
87	VVER PHYSICS EXPERIMENTS: HEXAGONAL LATTICES (1.22-CM PITCH) OF LOW-ENRICHED U(3.6, 4.4 WT.% U235)O_2 FUEL ASSEMBLIES IN LIGHT WATER WITH VARIABLE FUEL-ASSEMBLY PITCH	NRI	None used due to hex arrays.
88	CRITICAL LOADING CONFIGURATIONS OF THE IPEN/MB-01 REACTOR WITH HEAVY REFLECTORS COMPOSED OF CARBON STEEL AND NICKEL	IPEN	Not used due to no same SCALE decks and no significant contribution.
89	CRITICAL LOADING CONFIGURATIONS OF THE IPEN/MB-01 REACTOR WITH UO_2 AND BORATED STAINLESS STEEL PLATES	IPEN	Used only one case. Rest of cases were not significantly different.
90	CRITICAL LOADING CONFIGURATIONS OF THE IPEN/MB-01 REACTOR WITH UO_2 AND STAINLESS STEEL RODS	IPEN	Used only one case. Rest of cases were not significantly different.
91	CRITICAL LOADING CONFIGURATIONS OF THE IPEN/MB-01 REACTOR WITH UO_2, STAINLESS STEEL AND GD2O3 RODS	IPEN	Not used due to Gd rods.
92	CRITICAL LOADING CONFIGURATIONS OF THE IPEN/MB-01 REACTOR WITH SOLUBLE BORON	IPEN	Not used due to sufficient boron cases already and no SCALE sample input.
93	DEUTERIUM CRITICAL ASSEMBLY WITH 1.2% ENRICHED URANIUM VARYING COOLANT VOID FRACTION AND LATTICE PITCH	PNC	Not used since cases use D_2O rather than H_2O

Benchmark Number	Description	Lab	Selected
94	VVER PHYSICS EXPERIMENTS: REGULAR HEXAGONAL (1.10 CM PITCH) TWO-REGION LATTICES OF LOW-ENRICHED U(6.5 AND 4.4 WT.% 235U)O_2 FUEL RODS IN LIGHT WATER AT DIFFERENT CORE CRITICAL DIMENSIONS	Kurchatov Institute	None used due to hex arrays.

A.3.2 Selection of MOX Critical Experiments

Burned fuel contains a low concentration of plutonium (about less than 1 wt%), as well as the uranium and thus is actually Mixed Oxide (MOX) fuel. Most classical MOX experiments have plutonium concentrations at least twice as high as that contained in burned fuel. A series of experiments were performed in France, Haut Taux de Combustion (HTC) critical experiments, and purchased by the US for domestic use. These experiments model the uranium and plutonium concentration of 4.5 wt % U-235 fuel burned to 37.5 GWd/T [A.4]. This fuel has 1.1 wt% plutonium and 1.57 wt% U-235. All the HTC critical experiments used the same fuel pins. The criticality of these experiments was controlled by adjusting the critical water height. The fuel pins were used in 156 critical arrangements. . The experiments were performed in four phases.

HTC Phase 1 [A.5] consists of 17 cases where the pin pitch was varied from 1.3 cm to 2.3 cm and different quantities of pins were used to change the critical height. An 18th case was done where the array was moved to the edge of the tank, so the boundary was the steel tank followed by void. This condition is not typical of a spent fuel pool, so this case was not analyzed. HTC Phase 2 [A.6] consisted of 20 cases where gadolinium of various concentrations was dissolved in the water (Phase 2a) and 21 cases where boron was dissolved in the water (Phase 2b). Since Gd is not credited except as a fission product, Phase 2a cases are not selected for analysis. Phase 3 [A.7] consists of 26 experiments where the pins were arranged as 4 "assemblies." Each assembly used a 1.6 cm pin pitch. The assembly separation was varied, as well as the number of pins in each assembly. Eleven cases boxed the assemblies with an absorber (borated steel, Boral, or cadmium). All boxed cases, but the cadmium boxed assembly cases, are eliminated since no credit for boron absorber panels is taken. (Cadmium is credited as part of the control rod credit.) Finally, Phase 4 [A.8] consisted of redoing the same

type of experiments as Phase 3, except with lead and steel reflector screens. The cases without boxes or with Cadmium boxes and steel reflectors were selected. In review, a total of 78 HTC critical experiments were included.

Since the burnup requirements may exceed 37.5 GWd/MTU and so that the MOX cases came from more than one experimental facility, MOX critical experiments from the OECD/NEA handbook [A.3] were reviewed. There are only 63 low enriched MOX pin critical experiments documented in the OECD/NEA handbook. All of these are selected for analysis.

The total MOX set is 63 (OECD/NEA)+78 (HTC) or 141 critical experiments. Twenty four of the 63 OECD/NEA MOX experiments have plutonium content greater than 2 wt%. Since spent nuclear fuel never reaches greater than 2 wt% Pu these experiments were not used in the final determination of the bias and uncertainty for spent fuel. The bias and uncertainty from the MOX set was determined from 117 MOX critical experiments.

A.4. Modeling and Calculating k of the Critical Experiments

For most cases, input decks exist on the OECD/NEA handbook [A.3] disc. In general, these input decks were used with minor modifications. For example, none of the decks were for SCALE 6.0 or the ENDF/B-VII library, and the number of neutrons per generation and the number of generations were, in general, too low. All of the decks were modified to 6000 neutrons per generation and 1500 generations. This was sufficient to make the Monte Carlo uncertainty to be 0.0002 or about one tenth the experimental uncertainty. It was confirmed that the input decks matched the isotopic content given in the handbook. The geometric modeling in the decks also matched the descriptions in the handbook. In short, although there was considerable help by starting with the input files given in the handbook, the ownership of the files was taken, as required by NUREG/CR-6698 [A.2] and as stated in section 2.3:

For specific critical experiments, the facility or site may choose to use input files generated elsewhere to expedite the validation process. The site has the responsibility for ensuring that input files and the options selected are appropriate for use. Regardless of the source of the input file, the site must have reviewed the description of each critical experiment and determined that the representation of the experiment, including simplifying assumptions and

options, are consistent with the intended use. In other words, the site must assume ownership of the input file.

KENO case k convergence was verified using two techniques: 1) checking for satisfaction of the chi-squared test in the output, and 2) performing a statistical test that compares the average k of the first half of generations with the average k of the second half of generations within their respective uncertainties. This second technique is considered equivalent of viewing the plotted output and looking for a variation or trend which would indicate a lack of convergence. If either of these techniques failed and the output looked suspect, then the cases were rerun with more generations so that the tests succeeded.

Table A.4.1 shows the results of the analysis of the 204 UO2 critical experiments, along with parameters that are used to check for trends in the results. The spectral index, the Energy of the Average Lethargy of the neutrons causing Fission (EALF) is a calculated value from the SCALE output. Note that some of the critical experiments were actually slightly supercritical. For the supercritical experiments the calculated k's were divided by the measured k before being placed on Table A.4.1.

Table A.4.1: UO2 Critical Experiment Results with SCALE 6.0 and ENDF/B-VII

Benchmark ID	Case No.	Enrichment (wt% U-235)	Fuel Pin Diameter (cm)	Fuel Pin Pitch (cm)	EALF (eV)	Measurment Uncertainty (delta k)	Calculated k_{eff}
LCT-1	1	2.350	1.270	2.032	0.0960	0.003	0.9979
	2	2.350	1.270	2.032	0.0955	0.003	0.9978
	3	2.350	1.270	2.032	0.0945	0.003	0.9970
	4	2.350	1.270	2.032	0.0952	0.003	0.9974
	5	2.350	1.270	2.032	0.0939	0.003	0.9956
	6	2.350	1.270	2.032	0.0947	0.0027	0.9978
	7	2.350	1.270	2.032	0.0931	0.0031	0.9975
	8	2.350	1.270	2.032	0.0941	0.003	0.9964
LCT-2	1	4.310	1.415	2.540	0.1129	0.002	0.9974
	2	4.310	1.415	2.540	0.1128	0.002	0.9994
	3	4.310	1.415	2.540	0.1128	0.002	0.9982
	4	4.310	1.415	2.540	0.1117	0.0018	0.9978
	5	4.310	1.415	2.540	0.1101	0.0019	0.9963
LCT-6	1	2.596	1.417	1.849	0.2351	0.002	0.9977
	2	2.596	1.417	1.849	0.2420	0.002	0.9981
	3	2.596	1.417	1.849	0.2484	0.002	0.9985

Benchmark ID	Case No.	Enrichment (wt% U-235)	Fuel Pin Diameter (cm)	Fuel Pin Pitch (cm)	EALF (eV)	Measurment Uncertainty (delta k)	Calculated k_{eff}
	4	2.596	1.417	1.956	0.1812	0.002	0.9983
	5	2.596	1.417	1.956	0.1866	0.002	0.9979
	6	2.596	1.417	1.956	0.1913	0.002	0.9992
	7	2.596	1.417	1.956	0.1963	0.002	0.9988
	8	2.596	1.417	1.956	0.2018	0.002	0.9990
	9	2.596	1.417	2.150	0.1352	0.002	0.9987
	10	2.596	1.417	2.150	0.1388	0.002	0.9983
	11	2.596	1.417	2.150	0.1421	0.002	0.9985
	12	2.596	1.417	2.150	0.1456	0.002	0.9979
	13	2.596	1.417	2.150	0.1486	0.002	0.9986
	14	2.596	1.417	2.293	0.1142	0.002	0.9991
	15	2.596	1.417	2.293	0.1171	0.002	0.9991
	16	2.596	1.417	2.293	0.1196	0.002	0.9991
	17	2.596	1.417	2.293	0.1223	0.002	0.9990
	18	2.596	1.417	2.293	0.1249	0.002	0.9987
LCT-7	1	4.738	0.940	1.260	0.2406	0.0014	0.9965
	2	4.738	0.940	1.600	0.1089	0.0008	0.9986
	3	4.738	0.940	2.100	0.0707	0.0007	0.9976
	4	4.738	0.940	2.520	0.0605	0.0008	0.9983
LCT-8	1	2.459	1.206	1.636	0.2780	0.0012	0.9965
	2	2.459	1.206	1.636	0.2452	0.0012	0.9969
	3	2.459	1.206	1.636	0.2450	0.0012	0.9974
	4	2.459	1.206	1.636	0.2458	0.0012	0.9969
	5	2.459	1.206	1.636	0.2454	0.0012	0.9962
	6	2.459	1.206	1.636	0.2445	0.0012	0.9966
	7	2.459	1.206	1.636	0.2445	0.0012	0.9965
	8	2.459	1.206	1.636	0.2426	0.0012	0.9960
	9	2.459	1.206	1.636	0.2419	0.0012	0.9964
	10	2.459	1.206	1.636	0.2481	0.0012	0.9966
	11	2.459	1.206	1.636	0.2534	0.0012	0.9970
	12	2.459	1.206	1.636	0.2470	0.0012	0.9970
	13	2.459	1.206	1.636	0.2474	0.0012	0.9969
	14	2.459	1.206	1.636	0.2492	0.0012	0.9967
	15	2.459	1.206	1.636	0.2496	0.0012	0.9962
	16	2.459	1.206	1.636	0.2272	0.0012	0.9973
	17	2.459	1.206	1.636	0.1982	0.0012	0.9963
LCT-9	1	4.310	1.415	2.540	0.1126	0.0021	0.9983
	2	4.310	1.415	2.540	0.1119	0.0021	0.9978
	3	4.310	1.415	2.540	0.1123	0.0021	0.9980
	4	4.310	1.415	2.540	0.1121	0.0021	0.9982
	16	4.310	1.415	2.540	0.1135	0.0021	0.9981
	17	4.310	1.415	2.540	0.1128	0.0021	0.9986
	18	4.310	1.415	2.540	0.1136	0.0021	0.9981

Benchmark ID	Case No.	Enrichment (wt% U-235)	Fuel Pin Diameter (cm)	Fuel Pin Pitch (cm)	EALF (eV)	Measurment Uncertainty (delta k)	Calculated k_{eff}
	19	4.310	1.415	2.540	0.1129	0.0021	0.9991
	20	4.310	1.415	2.540	0.1136	0.0021	0.9979
	21	4.310	1.415	2.540	0.1128	0.0021	0.9988
	22	4.310	1.415	2.540	0.1136	0.0021	0.9989
	23	4.310	1.415	2.540	0.1128	0.0021	0.9989
	24	4.310	1.415	2.540	0.1120	0.0021	0.9982
	25	4.310	1.415	2.540	0.1118	0.0021	0.9984
	26	4.310	1.415	2.540	0.1119	0.0021	0.9986
	27	4.310	1.415	2.540	0.1117	0.0021	0.9982
LCT-10	5	4.310	1.415	2.540	0.3478	0.0021	0.9995
	6	4.310	1.415	2.540	0.2567	0.0021	1.0001
	7	4.310	1.415	2.540	0.2058	0.0021	1.0003
	8	4.310	1.415	2.540	0.1819	0.0021	0.9972
	9	4.310	1.415	2.540	0.1219	0.0021	1.0008
	10	4.310	1.415	2.540	0.1179	0.0021	1.0004
	11	4.310	1.415	2.540	0.1152	0.0021	1.0009
	12	4.310	1.415	2.540	0.1121	0.0021	0.9992
	13	4.310	1.415	2.540	0.1104	0.0021	0.9971
	14	4.310	1.415	1.892	0.3064	0.0028	1.0008
	15	4.310	1.415	1.892	0.2941	0.0028	1.0014
	16	4.310	1.415	1.892	0.2845	0.0028	1.0022
	17	4.310	1.415	1.892	0.2786	0.0028	1.0013
	18	4.310	1.415	1.892	0.2736	0.0028	1.0016
	19	4.310	1.415	1.892	0.2668	0.0028	1.0007
	24	4.310	1.415	1.892	0.5905	0.0028	0.9988
	25	4.310	1.415	1.892	0.5448	0.0028	1.0001
	26	4.310	1.415	1.892	0.5056	0.0028	1.0007
	27	4.310	1.415	1.892	0.4722	0.0028	1.0010
	28	4.310	1.415	1.892	0.4419	0.0028	1.0016
	29	4.310	1.415	1.892	0.4177	0.0028	1.0015
	30	4.310	1.415	1.892	0.3642	0.0028	0.9987
LCT-11	1	2.459	1.206	1.636	0.1677	0.0018	0.9970
	2	2.459	1.206	1.636	0.2436	0.0032	0.9963
	3	2.459	1.206	1.636	0.1915	0.0032	0.9967
	4	2.459	1.206	1.636	0.1917	0.0032	0.9974
	5	2.459	1.206	1.636	0.1926	0.0032	0.9967
	6	2.459	1.206	1.636	0.1937	0.0032	0.9968
	7	2.459	1.206	1.636	0.1949	0.0032	0.9975
	8	2.459	1.206	1.636	0.1962	0.0032	0.9968
	9	2.459	1.206	1.636	0.1971	0.0032	0.9969
	10	2.459	1.206	1.636	0.1854	0.0017	0.9942
	11	2.459	1.206	1.636	0.1622	0.0017	0.9942
	12	2.459	1.206	1.636	0.1664	0.0017	0.9939

Benchmark ID	Case No.	Enrichment (wt% U-235)	Fuel Pin Diameter (cm)	Fuel Pin Pitch (cm)	EALF (eV)	Measurment Uncertainty (delta k)	Calculated k_{eff}
	13	2.459	1.206	1.636	0.1466	0.0017	0.9945
	14	2.459	1.206	1.636	0.1498	0.0017	0.9949
	15	2.459	1.206	1.636	0.1382	0.0018	0.9953
LCT-13	1	4.310	1.415	1.892	0.2836	0.0018	1.0000
	5	4.310	1.415	1.892	0.2953	0.0032	1.0001
LCT-16	1	2.350	1.270	2.032	0.0951	0.0031	0.9973
	2	2.350	1.270	2.032	0.0948	0.0031	0.9958
	3	2.350	1.270	2.032	0.0947	0.0031	0.9974
	4	2.350	1.270	2.032	0.0949	0.0031	0.9964
	5	2.350	1.270	2.032	0.0945	0.0031	0.9966
	6	2.350	1.270	2.032	0.0955	0.0031	0.9970
	7	2.350	1.270	2.032	0.0953	0.0031	0.9970
	21	2.350	1.270	2.032	0.0967	0.0031	0.9978
	22	2.350	1.270	2.032	0.0964	0.0031	0.9976
	23	2.350	1.270	2.032	0.0960	0.0031	0.9974
	24	2.350	1.270	2.032	0.0964	0.0031	0.9974
	25	2.350	1.270	2.032	0.0960	0.0031	0.9977
	26	2.350	1.270	2.032	0.0965	0.0031	0.9976
	27	2.350	1.270	2.032	0.0959	0.0031	0.9975
	28	2.350	1.270	2.032	0.0943	0.0031	0.9977
	29	2.350	1.270	2.032	0.0942	0.0031	0.9966
	30	2.350	1.270	2.032	0.0943	0.0031	0.9967
	31	2.350	1.270	2.032	0.0943	0.0031	0.9978
	32	2.350	1.270	2.032	0.0942	0.0031	0.9970
LCT-17	4	2.350	1.270	2.032	0.1979	0.0031	0.9979
	5	2.350	1.270	2.032	0.1749	0.0031	0.9991
	6	2.350	1.270	2.032	0.1652	0.0031	0.9996
	7	2.350	1.270	2.032	0.1575	0.0031	0.9990
	8	2.350	1.270	2.032	0.1316	0.0031	0.9973
	9	2.350	1.270	2.032	0.1084	0.0031	0.9970
	10	2.350	1.270	2.032	0.0993	0.0031	0.9980
	11	2.350	1.270	2.032	0.0975	0.0031	0.9979
	12	2.350	1.270	2.032	0.0963	0.0031	0.9977
	13	2.350	1.270	2.032	0.0950	0.0031	0.9975
	14	2.350	1.270	2.032	0.0942	0.0031	0.9983
	15	2.350	1.270	1.684	0.1763	0.0028	0.9974
	16	2.350	1.270	1.684	0.1705	0.0028	0.9974
	17	2.350	1.270	1.684	0.1656	0.0028	0.9991
	18	2.350	1.270	1.684	0.1640	0.0028	0.9972
	19	2.350	1.270	1.684	0.1615	0.0028	0.9972
	20	2.350	1.270	1.684	0.1600	0.0028	0.9964
	21	2.350	1.270	1.684	0.1587	0.0028	0.9969
	22	2.350	1.270	1.684	0.1575	0.0028	0.9956

Benchmark ID	Case No.	Enrichment (wt% U-235)	Fuel Pin Diameter (cm)	Fuel Pin Pitch (cm)	EALF (eV)	Measurment Uncertainty (delta k)	Calculated k_{eff}
	26	2.350	1.270	1.684	0.3652	0.0028	0.9950
	27	2.350	1.270	1.684	0.3144	0.0028	0.9971
	28	2.350	1.270	1.684	0.2748	0.0028	0.9979
	29	2.350	1.270	1.684	0.2463	0.0028	0.9981
LCT-35	1	2.596	1.417	1.956	0.2073	0.0018	0.9981
	2	2.596	1.417	1.956	0.2111	0.0019	0.9971
LCT-39	1	4.738	0.940	1.260	0.2216	0.0014	0.9953
	2	4.738	0.940	1.260	0.2112	0.0014	0.9968
	3	4.738	0.940	1.260	0.1920	0.0014	0.9964
	4	4.738	0.940	1.260	0.1834	0.0014	0.9955
	5	4.738	0.940	1.260	0.1391	0.0009	0.9980
	6	4.738	0.940	1.260	0.1452	0.0009	0.9979
	7	4.738	0.940	1.260	0.2124	0.0012	0.9964
	8	4.738	0.940	1.260	0.2026	0.0012	0.9958
	9	4.738	0.940	1.260	0.1970	0.0012	0.9967
	10	4.738	0.940	1.260	0.1727	0.0012	0.9973
	11	4.738	0.940	1.260	0.2214	0.0013	0.9950
	12	4.738	0.940	1.260	0.2159	0.0013	0.9956
	13	4.738	0.940	1.260	0.2140	0.0013	0.9953
	14	4.738	0.940	1.260	0.2120	0.0013	0.9957
	15	4.738	0.940	1.260	0.2109	0.0013	0.9958
	16	4.738	0.940	1.260	0.2099	0.0013	0.9963
	17	4.738	0.940	1.260	0.2096	0.0013	0.9965
LCT-42	1	2.350	1.270	1.684	0.1680	0.0016	0.9972
	5	2.350	1.270	1.684	0.1765	0.0033	0.9983
LCT-48	1	3.005	1.094	1.320	0.6740	0.0025	0.9978
	2	3.005	1.094	1.320	0.6467	0.0025	0.9984
	3	3.005	1.094	1.320	0.6771	0.0025	0.9977
	4	3.005	1.094	1.320	0.6788	0.0025	0.9983
	5	3.005	1.094	1.320	0.6691	0.0025	0.9977
LCT-50	1	4.738	0.940	1.300	0.1992	0.0010	0.9976
	2	4.738	0.940	1.300	0.1906	0.0010	0.9972
	3	4.738	0.940	1.300	0.2072	0.0010	0.9970
	4	4.738	0.940	1.300	0.1976	0.0010	0.9967
	5	4.738	0.940	1.300	0.2218	0.0010	0.9983
	6	4.738	0.940	1.300	0.2134	0.0010	0.9986
	7	4.738	0.940	1.300	0.2094	0.0010	0.9988
LCT-51	1 C10	2.459	1.206	1.636	0.1468	0.0020	0.9960
	2 c11a	2.459	1.206	1.636	0.1953	0.0024	0.9979
	3 c11b	2.459	1.206	1.636	0.1951	0.0024	0.9973

Benchmark ID	Case No.	Enrichment (wt% U-235)	Fuel Pin Diameter (cm)	Fuel Pin Pitch (cm)	EALF (eV)	Measurment Uncertainty (delta k)	Calculated k_{eff}
	4 c11c	2.459	1.206	1.636	0.1968	0.0024	0.9970
	5 c11d	2.459	1.206	1.636	0.1974	0.0024	0.9974
	6 c11e	2.459	1.206	1.636	0.1989	0.0024	0.9967
	7 c11f	2.459	1.206	1.636	0.1991	0.0024	0.9972
	8 c11g	2.459	1.206	1.636	0.2000	0.0024	0.9970
	9 c12	2.459	1.206	1.636	0.1660	0.0019	0.9968
LCT-71	1	4.738	0.949	1.100	0.7553	0.00076	0.9943
	2	4.738	0.949	1.100	0.6915	0.00076	0.9945
	3	4.738	0.949	1.100	0.6563	0.00076	0.9943
	4	4.738	0.949	1.075	0.8432	0.0008	0.9938
LCT-72	1	4.738	0.949	1.600	0.1101	0.0012	0.9985
	2	4.738	0.949	1.600	0.1062	0.0012	0.9973
	3	4.738	0.949	1.600	0.1083	0.0012	0.9980
LCT-77	3	4.349	0.980	1.500	0.1618	0.0010	1.0005
LCT-82	3	4.349	0.980	1.500	0.1494	0.0010	1.0005
LCT-83	1	4.349	0.980	1.500	0.1512	0.0010	0.9999
LCT-84	1	4.349	0.980	1.500	0.1541	0.0010	0.9997
LCT-89	1	4.349	0.980	1.500	0.1529	0.0010	1.0000
LCT-90	1	4.349	0.980	1.500	0.1458	0.0010	0.9937

The HTC modeling utilized References A.5 through A.8 for all the details for the analysis. The modeling was straight forward. The references gave a simple modeling and a detailed modeling. The models created for this work followed the detailed modeling. Table A.4.2 shows the results of the SCALE calculations of the HTC experiments. The fuel pins for all the HTC cases are the same. The plutonium weight % is always 1.1 wt% Pu.

Table A.4.3 is the results of the SCALE calculations of the MOX critical experiments from the OECD/NEA handbook. [A.3]

Table A.4.2: HTC Critical Experiment Results with SCALE 6.0 and ENDF/B-VII

Experiment	k_{eff}	σ_{calc}	σ_{exp}	EALF (eV)	Pitch (cm)	Absorber
HTC-P1-C01	0.99924	0.00020	0.00182	0.0691	2.3	
HTC-P1-C02	0.99915	0.00019	0.00182	0.0662	2.3	
HTC-P1-C03	0.99929	0.00019	0.00182	0.0661	2.3	
HTC-P1-C04	1.00021	0.00024	0.00182	0.0845	1.9	
HTC-P1-C05	1.00028	0.00023	0.00182	0.0823	1.9	
HTC-P1-C06	0.99974	0.00022	0.00182	0.0817	1.9	
HTC-P1-C07	0.99992	0.00024	0.00182	0.1018	1.7	
HTC-P1-C08	0.99958	0.00024	0.00182	0.1002	1.7	
HTC-P1-C09	0.99917	0.00024	0.00182	0.0993	1.7	
HTC-P1-C10	1.00017	0.00025	0.00182	0.1397	1.5	
HTC-P1-C11	0.99882	0.00023	0.00182	0.1350	1.5	
HTC-P1-C12	0.99864	0.00023	0.00182	0.1331	1.5	
HTC-P1-C13	0.99834	0.00027	0.00182	0.2542	1.3	
HTC-P1-C14	0.99813	0.00024	0.00182	0.2322	1.3	
HTC-P1-C15	0.99766	0.00025	0.00182	0.2286	1.3	
HTC-P1-C16	1.00008	0.00023	0.00182	0.1010	1.7	
HTC-P1-C17	0.99937	0.00021	0.00182	0.0989	1.7	
						Boron ppm
HTC-P2-BOR-C01	0.99878	0.00024	0.00247	0.2451	1.3	100
HTC-P2-BOR-C02	0.99783	0.00026	0.00247	0.2426	1.3	106
HTC-P2-BOR-C03	0.99790	0.00024	0.00247	0.2530	1.3	205
HTC-P2-BOR-C04	0.99880	0.00024	0.00247	0.2612	1.3	299
HTC-P2-BOR-C05	0.99855	0.00022	0.00247	0.2721	1.3	400
HTC-P2-BOR-C06	0.99823	0.00023	0.00247	0.2688	1.3	399
HTC-P2-BOR-C07	0.99934	0.00027	0.00247	0.2776	1.3	486
HTC-P2-BOR-C08	0.99847	0.00022	0.00247	0.2847	1.3	587
HTC-P2-BOR-C09	0.99930	0.00022	0.00247	0.1652	1.5	595
HTC-P2-BOR-C10	0.99789	0.00022	0.00247	0.1600	1.5	499
HTC-P2-BOR-C11	0.99959	0.00023	0.00247	0.1555	1.5	393
HTC-P2-BOR-C12	0.99963	0.00021	0.00247	0.1492	1.5	295
HTC-P2-BOR-C13	0.99893	0.00024	0.00247	0.1445	1.5	200
HTC-P2-BOR-C14	1.00255	0.00026	0.00247	0.1391	1.5	89
HTC-P2-BOR-C15	1.00337	0.00024	0.00247	0.1026	1.7	90
HTC-P2-BOR-C16	1.00162	0.00024	0.00247	0.1066	1.7	194
HTC-P2-BOR-C17	1.00309	0.00021	0.00247	0.1098	1.7	286
HTC-P2-BOR-C18	0.99343	0.00020	0.00247	0.1152	1.7	415

Experiment	k_{eff}	σ_{calc}	σ_{exp}	EALF (eV)	Pitch (cm)	Absorber
HTC-P2-BOR-C19	1.00041	0.00023	0.00247	0.1041	1.7	100
HTC-P2-BOR-C20	0.99279	0.00020	0.00247	0.0892	1.9	220
HTC-P2-BOR-C21	0.99689	0.00026	0.00247	0.0857	1.9	110
HTC-P3-C7	0.99594	0.00018	0.00322	0.1278	1.6	Cd
HTC-P3-C8	1.00361	0.00017	0.00322	0.1381	1.6	Cd
HTC-P3-C9	0.99672	0.00019	0.00322	0.1325	1.6	Cd
HTC-P3-C10	0.99653	0.00021	0.00322	0.1288	1.6	Cd
HTC-P3-C11	0.99619	0.00019	0.00322	0.1364	1.6	Cd
HTC-P3-C12	0.99965	0.00024	0.00254	0.1121	1.6	
HTC-P3-C13	0.99956	0.00028	0.00254	0.1110	1.6	
HTC-P3-C14	0.99990	0.00023	0.00254	0.1111	1.6	
HTC-P3-C15	0.99938	0.00017	0.00254	0.1103	1.6	
HTC-P3-C16	0.99949	0.00027	0.00254	0.1098	1.6	
HTC-P3-C17	0.99991	0.00023	0.00254	0.1079	1.6	
HTC-P3-C18	0.99955	0.00023	0.00254	0.1060	1.6	
HTC-P3-C19	1.00008	0.00022	0.00254	0.1036	1.6	
HTC-P3-C20	0.99967	0.00023	0.00254	0.1016	1.6	
HTC-P3-C21	1.00014	0.00022	0.00254	0.1041	1.6	
HTC-P3-C22	1.00056	0.00023	0.00254	0.1065	1.6	
HTC-P3-C23	0.99996	0.00023	0.00254	0.1141	1.6	
HTC-P3-C24	0.99981	0.00025	0.00254	0.1497	1.6	
HTC-P3-C25	0.99952	0.00023	0.00254	0.1261	1.6	
HTC-P3-C26	0.99922	0.00026	0.00254	0.1148	1.6	
HTC-P4-ST-C14	1.00411	0.00017	0.00616	0.1486	1.6	Cd
HTC-P4-ST-C15	0.99846	0.00020	0.00406	0.1423	1.6	Cd
HTC-P4-ST-C16	0.99788	0.00018	0.00190	0.1358	1.6	Cd
HTC-P4-ST-C17	0.99585	0.00018	0.00190	0.1349	1.6	Cd
HTC-P4-ST-C18	0.99561	0.00019	0.00190	0.1335	1.6	Cd
HTC-P4-ST-C19	0.99517	0.00018	0.00190	0.1324	1.6	Cd
HTC-P4-ST-C20	0.99438	0.00019	0.00190	0.1316	1.6	Cd
HTC-P4-ST-C21	0.99887	0.00018	0.00237	0.1330	1.6	Cd
HTC-P4-ST-C22	1.00070	0.00023	0.00432	0.1724	1.6	
HTC-P4-ST-C23	1.00096	0.00024	0.00432	0.1650	1.6	
HTC-P4-ST-C24	0.99964	0.00024	0.00470	0.1573	1.6	
HTC-P4-ST-C25	0.99960	0.00021	0.00470	0.1557	1.6	
HTC-P4-ST-C26	0.99967	0.00017	0.00470	0.1543	1.6	
HTC-P4-ST-C27	0.99917	0.00024	0.00470	0.1533	1.6	

Experiment	k_{eff}	σ_{calc}	σ_{exp}	EALF (eV)	Pitch (cm)	Absorber
HTC-P4-ST-C28	0.99909	0.00025	0.00470	0.1523	1.6	
HTC-P4-ST-C29	0.99914	0.00023	0.00470	0.1431	1.6	
HTC-P4-ST-C30	0.99993	0.00023	0.00090	0.1335	1.6	
HTC-P4-ST-C31	0.99925	0.00021	0.00090	0.1278	1.6	
HTC-P4-ST-C32	0.99990	0.00028	0.00090	0.1244	1.6	
HTC-P4-ST-C33	0.99961	0.00022	0.00090	0.1224	1.6	

Table A.4.3: Results of Low Enriched MOX Critical Experiments Calculated with SCALE

Case ID	Reference	k_{eff}	sigma	EALF (eV)	Pu wt%	Pu 240 wt%	Am241/U238
093array	OECD-7	1.00201	0.00024	0.189	2	16	6.8162E-05
105al	OECD-7	0.99513	0.00025	0.136	2	16	7.5537E-05
105array	OECD-7	0.99680	0.00026	0.137	2	16	7.5537E-05
105b1	OECD-7	0.99202	0.00027	0.137	2	16	7.5537E-05
105b2	OECD-7	0.99304	0.00023	0.137	2	16	7.5537E-05
105b3	OECD-7	0.99359	0.00024	0.137	2	16	7.5537E-05
105b4	OECD-7	0.99450	0.00024	0.136	2	16	7.5537E-05
1143arra	OECD-7	0.99785	0.00024	0.116	2	16	8.1335E-05
132array	OECD-7	0.99689	0.00022	0.095	2	16	8.1335E-05
1386arra	OECD-7	0.99511	0.00023	0.090	2	16	6.9653E-05
epri70b	OECD-2	0.99893	0.00025	0.712	2	7.8	7.2865E-05
epri70un	OECD-2	0.99719	0.00026	0.536	2	7.8	7.2865E-05
epri87b	OECD-2	1.00160	0.00022	0.269	2	7.8	7.2865E-05
epri87un	OECD-2	0.99862	0.00025	0.184	2	7.8	7.2865E-05
epri99b	OECD-2	1.00083	0.00021	0.176	2	7.8	7.2865E-05
epri99un	OECD-2	1.00140	0.00028	0.133	2	7.8	7.2865E-05
k1mct009	OECD-9	0.99917	0.00026	0.508	1.5	8	1.0582E-05
k2mct009	OECD-9	0.99440	0.00024	0.290	1.5	8	9.7740E-06
k3mct009	OECD-9	0.99460	0.00024	0.151	1.5	8	8.9596E-06
k4mct009	OECD-9	0.99240	0.00024	0.114	1.5	8	8.9596E-06
k5mct009	OECD-9	0.99287	0.00022	0.094	1.5	8	8.9596E-06
k6mct009	OECD-9	0.99375	0.00024	0.090	1.5	8	9.7740E-06
omct61	OECD-6	0.99669	0.00024	0.373	2	8	2.6087E-05
omct62	OECD-6	0.99726	0.00024	0.190	2	8	2.2705E-05
omct63	OECD-6	0.99684	0.00024	0.137	2	8	2.5121E-05
omct64	OECD-6	0.99727	0.00024	0.116	2	8	2.2222E-05

Case ID	Reference	k_{eff}	sigma	EALF (eV)	Pu wt%	Pu 240 wt%	Am241/U238
omct65	OECD-6	0.99868	0.00022	0.095	2	8	2.2705E-05
omct66	OECD-6	0.99708	0.00021	0.090	2	8	2.3671E-05
mct8c1	OECD-8	1.00038	0.00024	0.137	2	24	7.9312E-05
mct8c2	OECD-8	0.99496	0.00027	0.138	2	24	7.2701E-05
mct8c3	OECD-8	0.99457	0.00022	0.137	2	24	8.5864E-05
mct8c4	OECD-8	0.99527	0.00024	0.137	2	24	9.8824E-05
mct8c5	OECD-8	0.99458	0.00023	0.137	2	24	9.5601E-05
mct8c6	OECD-8	0.99833	0.00024	0.372	2	24	7.2701E-05
mct8cal	OECD-8	0.99770	0.00024	0.247	2	24	8.5864E-05
mct8cb1	OECD-8	1.00459	0.00026	0.171	2	24	8.5864E-05
mct8cb3	OECD-8	1.00137	0.00023	0.142	2	24	8.5864E-05
mctcb2	OECD-8	1.00384	0.00026	0.106	2	24	8.5864E-05
mctcb4	OECD-8	1.00345	0.00023	0.092	2	24	8.5864E-05
mixo251k	OECD-5	1.00686	0.00024	0.087	4	18	1.5865E-04
mixo252k	OECD-5	0.99585	0.00025	0.354	4	18	1.5865E-04
mixo253k	OECD-5	0.99984	0.00026	0.187	4	18	1.5865E-04
mixo254k	OECD-5	0.99546	0.00026	0.137	4	18	1.5865E-04
mixo255k	OECD-5	1.00068	0.00024	0.116	4	18	1.5865E-04
mixo256k	OECD-5	1.00039	0.00022	0.095	4	18	1.5865E-04
mixo257k	OECD-5	0.99846	0.00024	0.090	4	18	1.5865E-04
saxtn104o	OECD-3	1.00023	0.00026	0.099	6.6	8.6	8.4292E-05
saxtn56bo	OECD-3	0.99971	0.00028	0.612	6.6	8.6	8.4292E-05
saxtn735o	OECD-3	0.99919	0.00028	0.182	6.6	8.6	8.4292E-05
saxtn792o	OECD-3	1.00015	0.00028	0.150	6.6	8.6	8.4292E-05
saxton52o	OECD-3	1.00000	0.00029	0.848	6.6	8.6	8.4292E-05
saxton56o	OECD-3	1.00067	0.00029	0.517	6.6	8.6	8.4292E-05
tca1	OECD-4	0.99609	0.00026	0.141	3	22	1.0448E-04
tca10	OECD-4	0.99949	0.00024	0.079	3	22	9.3066E-05
tca11	OECD-4	0.99960	0.00025	0.079	3	22	2.0582E-04
tca2	OECD-4	0.99693	0.00023	0.140	3	22	1.9931E-04
tca3	OECD-4	0.99716	0.00025	0.140	3	22	2.9620E-04
tca4	OECD-4	0.99695	0.00027	0.117	3	22	9.8780E-05
tca5	OECD-4	0.99768	0.00025	0.116	3	22	2.0175E-04
tca6	OECD-4	0.99797	0.00026	0.115	3	22	3.9026E-04
tca7	OECD-4	0.99826	0.00024	0.091	3	22	8.8781E-05
tca8	OECD-4	0.99817	0.00023	0.091	3	22	2.0338E-04
tca9	OECD-4	0.99906	0.00023	0.091	3	22	3.0189E-04

A.5. Statistical Analysis of the Data

The statistical treatment used follows the guidance provided in NUREG/CR-6698 [A.2]. The NUREG approach weights the calculated k's by the experimental uncertainty. This approach means the higher quality experiments (i.e.: lower uncertainty) affect the results more than the low quality experiments. The uncertainty weighting is used for the analysis of the set of experiments as a whole, as well as for the analysis for trends.

Spent fuel goes from having little plutonium to having about 1.5 wt% plutonium at discharge burnups. Since the bias is not the same for plutonium critical experiments as it is for uranium critical experiments, the bias would be expected to be a function of burnup. Rather than attempt to make the bias a function of burnup, analysis of the UO2 and MOX critical experiments are separated and the most limiting bias and uncertainty from the two sets will be used in the analysis of the spent fuel pool. The fresh fuel storage uses only the UO2 critical experiments.

The set of MOX experiments is more limited in geometric variation. Because of this, the only trending parameter used for the analysis of the MOX fuel is the spectral index Energy of the Average Lethargy of the neutrons causing Fission, EALF.

A.5.1 Statistical Analysis of the UO2 Critical Experiments

This section follows closely NUREG/CR-6698 so in order to help matching with the NUREG the equation numbers from the NUREG are given in parentheses.

The first step of the analysis is force all the experiments to be critical so the analysis is consistent over the entire set. This is done by converting supercritical experiments to critical experiments using the following equation (9):

$$k_{norm} = k_{calc} / k_{exp}$$

There are 204 critical benchmarks and the simple non-weighted mean k of the 204 samples is 0.9977 with a standard deviation of 0.0016.

NUREG/CR-6698 recommends weighting the data by its uncertainty. The combined error for each experimented is calculated (3):

$$\sigma_t = \sqrt{\sigma_{calc}^2 + \sigma_{exp}^2}$$

The weighted mean keff (6):

$$\bar{k}_{eff} = \frac{\Sigma \frac{1}{\sigma_i^2} k_{eff,i}}{\Sigma \frac{1}{\sigma_i^2}}$$

The bias is calculated as follows (8):

$$Bias = \bar{k}_{eff} - 1; \quad \text{the bias is set to zero if calculated to be greater than zero.}$$

The variance about the mean (4):

$$s^2 = \frac{\frac{1}{n-1}\Sigma\left\{\frac{1}{\sigma_i^2}\left[k_{eff,i} - \bar{k}_{eff}\right]^2\right\}}{\frac{1}{n}\Sigma\frac{1}{\sigma_i^2}}$$

The average total uncertainty (5):

$$\bar{\sigma}^2 = \frac{n}{\Sigma \frac{1}{\sigma_i^2}}$$

The square root of the pooled variance (7):

$$S_p = \sqrt{s^2 + \bar{\sigma}^2}$$

The uncertainty is calculated by multiplying the square root of the pooled variance by the one-sided lower tolerance factor. Since all the analysis has a sample size greater than 50, 2.065 is used as the single-sided lower tolerance factor.

The weighted mean is 0.9973 and the weighted standard deviation is 0.0024. These results show that the weighting has a small effect on the mean, but does increase the standard deviation. This increase in the standard deviation may be dominated by differences in the experimental uncertainty, which ranges from 0.0007 to 0.0032. Further, the average uncertainty of the experiments (interpreted as one sigma) is 0.0021. Since the total one sigma standard

deviation is only 0.0024, this suggests that the experimental uncertainty dominates the uncertainty and there is little to be gained with improved methods. Unless stated otherwise, all the results presented will come from the weighted analysis. The bias of the set as a whole is **0.0027**. The uncertainty is the standard deviation multiplied by the single-sided lower tolerance factor (taken as 2.065 from Table 2.1 of Reference 2), so it is **0.0049**.

As recommended by NUREG/CR-6698, the results of the validation are checked for normality. The National Institute of Standards and Technology (NIST) has made publicly available a statistical package, DATAPLOT [A.9]. The 204 critical experiments were tested with the Wilk-Shapiro normality test and were found not to adhere to a normal distribution. The test results are shown in Table A.5.1. Since the Wilk-Shapiro test does not show normality, a histogram plot of the data given on Figure A.5.1 is made. This plot suggests that a normal distribution assumption may be acceptable. Notice that the calculated k's are a little closer to the mean than expected in a normal distribution. This means assuming a normal distribution may be conservative for this data.

Table A.5.1: Wilk-Shapiro Test Results Output From DATAPLOT [A.9] For 204 UO2 Critical Experiments

WILK-SHAPIRO TEST k

WILK-SHAPIRO TEST FOR NORMALITY

1. STATISTICS:
   NUMBER OF OBSERVATIONS = 204
   LOCATION PARAMETER = 0.9976809
   SCALE PARAMETER = 0.1579199E-02

   WILK-SHAPIRO TEST STATISTIC VALUE = 0.9812083

2. CRITICAL VALUES:
   P-VALUE = 0.7890631E-02

3. CONCLUSIONS:
   AT THE 90% LEVEL, WE REJECT THE NORMALITY ASSUMPTION.
   AT THE 95% LEVEL, WE REJECT THE NORMALITY ASSUMPTION.
   AT THE 97.5% LEVEL, WE REJECT THE NORMALITY ASSUMPTION.
   AT THE 99% LEVEL, WE REJECT THE NORMALITY ASSUMPTION.

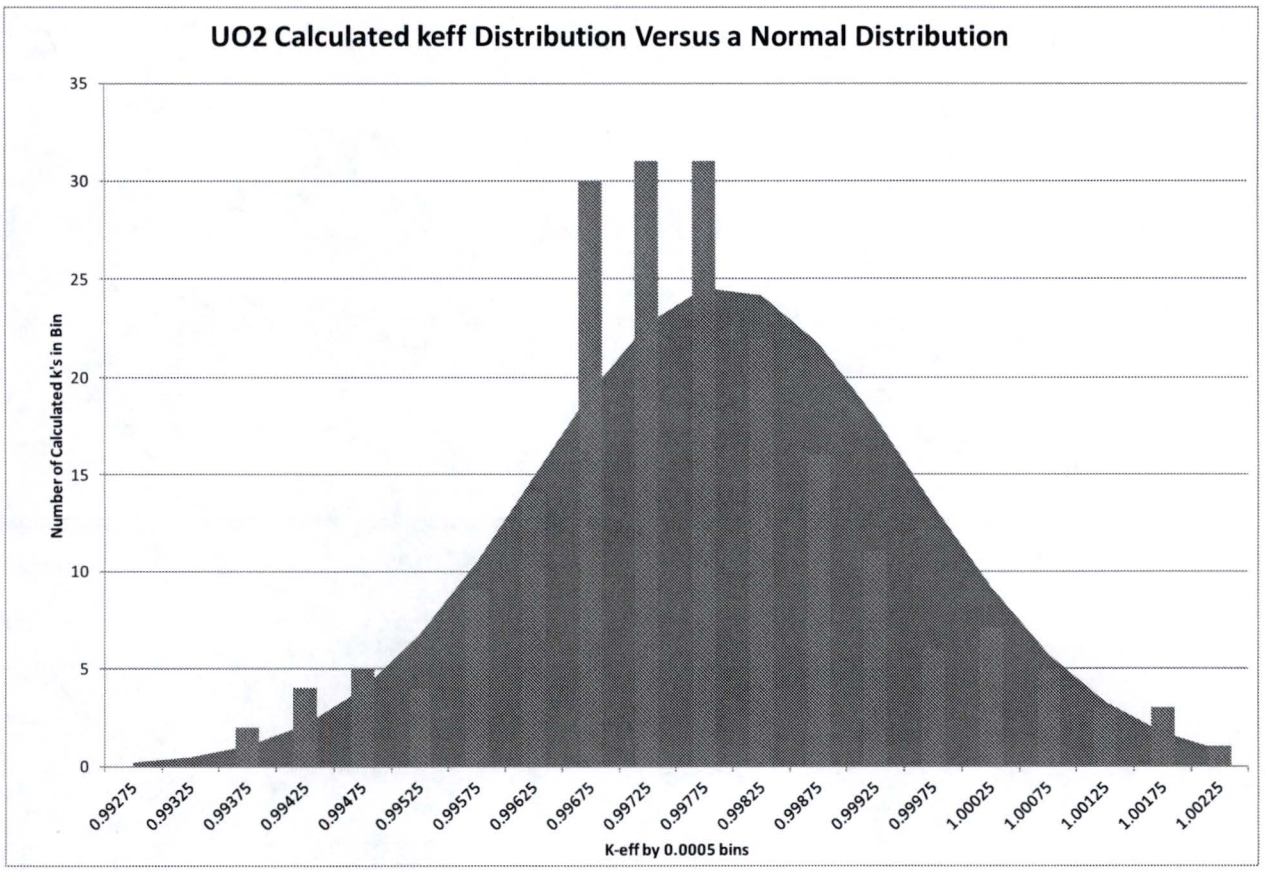

Figure A.5.1: Distribution of the Calculated k's Around the Mean for All the UO2 Benchmarks

Numerous sources [A.10, A.11, A.12] suggest that for the large sample size used here, normality testing is not important. For example, in the textbook, Statistics for Social Science by R. Mark Sirkin [A.12], it states:

> *"Law of large numbers. A law that states that if the size of the sample, n, is sufficiently large (no less than 30; preferably no less than 50), then the central limit theory will apply even if the population is not normally distributed along variable x …*
> *If: Then:*
> *n>= 100 It is always safe to relax the normality assumption*
> *50<=n<100 It is almost always safe*
> *30<=n<50 It is probably safe."*

The analysis in this validation assumes that the techniques used here are sufficiently robust for the limited normality data. However, a non-parametric check has been performed. The 204 cases were ranked by increasing k. 95% of the cases are above the 10th case. The k of the 10th case is 0.9950. Since the average of the experiments is 0.9977, a standard deviation of

(.9977-.9950)/1.96 = 0.0014 can be inferred. This inferred standard deviation is less than the standard deviation of 0.0024 (or the unweighted value of 0.0016) predicted assuming a normal distribution. Again, this is expected from a visual inspection of Figure A.5.1, since the predicted distribution shows a larger number of data points in the center compared to a normal distribution. In conclusion, although the data does not meet the normality tests, it will be treated as normally distributed, yielding a conservative bias uncertainty.

The next step in the analysis is to look for trends in the data. In the past it was assumed that unless there is a high confidence level (95%) that the slope was non-zero, the analysis would assume a zero slope (no trend) on the given parameter. Since the analysis will include consideration of the data as non-trended, it is more conservative to assume there is also a trend. Inverting the statistical test to requiring a high confidence that the slope is zero will result in all cases having a trend. At this time, although a test on the confidence of the trend is performed, the analysis assumes all calculated trends are real.

Before presenting the results of the analysis the following provides the equations used for the analysis. For these equations parameter y is for the dependent variable (k_{eff}), and parameter x is for the independent variables (e.g., enrichment, EALF).

First, the linear equation for the fit(10):

$$Y(x) = a + bx$$

The coefficients are calculated using the next three equations (11, 12, 13):

$$a = \frac{1}{\Delta}\left[\sum\frac{x_i^2}{\sigma_i^2}\sum\frac{y_i^2}{\sigma_i^2} - \sum\frac{x_i}{\sigma_i^2}\sum\frac{x_i y_i}{\sigma_i^2}\right]$$

$$b = \frac{1}{\Delta}\left[\sum\frac{1}{\sigma_i^2}\sum\frac{x_i y_i}{\sigma_i^2} - \sum\frac{x_i}{\sigma_i^2}\sum\frac{y_i}{\sigma_i^2}\right]$$

$$\Delta = \sum\frac{1}{\sigma_i^2}\sum\frac{x_i^2}{\sigma_i^2} - \left[\sum\frac{x_i}{\sigma_i^2}\right]^2$$

The weighted mean for the independent parameter (15):

$$\bar{x} = \frac{\sum \frac{1}{\sigma_i^2} x_i}{\sum \frac{1}{\sigma_i^2}}$$

The bias is calculated as follows (23):

$Bias = k_{fit}(x) - 1$; the bias is set to zero if calculated to be greater than zero.

Finally, the uncertainty is computed from (23):

$$S_{Pfit}\left\{\sqrt{2F_a^{(2,n-2)}\left[\frac{1}{n} + \frac{(x-\bar{x})^2}{\sum(x_i-\bar{x})^2}\right]} + z_{2P-1}\sqrt{\frac{(n-2)}{\chi^2_{1-\gamma,n-2}}}\right\}$$

where p = desired confidence (0.95) and the remaining parameters are computed as follows (25, 30, 28):

$$\gamma = \frac{1-p}{2}$$

$$s_{fit}^2 = \frac{\frac{1}{n-2}\sum\left\{\frac{1}{\sigma_i^2}\left[k_{eff,i} - k_{fit}(x_i)\right]^2\right\}}{\frac{1}{n}\sum\frac{1}{\sigma_i^2}}$$

$$S_{Pfit} = \sqrt{s_{fit}^2 + \bar{\sigma}^2}$$

The width of the tolerance band is a function of the trending parameter. When the value for the independent variable is known, it is used in the calculation of the uncertainty. For simplicity sometimes the maximum width of the tolerance band is for the range of data and is taken as the uncertainty.

In the final analysis, the calculated k of the system must be less than the minimum of k(x) minus the uncertainty minus the administrative safety margin. The uncertainty in k from other independent uncertainties, such as the manufacturing tolerances, burnup, and depletion uncertainties can be statistically combined with the uncertainty in the criticality validation. Now

this section will evaluate the trends in k as a function of trending parameters using the methods described above.

Neutron spectrum

Trends in the calculated k of the benchmarks were sought as a function of the neutron spectrum. Since a large number of things can affect the spectrum, a single index calculated by SCALE is used. This index is the Energy (eV) of the Average Lethargy causing Fission (EALF). Figure A.5.2 shows the distribution of k's around the mean k, which is shown as the red line. Visual inspection of the graph and the statistical analysis of the results of the statistical analysis suggest that there is a statistically significant trend on neutron spectrum. Using NUREG/CR-6698 [A.2] equations from above and the data from Table A.4.1, the predicted mean k as a function of EALF is:

k(EALF) = 0.99844 - 0.00488 * EALF

The units for EALF are eV. The uncertainty (in terms of k) about the trend is 0.0046 for EALF's less than 0.4 ev and 0.0055 for EALF's between 0.4 and 0.8 eV.

Geometry Tests

Two trend tests were performed to determine if lattice/geometric parameters are adequately treated by SCALE 6.0. The first parameter is the fuel pin diameter. A small, statistically significant trend was found when the critical experiment analysis results were correlated to the fuel pin diameter. The second lattice parameter tested is the lattice pitch. A statistically significant trend on lattice pitch was found. The trend on pitch or pin diameter could be caused by the spectral trend found in the previous subsection.

Using NUREG/CR-6698 [A.2] equations from above and the data from Table A.4.1, the predicted mean k as a function of pin diameter is:

k(Pin Diameter) = 0.99419 + (2.78E-03)*Pin Diameter

where the pin diameter is in cm. The predicted mean k as a function of pitch is:

$$\mathbf{k(Pitch) = 0.99421 + (1.87E\text{-}03)*Pitch}$$

where lattice pitch is in cm.

The maximum tolerance band widths, using the second term of NUREG/CR-6698 [2] equation 23, are 4.9E-03 and 4.9E-03 for the pin diameter and pitch, respectively. Figures A.5.3 and A.5.4 graphically present k_{eff} as a function of the pin diameter and the lattice pitch.

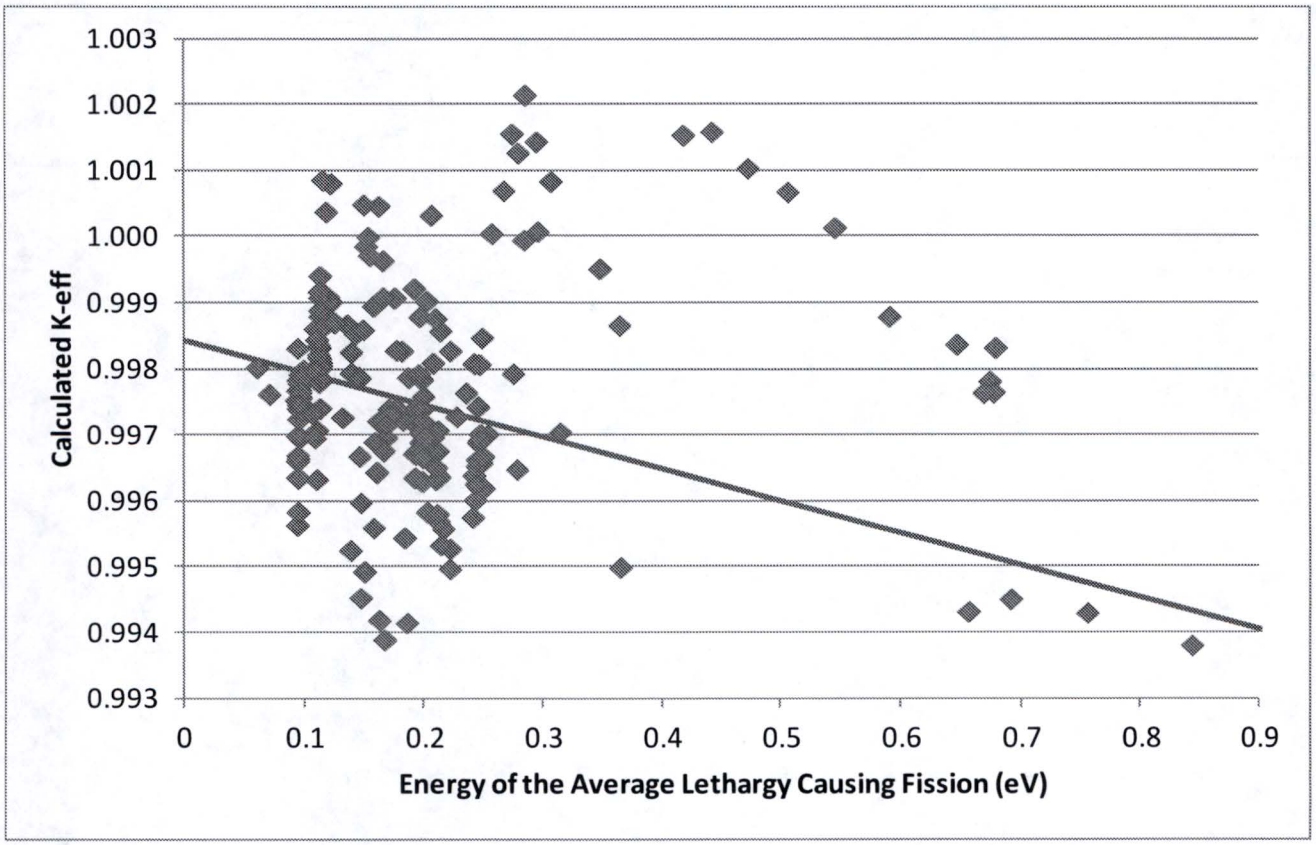

Figure A.5.2: Calculated k for the UO2 Critical Benchmarks as a Function of EALF

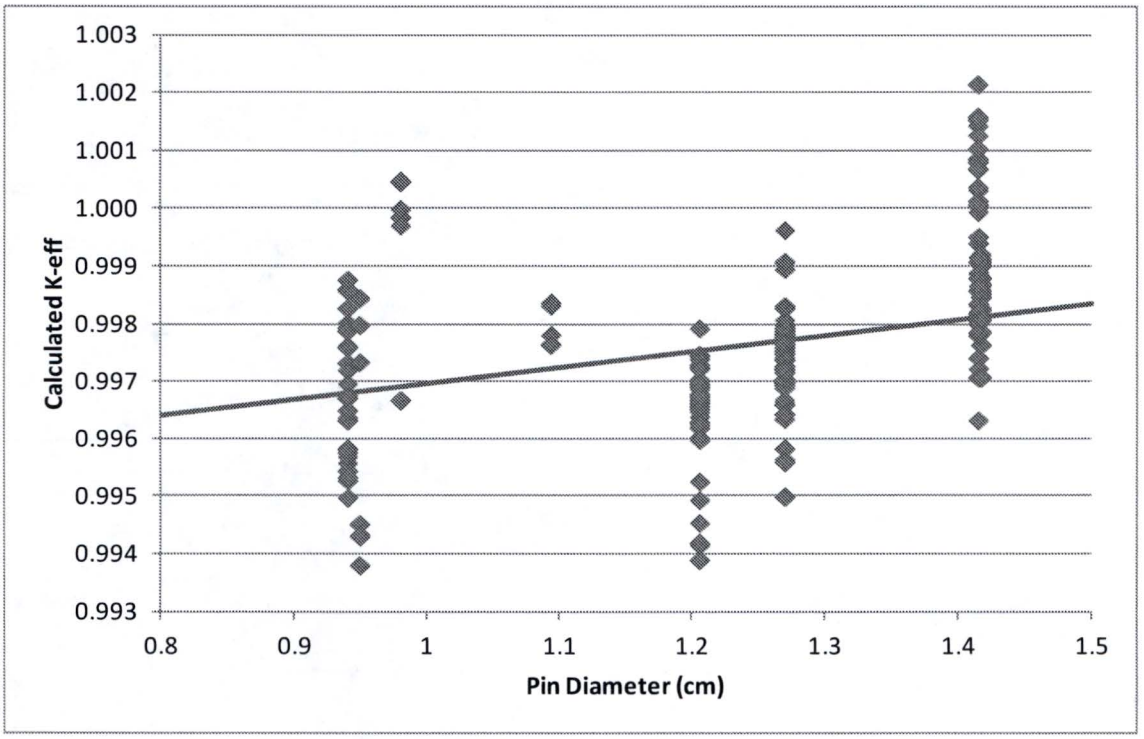

Figure A.5.3: Calculated k for the UO2 Critical Benchmarks as a Function of Pin Diameter

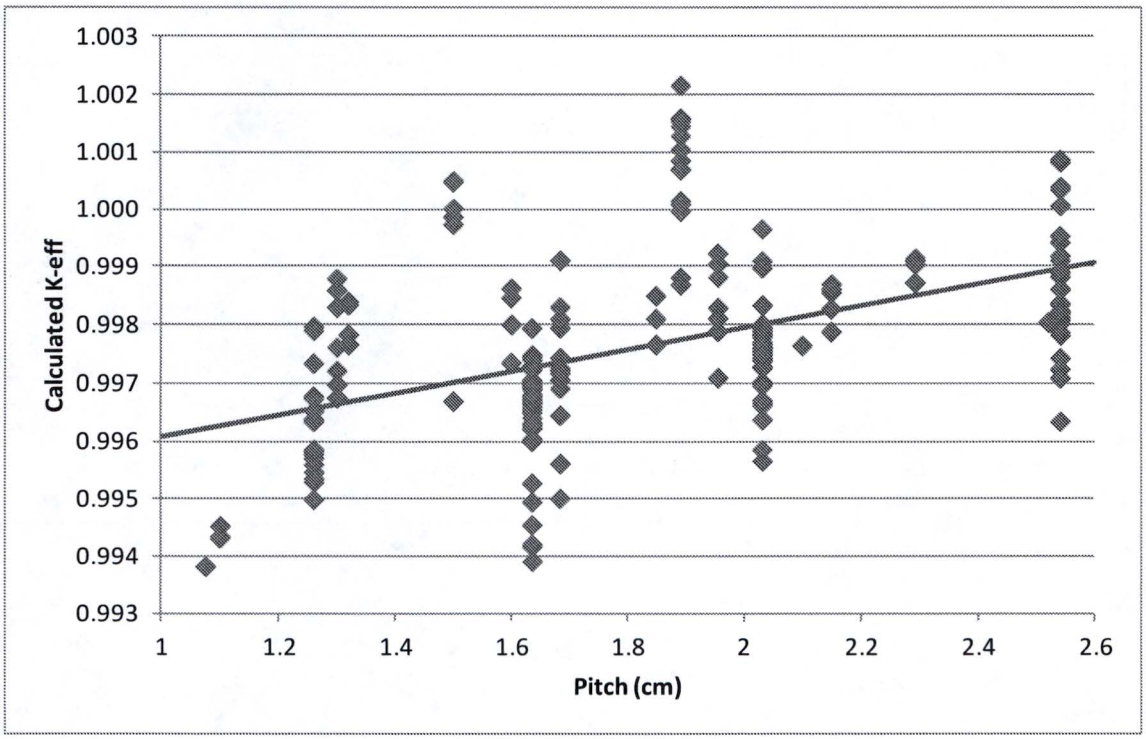

Figure A.5.4: Calculated k for the UO2 Critical Benchmarks as a Function of Fuel Pin Pitch

Enrichment

The fuel to be stored in the racks ranges in enrichment from 1.6 wt% ^{235}U to 5 wt% ^{235}U. It was determined that there is not a statistically significant trend on enrichment. However, to be conservative, both the zero slope and the calculated fit are used for determining the limiting k as a function of enrichment. Using NUREG/CR-6698 [A.2] equations from above and the data from Table A.4.1, the trend in the mean k is:

k(Enrichment) = 0.99705 + (6.96E-05)*Enrichment

where Enrichment is wt% ^{235}U.

The maximum tolerance band width is 5.00E-03. Figure A.5.5 graphically presents the results.

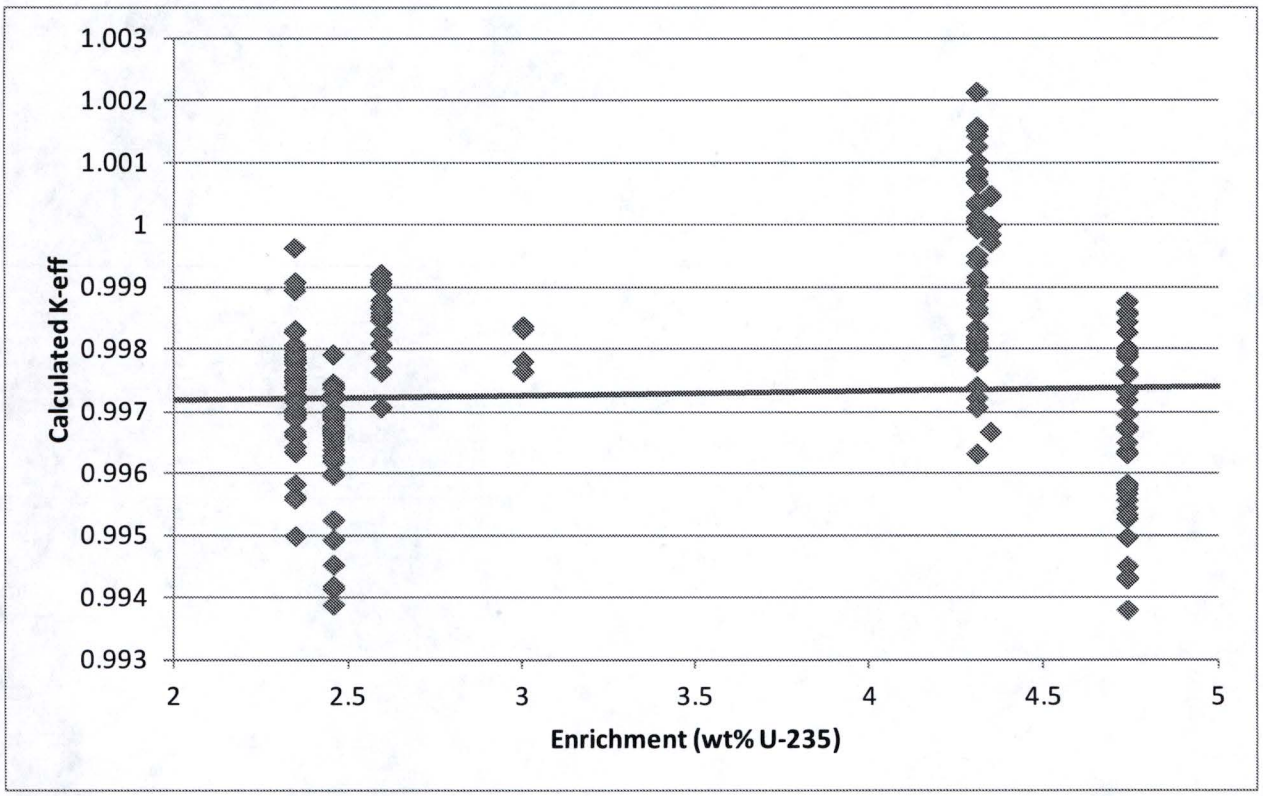

Figure A.5.5: Calculated k for the UO2 Critical Benchmarks as a Function of Enrichment

Soluble Boron Content

A fit of the calculated k's as a function of the soluble boron ppm was performed using the data from Table A.4.1 and Table A.5.2. The trend on soluble boron concentration is not statistically significance test compared to a zero slope. However, to be conservative, both the zero slope and the calculated fit are used for determining the limiting k as a function of soluble boron content.

The following equation is the best fit of the data for k versus soluble boron. Figure A.5.6 shows the results of the analysis. The uncertainty around the mean value given in the following equation is 0.0050.

k(ppm soluble boron) = 0.99727 + (1.038E-07)*ppm

Table A.5.2: UO2 Critical Experiment With Soluble Boron Results with SCALE 6.0 and ENDF/B-VII

Benchmark ID	Case No.	Soluble Boron ppm	Measurement Uncertainty (delta k)	k_{eff}
LCT-8	1	1511	0.0012	0.9965
	2	1334	0.0012	0.9969
	3	1337	0.0012	0.9974
	4	1183	0.0012	0.9969
	5	1181	0.0012	0.9962
	6	1034	0.0012	0.9966
	7	1031	0.0012	0.9965
	8	794	0.0012	0.9960
	9	779	0.0012	0.9964
	10	1245	0.0012	0.9966
	11	1384	0.0012	0.9970
	12	1348	0.0012	0.9970
	13	1348	0.0012	0.9969
	14	1363	0.0012	0.9967
	15	1362	0.0012	0.9962
	16	1158	0.0012	0.9973
	17	921	0.0012	0.9963
LCT-11	2	1037	0.0032	0.9963
	3	769	0.0032	0.9967
	4	764	0.0032	0.9974
	5	762	0.0032	0.9967
	6	753	0.0032	0.9968
	7	739	0.0032	0.9975
	8	721	0.0032	0.9968
	9	702	0.0032	0.9969
LCT-35	1	70	0.0018	0.9981
	2	147.7	0.0019	0.9971
LCT-50	3	822	0.0010	0.9970
	4	822	0.0010	0.9967
	5	5030	0.0010	0.9983
	6	5030	0.0010	0.9986
	7	5030	0.0010	0.9988
LCT-51	1 C10	143	0.0020	0.9960
	2 c11a	510	0.0024	0.9979
	3 c11b	514	0.0024	0.9973
	4 c11c	501	0.0024	0.9970
	5 c11d	493	0.0024	0.9974
	6 c11e	474	0.0024	0.9967
	7 c11f	462	0.0024	0.9972
	8 c11g	432	0.0024	0.9970
	9 c12	217	0.0019	0.9968

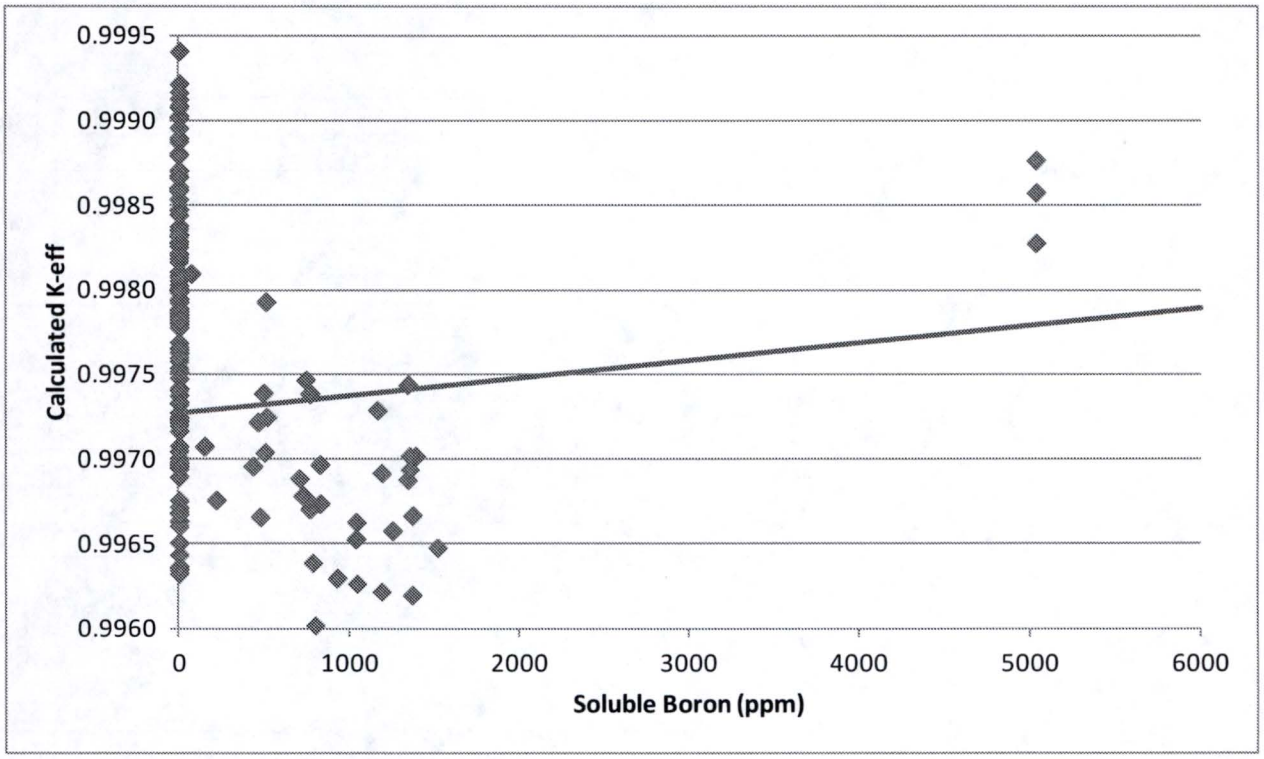

Figure A.5.6: Calculated k for the UO2 Critical Benchmarks as a Function of Soluble Boron

Establishing the Bias and the Uncertainty

To make the incorporation of the bias and bias uncertainty in the criticality analysis conservative, the most limiting bias and bias uncertainty from the trends in the range of interest is used. The lattice pitch for Westinghouse 17x17 fuel is 1.26 cm. The bias from the pitch trend is **0.0035**. The pin diameter is 0.95 cm where the bias as a function of pin diameter is 0.0032. The maximum bias from the enrichment trend is only 0.0028. The maximum bias as a function of soluble boron content is only 0.0027. There is a fairly strong trend with EALF. The bias increases with harder spectrum. The criticality analysis under normal operating conditions has an EALF of less than 0.4 eV. At 0.4 eV the bias is **0.0035**. For accident conditions the EALF may increase to 0.8 eV. For those conditions the bias is increased to a rounded 0.006. In conclusion the maximum bias for normal operating conditions is 0.0035 and for accident conditions 0.0060. For the optimum moderation of the new fuel storage area the EALF can be

as high as 1.1 eV. The calculated bias for this would be 0.0069. Due to some extrapolation this is rounded up to 0.007 for EALF of 1.1 eV.

The maximum uncertainty is also used but for this analysis if the bias is less than 0.0035, it is appropriate to subtract the differences in biases from the calculated uncertainties. The uncertainty in the EALF trend increases with spectral hardening so the uncertainty from 0.4 eV is appropriate for normal operations. Although it would be possible to use an uncertainty as a function of the EALF, the maximum uncertainty from 0.4 eV is 0.0046. The uncertainty at the 17x17 fuel pin pitch is also 0.0046. The uncertainty from the fuel pin diameter at the 17x17 fuel pin diameter is 0.0048. The uncertainty in the bias as a function of enrichment (not statistically significant trend) has a maximum of **0.0050**. For the uncertainty as a function of soluble boron (not statistically significant) , the uncertainty at 2000 ppm is 0.00505 but again the bias is less than 0.0030 so the net uncertainty is less than 0.0046. For the non-trended analysis the bias is 0.0027 and the uncertainty is 0.0049. Again the **limiting uncertainty is 0.0050**. Accident cases in the spent fuel pool may have a higher EALF. For a 0.8 eV EALF the uncertainty is 0.0054 but is rounded up to 0.0060. For the optimum moderation case of the new fuel storage area the EALF can be as high as 1.1. For that case an extrapolated uncertainty is 0.0063.

No Cadmium and Boron Subset

Since the new fuel storage area does not credit control rods or soluble boron, the statistical analysis was repeated where all the critical experiments with Cd or boron are eliminated. This reduces the set of critical experiments to 139 experiments. Table A.5.3 is a restatement of Table A.4.1 but with the excluded cases removed.

These 139 critical experiments passed the normality test. The analysis of this subset shows the trends to be about the same as shown previously. Further the bias and uncertainty selected for the whole UO2 set is about the same as for this limited set and bounds this set. **For the optimum moderation analysis the bias and uncertainty are 0.0070 and 0.0063 respectively.**

Table A.5.3: UO2 Critical Experiment With No Cd or B Results with SCALE 6.0 and ENDF/B-VII

Benchmark ID	Case No.	Enrichment (wt% U-235)	Fuel Pin Diameter (cm)	Fuel Pin Pitch (cm)	EALF (eV)	Measurement Uncertainty (delta k)	k_{eff}
LCT-1	1	2.350	1.270	2.032	0.0960	0.003	0.9979
	2	2.350	1.270	2.032	0.0955	0.003	0.9978
	3	2.350	1.270	2.032	0.0945	0.003	0.9970
	4	2.350	1.270	2.032	0.0952	0.003	0.9974
	5	2.350	1.270	2.032	0.0939	0.003	0.9956
	6	2.350	1.270	2.032	0.0947	0.0027	0.9978
	7	2.350	1.270	2.032	0.0931	0.0031	0.9975
	8	2.350	1.270	2.032	0.0941	0.003	0.9964
LCT-2	1	4.310	1.415	2.540	0.1129	0.002	0.9974
	2	4.310	1.415	2.540	0.1128	0.002	0.9994
	3	4.310	1.415	2.540	0.1128	0.002	0.9982
	4	4.310	1.415	2.540	0.1117	0.0018	0.9978
	5	4.310	1.415	2.540	0.1101	0.0019	0.9963
LCT-6	1	2.596	1.417	1.849	0.2351	0.002	0.9977
	2	2.596	1.417	1.849	0.2420	0.002	0.9981
	3	2.596	1.417	1.849	0.2484	0.002	0.9985
	4	2.596	1.417	1.956	0.1812	0.002	0.9983
	5	2.596	1.417	1.956	0.1866	0.002	0.9979
	6	2.596	1.417	1.956	0.1913	0.002	0.9992
	7	2.596	1.417	1.956	0.1963	0.002	0.9988
	8	2.596	1.417	1.956	0.2018	0.002	0.9990
	9	2.596	1.417	2.150	0.1352	0.002	0.9987
	10	2.596	1.417	2.150	0.1388	0.002	0.9983
	11	2.596	1.417	2.150	0.1421	0.002	0.9985
	12	2.596	1.417	2.150	0.1456	0.002	0.9979
	13	2.596	1.417	2.150	0.1486	0.002	0.9986
	14	2.596	1.417	2.293	0.1142	0.002	0.9991
	15	2.596	1.417	2.293	0.1171	0.002	0.9991
	16	2.596	1.417	2.293	0.1196	0.002	0.9991
	17	2.596	1.417	2.293	0.1223	0.002	0.9990
	18	2.596	1.417	2.293	0.1249	0.002	0.9987
LCT-7	1	4.738	0.940	1.260	0.2406	0.0014	0.9965
	2	4.738	0.940	1.600	0.1089	0.0008	0.9986
	3	4.738	0.940	2.100	0.0707	0.0007	0.9976
	4	4.738	0.940	2.520	0.0605	0.0008	0.9983
LCT-9	1	4.310	1.415	2.540	0.1126	0.0021	0.9983
	2	4.310	1.415	2.540	0.1119	0.0021	0.9978
	3	4.310	1.415	2.540	0.1123	0.0021	0.9980
	4	4.310	1.415	2.540	0.1121	0.0021	0.9982

Benchmark ID	Case No.	Enrichment (wt% U-235)	Fuel Pin Diameter (cm)	Fuel Pin Pitch (cm)	EALF (eV)	Measurement Uncertainty (delta k)	k_{eff}
	24	4.310	1.415	2.540	0.1120	0.0021	0.9982
	25	4.310	1.415	2.540	0.1118	0.0021	0.9984
	26	4.310	1.415	2.540	0.1119	0.0021	0.9986
	27	4.310	1.415	2.540	0.1117	0.0021	0.9982
LCT-10	5	4.310	1.415	2.540	0.3478	0.0021	0.9995
	6	4.310	1.415	2.540	0.2567	0.0021	1.0001
	7	4.310	1.415	2.540	0.2058	0.0021	1.0003
	8	4.310	1.415	2.540	0.1819	0.0021	0.9972
	9	4.310	1.415	2.540	0.1219	0.0021	1.0008
	10	4.310	1.415	2.540	0.1179	0.0021	1.0004
	11	4.310	1.415	2.540	0.1152	0.0021	1.0009
	12	4.310	1.415	2.540	0.1121	0.0021	0.9992
	13	4.310	1.415	2.540	0.1104	0.0021	0.9971
	14	4.310	1.415	1.892	0.3064	0.0028	1.0008
	15	4.310	1.415	1.892	0.2941	0.0028	1.0014
	16	4.310	1.415	1.892	0.2845	0.0028	1.0022
	17	4.310	1.415	1.892	0.2786	0.0028	1.0013
	18	4.310	1.415	1.892	0.2736	0.0028	1.0016
	19	4.310	1.415	1.892	0.2668	0.0028	1.0007
	24	4.310	1.415	1.892	0.5905	0.0028	0.9988
	25	4.310	1.415	1.892	0.5448	0.0028	1.0001
	26	4.310	1.415	1.892	0.5056	0.0028	1.0007
	27	4.310	1.415	1.892	0.4722	0.0028	1.0010
	28	4.310	1.415	1.892	0.4419	0.0028	1.0016
	29	4.310	1.415	1.892	0.4177	0.0028	1.0015
	30	4.310	1.415	1.892	0.3642	0.0028	0.9987
LCT-11	1	2.459	1.206	1.636	0.1677	0.0018	0.9970
	15	2.459	1.206	1.636	0.1382	0.0018	0.9953
LCT-13	1	4.310	1.415	1.892	0.2836	0.0018	1.0000
LCT-16	1	2.350	1.270	2.032	0.0951	0.0031	0.9973
	2	2.350	1.270	2.032	0.0948	0.0031	0.9958
	3	2.350	1.270	2.032	0.0947	0.0031	0.9974
	4	2.350	1.270	2.032	0.0949	0.0031	0.9964
	5	2.350	1.270	2.032	0.0945	0.0031	0.9966
	6	2.350	1.270	2.032	0.0955	0.0031	0.9970
	7	2.350	1.270	2.032	0.0953	0.0031	0.9970
	28	2.350	1.270	2.032	0.0943	0.0031	0.9977
	29	2.350	1.270	2.032	0.0942	0.0031	0.9966
	30	2.350	1.270	2.032	0.0943	0.0031	0.9967
	31	2.350	1.270	2.032	0.0943	0.0031	0.9978
	32	2.350	1.270	2.032	0.0942	0.0031	0.9970

Benchmark ID	Case No.	Enrichment (wt% U-235)	Fuel Pin Diameter (cm)	Fuel Pin Pitch (cm)	EALF (eV)	Measurement Uncertainty (delta k)	k_{eff}
LCT-17	4	2.350	1.270	2.032	0.1979	0.0031	0.9979
	5	2.350	1.270	2.032	0.1749	0.0031	0.9991
	6	2.350	1.270	2.032	0.1652	0.0031	0.9996
	7	2.350	1.270	2.032	0.1575	0.0031	0.9990
	8	2.350	1.270	2.032	0.1316	0.0031	0.9973
	9	2.350	1.270	2.032	0.1084	0.0031	0.9970
	10	2.350	1.270	2.032	0.0993	0.0031	0.9980
	11	2.350	1.270	2.032	0.0975	0.0031	0.9979
	12	2.350	1.270	2.032	0.0963	0.0031	0.9977
	13	2.350	1.270	2.032	0.0950	0.0031	0.9975
	14	2.350	1.270	2.032	0.0942	0.0031	0.9983
	15	2.350	1.270	1.684	0.1763	0.0028	0.9974
	16	2.350	1.270	1.684	0.1705	0.0028	0.9974
	17	2.350	1.270	1.684	0.1656	0.0028	0.9991
	18	2.350	1.270	1.684	0.1640	0.0028	0.9972
	19	2.350	1.270	1.684	0.1615	0.0028	0.9972
	20	2.350	1.270	1.684	0.1600	0.0028	0.9964
	21	2.350	1.270	1.684	0.1587	0.0028	0.9969
	22	2.350	1.270	1.684	0.1575	0.0028	0.9956
	26	2.350	1.270	1.684	0.3652	0.0028	0.9950
	27	2.350	1.270	1.684	0.3144	0.0028	0.9971
	28	2.350	1.270	1.684	0.2748	0.0028	0.9979
	29	2.350	1.270	1.684	0.2463	0.0028	0.9981
LCT-39	1	4.738	0.940	1.260	0.2216	0.0014	0.9953
	2	4.738	0.940	1.260	0.2112	0.0014	0.9968
	3	4.738	0.940	1.260	0.1920	0.0014	0.9964
	4	4.738	0.940	1.260	0.1834	0.0014	0.9955
	5	4.738	0.940	1.260	0.1391	0.0009	0.9980
	6	4.738	0.940	1.260	0.1452	0.0009	0.9979
	7	4.738	0.940	1.260	0.2124	0.0012	0.9964
	8	4.738	0.940	1.260	0.2026	0.0012	0.9958
	9	4.738	0.940	1.260	0.1970	0.0012	0.9967
	10	4.738	0.940	1.260	0.1727	0.0012	0.9973
	11	4.738	0.940	1.260	0.2214	0.0013	0.9950
	12	4.738	0.940	1.260	0.2159	0.0013	0.9956
	13	4.738	0.940	1.260	0.2140	0.0013	0.9953
	14	4.738	0.940	1.260	0.2120	0.0013	0.9957
	15	4.738	0.940	1.260	0.2109	0.0013	0.9958
	16	4.738	0.940	1.260	0.2099	0.0013	0.9963
	17	4.738	0.940	1.260	0.2096	0.0013	0.9965
LCT-42	1	2.350	1.270	1.684	0.1680	0.0016	0.9972

Benchmark ID	Case No.	Enrichment (wt% U-235)	Fuel Pin Diameter (cm)	Fuel Pin Pitch (cm)	EALF (eV)	Measurement Uncertainty (delta k)	k_{eff}
LCT-48	1	3.005	1.094	1.320	0.6740	0.0025	0.9978
	2	3.005	1.094	1.320	0.6467	0.0025	0.9984
	3	3.005	1.094	1.320	0.6771	0.0025	0.9977
	4	3.005	1.094	1.320	0.6788	0.0025	0.9983
	5	3.005	1.094	1.320	0.6691	0.0025	0.9977
LCT-50	1	4.738	0.940	1.300	0.1992	0.0010	0.9976
	2	4.738	0.940	1.300	0.1906	0.0010	0.9972
LCT-71	1	4.738	0.949	1.100	0.7553	0.00076	0.9943
	2	4.738	0.949	1.100	0.6915	0.00076	0.9945
	3	4.738	0.949	1.100	0.6563	0.00076	0.9943
	4	4.738	0.949	1.075	0.8432	0.0008	0.9938
LCT-72	1	4.738	0.949	1.600	0.1101	0.0012	0.9985
	2	4.738	0.949	1.600	0.1062	0.0012	0.9973
	3	4.738	0.949	1.600	0.1083	0.0012	0.9980
LCT-83	1	4.349	0.980	1.500	0.1512	0.0010	0.9999
LCT-84	1	4.349	0.980	1.500	0.1541	0.0010	0.9997
LCT-89	1	4.349	0.980	1.500	0.1529	0.0010	1.0000
LCT-90	1	4.349	0.980	1.500	0.1458	0.0010	0.9937

A.5.2 Statistical Analysis of MOX Critical Experiments

Tables A.4.2 and A.4.3 provides the raw results of the analysis of the MOX critical experiments. From the calculated k's provided in Tables A.4.1, A.4.2 and A.4.3 there is a clear trend on the plutonium content. Figure A.5.7 shows this trend.

Since there is a strong trend on plutonium content the critical experiments with plutonium content out of the range of spent fuel have been eliminated. Only the critical experiments with 2 wt% plutonium or less are included in the trending analysis for MOX critical experiments. This new set of MOX experiments consists of 117 critical experiments. The set does not have a normal distribution. Figure A.5.8 shows the histogram for the 117 calculated ks.

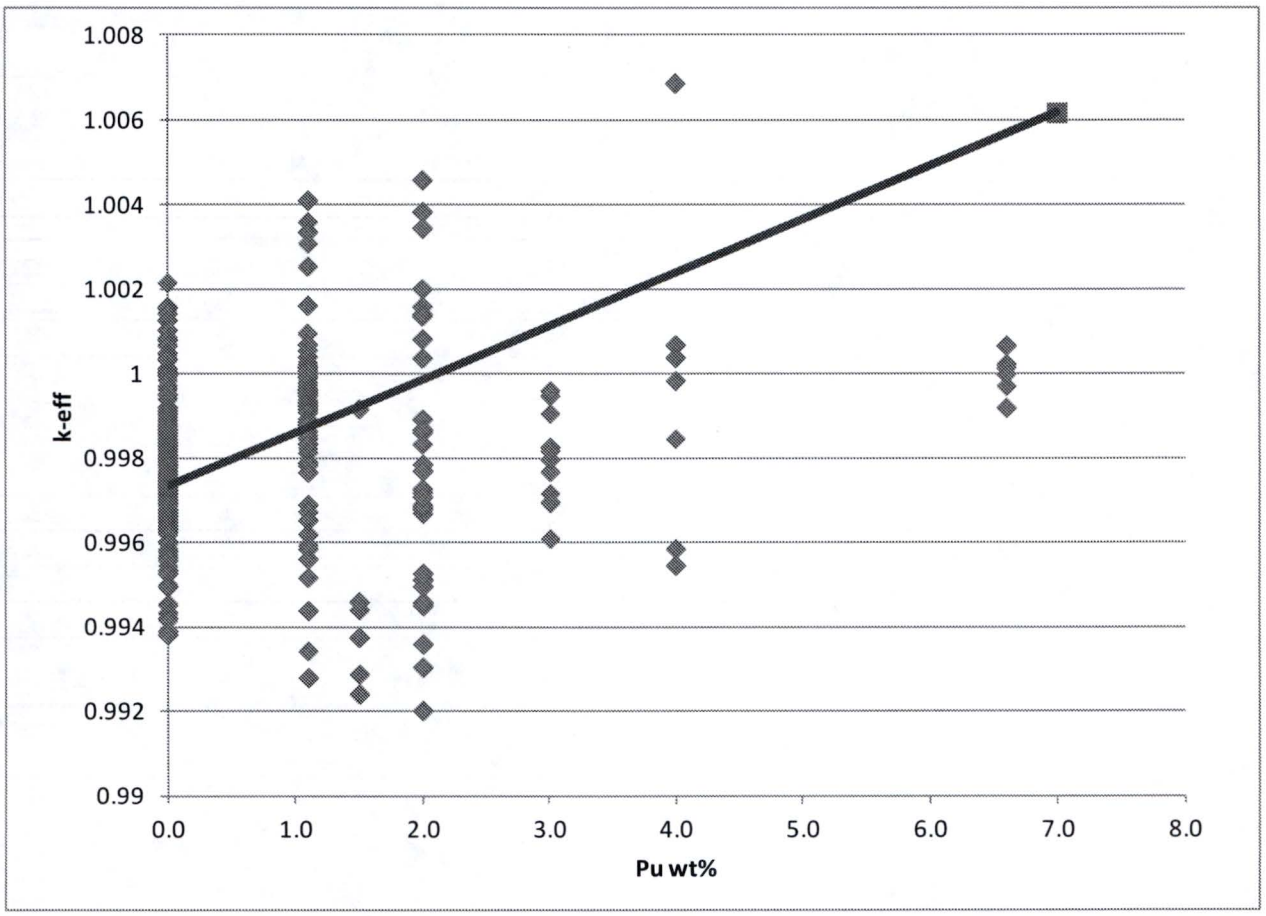

Figure A.5.7: Calculated k for the Critical Benchmarks as a Function of Plutonium Content

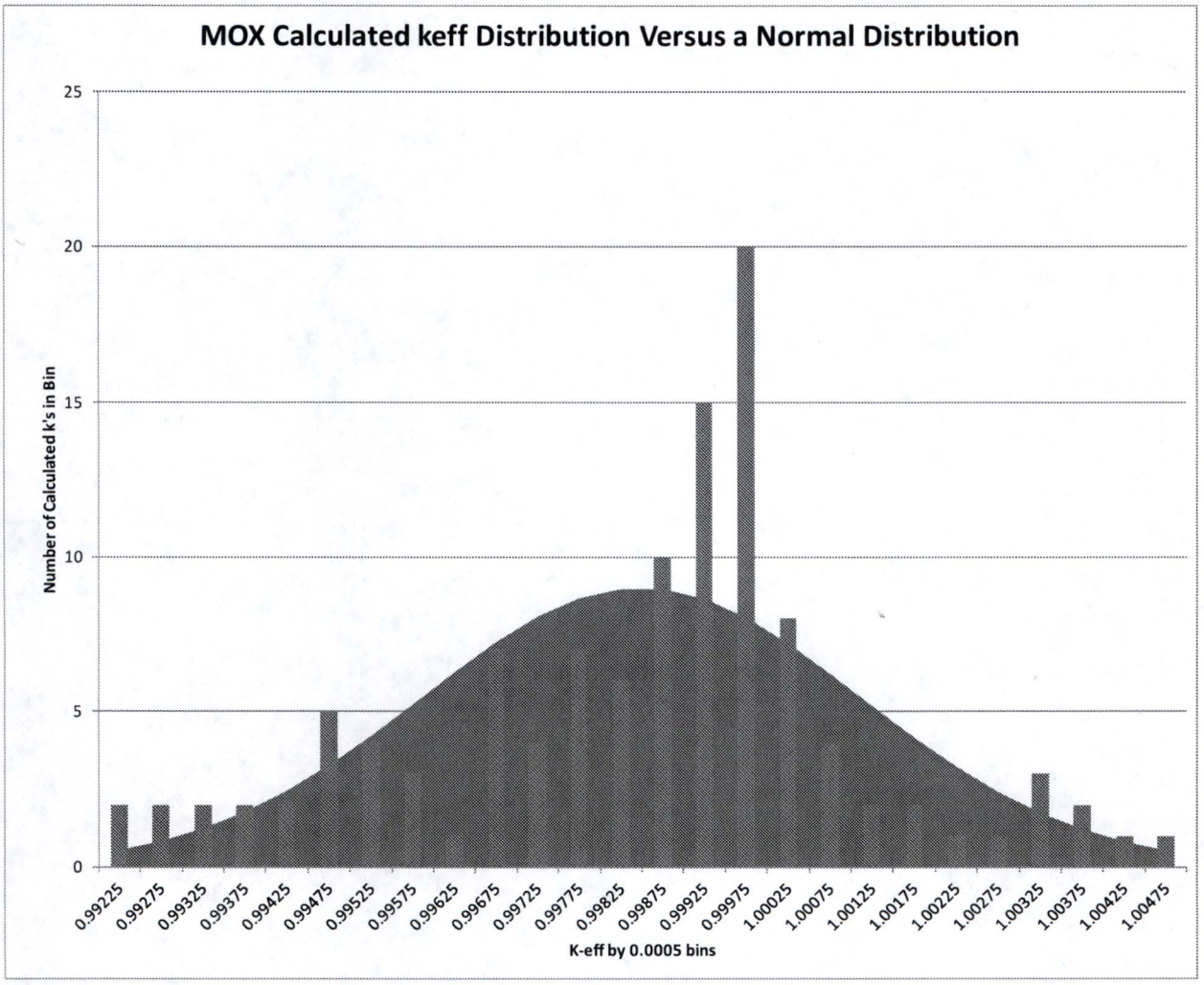

Figure A.5.8: Distribution of Calculated ks for the MOX Critical Benchmarks

The calculated ks have been ordered and the 5th lowest calculated k is 0.99304. The mean k of this set is 0.99849. 95% of the ks are above the mean k minus 0.006. Even though the set is not normal the rest of the analysis will be performed as though it is normal and it is found that the uncertainty is greater than 0.006.

As with the UO2 set the MOX set has a trend with EALF. That trend is:

$$k(EALF) = 0.999497 - 0.00364 * EALF$$

This is graphically presented as Figure A.5.9. **At EALF of 0.4 eV the bias is 0.0020 and the uncertainty is 0.0089**. At lower EALF both the bias and uncertainty decrease. For accident conditions the in the EALF range of 0.4 to 0.8 eV the bias is 0.0034 and the uncertainty is 0.0135. Note that the range of EALF in the MOX criticals is from 0.07 to 0.71 eV so some extrapolation of the data was needed to get the bias and uncertainty at 0.8 eV.

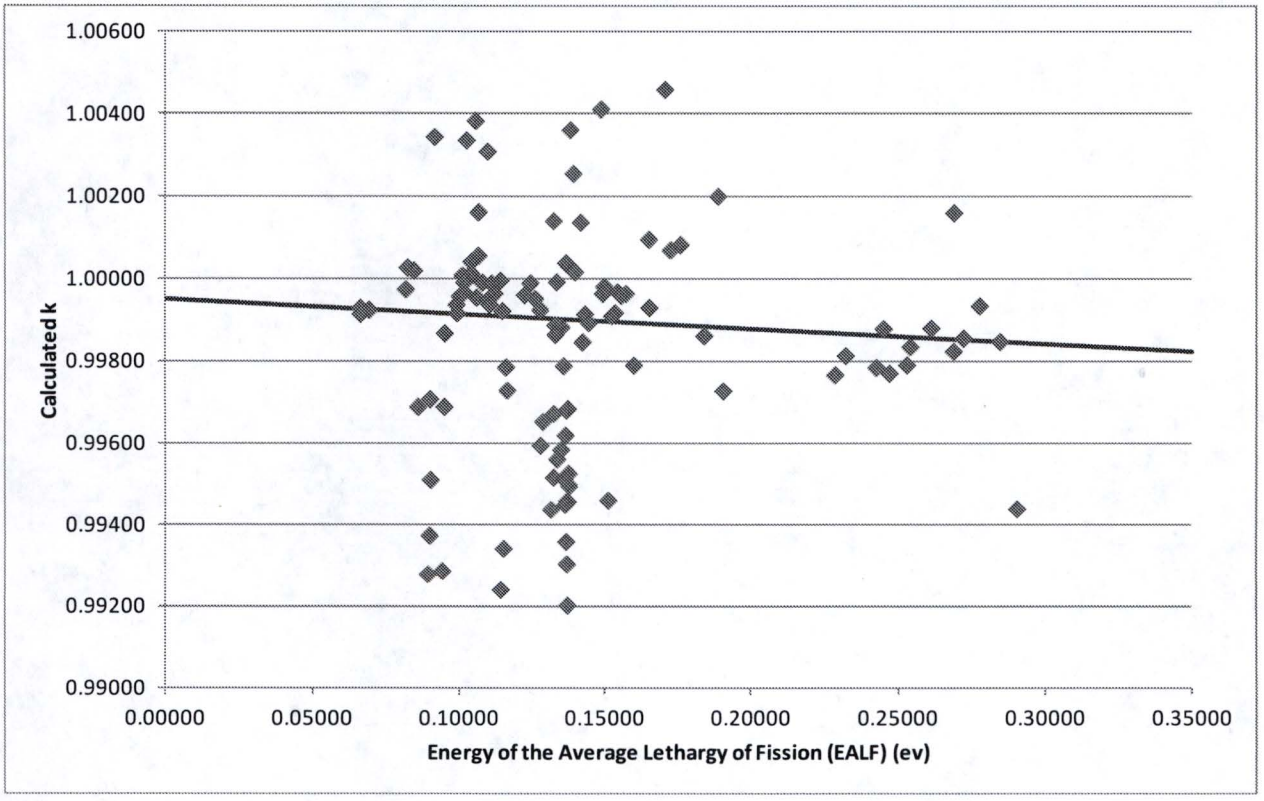

Figure A.5.9: Calculated MOX Critical k as a Function of EALF

The bias for the MOX set is smaller than the UO2 set so it would seem that the UO2 would be more limiting. However, the uncertainty for the MOX data is much higher than the UO2 data. Until the rack up of uncertainties in the spent and new fuel storage area is done it is not clear whether the bias or uncertainty is more important. Therefore both the UO2 and MOX bias and uncertainty are used in determining the most limiting condition.

A.5.3 Subcritical Margin

In the USA, the NRC has established subcritical margins for rack analysis. The subcritical margin for borated spent fuel pools, casks, and fully flooded dry storage racks is 0 when the analysis is performed with unborated water. This is actually saying the subcritical margin is contained in the uncredited soluble boron. To make sure there is sufficient soluble boron, analysis is also performed with soluble boron and a subcritical margin of 5% in k is required. For dry storage racks analyzed with optimum moderation, the subcritical margin is 2% and 5% with full moderation. In the analysis of 204 critical experiments, which generously cover the range of expected conditions, the lowest calculated k was 0.9938. The additional 117 MOX experiments also support this subcritical margin since the lowest calculated k is 0.9920. The subcritical margin is more than sufficient.

A.6. Area of Applicability (Benchmark Applicability)

The critical benchmarks selected cover both the new fuel storage area and the spent fuel pool of North Anna. To summarize the range of the benchmark applicability (or area of applicability), Table A.6.1 is provided below.

Table A.6.1: Area of Applicability (Benchmark Applicability)

Parameter	Range	Comments
Fissionable Material/Physical Form	UO_2	The fuel material is the same as in the benchmark experiments
Enrichment (wt% U-235)	2.35 to 4.74	The first core enrichments require extrapolation of the bias to lower enrichments. Assuming the enrichment is zero the bias would be 0.00295. The limiting bias which will be used in the application is 0.0035 (from the EALF trend). This 18% larger than the extrapolated bias which is sufficient margin for the extrapolation for lower enrichments. An extrapolation from 4.74 to 5 wt% will also be needed but in this direction the bias is decreasing so the data is adequate for this extrapolation.

Parameter	Range	Comments
Spectrum - EALF (eV)	0.0605 to 0.8485	Expected range in spent fuel pool applications: 0.1 to 0.8 eV The experiments cover the entire expected range of limiting conditions. For optimum moderation in new fuel storage area the EALF may be as high as 1.1 eV for this some extrapolation of the data is done.
Lattice Characteristics Type Pin Pitch (cm)	 Square 1.075 to 2.54	Hex lattices have been excluded. W 17x17 pin pitch is 1.26.
Assembly Spacing in Racks Distance between Assemblies (cm)	0 to 15.4	This covers all spacing. Neutron transport through larger than 15.4 cm has a small effect on k. Note that the spacing is assumed to be filled with full density water. If the water density is less, this separation effectively decreases. Therefore, optimum moderation cases of wide spaced racks are covered.
Absorbers Soluble Boron Concentration	0 to 5030 ppm	All designs are within this range.
Absorbers Cd (for Ag-In-Cd rods)	Cd Absorber panels	Although Cd is in panels, the inclusion or exclusion had no significant affect on the bias and uncertainty so credit for control rods is acceptable.
Reflector Experiments included water and steel	Reflectors adequately covered	Most racks are reflected by water, steel, and concrete which was covered in the set of experiments.
Temperature	Room Temperature (Reference 9 provides a bias for up to 85° C)	The criticality calculations are performed with the fuel at low temperatures. A separate set of experiments are used for a temperature bias covered in Reference 9.
Moderating material	Water	The moderator in all benchmark experiments is water, therefore water as a moderating material is covered

A.7. Summary and Recommendations

204 UO2 and 117 MOX critical experiments were analyzed with SCALE 6.0 and the 238 group ENFD/B-VII cross section set. The calculated k's were analyzed for trends using the statistical approach recommended in NUREG/CR-6698. Table A.7.1 provides the maximum bias and uncertainty for each trend.

For the spent fuel pool, the bias and uncertainty depends on the burnup since at low burnup the dominant fissile material is U-235 and at high burnup the dominant fissile material is Pu-239. In order to avoid trying to properly weight the critical experiments for the amount of U-235 and Pu-239 it is recommended to use two sets of bias and uncertainty, one from the fresh UO2 critical experiments and one from the MOX critical experiments. The final bias and uncertainty to be used will be that which produces the highest $k_{95/95}$. The UO2 critical experiments have a higher bias but lower uncertainty than the MOX experiments. Since the uncertainty of the bias is statistically combined with other uncertainties, it is not possible to determine which set is more limiting until the other uncertainties (due to factors such as manufacturing tolerances) are determined. Using the values from Table A.7.1 the UO2 based bias and uncertainty for EALF less than 0.4 eV (all unborated cases) is 0.0035 and 0.0050 respectively. For cases with an EALF greater than 0.4 eV but less than 0.8 eV, the UO2 bias and uncertainty is rounded up to 0.0060. Simultaneously, the analysis must be performed using the MOX bias and uncertainty. For EALF up to 0.4 eV, the MOX bias and uncertainty is 0.0020 and 0.0089 respectively. For the harder spectra, 0.4 to 0.8 eV, the MOX based bias and uncertainty is 0.0034 and 0.0135 respectively. Table A.7.2 summaries this paragraph.

Table A.7.1: Summary of the Trend Analysis

Trend	Equation	Maximum Bias	Maximum Uncertainty
UO2 Critical Experiments			
No trend (not weighted)	n/a	0.0023	0.0033
No trend (weighted)	n/a	0.0027	0.0049
EALF	0.99844-0.00488*EALF (ev)	0.0035 (@0.4 eV) 0.0055 (@0.8 eV) 0.0069 (@1.1 eV)	0.0046 (@0.4 eV) 0.0054 (@0.8 eV) 0.0063 (@1.1 eV)
Fuel Pin Diameter	0.99419+2.78E-03*Pin Dia. (cm)	0.0032	0.0049
Lattice Pitch	0.99421+1.87E-03*Pitch (cm)	0.0034	0.0049
Enrichment	0.99705+ 6.96E-05)*U235wt%t	0.0028	0.0050
Soluble Boron	0.99727+1.038E-07*ppm	0.0027	0.0050
MOX Critical Experiments			
No trend (not weighted)	n/a	0.0015	0.0054
No trend (weighted)	n/a	0.0010	0.0064
EALF	0.999497-0.00364*EALF (ev)	0.0020 (@0.4 eV) 0.0034 (@0.8 eV)	0.0089 (@0.4 eV) 0.0135 (@0.8 eV)

Table A.7.2: Final Bias and Uncertainty for Burned Fuel
(Calculate with both UO2 and MOX bias and uncertainty and use the set that provides the highest $k_{95/95}$)

	EALF Range (eV)	UO2	MOX
Bias			
	< 0.4	0.0035	0.0020
	0.4 – 0.8	0.0060	0.0034
	0.8 – 1.1	0.0070	
Uncertainty			
	< 0.4	0.0050	0.0089
	0.4 – 0.8	0.0060	0.0135
	0.8 – 1.1	0.0063	

For unburned fuel in the spent fuel pool use only the UO2 set from the above.

For the new fuel storage area in the fully flooded condition use the UO2 set from the above. For the optimum moderation case the spectrum can be higher. It is recommended to use extrapolated values for the bias and uncertainty. The range of the EALF in the criticality data is 0.06 to 0.84 eV. The optimum moderation case will need a bias and uncertainty for 1.1 eV. The extrapolation needed is only a third of the range. The bias and uncertainty from extrapolation to 1.1 eV are 0.0070 and 0.0063 respectively.

A.8. Temperature Bias

All of the critical experiments used thus far have been at room temperature. There could be a bias in k in the temperature range of interest to spent fuel pools and dry storage racks (0 to 100 C). There is one critical benchmark evaluation in the OECD/NEA handbook [A.3] that performed measurements with elevated temperatures in this range, LEU-COMP-THERM-046 (shortened to LCT-046). LCT-046 consists of 22 experiments but the last 5 experiments contain copper rods. Since copper is not in North Anna's spent fuel pool only the first 17 experiments are analyzed.

The 17 LCT-046 experiments have been analyzed using SCALE 6.0 [2] and the 238 ENDF/B-VII cross section library. Section 3 of LCT-046 provides the details for analysis of the critical benchmark. The SCALE models used follows that specification. All the expansion factors from Table 29 of LCT-046 were applied to all the x-y dimensions. That means that the same stainless steel component expansion factor was applied to pitch and the inner and outer diameter of the clad. This is consistent with the MCNP samples given in the Appendix of LCT-046. For the axial expansion, only the fuel was expanded. As with the MCNP sample input, the same expansion factor was used for the radius and the axial direction. The fuel column is 54.84 cm long (unexpanded). Due to the control rod bottom plug which hangs into the fuel region, the fuel is modeled as a 53.44 cm long (unexpanded) zone followed by two shorter zones. For this effort only the 53.44 cm long segment was expanded axially by the expansion factor. This approach assures that the axial position of the control rod and bottom plug is not changed.

Table A.8.1 shows the corrected SCALE 6.0 ENDF/B-VII results for the 17 critical experiments. Corrected results in this case means they were divided by the k of the benchmark which was not quite 1.0.

Table A.8.1: LCT-046 with Full Thermal Expansion Calculated with SCALE 6.0 and ENDF/B-VII

Case	Temperature (K)	Corrected SCALE k	SCALE sigma
1	297.05	0.998901	0.00007
2	310.41	0.998867	0.00007
3	315.43	0.998710	0.00007
4	319.96	0.998915	0.00007
5	324.93	0.998558	0.00007
6	332.53	0.998697	0.00007
7	287.22	0.999163	0.00007
8	315.91	0.998854	0.00006
9	330.27	0.998669	0.00007
10	337.44	0.998566	0.00007
11	351.99	0.998625	0.00007
12	303.60	0.998632	0.00007
13	312.95	0.998616	0.00007
14	321.16	0.998511	0.00007
15	328.24	0.998258	0.00007
16	338.26	0.998147	0.00007
17	358.31	0.998057	0.00007

Figure A.8.1 plots the results of the analysis as a function of case. As can be seen from this plot, there does appear to be a trend with temperature. Figure A.8.2 shows the data plotted against temperature with the least squares linear fit. The nominal slope of the fit is -1.14E-05 Δk/ΔC. Using the EXCEL regression function the most limiting slope with 95% certainty is -1.7E-05 Δk/ΔC.

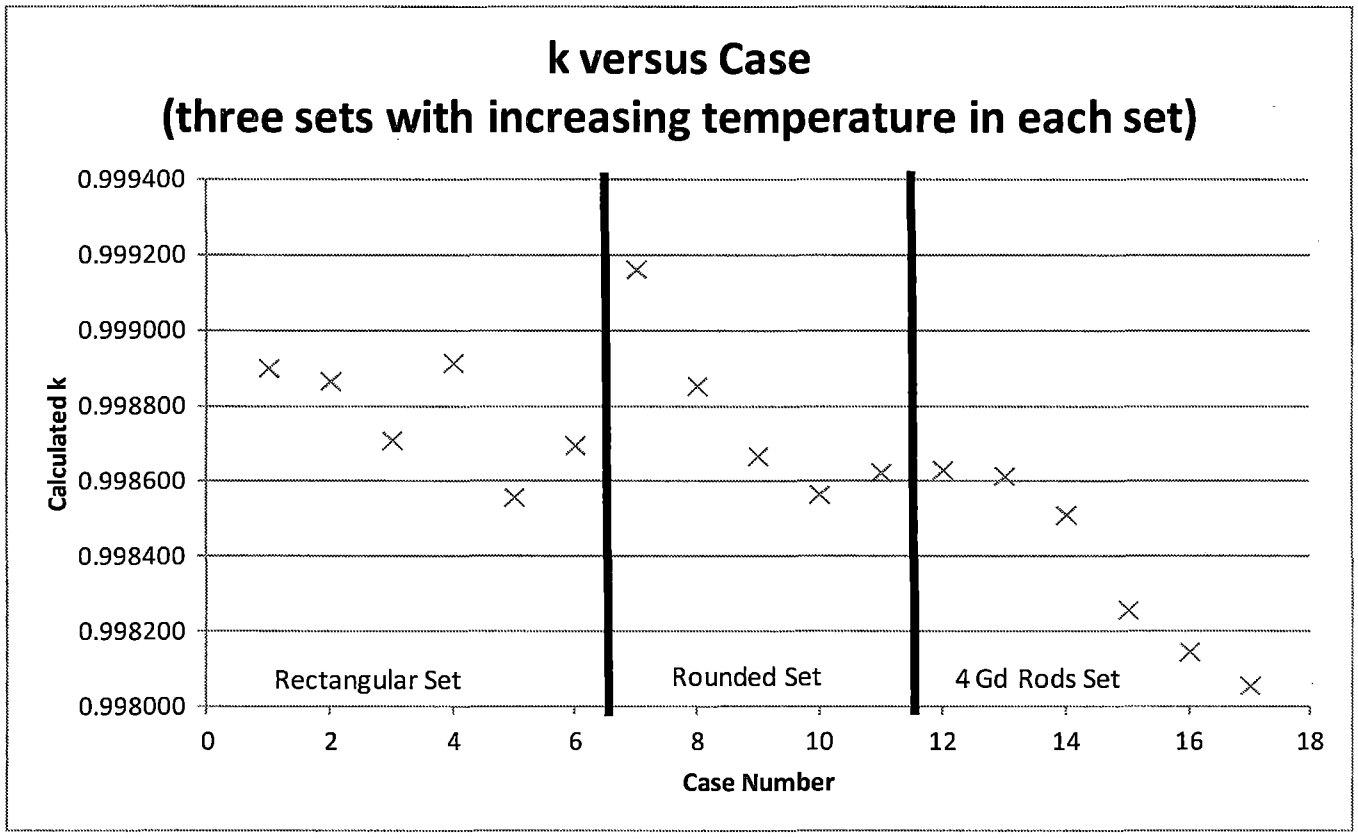

Figure A.8.1: LCT-046 Corrected Calculated k per Case

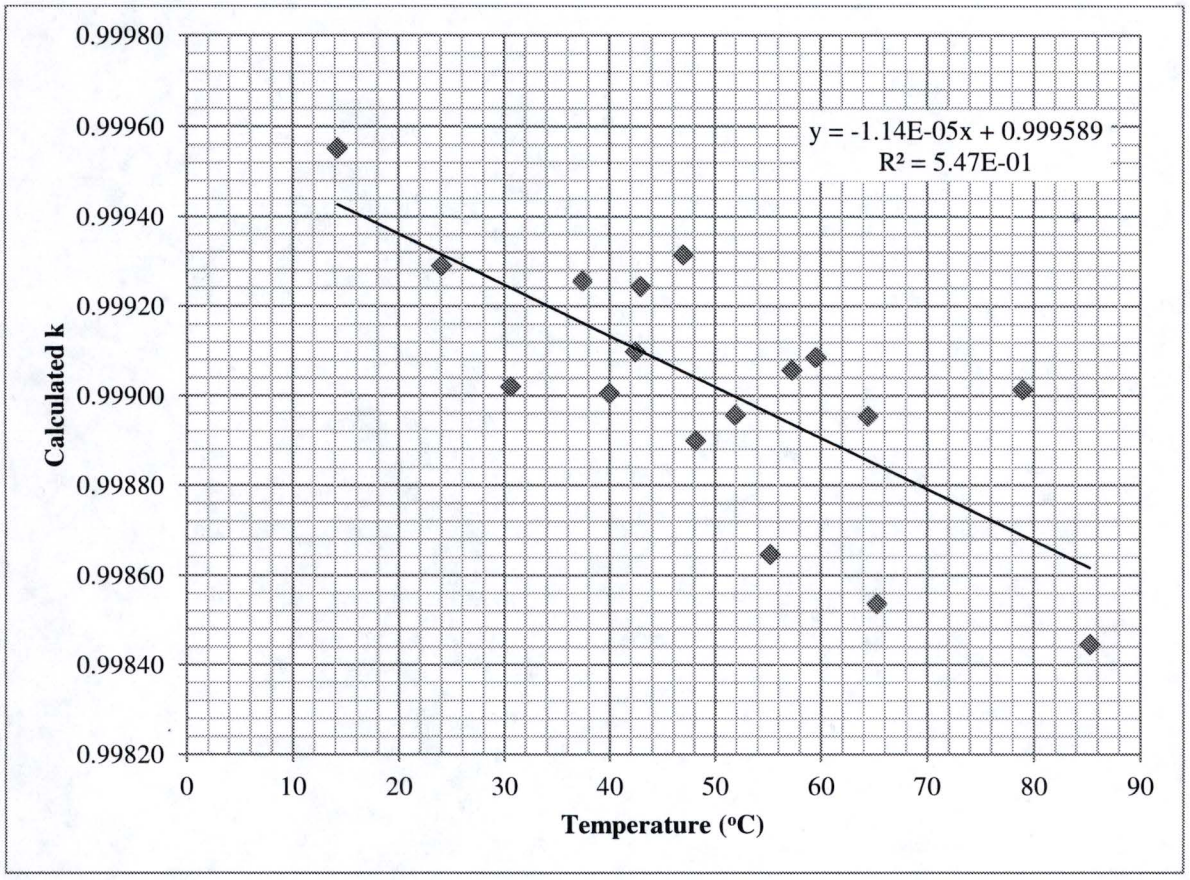

Figure A.8.2: LCT-046 k versus Temperature

The analysis of the only set of thermal critical experiments in the International Handbook that uses elevated temperatures in the range of 0 to 100 C has shown a small increase in the bias with temperature. This increase can be conservatively handled by a bias from room temperature of 1.7E-05 $\Delta h/^{o}C$. This bias is the lower (most negative slope) 95% confidence slope of the fit line.

A.9. Appendix References

[A.1] *SCALE: A Modular Code System for Performing Standardized Computer Analyses for Licensing Evaluation*, ORNL/TM-2005/39, Version 6, Volumes 1-3, January 2009.

[A.2] J.C. Dean and R.W. Tayloe, Jr., *Guide for Validation of Nuclear Criticality Safety Calculational Methodology*, NUREG/CR-6698, Nuclear Regulatory Commission, Washington, DC January 2001

[A.3] *International Handbook of Evaluated Criticality Safety Benchmark Experiments*, NEA/NSC/DOC(95)3, Volumes IV and VI, Nuclear Energy Agency, OECD, Paris, September, 2010.

[A.4] D. E. Mueller, K. R. Elam, and P. B. Fox, *Evaluation of the French Haut Taux de Combustion (HTC) Critical Experiment Data*, NUREG/CR-6979 (ORNL/TM-2007/083), prepared for the US Nuclear Regulatory Commission by Oak Ridge National Laboratory, Oak Ridge, Tenn., September 2008.

[A.5] F. Fernex, "Programme HTC – Phase 1 : Réseaux de crayons dans l'eau pure (Water-moderated and reflected simple arrays) Réévaluation des expériences," DSU/SEC/T/2005-33/D.R., Institut de Radioprotection et de Sûreté Nucléaire, 2008.

[A.6] F. Fernex, *ProgrammeHTC – Phase 2 : Réseaux simples en eau empoisonnée (bore et gadolinium) (Reflected simple arrays moderated by poisoned water with gadolinium or boron) Réévaluation des expériences*, DSU/SEC/T/2005-38/D.R., Institut de Radioprotection et de Sûreté Nucléaire, 2008.

[A.7] F. Fernex, *Programme HTC – Phase 3 : Configurations "stockage en piscine" (Pool storage) Réévaluation des expériences*, DSU/SEC/T/2005-37/D.R., Institut de Radioprotection et de Sûreté Nucléaire, 2008.

[A.8] F. Fernex, *Programme HTC – Phase 4 : Configurations "chateaux de transport" Réévaluation des expériences*, DSU/SEC/T/2005-36/D.R., Institut de Radioprotection et de Sûreté Nucléaire, 2008.

[A.9] DATAPLOT is statistical software supported by the National Institute of Standards and Technology. It can be down loaded at: http://www.itl.nist.gov/div898/software/dataplot/

[A.10] Kleinbaum, Kupper, and Muller, Applied Regression Analysis and Other Multivariable Methods, Second Edition, page 48, PWS-KENT Publishing Company, Boston, MA 1988.

[A.11] "PROPHET StatGuide: Examining normality test results," http://www.basic.northwestern.edu/statguidefiles/n-dist_exam_res.html, located on 6/8/09.

[A.12] R. Mark Sirkin, Statistics for the Social Sciences, Third Edition, 2005, page 245, Sage Publications, Thousand Oaks, CA.